BIOLOGICAL GENERATION OF REACTIVE ALKALINE SPECIES AND THEIR APPLICATION IN A SUSTAINABLE BIOPROCESS FOR THE REMEDIATION OF ACID AND METAL CONTAMINATED WASTEWATERS

A thesis submitted in the fulfilment of the
requirements for the degree of

DOCTOR OF PHILOSOPHY

in the
Department of Biochemistry and Microbiology
Rhodes University

by

Robert Paul van Hille

December 2001

This thesis is dedicated to the memory
of my grandparents Bob and Gerda van Hille
whose love of science and nature and willingness
to indulge a curious child helped me decide on
a future career at an early age.

Thanks to you I was never going to be a cowboy

PUBLICATION LIST

Parts of this thesis published as:

van Hille, R.P., Boshoff, G.A., Rose, P.D. and Duncan J.R. 1999. A continuous process for the biological treatment of heavy metal contaminated acid mine water. *Resources, Conservation and Recycling*, **27**: 157-167.

Duncan, J.R., Stoll, A., Wilhelmi, B.S., Zhao, M. and van Hille, R.P. 1997. The use of algal and yeast biomass to accumulate toxic and valuable heavy metals from wastewater. *Water Research Commision Report*, No. 616

Rose, P.D., Boshoff, G.A., van Hille, R.P., Wallace, L.C.M., Dunn, K.M. and Duncan, J.R. 1998. An integrated algal sulphate reducing high rate ponding process for the treatment of acid mine drainage wastewaters. *Biodegradation*, **9**(3-4): 247-257.

International conference presentations:

van Hille, R.P. and Duncan J.R. 1996. Bioremediation of heavy metal polluted acid mine effluent by *Spirulina sp.* - Presented at the 7th conference of the International Association of Applied Algology. Published as an abstract in *Journal of Applied Phycology* **8:** 461 (1996)

Duncan, J.R., Wilhelmi, B.S., Stoll, A., Zhao, M., van Hille, R.P. and Wallace, L. 1997.Bioacculmulation of metals from industrial and mining effluents. Published in conference proceedings for IBS 97/Biomine

van Hille, R.P., Boshoff, G.A., Rose P.D. and Duncan J.R. A continuous process for the biological treatment of heavy metal contaminate acid mine water. - Presented at the International Society of Environmental Biotechnology Conference in Belfast in June 1998.

van Hille, R.P., Nightingale, L., Rose, P.D. and Duncan, J.R. Biogenic alkalinity - a viable alternative to existing strategies for acid mine drainage remediation. - Presented at the International Society of Environmental Biotechnology Conference in Noordwijkerhout, Netherlands in April 2000.

Patents awarded:

van Hille, R.P., Boshoff, G.A., Rose P.D. and Duncan, J.R. Mine water treatment process. RSA patent number 98/7698, USA patent number 6,110,370

Rose, P.D., Duncan, J.R., van Hille, R.P. and Boshoff, G.A. Alkalinity and Biorefining. RSA patent number 99/4586, USA patent application number 09/364,820

Rose, P.D., Duncan, J.R., van Hille, R.P. and Boshoff, G.A. Use of Ponds to Treat Sulphate Solutions and ASPAM Process. RSA patent number 99/4585, USA patent application number 09/364,126

ABSTRACT

This project focused on the development of an integrated biological system for the treatment of acidic and metal-laden effluents, based on the sustainable biological generation of reactive alkaline species.

Initial studies concentrated on the binding and accumulation of heavy metals by biomass of the cyanobacteria, *Spirulina* sp. Metal binding was rapid, with saturation reached in 30 minutes, and followed an affinity series of Pb > Cu > Zn >> Fe. The binding capacity of the *Spirulina* for each of the metals was relatively low when compared to a range of other biosorbents. The toxicity thresholds of the algae was determined for copper and zinc. These were low (< 10μmoles/g) and as such, the algae were not suitable for application in a treatment system in which they came into direct contact with the toxic metals.

The algae were able to increase the pH of the surrounding medium. This occurred as a result of the accumulation of inorganic carbon, from bicarbonate, as a response to low concentrations of carbon dioxide in the medium. The resulting release of a hydroxide ion into solution led to the increase in pH. The increase in pH was shown to be due to a reduction in acidity, rather than an increase in alkalinity. The enzyme carbonic anhydrase was shown to be pivotal in this system. Attempts to determine the enzyme activity directly were unsuccessful, due to the inherent inaccuracy of the assay system. An indirect method of determining enzyme activity, by measuring changes in the carbonate species equilibrium, was developed. Under optimal conditions *Spirulina* was able to reduce the acidity by an amount equivalent to the addition of 3670μmoles NaOH g^{-1} h^{-1}. Predictive modelling showed that this enhanced the potential of the medium to effect metal precipitation.

For the algal system to be sustainable, a readily available source of bicarbonate was needed. This was achieved by the oxidation of organic carbon, under sulphidogenic conditions, by a bacterial consortium isolated from the anaerobic component of a facultative pond. The consortium was shown to consist of sulphate reducing (most likely *Desulvovibrio* and *Desulfotomaculum*)and acetogenic bacteria. Sulphate removal rates of 500mg l^{-1} day^{-1} and 135mg l^{-1} day^{-1} were achieved in a 2l agitated and 28l upflow reactor respectively. The bicarbonate generation rate in the 28l reactor was calculated as 4033μmoles l^{-1} day^{-1}, which proved sufficient to act as a feed for the algal system. Sparging the anaerobic digester overflow with air and nitrogen resulted in a reduction in the aqueous sulphide concentration. Using nitrogen, a 70% recovery of sulphide, as H_2S gas, was achieved in 60 minutes, while with air, this dropped to 40%, due to the oxidation of the aqueous sulphide. The stripping of H_2S resulted in an increase in pH. The H_2S gas was used for the selective precipitation of copper and lead in the integrated system.

The dynamics of metal precipitation was investigated. For simple reactions, between individual

metal and base species, it was possible to generate an accurate predictive model and confirm the precipitating species using wavelength dispersive X-ray spectroscopy (WDS). In more complex systems, where precipitation of the artificial acid mine drainage was examined, the predictive modelling and WDS could not accurately describe the system. The addition of aqueous sulphide to copper and iron resulted in the formation of metastable, amorphous precipitates, which remained in suspension. Ageing of the copper precipitate resulted in the evolution of a stable crystalline structure (covellite) and the aggregation and settling of the precipitate. In the case of iron, the amorphous precipitate underwent oxidation before a stable iron sulphide could evolve and the settled precipitate was an iron oxide or oxyhydroxide. The artificial acid mine drainage was treated with sulphide, hydroxide, anaerobic digester overflow and algal overflow. The best metal removal was achieved with the sulphide and hydroxide, while the algal overflow outperformed the anaerobic digester overflow. The precipitate generated by the addition of sulphide was the most compact, followed by the algal overflow, the anaerobic digester overflow and the hydroxide. Efficient precipitation of all the heavy metals, except manganese, was achieved using the algal overflow at an acidity to alkalinity ratio of 1:2. This ratio was selected for use in the pilot system.

The *Spirulina* based pilot system was effectively used to treat an effluent from the Black Mountain base metal mine. The necessity to maintain the algae in suspension and avoid biomass washout were practical considerations which counted against this system. The replacement of the *Spirulina* by *Oscillatoria*, which adhered to a solid support, overcame these problems. The integrated biological system was able to effectively treat an artificial acid mine drainage for 90 days, reducing the concentration of all metals, except manganese, to below the acceptable environmental risk levels. The treatment of the final effluent in a second anaerobic digester reduced the manganese concentration to 4.5μM and proved that the sulphate reducing bacteria could be cultivated on enriched, partially treated acid mine drainage.

The integrated biological treatment system performed well, effectively treating an effluent modelled closely on the quality of the water being discharged from the East Rand Basin. The cost of such a system would be considerably less than a "high tech" physico-chemical system. This, coupled with the potential long term sustainability of a biological system, would make it a potentially attractive option for the treatment of future acid mine drainage discharges.

TABLE OF CONTENTS

List of Figures		Page
Figure 1.1:	Observed decline in iron over time during flushing of Wheal Jane mine, Cornwall, compared with model output obtained using equation (8) (Younger, 2000)	19
Figure 1.2:	New classification scheme for minewaters: Fields in which minewaters of different origins and affinities plot (Younger, 1995)	24
Figure 1.3:	Aqueous and solid phase equilibrium for ferrous hydroxide at infinite dilution (Loewenthal *et al.*, 2001)	26
Figure 2.1:	Lithostratigraphic section of the East Rand geology (after Scott, 1995)	45
Figure 2.2:	Three dimensional relationships of: Main Reef basins, base of the dolomite (Black Reef) and surface topography (after Scott, 1995)	48
Figure 2.3:	The East Rand region showing breaks in mine boundary pillars allowing water movement. The regions of major groundwater inflow and preferred flow paths to the predicted discharge site are shown (after Scott, 1995)	55
Figure 3.1:	Scanning electron micrograph of healthy *Spirulina*	63
Figure 3.2:	Percentage metal accumulation in batch flasks by *Spirulina* as a function of time (n=3 ± SD). Initial metal concentration 200μM. Data for individual metals obtained from separate experiments and combined	72
Figure 3.3:	Graph showing mean (n=3) algal concentration vs time for effluent treatment studies. Viable algal mass was determined using the linear relationship between Chlorophyll *a* and dry mass. Chlorophyll determinations terminated after day 25 due to death of most cultures	74
Figure 3.4:	Graph of pH vs time for effluent treatment studies (mean values, n=3)	74
Figure 3.5:	Graph of cumulative copper removal vs time for the effluent treatment studies (mean values, n=3)	75
Figure 3.6:	Graph of cumulative zinc removal vs time for effluent treatment studies (mean values, n=3)	76
Figure 3.7:	Comparison of pH change vs time for experimental (a) and algal free control (b) flasks (mean values, n=3)	77
Figure 3.8:	Mean pH vs time for copper toxicity study (n=3)	78
Figure 3.9:	Mean algal concentration vs time for copper toxicity study (n=3). Algal concentration determined from chlorophyll extractions	79

ACKNOWLEDGEMENTS

To the staff members of the Biochemistry and Microbiology Department , Rhodes University, my sincere thanks for generous assistance throughout my postgraduate studies. In particular, I would like to thank Professor J. Duncan and Professor P. Rose for their supervision of this project.

To my collegues, Paula Antunes, Genevieve Boshoff, Leigh Nightingale, Rosemary Payne, Neil Rein and Douglas Sanyahumbi, thank-you for your friendship and assistance.

To Doctor Paul Younger, thank-you for your invaluable assistance in helping me understand the hydrogeology of abandoned mine systems.

I am indebted to Doctor Malcolm Roberts and Mr Robin Cross for their assistance with the wavelength dispersive X-ray spectroscopy and the electron microscopy.

Financial support for the project from the Water Research Commission and the National Research Foundation is gratefully appreciated.

Thank-you to Heather Benney, Douglas Sanyahumbi and Arno Venter for proof-reading this thesis.

Most importantly, a special thank-you to Heather for her understanding, encouragement and loving support throughout the writing up of this thesis, and to my family; including Erik; who have always been encouraging and supportive.

CHAPTER 1. GENERAL INTRODUCTION

1.1 Water as a resource in South Africa

South Africa (SA) is a developing country that is water scarce and water stressed. While water conservation (WC) and demand management (DM) are topics that are commonly referred to in water resources literature in South Africa, the need and value of WC/DM principles have only recently been fully recognised and appreciated. The realities of the new democratic South Africa demand improved management of the country's limited water resources (DWAF, 1999).

The demand on South Africa's limited water resources is growing as a result of a high population growth rate, a developing economy and the urgent need to supply water services to millions of people who have previously been without them. The sustainability of SA's water resources is threatened both in terms of quantity and quality. If the current patterns of water usage are maintained, all renewable water resources in SA will be fully committed (Odendaal, 1997; DWAF, 1999). Already there are a number of regions in the country that rely on expensive transfer schemes as water demand has far exceeded water availability.

Some of the reasons contributing to the challenges of ensuring sustainable water resources for the future are:

- While the climate varies from rain forest to desert, the typical climate of SA is semi-arid, with the average rainfall, 475mm per annum, being just over half the global average.
- Rainfall patterns are variable, with droughts followed by floods commonly occurring.
- The distribution of rainfall is uneven, with 60% of the river flow arising from only 20% of the land area.
- Limited groundwater.
- Some metropolitan and industrial growth centres have developed around mineral deposits and are far from major water resources.
- South Africa's average evaporation rate exceeds its precipitation rate.
- A population growth rate of 2-3% per annum.
- A large backlog of housing and service delivery.

While alternative water sources, such as desalination and icebergs, are possible they are prohibitively expensive in view of South Africa's socio-economic needs. Therefore, the need to develop effective WC/DM strategies is acute (DWAF, 1999).

Reducing water demand reduces water withdrawals impacting on the environment and results in increased stream flows and reduced demand on groundwater sources. Current land and water utilisation in South Africa is having a detrimental effect on the ecology of rivers, lakes, wetlands and estuaries. These threatened ecosystems need to be protected from the over utilisation of water resources and the continued development of new dams (DWAF, 1999).

The protection of existing water resources through conservation measures is of great importance. Examples include:

- The removal of alien vegetation, which has reduced surface runoff and the yield of existing resources. Catchments cleared of invading alien plants show improved yields of up to 10%.
- Rehabilitation of wetlands.
- Protection of groundwater resources.
- Minimising pollution of water resources.

1.2 Water resource policy and legislation

Management of natural resources and the environment has progressed rapidly in South Africa in recent years. This is a result of the global trend towards increased knowledge of the environment and the need to protect it, as well as a massive change in the political perspectives in the country (Harris *et al.*, 1999).

The Department of Water Affairs and Forestry has reviewed water laws, both locally and abroad in preparation for new legislation designed to reflect democratic principles and equitable resource access by all. The development of new legislation presented an ideal opportunity to achieve the objectives of providing more equitable access to water resources and consolidate

much of the recent development in water resource thinking (Harris *et al.*, 1999; Singh and Constantinides, 2000).

The Department's slogan of "some for all, forever" succinctly captures the goal for water resource management and service provision in South Africa. It recognises that water is an essential, finite resource and indicates a fundamental commitment to equitable allocation. Finally it acknowledges the goal of sustainable use.

1.2.1 Ecological integrity

Ecosystems have an inherent recovery capacity in response to variable conditions, such as floods and droughts, but this ability is finite. As the maximum recovery capacity is assumed to exist in a natural, unmodified system, the degree to which a specific component of the water resource differs from its natural state is important in estimating its ability to recover. The degree of modification of a particular part of a water resource can be assessed by measuring components of its ecological integrity (Harris *et al.*, 1999).

The ecological integrity of a water source is its ability to maintain a balanced, integrated composition of physico-chemical habitat characteristics and biotic components on a temporal and spacial scale. These should be comparable to the natural characteristics of ecosystems in the region. Ecological integrity implies the ecosystem's structure and functions are not impaired by anthropogenic stresses. A resource will only be able to provide for long term water uses if its ecological integrity is assured (Harris *et al.*, 1999; Singh and Constantinides, 2000).

Many of South Africa's water resources have already been modified by use and development and are no longer in their natural state, but this does not mean they are no longer sustainable. In such cases the effects of these uses need to be determined and those uses that can be sustained by the water resource, so that its integrity remains at an acceptable level, need to be identified (Harris *et al.*, 1999).

The concept of a water "Reserve" has been defined and is intended to protect water resources, so that basic human needs can be met and ecological functions and processes can be sustained. The Reserve consists of two parts, the basic human needs reserve and the ecological reserve. The basic human needs reserve provides for the essential needs of individuals served by the water resource in question and includes water for drinking, for food preparation and for personal hygiene. The ecological reserve relates to the water required to protect the aquatic ecosystem of the water resource. The Reserve for all or part of any significant water resource is determined by the Minister of Water Affairs and Forestry (National Water Act, 1998).

Components of ecological integrity, such as the chemical and physical characteristics of the water, the quantity of water, the habitat and the structure and function of the associated biotic communities are measured to ensure the Reserve does indeed protect the ability to meet human needs and sustain ecological functions. The ongoing monitoring and assessment of the condition of the water resources, their response to impacts and the state of the Reserve are critical to the management and protection of resources. The aim is for management decisions to be made on the basis of sound scientific and technical information and understanding (Harris *et al.*, 1999; Singh and Constantinides, 2000).

1.2.2 Policy for protecting water resources

The enactment of the National Water Act (1998) and the Water Services Act (1997) made various requirements and provisions for the implementation of water conservation and demand management principles. The Water Services Act sets out a framework to ensure the provision of basic water supply and sanitation and a regulatory framework for water services institutions. The National Water Act ensures that the nation's water resources are protected, used, developed, conserved, managed and controlled in ways which take into account, amongst other factors, promoting the efficient, sustainable, and beneficial use of water in the public interests. Furthermore, the Act gives the Minister broad powers to make regulations limiting or restricting the purpose, manner or extent of water use as well as the attachment of conditions relating to water resource protection to every authorisation or licence issued. Finally the Act requires the establishment of a national water resource strategy and a catchment management strategy, to

provide for the development, management and protection of water resources and catchments (DWAF, 1999).

The policy integrates resource-directed measures for protection (such as resource quality objectives) with source-directed measures (such as effluent standards). It includes:

- Setting water resource-based objectives which clearly define acceptable values for water resources for each of the components (chemical, physical, biological) of ecological integrity.
- Use of source-directed standards which clearly define acceptable values for waste discharge or impact generation and encourage movement towards minimisation of waste disposal and impacts.
- Where source-directed standards cannot be met in the short term, a temporary exemption from the standards could be considered if an impact assessment indicates that the water resource-based objectives could still be met.

Before any potentially hazardous waste can be disposed of, a waste disposal site permit needs to be issued by the Department of Water Affairs and Forestry. The applicant is required to adhere to a series of "minimum requirements" before a permit is issued. The objectives of the minimum requirements are to ensure the protection of SA's water resources, to ensure a nationally uniform approach to waste disposal and to make South African waste management practices internationally acceptable (DWAF, 1998).

The minimum requirements are enforceable under the National Water Act (1998) and the Environment Conservation Act (1989). They allow for the suspension and revocation of disposal permits and the recovery of remediation costs from any person responsible for the pollution of water resources.

A cornerstone of the minimum requirements is the determination of the estimated environmental concentration (EEC) for particular hazardous substances. The EEC is calculated based on acceptable risk criteria. The aquatic environment has been chosen to quantify the risk to man and

the environment. Since the aquatic environment is extremely sensitive to contamination and pollution it is possible to prove that if the aquatic environment is not at risk (being within acceptable risk), that man and more robust ecosystems should also not be exposed to unacceptable risk. The acceptable risk levels have been set at one tenth of the LC_{50} (the concentration determined to kill 50% of specific warm and cold water fish or aquatic invertebrate species) and have been statistically shown to result in a mortality incidence of 1 in 300 000 in the aquatic environment (DWAF, 1998). The acceptable risk values for the elements of interest to this study are listed in appendix A.

1.3 Water pollution

Human activities have resulted in the widespread pollution of the natural environment by both organic and inorganic contaminants. This study concentrates on inorganic contaminants, particularly heavy metals and salinity.

A study by the Council for Scientific and Industrial Research (CSIR) in 1991 indicated that the quality of South Africa's water resources is declining, primarily as a result of salinisation, but also as a result of metal pollution and eutrophication (Neytzell-De Wilde, 1992). The major ions responsible for salinity related problems are calcium, magnesium, sodium, chloride, sulphate and bicarbonate. High concentrations of these ions may detrimentally affect plant and animal health by affecting water and nutrient intake. While a portion of these ions may enter waters naturally, by leaching from sedimentary deposits, the major source is anthropogenic, primarily as a result of mining and related industries and to a lesser extent agriculture (Backeburg *et al.*, 1996; Casey *et al.*, 1996).

The heavy metals consist of a group of elements with densities greater than five. Many of these elements are essential micronutrients, but at elevated concentrations they become acutely toxic to living organisms. The incidence of heavy metal pollution in surface and groundwaters is a direct result of industrial activities, primarily mining, refining, electroplating and manufacturing.

Heavy metals have a profound effect on aquatic ecosystems. At low (sub-lethal) concentrations they are accumulated by many microbial species and are increasingly concentrated at higher levels in the food chain. Higher concentrations of acutely toxic metals such as copper, lead, zinc, cadmium, nickel and mercury have a devastating effect on aquatic organisms. Their effect on the organisms is diverse and includes the denaturation of proteins (Gadd and Griffiths, 1978), the inactivation of enzymes (Teisseire and Vernet, 2000), the retardation of electron transport chains and photosynthesis (Asthana *et al.*, 1992; Abalde *et al.*, 1995; Barón *et al.*, 1995; Jin *et al.*, 1996) and the destabilisation of membrane structures (Brady and Duncan, 1994; Franklin *et al.*, 2000).

While metals such as iron, aluminium and manganese are less toxic to aquatic organisms, they form bulky hydroxide and oxide precipitates in oxygen-rich waters. These precipitates can still have a serious effect on aquatic invertebrates by coating their gills and breathing apparatus as well as reducing adhesion points to the substrate (Younger, 1995; Jooste and Thirion, 1999).

The major source of both salinity and heavy metal contamination of water resources in SA is acid mine drainage, originating from operating and abandoned mines as well as rock piles and tailings.

1.4 Acid Mine Drainage

"Acid mine drainage" (AMD) has been described as a major source of water pollution worldwide. Currently over 700km of streams and rivers have been affected in Great Britain (Jarvis and Younger, 2000) and over 3000km in the United States (Hedin, 1997). It arises from the bacterially catalysed oxidation of sulphide minerals, most commonly pyrite (FeS_2). The oxidation of sulphide minerals can occur in working and abandoned mines, where mining has exposed them to the atmosphere, as well as in waste rock piles and tailings generated by the processing of the mined ore (Johnson, 1995).

1.4.1 Oxidation of pyrite and other sulphide minerals

Pyrite is widely disseminated in deposits of coal and both precious and base metals. The initial oxidation of pyrite may be written as follows:

$$FeS_2 + {}^7/_2O_2 + H_2O \rightarrow Fe^{2+} + 2SO_4^{2-} + 2H^+ \quad (1)$$

For vigorous pyrite oxidation to occur a number of criteria must be simultaneously satisfied. Reaction (1) indicates that water and atmospheric oxygen are required. These criteria are typically met only in the unsaturated zone of the sub-surface, above the water table. The composition of the pyrite affects its oxidation rate, with fine grained "framboidal" pyrite being significantly more reactive than coarse crystals of pyrite. The sulphur content of the ore affects its acid generating potential, with values of 4-6wt% indicating a high acid potential (Younger, 1998). Values of this range are often associated with strata deposited in brackish water and are geologically mapped as "marine bands". The final criterion for substantial pyrite oxidation is the presence of bacterial catalysis. Reaction (1) is bacterially catalysed in at least two ways. Firstly iron oxidising bacteria such as *Acetothiobacillus ferrooxidans* are responsible for the rapid oxidation of ferrous iron (Fe^{2+}) to ferric iron (Fe^{3+}) by the following reaction:

$$Fe^{2+} + {}^1/_4O_2 + H^+ \rightarrow Fe^{3+} + {}^1/_2H_2O \quad (2)$$

The bacterial action can speed up the reaction rate by a factor of up to one million and provide a supply of ferric ions for the further oxidation of pyrite in the absence of oxygen:

$$FeS_2 + 14Fe^{3+} + 8H_2O \rightarrow 15Fe^{2+} + 2SO_4^{2-} + 16H^+ \quad (3)$$

The reaction proceeds rapidly, especially at low pH. This reaction is particularly important in AMD generation in rock piles and tailings, where only a small fraction (the outer 1m) is exposed to sufficient oxygen for reaction (2) to be efficient. The water percolating through the anoxic portion is rich in ferric iron and allows further leaching of pyrite (Johnson, 1995). The second

bacterially catalysed reaction is the oxidation of reduced sulphur compounds to SO_4^{2-} by bacteria such as *Acidothiobacillus thiooxidans*.

The above acid and metal generating reactions are not restricted to pyrite and other members of the pyrite family, such as chalcopyrite and arsenopyrite can be similarly oxidised to generate proton acidity and release copper and arsenic into solution along with iron. A number of other metal sulphide minerals such as galena (PbS) and sphalerite (ZnS), which are found in association with coal or gold bearing strata, readily release their metals into acidic solutions (Younger, 1998). Oxidation of these minerals does not directly generate proton acidity. An example is shown below:

$$PbS + 2O_2 \rightarrow Pb^{2+} + SO_4^{2-} \quad (4)$$

1.4.2 Hydrolysis of Fe^{3+}

As the groundwater containing the ferrous iron which has been released by pyrite oxidation is discharged at the earth's surface, where the environment is sufficiently oxidising, the hydrolysis of ferric iron can occur (Younger, 1995). This reaction generates further proton acidity:

$$Fe^{3+} + 3H_2O \rightarrow Fe(OH)_3 + 3H^+ \quad (5)$$

The above mentioned processes can be combined into an overall reaction which summarises the process resulting in the surface discharge of AMD:

$$FeS_2 + {}^{15}/_4O_2 + {}^{7}/_2H_2O \rightarrow Fe(OH)_3 + 2SO_4^{2-} + 4H^+ \quad (6)$$

This shows that each mole of pyrite oxidised ultimately produces four moles of proton acidity (H^+). As such, it is one of the most prolific acid producing reactions in nature (Appelo and Postma, 1993). The acid generated by these reactions can be responsible for further leaching of acid labile minerals resulting in a "classical" AMD discharge having a low pH, high sulphate and iron load and potentially dangerous levels of other metals such as manganese (Mn), aluminium

(Al), copper (Cu), lead (Pb), zinc (Zn), nickel (Ni) and arsenic (As). In addition, if the AMD is generated from pyrite exposure as a result of precious metal mining the discharge may contain metals such as silver (Ag), gold (Au) and platinum (Pt) at concentrations which make their recovery financially viable.

1.4.3 Formation of acid generating salts (AGS)

Due to the constant dewatering that occurs in most deep level mines, reaction (6) tends not to run to completion as most of the pyrite oxidation occurs in the unsaturated zone. As a result, the quality of the pumped water tends not to be seriously affected by dissolved metals or proton acidity. In these unsaturated zones pyrite oxidation results in the formation of intermediate solid phase minerals (Younger, 2000; Bayless and Olyphant, 1993). These are most often ferrous/ferric hydroxy-sulphates and members of the jarosite family and have collectively been labelled acid generating salts (AGS) by Bayless and Olyphant (1993). They may also be formed by the evaporation of mine drainage (Nordstrom *et al.*, 1979). A number of typical AGSs are shown in table 1.1 below.

Table 1.1: Chemical formulas for commonly occurring acid generating salts (AGSs)

Hydroxy-sulphates	
Melanterite	$FeSO_4 \cdot 7H_2O$
Römerite	$Fe^{2+}Fe_2^{3+}(SO_4)_4 \cdot 14H_2O$
Copiapite	$Fe^{2+}(Fe^{3+})_4(SO_4)_6(OH)_2 \cdot 20H_2O$
Rozenite	$FeSO_4 \cdot 4H_2O$
Jarosite family	
Potassium jarosite	$KFe_3(OH)_6(SO_4)_2$

Most AGSs have distinctive yellow, white or pale-green colours and form conspicuous encrustations on pyrite beds within mines. The kinetics of formation of these minerals is rapid (<1 hour) making them a relatively "instant" source of contamination (Bayless and Olyphant, 1993).

The formation of AGS releases less acidity than the complete oxidation of pyrite, shown in reaction (6).

$$3FeS_2 + {}^{23}/_2O_2 + 15H_2O \rightarrow Fe^{2+}Fe_2^{3+}(SO_4)_4 \cdot 14H_2O + 2SO_4^{2-} + 2H^+ \quad (7)$$

For example, the ratio of product protons to source pyrite for römerite is 0.6:1 compared to 4:1 for reaction (6). However, when an AGS encounters abundant water it dissolves rapidly releasing ferrous and ferric iron into solution. Ultimately the ferrous iron will oxidise to ferric, which will undergo hydrolysis to release the "missing" protons. Essentially AGSs store acidity in the unsaturated zone during dewatering. The stored acidity is rapidly dissolved during groundwater rebound after dewatering ceases. As a result of their high solubilities (4860g/l for melaterite) it is not unusual to find that AGS dissolution during mine flooding leads to a pH drop of 3 units and an increase in dissolved iron of two orders of magnitude (Younger, 2000; Bayless and Olyphant, 1993).

1.5 Mine closures

The closure of a significant number of mines is a relatively new phenomenon in South Africa. The increase in working costs and fixing of the gold price resulted in the closure of a number of gold mines during the 1960's. The onset of serious environmental problems has been delayed by the fact that most of the mines are interconnected as a result of the boundary pillars between them being mined out for safety reasons or to extract further gold. As a result the mines that remain operational have taken over the dewatering responsibilities (van Wyk and Munnik, 1998).

In contrast, the United Kingdom (UK) has sustained a major mining industry for many centuries and has historically been a major producer of tin, copper, lead, coal and oil shale. Mining activity was at its peak in the early 20th century and has steadily declined since then (Adams *et al.*, 2000). As a result the effect of mine closure on ground and surface waters has been extensively studied, particularly in the coalfields of England (Sherwood and Younger, 1994; Younger 1995, Younger, 1997; Younger and LaPierre, 2000) and Scotland (Wood *et al.*, 1999, Younger 2001).

1.5.1 Dewatering and groundwater rebound

The extraction of minerals by deep-level mining has resulted in major modifications of the hydrology of the host catchments. The sinking of shafts required for deep mining cut the water table and necessitates the continued dewatering of the mine to avoid flooding of the underground workings. This has been achieved by two methods. During the 18th and 19th centuries dewatering was almost exclusively achieved by the construction of drainage adits, often up to several kilometres long. More recently the majority of dewatering is achieved by pumping, either using shafts/boreholes outside the working area or by collecting water in the workings in sumps and then pumping it to the surface (Adams *et al.*, 2000; van Wyk and Munnik, 1998). The result of mine dewatering is a regional lowering of the water table. In the Durham coalfield a combined total of 105Ml d^{-1} of groundwater is pumped out by nine pumpstations, resulting in a drop in the water table of over 100m beneath an area in excess of 2000km^2 (Adams *et al.*, 2000). In South Africa mining occurs at far greater depths, up to 3500m in the Witwatersrand conglomerate reefs (Warwick *et al.*, 1987). As a result the effects of dewatering are likely to be exaggerated. For example the Grootvlei mine, which drains the Far East Rand Mining Basin (FERB), pumps 110Ml d^{-1} to the surface.

The dewatering of mines is a costly operation, typically accounting for up to 10% of the mine's operating cost (Scott, 1995). During the 1997/1998 financial year dewatering of the FERB cost in excess of R45 million rand. Approximately half of the cost was subsidised by the state, based on the mine's marginal status and the fact that it would have to close within five years as a result of the inflow of extraneous water (van Wyk and Munnik, 1998). Previous attempts to reduce the cost of dewatering in the West Rand goldfields proved unsuccessful. The gold bearing rocks of the Witwatersrand are covered throughout the area by the Proterozoic Malmani dolomite, which carries large quantities of water in secondary openings and zones of porous dolomite weathering products. This water enters the mine workings through natural fissures and shafts from the surface which pass through the dolomite. In the 1960's a number of these secondary compartments were pumped dry to prevent the stored water from entering the mine workings. The results were catastrophic, with compaction subsidences and sinkholes resulting in 30 deaths and millions of rands worth of damage to residential and industrial properties. As a consequence

mining companies in other dolomite compartments have been forced to maintain the water table by returning water pumped from the underground workings to the compartments via boreholes, thereby increasing costs (Warwick *et al.*, 1987).

The cost of dewatering is such that it is not a feasible long-term option, particularly once the mine stops generating income. Dewatering has ceased over large areas in the UK coalfields (Sherwood and Younger, 1994; Younger, 1997).

The major hydrological consequences of the cessation of dewatering are associated with the process of minewater rebound. During this process previously dewatered voids gradually fill with water until a surface overflow point is encountered (Younger, 1997). Rebound does not only result in a repositioning of the water table and surface discharges, but can also have a significant effect on the quality of the groundwater, with a marked deterioration often occurring. The reason for this can be explained by looking at the flow path of water through the mine workings. During dewatering, water passes through the mine along discrete flow-paths. These paths are well washed and as such any soluble minerals are flushed from them. When the workings are left to flood, all the void space comes into contact with water. Areas that have been unsaturated in the past are likely to be encrusted with acid generating salts, as described in the previous section. These rapidly dissolve and introduce both mineral and proton acidity, as well as sulphate salinity, into the water. The resulting low pH can be responsible for the mobilisation of further metals from carbonate minerals, such as siderite ($FeCO_3$) and rhodocrosite ($MnCO_3$). The simultaneous release of carbonate ions can result in some pH neutralisation, explaining why some minewaters have high metal loadings without being excessively acidic (Adams *et al.*, 2000). The discharge of ferruginous (iron loaded) minewaters can have a dramatic impact on receiving waters. The most obvious is the deposition of thick orange or red ochre (ferric hydroxide) on stream beds. They do not only have a visual impact, but smother the benthic fauna and flora and preclude photosynthesis, thus removing the foundation from the local food chain (Younger, 1997).

The process of minewater rebound can have a number of consequences aside from surface water pollution (Adams *et al.*, 2000). These include:

- localised flooding of agricultural and industrial land
- temporary loss of dilution of municipal or industrial effluents in the period between cessation of pumping and commencement of surface discharge
- pollution of overlying aquifers by upward migration of minewater
- temporarily accelerated mine gas emissions, especially in relation to dense gases such as carbon dioxide and radon which literally 'ride up' on the rising water table
- the increased risk of subsidence (sinkhole formation) as rising waters weaken support pillars

1.6 Longevity of minewater pollution

Once rebound has occurred in an abandoned mine and the resulting discharge contains unacceptable levels of contaminants, it is important to be able to predict for how long the contamination will persist and what changes in the composition of the discharge can be expected over time. This information is important when considering what type of treatment strategy to implement (Younger, 1998).

Prior to the mid 1980's the question of predicting the longevity of minewater pollution had been given little consideration. Frost (1979) derived a conceptual model based on studying data from the abandoned Mainsforth Colliery, where the water table had been held at a constant level by pumping. He showed that the iron content of the minewater at Mainsforth declined according to an approximately exponential law. Frost optimistically predicted that chronic pollution would persist for no longer than five years. A similar "rule of thumb" was proposed by Glover (1983) stating that the iron concentration in an uncontrolled discharge decreases by 50% in each subsequent period equal to that taken for the abandoned workings to fill with water after pumping ceased. The fact that several UK mines have discharged highly polluted waters for over 70 years clearly attests to the inadequacy of these models (Younger, 1997).

The optimistic projections of the persistence of minewater pollution implicitly suggests the following:

(i) pyrite oxidation stops after water table rebound
(ii) the residence time of polluted groundwaters in the abandoned mine is relatively short

The first assumption is only partially correct. While pyrite oxidation at depth in an abandoned mine will be negligible due to the absence of dissolved oxygen, significant amounts of acidity can be generated seasonally where the water table lies near the surface. As the water table fluctuates pyrite oxidation can occur in the unsaturated zone to form acid generating salts. These can dissolve when the water table rises, exposing fresh pyrite the next time the water table falls. In this manner it is theoretically possible for flooded mines to continue generating AMD until the pyrite source is exhausted, which may take centuries (Younger, 1997).

In practical terms it is necessary to distinguish between vestigial and juvenile acidity. Vestigial acidity arises from the dissolution of pyrite oxidation products, including AGS, during regional water table rebound. This represents a highly polluted "first flush". In contrast juvenile acidity arises primarily from pyrite oxidation as a result of seasonal water table fluctuations (Younger, 1997; Younger, 1998). In terms of these two components the longevity of minewater pollution at a given site is a function of (Younger, 1997; Wood *et al.*, 1999):

(i) the rate of depletion of vestigial acidity, which is primarily controlled by the following hydraulic factors:
    (a) the volume of the interconnected, flooded mine system where depletion will be fastest where systems are small and flowpaths short
    (b) the hydraulic connectivity and conductivity of the mine system, with depletion being more rapid where connectivity and conductivity are highest
    (c) the rate of recharge - hydrological residence times will be shorter where recharge is higher

(ii) the scope for generation of juvenile acidity, which:

(a) will be important where pyrite oxidation can occur above a fluctuating water table, but can also occur above or below the water table where other soluble iron minerals are present

(b) will diminish over time only if and when mineral sources are depleted by dissolution in the shallow workings, which may require centuries

(c) can be reduced as a result of carbonate dissolution after acid generation, if there are associated limestone horizons

(d) can be reduced by armouring of the pyrite surfaces by deposition of insoluble iron hydroxide which provides an oxygen barrier and prevents further pyrite oxidation.

1.7 Predicting changes in minewater quality during flushing

Younger (2000) analysed data from 81 abandoned deep coal mine discharges in the UK and used the information to derive practical prediction guidelines for pollution for the initial period following complete flooding of the mine voids. He identified two features of this period that are most critical to predict. They are:

- the peak contaminant concentrations following the dissolution of all AGS in the workings during flooding, and
- the duration of the main period of flushing, as contaminant concentrations decline to their long-term levels

Peak iron and sulphate concentrations in any mine system are clearly related to the availability of AGS in the mined strata. Data from the UK coalfields has suggested that total sulphur content is a good proxy measure for the availability of AGS in the worked seams and adjoining disturbed strata. Table 1.2 shows predictions for first approximation estimates of peak (immediately after mine flooding) and long-term (after complete flushing) iron concentrations from the data for 81 UK coalfield discharges.

Table 1.2: Estimates for peak and long-term iron concentrations based on total sulphur content of worked seams (after Younger, 2000).

Total S content (wt%)	Peak Fe conc. (mg/l)	Long-term Fe conc. (mg/l)
$S < 1$	0.15 ± 0.27	0.02 ± 0.76
$1 < S \leq 2$	98 ± 14	12 ± 8
$2 < S \leq 3$	267 ± 40	34 ± 22
$3 < S \leq 4$	873 ± 163	110 ± 78
$4 < S \leq 5$	1494 ± 248	190 ± 127

The duration of the first flush depends primarily on the volume of the mined system and the rate of recharge (Younger, 1997). The hydraulics of flushing are more complex and cannot be described by the above factors alone. Attempts to model discharge from the Wheal Jane tin mine in Cornwall, UK, using a simple "well-mixed reactor" model proved inadequate and significantly underestimated the duration. In a well-mixed batch reactor, flushing of conservative contaminants would take a certain time (t_f) defined by the ratio of the void volume (V_0) to the rate of discharge from the mine (Q). At steady state the discharge rate equals the recharge rate. This model predicted that the conservative contaminants would be flushed from the Wheal Jane mine within nine months, while in reality the first flush lasted 42 months (Younger, 1997; Younger 2000). The delay can be attributed to the tortuosity and heterogeneous permeability of the old mine workings. In natural hydrogeological systems these phenomena are explained using the blanket concept of dispersion (Younger, 2000).

The most common technique to model dispersion in groundwater bodies is the advection-dispersion equation. This equation, developed by Sauty (1980), applies to a simple one-dimensional flow system where contaminants are continuously injected at the upstream boundary and predicts breakthrough at the downstream end of the system, a distance L from the injection site. Younger (2000) modified the classic equation so that it can be used to model the displacement of contaminated groundwater from abandoned mines by fresh recharge. The modified solution can be written as:

$$C(t) = 0.5C_0\,[\mathrm{erfc}(\{L\text{-}v_a t_w\}/\{2(Dt_w)^{0.5}\}] + C_a \quad (8)$$

where:

$C(t)$ = concentration at the downstream boundary at time t (elapsed time since the mine began to overflow)

$C_0 = C_p - C_a$

C_p = peak iron concentration at the end of the flooding process

C_a = asymptotic iron concentration at the end of main flushing period

v_a = average groundwater flow velocity within the mine system (L/T)

t_w = "working time", the difference between the total length of the main flushing period (found on a trial and error basis) and the total number of days since overflow started

D = longitudinal dispersion coefficient ($L^2.T^{-1}$)

if molecular dispersion is neglected, then $D \approx \alpha_L v_a$, where α_L is the longitudinal dispersivity (L)

erfc = complementary error function (values for which are widely tabulated)

While this equation is based on sound physical principals it is still difficult to parameterise in a meaningful manner for real systems. An excellent match was obtained with the iron decay curve for the flushing of the Wheal Jane mine (Figure 1.1), but the values for L and α_L were arbitrarily selected and could not be measured in the field. Flushing equations such as equation (8) serve to illustrate the physics of flushing in abandoned deep mines, but are not recommended as practical tools for field use (Younger, 2000).

In terms of practical applications a simpler methodology is proposed, which is consistent with the concepts discussed above. This method is based on the prediction of Glover (1983), who hypothesised that the half-life for the decline in contaminant concentrations for an uncontrolled discharge from a given mine system will generally equal the total time period which was required for rebound. While there are few complete data sets available to test the validity of the

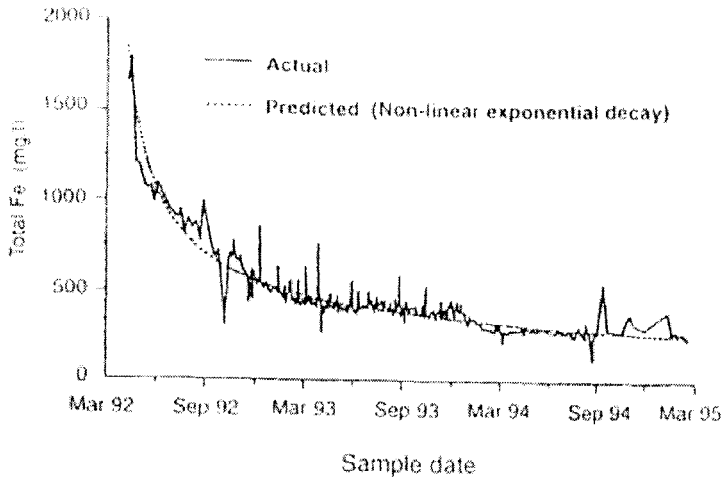

Figure 1.1: Observed decline in iron over time during flushing of Wheal Jane mine, Cornwall, compared with model output obtained using equation (8) (Younger, 2000)

hypothesis, those that have been tested have yielded estimates within the correct order of magnitude (Younger, 2000).

Glover's method fails to take juvenile acidity into account and predicts the decline in contaminant concentration will continue to negligible levels. In order to extend the analysis to cover contaminant reduction to an asymptotic level it is necessary to take into account the ratio between the initial and final concentrations during the flushing period (R_f). If the half-life of decay is taken to equal the time taken for the mine system to flood completely (t_r) as Glover (1983) proposed, then the time required for the flushing of conservative contaminants (t_f) can be calculated as:

$$t_f = (R_f/2)t_r \tag{9}$$

The data from the 81 studied sites generated a mean value for R_f of 7.9 which was valid at the 95% confidence level in relation to the source data. This allows equation (9) to be rewritten as follows:

$$t_f = (3.95 \pm 1.2)t_r \tag{10}$$

Modelling techniques have recently been developed for predicting the time required for groundwater rebound (t_r) in systems that have not yet been allowed to flood (Sherwood and Younger, 1997). Therefore equation (10) provides a simple basis for *a priori* estimates of the duration of future flushing periods for such systems to a first approximation (Younger, 2000).

Evidence from the analysis of the UK coalfield data indicates that the concentration of contaminants emerging from a recently flooded mine, during the first flush, can be expected to decrease in accordance with exponential decay laws to an asymptotic point which is likely to persist until the available reduced minerals have been exhausted. The long-term concentration of contaminants, after the first flush is completed, is generally one eighth of the peak value. Younger (2000) proposed a simple model (equation 10) to predict the duration of the first flush, but concedes that a significant amount of further research is necessary to be able to refine the proposed models and develop more elegant process-based models for groundwater quality evolution in flooded underground mines.

1.8 Classification of minewaters

The production of acid waters from pyrite oxidation is just the starting point in the evolution of many minewaters. Acidic minewaters may be subject to neutralisation by a number of mechanisms, all of which result in the release of additional ions into solution. Similarly, processes such as ion exchange and mixing with other subsurface waters (brines or more fresh groundwaters) can further neutralise the water and increase the complexity of the solution (Younger, 1998).

The characteristics of the minewaters have a profound effect on the design of subsequent treatment facilities and as such it is necessary to classify them into a number of major categories (Hedin *et al.*, 1994). Younger (1995) conducted a survey on minewaters flowing from abandoned coal workings in County Durham and used this information to evaluate a number of hydrochemical classification schemes which might be used to describe them.

1.8.1 Piper classification

This is a standard technique for evaluating groundwater resources. It has limited application to minewater examples as it neglects ion species which typically dominate minewaters (Fe, Mn) in favour of those that compose most natural groundwaters (Na, Ca, Mg, Cl, SO_4). Furthermore it is not designed to incorporate pH into the classification.

1.8.2 Glover classification

As this scheme was specifically designed for minewaters it does not suffer from the limitations of Piper-type approaches. Iron content and pH form the cornerstones of Glover's classification with valence state of iron in solution, the presence of suspended iron compounds and the degree of acidity being used to divide the waters into five categories (Glover, 1975). These are:

1. Acidic with low total Fe concentration
2. Acidic with high Fe^{3+} concentration
3. Acidic with high Fe^{2+} concentration
4. Neutral with high Fe^{2+} concentration
5. Suspended ferric hydroxide (combined with dissolved Fe^{2+} or Fe^{3+})

The practical implementation of this scheme is however not easy, based on the difficulty of obtaining reliable measures of Fe^{2+} and Fe^{3+}. In most cases it has proven more practical to measure total iron concentration and predict the speciation in solution by modelling. An additional shortcoming of this classification is that Glover (1975) derived the scheme by analysing waters from working mines, which differ markedly in terms of modal chemistry for waters discharging from abandoned mines. Furthermore, the focus on only pH and iron limits the geochemical utility of the scheme. By neglecting to take into account other major ions (ie those analysed in Piper diagrams) little information can be inferred regarding the genesis of the particular minewater and its treatability (Younger, 1995).

1.8.3 US Bureau of Mines classification

This scheme was designed by Hedin and co-workers (1994) and classifies minewaters according to their treatability by different passive treatment systems. The scheme allows the classification of waters based on two simple titrations, one for acidity and one for alkalinity. The results for both these titrations are represented as mg/l $CaCO_3$ equivalent. Alkalinity is the capacity of a solution to neutralise strong acid (usually H_2SO_4) to a specific end-point, usually pH 4.5. In most examples, where alkalinity is present, the dominant species is the bicarbonate (HCO_3^-) ion, although where the waters have been affected by bacterial action other species may be significant (HS^- and polythiones). Acidity is different from pH and represents the capacity of a solution to neutralise a strong base (usually NaOH) to a specific end-point, usually pH 8.3. As such acidity measures not only the hydrogen ion content (pH), but also the "mineral acidity" generated by the hydrolysis of metals such as iron (Fe), aluminium (Al) and manganese (Mn). These reactions generate protons, as shown in reaction (5) above. It is possible to calculate a theoretical mineral acidity if the concentration of the specific cations are known by using the equation below:

$$Acidity_{calc} = 50[(2Fe^{2+}/56) + (3Fe^{3+}/56) + (3Al/27) + (2Mn/55) + (1000(10^{-pH}))] \quad (11)$$

All metal values are in mg/l and acidity is calculated as mg/l $CaCO_3$ equivalents. Experimental results have shown that acidities calculated using this formula correlate well (within 10%) with corresponding titrated acidities (Hedin *et al.*, 1994). Acidity and alkalinity relate to different components of the water and are not mutually exclusive. It is possible for a water with a pH of 6 to contain significant amounts of bicarbonate alkalinity. Hedin *et al.* (1994) used the above definitions to classify minewaters into two groups:

1. Net alkaline minewaters (alkalinity > acidity)
2. Net acidic minewaters (acidity > alkalinity)

The scheme considers the relative importance of six major parameters, alkalinity, pH, Fe^{2+}, Fe^{3+}, Al and Mn, commonly occurring in minewaters and is useful in classifying the waters according

to their amenability to different treatment approaches. The only real shortcoming of this system of classification is that it does not consider the anion chemistry of the water. The relative concentrations of the major anions, chloride and sulphate, reveal important information regarding the genesis of the minewater (Younger, 1995).

1.8.4 Younger classification

Younger (1995) extended the classification of the US Bureau of Mines (Hedin *et al.*, 1994) by incorporating major anion species as follows:

1. As the units for alkalinity and acidity are the same, the net acidity or net alkalinity of a solution can be quantified by calculating the acidity or alkalinity as a percentage of the total $CaCO_3$ equivalent species (acidity + alkalinity).
2. The major anion species other than bicarbonate (sulphate and chloride) are clues to the genesis of a particular minewater. The processes which favour dominance of one over the other represent opposite ends of a hydrogeological spectrum ranging from undisturbed coal measures (high chloride from brines) to extensively mined coal measures in which pyrite oxidation dominates water quality evolution, leading to high sulphate concentrations. It is thus logical to plot the ratio of sulphate to chloride (% total milliequivalents) on a single axis.

The information allows the construction of a simple diagram (Figure 1.2) on which various fields have been defined by using information on minewaters of known origin. A diagram such as this makes basic geochemical process interpretations feasible. For example, a "classic" polluting mine drainage, having high sulphate and being net acidic, will plot close to the lower left field on the graph. Displacement of the plot position towards increased alkalinity and lower sulphate will be indicative of sulphate reduction (the desired process in anaerobic wetlands). An increase in alkalinity without a corresponding drop in sulphate levels would indicate alkalinity generation by carbonate dissolution (the desired process in anoxic limestone drains).

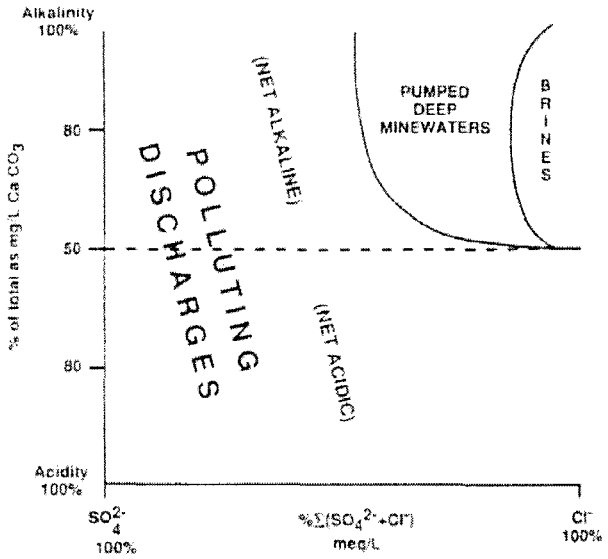

Figure 1.2: New classification scheme for minewaters: Fields in which minewaters of different origins and affinities plot (Younger, 1995)

Younger (1995) feels that this classification scheme has the potential to assist in identifying or documenting:

(i) the hydrological affinity of a given water type (brine, pumped hybrid water, polluting discharge)

(ii) hydrogeochemical processes occurring during transport through the subsurface

(iii) processes occurring during passive treatment of minewater discharges using constructed wetland technology

While this classification scheme was specifically designed using examples related to the coal mine discharges it is applicable to other types of mine drainages.

1.9 Treatment strategies

1.9.1 Chemical precipitation

Chemical treatment strategies for AMD remediation have two primary goals, the neutralisation of pH and the precipitation of heavy metals. The most commonly employed chemical treatment method is the addition of lime. The lime may be added in the unslaked, hydrated ($Ca(OH)_2$) or dolomitic ($CaMg(CO_3)_2$) form. Each form has associated advantages and disadvantages, for example hydrated lime reacts faster than the dolomitic form, but is almost three times as expensive and produces greater sludge volumes (Maree *et al.*, 1992).

All heavy metals encountered in AMD waters form complexes with hydroxide species. These complexes affect the solubility of the particular mineral. Considering the generic divalent metal ion (M^{2+}) it is clear that up to three hydroxide complexes can be formed (MOH^+, $M(OH)_2^0$ and $M(OH)_3^-$) depending on the pH. While the positive charged complex has meaning considering the aqueous phase alone, the remaining two only have significance in determining metal ion solubility (Loewenthal *et al.*, 2001). The two phase equilibrium diagram (Figure 1.3) for ferrous iron illustrates this phenomenon. This has implications for lime dosing, with a relatively specific amount needing to be added to achieve optimal metal removal. From figure 1.3 it is evident that optimal $Fe(OH)_2$ precipitation is only achieved in the region of pH 11 and that below pH 10 the Fe^{2+} and $Fe(OH)^+$ species dominate.

As ferrous iron is the dominant heavy metal in most AMD discharges and the efficient precipitation of $Fe(OH)_2$ requires a high pH, a modified process is most commonly employed. The high density sludge (HDS) process involves the initial oxidation of the ferrous iron to the ferric form at a high oxygen concentration and a relatively low pH. The ferric iron subsequently precipitates and settles (at pH 6) as amorphous ferric hydroxide which upon dehydration changes to FeOOH and Fe_2O_3 as the final products. The sludge is recycled and contacted with lime in order to induce crystallisation. This process has proven effective for iron removal, but has little capacity to remove heavy metals and salinity (Loewenthal *et al.*, 2001).

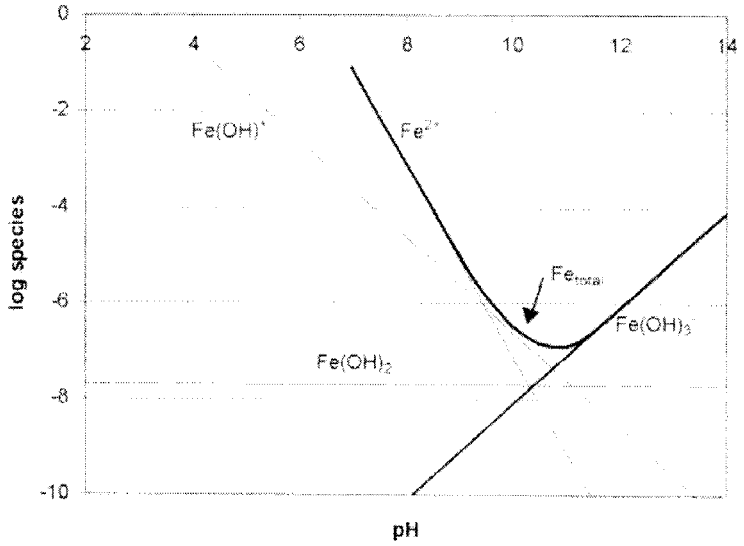

Figure 1.3: Aqueous and solid phase equilibrium for ferrous hydroxide at infinite dilution (Loewenthal *et al.*, 2001)

An alternative to the HDS process is a sequential process where neutralisation and the precipitation of some heavy metals as hydroxides is achieved by lime addition and ferrous iron is removed by sulphide addition. A range of sulphide salts has been utilised, but barium sulphide (BaS) is preferential as the barium will not persist in solution in the presence of sulphate ions. Therefore, the use of BaS can reduce the salinity of the AMD (Larson *et al.*, 1973). The precipitation of ferrous iron by sulphide addition is not without disadvantages, the main one being the formation of a colloidal precipitate that has poor settling characteristics. The potential of biologically generated hydrogen sulphide has also been investigated and will be discussed in more detail later.

Based on the shortcomings of the above processes a number of authors have proposed an alternative system, the Ferrite Process, which is capable of removing iron and heavy metals in a single process, without the necessity of further sludge treatment (Wang *et al.*, 1996; Barrado *et al.*, 1998; Loewenthal *et al.*, 2001). The term "ferrite" refers to magnetic oxides containing other metals in addition to iron. The general chemical formula of ferrites is MFe_2O_4, where M is any divalent ion with an unhydrated ion radius of between 0.6 an 1.0Å.

Ferrite is formed via partial oxidation of ferrous species at pH values of greater than 7. The reaction has been shown to proceed through two pathways, depending on the pH and rates of oxidation. At pH values of 7-10 and relatively slow oxidation rates, ferrites form through the Green Rust (GR) path. At pH values of 10.5 and greater they form from the FeOOH phase. Green rusts are unstable green-blue compounds consisting of a mixture of ferrous and ferric ions accompanied by Cl^-, SO_4^{2-} or CO_3^{2-} and OH^- ions. Ferrite formation through the GR pathway at pH<10 has been shown to result in relatively high residual iron and heavy metal concentrations in solution, as well as inferior sludge settling properties (Perez *et al.*, 1998; Loewenthal *et al.*, 2001).

Ferrite formation at pH>10 showed excellent removal efficiencies (>99%) and good sludge characteristics. Barrado *et al.* (1998) proposed the following reactions for ferrite formation from ferrous at pH>10.5:

1) In the absence of heavy metals and controlled oxidation rate

$$3FeSO_4 + 6NaOH + 0.5O_2 \rightarrow Fe_3O_4 + 3Na_2SO_4 + 3H_2O \quad (12)$$

2) In the presence of heavy metals and controlled oxidation rate

$$xM^{+n} + 3FeSO_4 + 6NaOH + 0.5O_2 \rightarrow M_xFe_{3-x}O_4 + 3Na_2SO_4 + 3H_2O + xFe^{+n} \quad (13)$$

Fe^{+n} represents the total concentration of iron whose precipitation as ferrite is impeded by the other metal cations present in the water. If the pH is maintained at greater than 10 these ferrous and ferric ions will react again to form magnetite (Fe_3O_4).

The ferrite process is most efficient where the iron to heavy metals ratio is 10-20:1. To achieve this, $FeSO_4$ is added to the solution. The pH is raised to over 10 at 65°C and oxygen is introduced to effect the partial oxidation of ferrous iron. The resulting precipitates are stable and can be easily recovered by magnetic filtration. In addition, as the heavy metals are incorporated into the lattice structure they are not susceptible to leaching from the sludge upon ageing. The major disadvantage of the standard ferrite process is the high temperature, which introduces prohibitive energy costs. The major focus of research in this field is on developing an efficient ambient temperature process (Loewenthal *et al.*, 2001).

1.9.2 Adsorption and ion exchange

One of the major drawbacks of treatment systems based on chemical precipitation is their poor efficiency when treating effluents with low metal concentrations. The removal of inorganic pollutants from dilute aqueous media can be achieved by adsorption and ion exchange mechanisms. Adsorption refers to the binding of charged species in solution to reactive groups, of opposite charge, on a solid support. Much of the research in recent years has focussed on the use of cells or sorbents derived from biological material (Kratochvil and Volesky, 1998). A wide range of biosorbents have been tested, including yeast (Brady and Duncan, 1994; Ashkenazy *et al.*, 1997), fungi (Tobin *et al.*, 1990; 1993), algae (Ting *et al.*, 1989; Holan *et al.*, 1993; Leusch and Volesky, 1995; Kratochvil and Volesky, 1998) and the aquatic fern *Azolla* (Zhao and Duncan, 1998; Sanyahumbi *et al.*, 1998). The most important metal binding sites on the surface of biological material are the carboxyl, phosphoryl, amino and thiol groups.

Ion exchange refers to the replacement of toxic heavy metal ions in solution by more benign counter-ions that balance the surface charge of the solid exchanger. The ion exchange resins are derived from both natural (zeolite) and synthetic (synthetic polymers) sources and can be manufactured to contain single or multiple functional groups, depending on the application (Ahmed *et al.*, 1998; Chiarle *et al.*, 2000).

Both biosorbents and ion exchange resins have been successfully utilised in low volume effluent treatment systems. The most common reactor configurations are the packed and fluidised bed reactors, as well as a number of column designs. Their application to high volume effluents such as AMD are limited by reactor design and flow dynamics, with a typical unit containing between 20 and 100kg of biomass (Gadd and White, 1993).

1.9.3 Membrane technologies

A number of membrane based technologies have been developed for the treatment of wastewaters polluted with heavy metals. Both electrodialysis and tubular reverse osmosis reactors have demonstrated the ability to desalinate non-scaling mine waters, with the former

producing water fit for human consumption. The majority of AMD waters contain high concentrations of sodium and sulphate, leading to scale formation on the membrane surface. There have been some advances in the field with the development of the SPARRO (Slurry Precipitation and Recycle Reverse Osmosis) process, which partially overcomes the scaling problem and reduces operation costs (Juby *et al.*, 1996). The construction and operation costs of membrane reactors, coupled with the volume of polluted water discharges from South African mines limit the large scale application of this technology.

1.9.4 Active biological treatment systems

Active biological systems for the treatment of AMD are primarily dependent on the action of sulphate reducing bacteria (SRB). The bacteria are able to utilise sulphate as the terminal electron acceptor to oxidise organic carbon, producing bicarbonate and hydrogen sulphide as by-products. The biochemical pathways involved are complex and will be discussed in greater detail in the relevant chapter of this thesis. A simplified overview of the reaction is shown below:

$$2CH_2O + SO_4^{2-} \rightarrow 2HCO_3^- + H_2S \qquad (14)$$

The form of the alkalinity and the sulphide will depend on the pH and aqueous chemistry of the system. The sulphide reacts with metals in solution to form insoluble metal sulphides and the bicarbonate alkalinity helps to raise the pH of the AMD.

The SRB are grown in purpose built bioreactors under controlled conditions. A number of reactor designs have been tested, including anaerobic filters (Chian and De Walle, 1983), packed bed anaerobic reactors (Maree *et al.*, 1987), mixed systems (Maree and Hill, 1989), fluidised bed systems (van Houten *et al.*, 1994), sequencing batch reactors (Herrera *et al.*, 1991) and upflow anaerobic sludge blanket systems (Barnes *et al.*, 1991). A wide range of simple and complex organic carbon sources have been investigated.

There have been few successful industrial scale applications of this technology, although Shell Research Ltd successfully ran a pilot plant at the Budelco BV zinc refinery in the Netherlands,

which was later scaled up to a system capable of treating 7Ml day^{-1}. The system uses a selected, but undefined consortium of sulphate reducing bacteria, with ethanol as the carbon source. The final concentration of all heavy metals was reduced to the ppb range and the sulphate concentration was reduced by over 80% (Barnes *et al.*, 1991).

1.9.5 Passive treatment systems

Natural processes commonly ameliorate mine drainage pollution. As contaminated mine drainage flows through receiving systems (streams, rivers and lakes) its toxicity decreases naturally as a result of biological and chemical reactions as well as by dilution with uncontaminated waters. The low pH typical of many mine drainages increases as the water mixes with less acidic water or through dissolution of carbonate minerals. Metals contained in the mine water then precipitate as oxides or hydroxides under the aerobic conditions found in most surface waters. Ferric iron, aluminium and to a lesser extent manganese are the first metals to precipitate out (Hedin *et al.*, 1994).

The passive treatment of mine water developed from pilot scale plants to full scale field implementation during the 1980's. Passive treatment technologies take advantage of natural chemical and biological processes. Ideally these systems require no addition of chemicals and little or no operation and maintenance inputs. Passive systems depend on processes that are slower than those of active treatments and thus require longer retention times and larger areas to achieve similar results (Hedin *et al.*, 1994).

The goal of passive systems is to enhance natural processes so that they occur within the treatment area and not in the receiving water body. There are two factors which determine if this can be achieved, the kinetics of the contaminant removal processes and the retention time within the system. The retention time for a particular site is often determined by the available land area. However, the kinetics of contaminant removal processes can often be affected by manipulating the environmental conditions that exist within the passive treatment system. Efficient manipulation of contaminant removal processes requires that the nature of the rate-limiting aspects of each removal process be understood (Hedin *et al.*, 1994). The development of passive

systems from an experimental concept to full scale field application occurred during the 1990's. While over 200 wetlands have been operating in the Appalachia region of the US, their application has been limited to acid waters with low metal content (Gazea *et al.*, 1996).

1.9.5.1 History of passive treatment

The interest in passive systems was sparked by research in the late 1980's which indicated that natural *Sphagnum* wetlands improved the quality of mine drainage without incurring any obvious ecological damage (Wieder and Lang, 1992). A number of experimental wetlands were constructed to mimic the *Sphagnum* moss wetlands. However, *Sphagnum* moss was not readily available, proved difficult to transplant, and had the tendency to accumulate metals to toxic levels within several months (Spratt and Wieder, 1988). Despite these initial setbacks research continued and eventually a design evolved that proved tolerant to years of exposure to contaminated mine drainage and was effective at lowering the concentrations of dissolved metals. They typically consisted of a series of small wetlands (<1 ha) vegetated with cattails (*Typha latifolia*) (Wieder, 1989).

During the development of the most recently applied passive treatment schemes the importance of anaerobic processes in metal removal was identified. In such systems a complex ecosystem is not needed and the treatment cells operate effectively without plants. Pretreatment systems have also been developed which involve contacting the acidic waters with limestone in an anoxic environment before it enters a settling pond or wetland system (Gazea *et al.*, 1996).

1.9.5.2 Mechanisms for contaminant removal

A number of physical, chemical and biological processes are known to occur within passive treatment systems to reduce metal concentrations and neutralise the acidity of the influent water. The relative importance of the various processes is difficult to assess due to a lack of accurate quantitative data (Gazea *et al.*, 1996).

The simplest mechanism encountered in a passive wetland system is the dilution of contaminants by inflows of uncontaminated water. Large volume inflows may cause significant changes in the water chemistry that might be mistakenly attributed to biological or chemical processes (Hedin *et al.*, 1994).

After accounting for dilution there are four major processes which can occur in passive systems to reduce the acidity and lower the concentration of metal ions in solution. These are:

- oxidation and hydrolysis
- metal removal by plants, algae and organic substances
- reduction
- limestone addition

1.9.5.3 Oxidation and hydrolysis

The mechanism of oxidation of ferrous to ferric iron has been previously covered. This process occurs abiotically, but can also be catalysed by bacteria. The kinetics of both mechanisms are pH dependent. At pH values of 5 and above the kinetics of oxidation can be described by the following equation:

$$-(d[Fe^{2+}]/dt) = k_1[Fe^{2+}][OH^-]^2{}_pO_2 \quad (15)$$

where $k_1 = 8.0 \times 10^{13}$ min^{-1} atm^{-1} mol^{-2} l^2

${}_pO_2$ = partial pressure of oxygen

From the $[OH^-]^2$ it is clear that for each unit the pH is raised, above 5, the reaction rate increases 100-fold. Under these conditions the most important role of the constructed wetland is to provide a retention time that is sufficient for the dissolved iron to oxidise and precipitate (Gazea *et al.*, 1996).

At lower pHs (pH < 3.5) the kinetics of abiotic oxidation is described by the following equation:

$$-(d[Fe^{2+}]/dt) = k_2[Fe^{2+}]_P O_2 \quad (16)$$

where $k_2 = 1.0 \times 10^{-7}$ min^{-1} atm^{-1}

Under these conditions the oxidation is clearly slow and the contribution of iron oxidising bacteria becomes important. Species such as *Acidothiobaccillus* and *Leptobacillus ferrooxidans* have a pH optimum of between pH 1.5-3.5. They are able to increase the ferrous iron oxidation rate by several orders of magnitude. In experimental aerobic wetland systems the numbers of iron oxidising bacteria has been positively correlated with iron oxidation and removal (Gazea *et al.*, 1996).

As ferrous iron is oxidised to ferric, it is subjected to hydrolysis that results in the rapid precipitation of ferric hydroxide and the release of proton acidity, the mechanisms of which have been discussed previously. Based on the solubility of ferric hydroxide ($K_{sp} = 6.0 \times 10^{-38}$) it is clear that under equilibrium conditions negligible concentrations of dissolved ferric iron exist at pH values above 3. Natural or constructed aerobic wetlands that receive neutral iron containing waters typically discharge acid water (pH 2-3) as a result of iron oxidation and hydrolysis (Gazea *et al.*, 1996).

Manganese is the second important component of most acid mine drainages that can be removed by oxidation and hydrolysis. Typically manganese is discharged to the surface as the Mn^{2+} ion and for efficient hydroxide precipitation to occur requires the oxidation of the Mn^{2+} to a higher oxidation state. The exact mechanisms occurring in aerobic wetlands have not been fully elucidated, but it has been suggested that Mn^{2+} is oxidised to either the trivalent or tetravalent form, which then precipitates as MnOOH (Hedin *et al.*, 1994). The proposed reaction is shown below:

$$4Mn^{2+} + O_2 + 6H_2O \rightarrow 4MnOOH + 8H^+ \quad (17)$$

Over time the MnOOH is likely to oxidise to the thermodynamically more stable MnO_2. As with iron, the oxidation of manganese is strongly dependent on pH and occurs very slowly at pH values below 8. The process may be accelerated by the action of manganese oxidising bacteria, which are most readily found at pHs of 7 and above (Gazea *et al.*, 1996). The bacteria oxidise Mn^{2+} to MnOOH or the manganate ion (Mn^{4+}).

In alkaline environments manganese can also precipitate in the carbonate form. In the presence of atmospheric oxygen the carbonate may oxidise further to the more stable oxide as shown below:

$$Mn^{2+} + HCO_3^- \rightarrow MnCO_3 + H^+ \quad (18)$$

$$2MnCO_3 + O_2 \rightarrow 2MnO_2 + 2CO_2 \quad (19)$$

Data collected from wetland applications has shown that when a minewater contaminated with both iron and manganese passed through the system the manganese removal was far less effective than the iron and occurred sequentially, not simultaneously (Hedin *et al.*, 1994). There are two main factors which contribute to this phenomenon. Both mechanisms are pH dependent, but the oxidation of iron occurs more readily and is optimal at lower pH values. The oxidation and hydrolysis of iron releases further proton acidity which makes the conditions for manganese oxidation even less favourable. The second factor is the reduction of oxidised manganese by ferrous iron:

$$MnOOH + Fe^{2+} \rightarrow FeOOH + Mn^{2+} \quad (20)$$

The net result is that manganese removal in passive aerobic systems is a slow and inefficient process, even in situations where ferrous iron concentrations are low (Gazea *et al.*, 1996).

1.9.5.4 Metal removal by plants and algae

Emergent vegetation is one of the components of aerobic wetland systems. While accumulation of metals in the plant tissues plays only a minor role in metal removal the presence of plants has

a number of associated benefits. Plants are able to diffuse oxygen from their roots, generating localised oxidising zones within the substrate which promote metal removal by oxidation.

Decaying plant material is an important component of a number of other processes which occur in the wetland. It is used as an organic carbon source for sulphate reducing bacteria and contains carboxylic and phenolic acids which are able to complex metal ions from solution. In addition, the presence of emergent vegetation enhances the aesthetics of the treatment system and reduces erosion and dispersal of metal precipitates by wind during dry periods (Gazea *et al.*, 1996).

A considerable amount of research has been conducted on the ability of algae to reduce the concentration of metals in solution. This is achieved by adsorption onto charged functional groups on the cell surface and by accumulation of the metal inside the cell. The mechanisms involved will be discussed in greater detail in chapter three.

1.9.5.5 Reduction processes

Bacterial sulphate reduction under anaerobic conditions can be an important factor in determining the final water quality discharged from the passive treatment system. Sulphate reduction occurs in the organic substrate layer, where bacteria such as members of the *Desulfovibrio* species use sulphate to oxidise organic matter and release bicarbonate and hydrogen sulphide (Kalin *et al.*, 1991). The range of species involved, carbon sources utilised and biochemical mechanisms will be discussed in greater detail in chapter five.

Bacterial sulphate reduction is limited to certain environmental conditions. The process is curtailed at pH values below 4 and in the presence of oxidising agents such as O_2, Fe^{3+} and Mn^{4+}. Typically the conditions which favour bacterial sulphate reduction can be maintained in an anoxic wetland environment (Gazea *et al.*, 1996).

The hydrogen sulphide reacts with some dissolved metal ions to form insoluble metal sulphides, which may then precipitate. The removal of dissolved metals in the sulphide form depends on the pH, the solubility of the specific metal sulphide and the concentration of reactants.

While low pH values inhibit the growth and activity of SRB, their activity results in an increase in alkalinity and pH in the surrounding micro-environment. As a result they have been found to be active in sediments below extremely acidic waters (Herlihy *et al.*, 1987). They are also tolerant of relatively high concentrations of toxic heavy metals, with exposure to zinc, lead and nickel at concentrations of 60mg/l not resulting in significant inhibition.

While sulphate reduction is the most important source of alkalinity in recently commissioned wetlands, there is evidence to suggest that in more established wetlands the reduction of ferric iron to ferrous iron is the major source of alkalinity (Vile and Wieder, 1993).

1.9.5.6 Limestone addition

The addition of limestone may be employed where the mine drainage has a particularly high acidity. The limestone dissolves to produce calcium and bicarbonate alkalinity, which neutralises acidity and buffers the pH. The solubility of limestone depends on pH, temperature and carbon dioxide concentration. When acid water, pH < 6.4, contacts limestone, the limestone reacts according to the equation:

$$CaCO_3 + 2H^+ \rightarrow Ca^{2+} + H_2CO_3^* \qquad (21)$$

Dissolved carbon dioxide, conventionally noted as $H_2CO_3^*$, is a weak acid and continues to react with limestone, producing calcium and bicarbonate alkalinity which is available for acid neutralisation reactions (Gazea *et al.*, 1996).

In practice, the effectiveness of this process is reduced where the influent water is high in ferrous iron and contacts limestone in an oxidising environment. The resulting formation of ferric hydroxide precipitates leads to coating of the limestone surface and reduces dissolution to almost nil. In anoxic environments, where the iron is maintained in the ferrous form and no precipitate forms at pH < 5.5, limestone addition can be an effective method of reducing acidity (Gazea *et al.*, 1996).

1.9.6 Types of passive treatment systems

There are three principal types of passive technologies developed for the treatment of mine discharges. They are:

1. aerobic wetland systems
2. anaerobic organic substrate systems
3. anoxic limestone drains

1.9.6.1 Aerobic wetland systems

Aerobic wetlands have been effectively used to treat net alkaline waters, which typically contain enough alkalinity to buffer the acidity produced by metal hydrolysis reactions. The system relies on oxidation reactions and metals precipitate primarily as hydroxides, oxyhydroxides and oxides. The aerobic wetland cells are designed to retard the flow of water long enough for metal oxidation and hydrolysis to occur and for the resulting precipitates to settle. The hydrolysis process releases proton acidity, which retards the oxidation rate. In some cases an amount of crushed limestone is initially added to mediate this effect. Ideally the pH of the wetland is maintained at between 5.5 and 6.5, which enhances the precipitation of iron, manganese and aluminium, the primary constituents of net alkaline minewaters (Younger, 1995; Gazea *et al.*, 1996).

The design is similar to that of a "natural" wetland and consists of basins or channels with a relatively impermeable bottom layer to prevent seepage. This is covered with soil or a similar medium suitable for supporting vegetation. The efficiency of aerobic wetlands for removing iron is limited by dissolved oxygen concentrations. To enhance efficiency, wetlands are often designed with features to enhance aeration, such as steps or waterfalls, followed by quiescent areas. Each aeration step provides sufficient oxygen to remove 50mg/l Fe^{2+}, so where iron concentrations are higher, a series of aeration steps needs to be incorporated (Hedin *et al.*, 1994). The water depth is typically shallow (10-50cm) to further enhance aeration (Younger, 1995), but not consistent throughout the wetland, with deeper (1-2m) areas providing regions for sludge

accumulation (Hedin *et al.*, 1994). The length to width ratio is typically over 10 to ensure sufficient residence time. The presence of vegetation helps to regulate the water flow, introduces additional oxygen into the water and sediment, assists in the removal of iron flocs and reduces the erosion potential of the precipitates (Gazea *et al.*, 1996).

1.9.6.2 Anaerobic (compost) wetlands

The compost wetland is one of the systems available for the treatment of net acidic mine waters. In these cases the system is required to generate sufficient alkalinity to neutralise excess acidity. Compost wetlands generate alkalinity through a combination of bacterial activity and limestone dissolution. The SRB require a rich organic substrate in which anaerobic conditions will develop (Hedin *et al.*, 1994; Gazea *et al.*, 1996).

A wide range of organic substrates have been tested and are typically low-cost natural products and wastes, such as horse and cow manure, spent mushroom compost, hay bales, peat, wood chips or sawdust. Some substrates, such as mushroom compost contain limestone, while those that don't are usually supplemented with limestone. The substrate is placed in a non-compacted layer, typically 30-45cm thick A compost loading of 250-300kg.m^{-2} is usually employed (Hedin *et al.*, 1994). The bacteria reduce sulphate to assist in the oxidation of labile organic carbon. The sulphide which is released reacts with metal ions in solution and the bicarbonate assists in neutralising excess acidity. As the bacterial metabolism is influenced by temperature, the efficiency of the system is affected by seasonal fluctuations in temperature. The loss of efficiency in winter may be reduced by limestone addition and by directing the water flow through the compost layer, rather than over the surface (Younger, 1995; Gazea *et al.*, 1996).

1.9.6.3 Anoxic limestone drains (ALDs)

Anoxic limestone drains (ALDs) have become an increasingly popular passive "pre-treatment" technology (Younger, 1995). Essentially these consist of trenches filled with limestone gravel or cobbles (10cm diameter) that are overlayed with a plastic sheet and a layer of clay to exclude oxygen. They are used to raise the pH of net acidic waters by carbonate dissolution prior to metal and/or acidity removal in wetlands (Younger, 1995; Gazea *et al.*, 1996).

ALDs are operated under saturated conditions to further minimise the infiltration of atmospheric oxygen. Their dimensions vary considerably, with most of the early systems consisting of long, narrow (0.6-1m wide) trenches (Hedin *et al.*, 1994), although more recently systems have been installed that are 10-20m wide, without a significant reduction in efficiency.

The mass of limestone required to neutralise a certain discharge for a specific period of time can be calculated based on the minewater flow rate and the alkalinity-generating performance of the ALD. Research has shown that a 14 hour contact time between the minewater and the limestone is required to achieve a maximum concentration of alkalinity (275-300mg/l). To achieve a contact time of 14 hour approximately 3000kg of limestone is required for each litre per minute of minewater flow. In the above situation the limestone would dissolve at a rate of 160kg per year for each litre per minute of minewater flow (Hedin *et al.*, 1994).

The major problem associated with the use of ALDs is the armouring of the limestone surfaces by iron and aluminium precipitates. If the influent minewater contains over 2mg/l of Fe^{3+} or Al^{3+}, or has a high dissolved oxygen content the efficiency of the ALD system decreases rapidly as a result of armouring, although this is not common in discharges originating from deep level mining, where the vast majority of Fe and Al is in the divalent state (Hedin *et al.*, 1994; Gazea *et al.*, 1996).

The precipitation of metals should ideally not occur within the ALD, so its primary function is to add alkalinity to the water. Therefore they need to be utilised in conjunction with other passive treatment components.

1.9.7 Wetland size

The sizing design for wetlands has been developed by Hedin *et al.* (1994) and is based on two key principals:

(i) The pollutant loading which the wetland will receive is calculated as:

$$\text{Loading (g/day)} = Q \text{ (l/min)} \times \text{concentration (mg/l)} \times 1.44 \quad (22)$$

where Q is the peak flow rate

Where the water is net alkaline, iron is typically the main polluting component. Iron removal occurs most effectively by oxidation processes in aerobic wetlands. However, where waters are net acidic, iron removal must be accompanied by the neutralisation of total acidity (proton and mineral) in order to generate a satisfactory final effluent. This is best achieved using an anaerobic wetland. Based on this, loadings are determined with reference to iron alone in the case of net alkaline waters and total acidity loadings where net acid waters are to be treated (Hedin *et al.*, 1994; Younger, 1995).

(ii) The minimum size of a constructed wetland is determined by dividing the appropriate loading by an empirical removal rate (RR), which has been determined by the US Bureau of Mines based on existing systems. That is:

$$\text{Wetland size } (m^2) = \text{Loading (g/d)} / \text{RR } (g/d/m^2) \quad (23)$$

Hedin *et al.* (1994) recommended two distinct suites of RR values based on the legal conditions relating to the remediation of the site. Where strict compliance with discharge standards is required a "conservative criterion" (CC) must be used. In this situation a removal rate of 10g of iron per m^2 d^{-1} should be assumed when designing aerobic wetlands receiving net alkaline waters and an acidity removal rate of 3.5g total acidity per m^2 d^{-1} when designing an anaerobic wetland to treat net acidic discharges. The use of these strict compliance criteria will yield large wetland areas and as such will only be popular where legal obligations exist. In many cases the pollution

is associated with long abandoned mines, where liability cannot be traced to an existing company. In these cases application of the CC may prove too costly so a second set of RR values, based on "reasonable improvement criteria" (RIC) has been proposed. The RR values are 20 for aerobic wetlands and 7 for anaerobic wetlands, resulting in smaller, less expensive wetlands (Hedin *et al.*, 1994; Younger, 1995).

1.9.8 Integrated biological treatment systems

Both active and passive biological systems have been used for the treatment of acid mine drainage, but there are serious constraints to their widespread implementation, particularly in SA. The land area necessary to treat high volume AMD discharges has restricted the use of passive systems, particularly as the affected areas are typically surrounded by industrial development. The three major factors constraining the active biological treatment approach are the reactor configuration used, the cost of construction and the cost and availability of the carbon source and the electron donor for the microbial reduction processes (Rose *et al.*, 1998).

Research at Rhodes University has focused on the utilisation of cheap or waste carbon sources for sulphate reduction and the integration of SRB and algal based technologies for AMD treatment (Rose *et al.*, 1998; Boshoff, 1999; van Hille *et al.*, 1999). Algal waste stabilisation pond (WSP) technology has been developed over the past 40 years (Mara *et al.*, 1996). While WSPs have been used to treat a diverse range of effluents little attention has focused on their potential to treat AMD.

Rose *et al.* (1998) reported on the treatment of tannery effluent in an Algal Integrated Ponding System (AIPS), similar to the type developed by Oswald (1991). The system consisted of a facultative pond, containing both an anaerobic and an aerobic component. Efficient sulphate reduction and metal precipitation was observed in the anaerobic compartment, while the aerobic cap was responsible for the re-oxidation of excess sulphide, which eliminated potential odour and toxicity concerns. This work led to the consideration of algal ponding as a possible system for the treatment of AMD.

Boshoff (1999) developed an integrated biological system for the treatment of acid mine drainage, utilising tannery effluent or primary sewage sludge as the carbon source for sulphate reduction.

1.10 General research hypothesis

The mining industry has been a cornerstone of the South African economy for over a century. The abandonment of mines due to ore depletion and economic conditions has created a serious environmental problem that is likely to intensify in the near future and persist for several centuries.

While chemical treatment strategies are being successfully employed for the remediation of acid mine drainage, they are expensive and therefore not a feasible long-term strategy. Based on the predicted volume of the discharges and the level of contamination the land area required for complete treatment by passive biological systems would be prohibitive. In addition, passive systems do not allow flexibility in terms of operational control.

The reactive alkaline species, sulphide, hydroxide, carbonate and bicarbonate, that are used to drive precipitation in chemical treatment systems can be generated biologically by the action of sulphate reducing bacteria and algae. The bacteria are able to utilise sulphate and a carbon source to generate sulphide and bicarbonate, which in turn can be used as a source of carbon for algal photosynthesis. The algae split the bicarbonate into carbon dioxide, which is accumulated, and a hydroxide ion which is released into the surrounding medium. The kinetics of the biological reactions are such that the reactive alkaline species can be generated at a suitable rate to drive an effective treatment process.

Such an integrated biological treatment system, based on the biological generation of reactive alkaline species, offers a number of potential advantages over conventional methodologies. The systems depend on the same naturally occurring biological and geochemical reactions as passive systems, but the compartmentalisation of different components allows for a greater degree of optimisation and finer control. This will result in reduced land usage and an increased potential to deal with fluctuations in discharge volume and quality. The reactor systems described in this

study are cheaper to construct and require less inputs than those employed in other active biological systems.

If correctly implemented, an integrated biological treatment system based on biogenic alkalinity offers the potential for a low-cost, sustainable solution to the problem of long-term discharge of acid and metal contaminated water from abandoned mines, rock piles and tailings.

CHAPTER 2. THE EAST RAND: A CASE STUDY FOR MODELLING AND RISK ASSESSMENT

2.1 Introduction

This chapter serves to put the problem of acid mine drainage in a South African context and highlight the current inadequacies in terms of predictive modelling and the application of remediation systems. The East Rand region was chosen to illustrate this as it represents the most immediate threat from a high volume, uncontrolled AMD discharge. While the coal mining industry has been responsible for some AMD pollution, this has been localised and on a relatively small scale. Of the gold mining regions in South Africa the East Rand is the closest to exhausting its reserves, with active mining expected to cease within the next five years.

2.2 Description of the investigation area

The study area is referred to as the East Rand and covers an area of 768km^2. The area includes all or portions of the municipal districts of Boksburg, Brakpan, Benoni, Springs, Nigel and Heidelberg. The mined basin is geographically and geohydrologically distinct from the other mined basins on the Witwatersrand, South Africa.

There are two main watercourses draining the area, the Blesbok Spruit, which drains the northern and eastern regions and the Riet Spruit, which drains the central and western parts. The Blesbok Spruit catchment covers 1427km^2, almost double that of the Riet Spruit. Both streams form part of the Vaal River Barrage catchment, which is responsible for providing water to the Gauteng region. Both streams have historically had intermittent flow, but the disposal of municipal and industrial effluent into them have resulted in a more constant flow pattern (Scott, 1995).

2.2.1 Geology

A generalised lithostratigraphic section giving the geological succession to be expected in this area is shown in figure 2.1. The average thickness of the main lithologies and economic horizons is indicated.

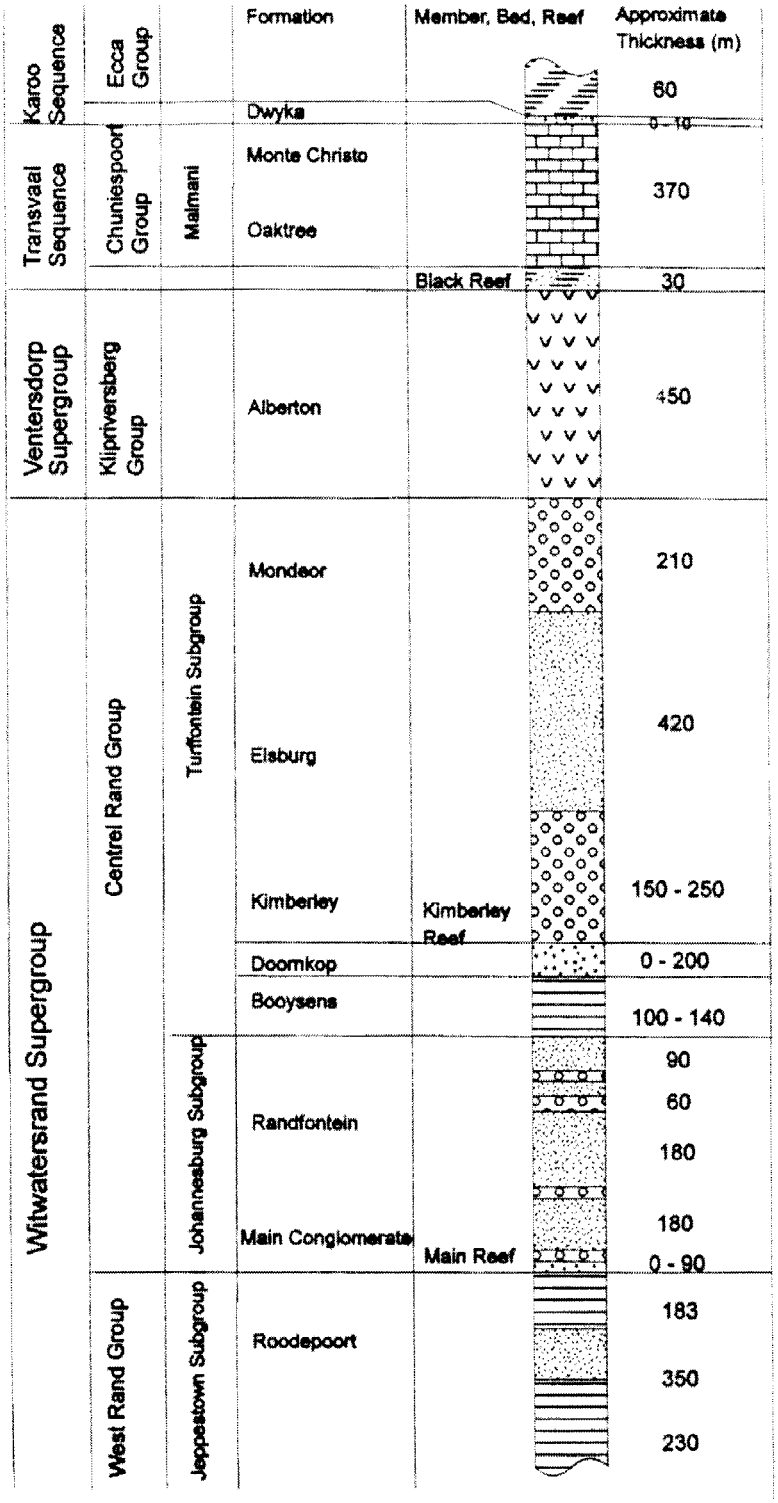

Figure 2.1: Lithostratigraphic section of the East Rand geology (after Scott, 1995)

The East Rand Basin has been described as a relatively shallow, lagoon-like extension of the main Witwatersrand Supergroup Basin. The sediments making up the basin lie on pre Witwatersrand basement rocks and have been gently folded (Wagener, 1972).

In the western portion of the East Rand the Witwatersrand Supergroup sediments are either exposed or overlain by Ventersdorp Supergroup and lower units of the Transvaal Supergroup, with some remnants of a Karoo sill. In the central portion of the area Witwatersrand Supergroup sediments are overlain by Karoo Sequence. In the north-eastern and eastern sections the Witwatersrand Supergroup sediments are overlain by Black Reef and dolomites, which are predominantly covered by Karoo.

2.2.2 Groundwater

There are two distinct dolomite aquifers in the region. The first occurs in the northern part of the area and overlies the Witwatersrand sediments. It is up to 200m thick. A prominent set of sills occurs in this dolomite below 60m and is referred to as the Green Sill. They have resulted in the development of a perched water table, characterised by relatively shallow water levels. Major fissures occur from the dolomites into the mine workings. These are more significant in the shallower Black Reef workings, since much of the off reef development is in the dolomite (Scott, 1995).

The second dolomite aquifer occurs in the south-western portion of the area. It overlies the Ventersdorp supergroup rocks, which form a hydraulic barrier between it and the Witwatersrand sediments. As a result it plays little part in the inflows into the mines and as such will not be considered further.

2.3 Mining history

Both coal and gold have been mined in the region, although the last coal mines were abandoned in 1953. The coal deposits occurred in the Karoo Sequence and while these have been extensively worked out, the workings were all relatively shallow, with a maximum depth of 50m.

The shallow nature of the workings has resulted in significant subsidence, either as broad depressions or cone shaped collapses. These typically contain permanent water at a similar depth to nearby boreholes (Scott, 1995).

Gold mining began in the area in 1886, with the peak period of production occurring in the 1940's and 1950's. In 1955 there were 24 mines operating 90 shafts, but the fixing of the gold price and an increase in operating costs has resulted in a steady decrease in the number of operating mines, with the result that by 1995 only Grootvlei and Consolidated Modderfontein Mines were still operational (Scott, 1995).

Three major reefs have been exploited in the region. The Main Reef has been mined out, while the Black Reef and Kimberley Reef have been more sporadically mined and still contain economically viable deposits.

The long term result of mining has been the excavation of underground basins which follow the undulations and shape of the reefs. The exploitation of the Main Reef has led to the development of basins at three different levels. This is shown in figure 2.2. On the Kimberley Reef, approximately 600m above Main Reef, a basin has developed which corresponds to the East Rand Basin. This basin is likely to expand as the Kimberley Reef continues to be worked (Scott, 1995; van Wyk and Munnik, 1998).

2.4 Dewatering history

Historical records relating to the ingress of water into the mines in this region date back to 1909 and dewatering has been an integral part of mine operation since then. Initially, each individual mine was responsible for dewatering their own workings as they were physically separated from neighbouring mines by unworked boundary pillars. In time, these boundary pillars were mined out, both to extract gold and for safety reasons. As a result the mines became extensively interconnected and water was able to flow unhindered between the individual mines (van Wyk and Munnik, 1998).

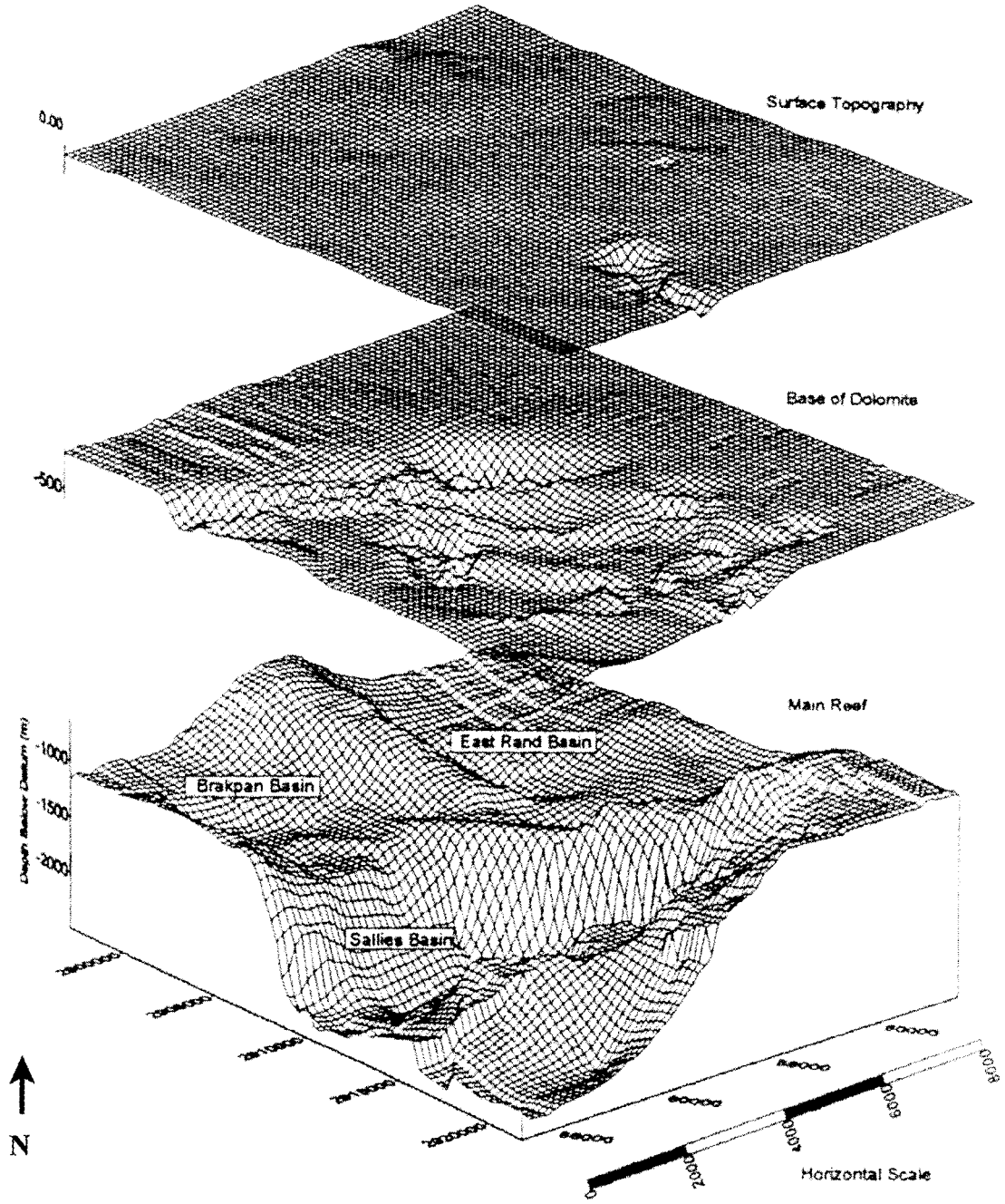

Figure 2.2: Three dimensional relationships of: Main Reef basins, base of the dolomite (Black Reef) and surface topography (after Scott, 1995)

As the underground workings became interlinked the task of dewatering was carried by fewer mines, with those operating in the deeper parts of the basin carrying a greater burden than those operating near the perimeter. To avoid uneven distribution of the financial burden, water committees were formed to ensure that all benefactors could contribute to the pumping cost. The

closure of an increasing number of mines led the state to begin subsidising the cost of pumping in 1963 (van Wyk and Munnik, 1998). At this stage only three mines, Grootvlei, South African Lands and Exploration Gold Mining Company (Sallies) and Vlakfontein, were responsible for dewatering the entire basin and the water level was maintained at 1606mbd. Sallies and Vlakfontein ceased operations in 1976 and 1977 respectively, but their pumpstations continued to operate until June 1991. At this point the water level was allowed to rise to the level of the newly constructed Grootvlei pumpstation, approximately 1030mbd, which occurred in November 1995. Grootvlei has now become responsible for dewatering the entire East Rand Basin. The shifting of the bulk of the dewatering burden from Sallies, which discharged into the Riet Spruit, to Grootvlei, which discharges into the Blesbok Spruit, has resulted in severe hydraulic overloading of the Blesbok Spruit (Scott, 1995; van Wyk and Munnik, 1998). The untreated water was discharged directly into the Blesbok Spruit, resulting in the addition of over 23 000 tons of iron and 200 000 tons of sulphate to the system per day (Boshoff, 1999). This was deemed unacceptable by the Department of Water Affairs and Forestry and the dewatering permit was withdrawn in May 1995. Subsequent to this a number of temporary permits were issued based on the undertaking that a permanent clarifier (high density sludge (HDS) plant) be established by September 1996 (van Wyk and Munnik, 1998).

The current situation is that a volume of approximately 110Ml day^{-1} is being pumped from the underground workings and treated by aeration and lime addition in a HDS plant to remove iron.

2.5 Financial implications

In March 1996 the South African government appointed a committee to conduct a cost-benefit analysis (CBA) in order to be in a position to make an informed decision on the future of mining in the East Rand Basin. For the purpose of the investigation the situation prior to the commencement of pumping by Grootvlei was used as a base case. Three scenarios were identified in the Grootvlei preliminary CBA. These were:

Scenario 1 Mining and pumping of the underground mine water cease immediately

Scenario 2 Mining and pumping continues, with only clarification of the underground water (the current situation)

Scenario 3 Mining and pumping continues, with clarification and desalination of the underground mine water

The CBA incorporated revenue generated from mining, agriculture, eco-tourism and the sale of treated water as well as the capital and operating costs of treatment strategies and the downstream impact on the Vaal River system (van Wyk and Munnik, 1998). The findings of the CBA are summarised in table 2.1.

Table 2.1: Results of preliminary CBA on the Grootvlei-Blesbok Spruit system (van Wyk and Munnik, 1998)

		Changes due to different scenarios		
	Base case	Scenario 1	Scenario 2	Scenario 3
Total impact	R million	R million	R million	R million
GDP of agriculture	178	-80	-178	
GDP of mining	2 498	-2 498		
GDP of eco-tourism	1		-1	
Impact on Vaal river system	-69	+36		+69
Capital cost of treatment and brine disposal			-20	-339*
Operating cost of treatment and brine disposal			-92	-326*
Selling of treated water			+3	+163
Total impact on economy	2 608	-2 542	-288	-433

* The cost of full desalination was predicted at an exchange rate of 1US$ = R4.50. The current exchange rate of 1US$ = R12.35 (December 2001) will result in a significant increase in the cost of desalination.

The CBA indicated that Scenario 2 would be the most economically viable option, although environmental concerns led to Scenario 3 being regarded as the best long term strategy (van Wyk and Munnik, 1998).

2.5.1 Desalination options

Based on the results of the preliminary CBA the Grootvlei Joint Venture Committee recommended the construction of a full scale desalination plant. Three desalination options, reverse osmosis (RO), electrodialysis (ED) and ion-exchange (IX) were evaluated to estimate performance and the economics of the processes for the treatment of the mine water. For the purpose of the evaluation a feed rate of 80Ml day^{-1} was used and performance was predicted using a best, probable and worst case scenario for water quality. Table 2.2 summarises the relative costs and predicted performance levels for the three systems evaluated. In each case the costs have been calculated to treat the worst case water (Schoeman and Steyn, 2001).

Table 2.2: Summary of the predicted costs and performance levels for three physico-chemical treatment systems. SRO = spiral reverse osmosis, EDR = electrodialysis reversal, GYP-CIX = ion exchange based process (Schoeman and Steyn, 2001).

	Treatment system		
	SRO	EDR	GYP-CIX
Feed (Ml/day)	80	80	80
Brine (Ml/day)	12	28	36.8
Potable water recovery (%)	85	65	54
Plant cost (R million)	325.5	495.7	248.3
Brine disposal cost (R million)	167.4	390.6	512.4
Total capital cost (R million)	492.9	886.3	760.7
Operating cost (R/kl)	8.19	4.43	5.67
Daily operating cost (R)	655 200	354 400	453 600

The plant costs estimate for the SRO and EDR plants include a component for pretreatment of the minewater to remove heavy metals. The existing HDS plant could accomplish this task,

thereby reducing the plant cost to a degree. The GYP-CIX ion exchange process is capable of treating raw minewater, so there would be no significant saving.

Despite the fact that the JVC recommended that a full-scale desalination plant be operational by 1 December 1999, no progress has yet been made towards this almost two years after the deadline. Given the limited gold reserves remaining it seems unlikely that desalination of the minewater will become a reality. The most likely scenario is that Grootvlei will continue to discharge large volumes of partially treated water into the Blesbok Spruit, with the associated environmental risks.

2.6 Ecological risk assessment

Jooste and Thirion (1999) conducted a biotic integrity assessment of a 3.8km stretch of the Blesbok Spruit that had been impacted by AMD discharge. The ecological integrity of the stream was assessed using the benthic invertebrate-based SASS4 index developed by Chutter (1998). The results showed that only seven macroinvertebrate families were present at the site. With the exception of one family they are all considered acid tolerant, clearly indicating acid pollution at the site. Furthermore the complete absence of oligochaete worms indicates metal pollution. Although oligochaetes are generally very tolerant organisms they are sensitive to metal pollution. The presence of metal hydroxide precipitates, primary iron hydroxide, effectively blankets the stones-in-current biotope, interfering with the feeding and respiratory processes of the insect larvae (Jooste and Thirion, 1999).

Daphnia pulex was used as a surrogate organism for this ecosystem in controlled toxicity tests. The results indicated that even at near neutral pH the metal concentration of the water dominates the toxicity toward *D. pulex*. At the current concentrations of metals, notably zinc and manganese, in the water, a high risk to aquatic life exists. Zinc and manganese are serious problems as they are the AMD components least likely to be removed in the high density sludge (HDS) plant (Jooste and Thirion, 1999; Stumm and Morgan, 1996).

A shortcoming of the risk assessment is the fact that the toxicity bio-assessment was not performed on a greater number of in-stream organisms. This limits the estimation of the variability of organism susceptibility. In the Blesbok Spruit system the potential exists for significant downstream precipitation of metal, particularly manganese, as it is oxidised and undergoes hydrolysis. While this would have little effect on the *Daphnia pulex* used in toxicity bioassays it would have a significant effect on sediment dwelling organisms and it is possible that the environmental risk may be considerably higher than the estimates presented by Jooste and Thirion (1999).

While the current HDS treatment plant significantly improves the water quality it does not eliminate the risk posed to the aquatic environment by AMD discharge.

2.7 Post-mining predictions

The gold reserves remaining in the Kimberley and Black Reefs are limited and mining of the East Rand Basin should cease by 2006. With no revenue being generated the cost of dewatering mine workings will become prohibitive and groundwater rebound will continue uninterrupted.

There is very limited outcrop of Witwatersrand sediments in the area, so direct recharge to the mine aquifer is either negligible or is limited to periods of excessive flooding along the upper reaches of the Blesbok Spruit, where outcrop does occur (Scott, 1995).

The northern dolomitic aquifer covers an area of approximately 100km^2. Historical records have shown that during mine development and shaft sinking most of the significant inflows encountered by the mines were derived from the dolomites (de Jager, 1986). During peak operation, 12 of the 19 mines, which made up approximately half the mined area, were overlain by dolomite and these were responsible for 85% of the total water pumped.

Wagener (1972) calculated that the volume of water in the dolomite was approximately 1.4 million Ml, based on an average porosity of 3%. The volume of water pumped by the mines

annually accounted for less than 2% of the total stored volume. The recharge potential of the dolomite can be calculated according to the following formula:

Recharge volumes = area x rainfall x recharge %

The recharge percentage is calculated using the environmental chloride method which compares the chloride concentration of rainwater with that of freshly recharged groundwater (van Tonder and Kirchner, 1990). For the East Rand region the recharge is 16% or 119mm $year^{-1}$, which is consistent with the relatively flat topography. This would result in the recharge of an average of 34.1Ml day^{-1}.

Scott (1995) concluded that, given the rate of aquifer recharge by rainfall and the fact that the chemistry of the aquifer water indicated recharge from other surface sources, the average mine inflow could occur without dewatering the groundwater resources of the area. However, since 1995 the rate of dewatering has increased from 64.5Ml day^{-1} to 110-120Ml day^{-1}, it is likely that the some depletion of the groundwater resources is occurring.

Scott has predicted that recharge to surface will occur nine years and eleven months after pumping at Grootvlei stops. This prediction is generated using calculated mined-out volumes and the historical rate of recharge. Between July 1991, when pumping at Sallies ceased, and August 1994 the water level had risen 385m at an average rate of 0.34m day^{-1} (Scott, 1995). The predictions were, however, based on the fact that no further mining or pumping would occur. A more likely scenario is that rebound to surface will occur approximately 12.5 years after pumping ceases, assuming mining activity stops early in 2006 and the rate of dewatering remains at its current levels. The increased time taken to rebound will occur as a result of the expansion of the Kimberley Basin by current mining activities and the fact that the dolomitic aquifer is being dewatered at almost double the predicted recharge rate.

The most likely surface discharge point will be the Nigel No. 3 shaft, which is 24m below the predicted piezometric level (piezometric level = shaft elevation (1623) - major inflow depth (50)). The shaft is inclined and has been ineffectively filled by dumped rubble, but this will not

affect its potential to become free flowing. The predicted subsurface water flow through the interconnected mines in the region is shown in figure 2.3.

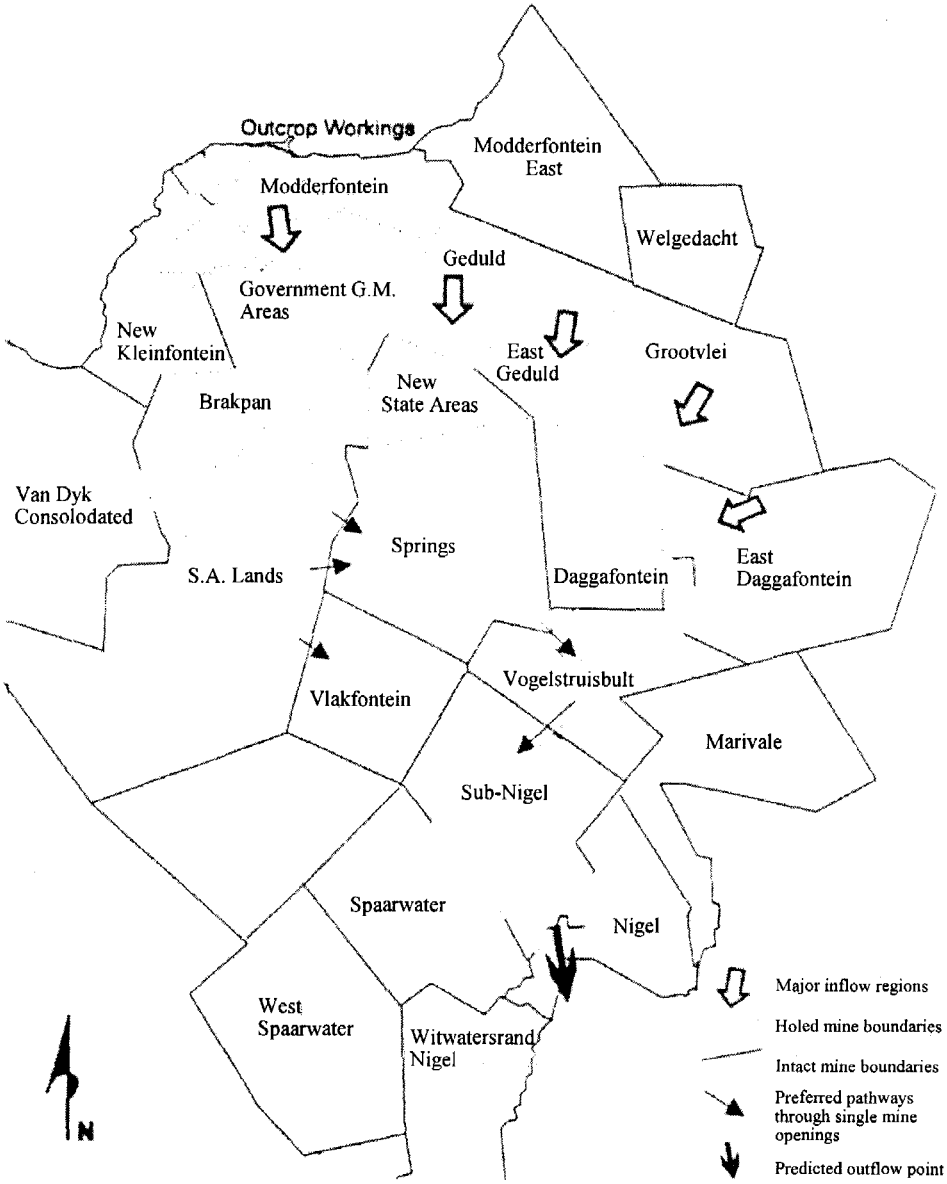

Figure 2.3: The East Rand region showing breaks in mine boundary pillars allowing water movement. The regions of major groundwater inflow and preferred flow paths to the predicted discharge site are shown (after Scott, 1995)

While Scott (1995) acknowledges that predicting the exact volume of the discharge is difficult it should be of a similar order of magnitude to the Blesbok Spruit flow rate before mining and effluent disposal altered the surface and groundwater flow situation. At that time the main flow in the river was derived from groundwater and the river was dry for half the year. Using historical flow rate data Scott has predicted that surface discharge from the East Rand Basin will be approximately 33Ml day^{-1}.

2.7.1 Water quality

The majority of the water recharging the mine aquifer is derived from the dolomite. Therefore the quality of the groundwater is significant in determining the quality of the surface discharge. Scott (1995) conducted a survey of groundwater in the region and found the quality to be spatially variable, with excellent quality being encountered in the extreme north and the south-west. The water in the vicinity of the Blesbok Spruit, north and east of Springs indicated varying levels of sulphate contamination. This appears to be related to either abandoned coal workings or effluent disposal.

A survey conducted by Scott (1995) investigated the quality of water pumped from the Sallies and Grootvlei pump stations. This data was modelled using the PHREEQE geochemical equilibrium model to predict the quality of the water that would eventually discharge to the surface. Scott made a number of assumptions relating to the water rising in the mines:

- the rising water would permeate the dolomite, rather than following a preferred flow-path
- the rising water was equilibrated under assumed new environmental conditions in a cavernous dolomite. For example, it was saturated with oxygen and oversaturated minerals were precipitated
- the water was allowed to dissolve dolomite to equilibrium. Unnatural over saturation that may have developed during the simulations was constantly removed by precipitation

The results of the modelling, for the worst case scenario, are given in table 2.3. Based on this data Scott predicted that heavy metal pollution would not be a major concern, although the total

dissolved solids (TDS) would be unacceptably high, primarily due to the elevated sulphate levels. The modelled data for the water of "typical" quality originating from the East Rand Basin predicts negligible concentrations on heavy metals, a sulphate concentration of below 600mg/l and a pH of approximately 6.5. The mean chloride concentration of the "typical" water is 165mg/l. Therefore, this water can be classified as a marginally polluting, net alkaline water according to the Younger classification system (Younger, 1995).

Scott's predictions fail to take into account any possible changes in water quality as a result of the dissolution of AGSs. The underground conditions experienced during active mining would promote the partial oxidation of pyrite and the formation of AGSs. There is evidence to suggest that this is already occurring. The iron content in the water that was pumped from the Sallies pump station was in the region of 20mg/l. This has increased to 210mg/l in the water that is currently being pumped from Grootvlei. There has been a similar increase in sulphate concentration from 500mg/l to over 1800mg/l. This can be accounted for by the dissolution of AGSs as the water level in the underground workings rose from the level of the Sallies pump station to the Grootvlei pumpstation.

Table 2.3: Results of PHREEQE modelling on worst case water in East Rand mines (Scott, 1995)

Component	Initial water	Equilibrated	Surface discharge
pH	2.71	2.30	4.55
Ca (mg/l)	179.56	179.51	2814.37
Mg (mg/l)	42.06	42.13	1640.40
Na (mg/l)	363.24	364.03	364.03
Fe (mg/l)	34.07	0.00	0.00
Mn (mg/l)	2.29	2.29	2.29
Al (mg/l)	29.68	29.64	29.64
Cl (mg/l)	563.70	564.60	564.60
HCO_3 (mg/l)	148.27	57.15	1570.53
SO_4 (mg/l)	1479.35	1360.96	1360.96

The full effect of the dissolution of AGSs has probably not been realised yet, as a result of preferred flow paths. Figure 2.3 indicates that the majority of the inflow is derived from the north and eastern region, close to Grootvlei. Therefore, the majority of the water pumped out of Grootvlei is most likely derived from fresh inflow, rather than water that has seeped up from the Sallies basin. Figure 2.2 shows that the Sallies basin is further to the south and west, closer to the most likely discharge point at Nigel.

Once pumping at Grootvlei has stopped the natural hydraulic gradient will be restored and the flushing of the Sallies basin will be more complete. There will be further dissolution of AGSs as the water level rises to the point where surface discharge is reached. Thus the quality of the water discharged to the surface initially is likely to be significantly poorer than that being pumped from Grootvlei at present, with iron levels in excess of 1000mg/l as would be expected based on the sulphur content of the mined ore.

2.7.2 Model for future discharge

Based on the evidence presented above it is possible to develop a conceptual model of the East Rand system, using the proposals of Younger (2000). To implement this model several assumptions need to be made. Firstly, it must be assumed that only a portion of the contaminants which dissolved as the Sallies basin was flooded has been pumped out at Grootvlei, as a result of the fact that Grootvlei is primarily pumping fresh recharge. Therefore, when determining the time taken for the mine system to flood completely, the time taken for the water level to rise from the Sallies pump station to the Grootvlei pump station cannot be completely neglected. Assuming that the Sallies basin will flush completely once rebound is complete will conservatively add three years to the total flush duration. Therefore, the time taken for complete flushing (t_f)can be estimated as:

$$t_f = (7.9/2)15.5$$
$$= 61.2 \text{ years}$$

The initial iron concentration can be expected to be in the region of 1000mg/l, although if the predicted decline in contaminant concentration is followed the iron concentration will be reduced to approximately 200mg/l within 15 years. Despite Scott's suggestions that the high pH of the dolomitic inflow and the oxygenation and hydrolysis of iron while the water is still below ground would result in complete removal of iron before discharge to surface, this is unlikely to occur. While the pH of the water in the dolomite is high (± pH 8.5) the alkalinity, and hence the capacity to neutralise acidity, is not. The published solubility product values of dolomite vary between $10^{-16.5}$ to $10^{-19.5}$, due to a lack of understanding of the dolomite precipitation process, indicating that only a small amount of alkalinity will be added to the water before saturation occurs (Stumm and Morgan, 1995). This is confirmed by borehole samples analysed for this study, where alkalinity measurements were below 150mg/l $CaCO_3$, despite the alkaline pH. Although 30% of the study area is overlain by dolomite, the existence of preferred flow paths should preclude much of the minewater from permeating through the dolomite to reach the surface. In terms of oxidation and precipitation of iron, it is unlikely that the amount of oxygen present at the depths concerned is sufficient to oxidise a significant amount of iron. Surface water at 25°C is at equilibrium with the atmosphere at a dissolved oxygen concentration of 8.4mg/l (Henry's law constant, $K_H = 1.26 \times 10^{-3}$ M atm^{-1}). Hedin *et al.* (1994) has calculated that this is sufficient to oxidise 50mg/l of Fe^{2+}. Dissolved oxygen values obtained from water pumped from 30m boreholes, surrounding Springs (in the study area), ranged from 0.5mg/l to a maximum of 2.3mg/l. Therefore, it is unlikely that there will be significant iron oxidation occurring prior to the minewater discharging to the surface.

The long-term situation, however, should not be as serious as would be predicted using the sulphur percentage of the mined ore. This is again related to the lack of availability of oxygen to the exposed pyrite in the flooded workings. Juvenile acidity generation is a serious problem in the coalfields of the UK, but the workings there are much shallower which allows the pyrite to be exposed to significant amounts of oxygen, particularly at the air-water interface. Of the three reefs in the East Rand region, only the relatively minor Black Reef is shallow enough for potential exposure to the air as the level of the water table fluctuates. The vast majority of the worked areas will be permanently flooded and not exposed to sufficient oxygen for further pyrite oxidation to occur.

2.7.3 Long term treatment options

Despite the predicted low-level impact of juvenile acidity on the region, a treatment strategy will need to be in place for at least 60 years. The evaluation of the desalination options clearly indicates that they will not be financially viable options. Similarly, continued pumping from the Grootvlei pump station cannot be sustained for financial reasons. As the predicted discharge will occur some distance from Grootvlei the existing HDS plant will also not be effective. A relatively low cost, sustainable system will need to be built to the discharge point, to avoid costly pumping of the water.

2.7.3.1 Evaluation of a passive anaerobic wetland system

A passive wetland based system would be one possible long-term option. Using the sizing procedure developed by Hedin *et al.* (1994) it is possible to determine the size requirement of an anaerobic wetland system capable of treating the predicted discharge. The following input data have been selected:

Flow rate (Q)	= 22 917l/min
Fe concentration (peak)	= 1000mg/l
Mn concentration (peak)	= 35mg/l
Al concentration (peak)	= 30mg/l
pH (worst)	= 3.0

This would yield a loading rate of 40 095kg/d of total acidity (mineral + proton). In order for the treated water to be safe for discharge to the aquatic environment (ie Blesbok Spruit) an empirical removal rate of 3.5g total acidity m^{-2} day^{-1} was calculated. Therefore, to effectively treat the predicted initial discharge an anaerobic wetland of 11.5 million m^2 would be required. This would not be a suitable treatment system until the level of contamination in the discharge decreased significantly.

2.8 Conclusions

The gold reserves in the East Rand region are limited and mining is unlikely to continue beyond 2006. As a result dewatering is expected to be discontinued soon afterwards. This will lead to the rebound of groundwater through the abandoned workings until a level is reached where discharge to the surface will occur, presumably from the Nigel No. 3 shaft. It is predicted that the time required to flush conservative contaminants from the East Rand Basin will be in the region of 60 years. The initial water quality is likely to be very poor, with a low pH and unacceptably high levels of heavy metal and sulphate, but should show a steady improvement with time. Juvenile acidity should not represent a serious concern as a result of the depth of the worked reefs. If the initial discharge is allowed to flow, untreated, into the Blesbok Spruit it would represent an ecological disaster. No effective treatment mechanisms are currently in place. Desalination options have been considered, but do not represent an economically viable option. While a passive wetland based system would be impractical for the treatment of the initial discharge it could represent a feasible solution in the longer term. If suitable remediation measures are not put in place prior to surface discharge of the rebounding minewater, a very real and serious risk to the aquatic environment exists.

The pilot plant studies described later in this thesis have been conducted using a synthetic acid mine drainage, the general characteristics of which are based directly on the water which is currently being pumped from the Grootvlei pumpstation.

CHAPTER 3. DIRECT TREATMENT OF AMD BY ALGAL BIOMASS - EFFICIENCY AND TOXIC EFFECTS

3.1 Introduction

During the last decade a considerable amount of attention has been focused on the ability of both viable and non-viable algal biomass as a potential tool for the extraction and recovery of toxic and valuable heavy metals from aqueous solutions. The studies have focused on both unicellular algae (Gardea-Torresdey *et al.*, 1990; Roy *et al.*, 1993; Pascucci, 1993; Garnham *et al.*, 1993; Wilde and Benemann, 1993) and cyanobacteria (Karamushka *et al.*, 1995) as well as macroalgae (Kratochvil *et al.*, 1995; Fourest and Volesky, 1996) and complex algal mats (Lawrence *et al.*, 1998).

The biosorption of the metal by the algal biomass arises from the coordination of the ions to different functional groups in or on the algal cell. These groups are found on proteins, lipids and carbohydrates and include amino, thioether, sulfhydral, carboxyl, carbonyl, imidazole, phosphate, phenolic, hydroxyl and amide moieties (Gardea-Torresdey *et al.*, 1990).

The specific binding mechanism depends on the species of metal ion, the specific organism and the chemical composition of the metal ion solution. Several researchers have demonstrated the release of protons during metal accumulation, suggesting an ion-exchange mechanism (Greene *et al.*, 1987; Crist *et al.*, 1994a; 1994b), while electrostatic interactions and covalent bonding have also been demonstrated (Volesky, 1987).

Many heavy metals are required by algae in trace concentrations as essential micronutrients and as such the organisms have developed specific transport pathways for accumulating these metals. At elevated concentrations these metals become toxic to the cells. Copper and zinc have both been used to control nuisance algal blooms, due to their high toxicity to cyanobacteria in particular (Meador *et al*, 1998). As a result, algae are often used as indicator organisms in toxicity testing protocols (Lam *et al.*, 1999). The effect of metal toxicity is therefore an important consideration in the development of algal based bioremediation systems.

Spirulina sp. was chosen for the initial algal studies as it was readily available and its cultivation on a large scale has been documented (Ciferri, 1983). In addition, it has been used on an industrial scale to treat municipal waste and is able to tolerate a wide range of pHs and salinities (Vonshak *et al.*, 1996). Due to its filamentous nature it is easy to harvest by filtration, using a nylon mesh, which reduces the problems associated with solid-liquid separation.

3.1.1 Characteristics of Spirulina

Spirulina is a multicellular, filamentous, non-heterocystous cyanobacterium. The filaments are composed of cylindrical cells arranged in unbranched, helicoidal trichomes (Figure 3.1). The filaments are motile, gliding along their axis (Ciferri, 1983; Martel *et al.*, 1992; Vonshak *et al.*, 1996).

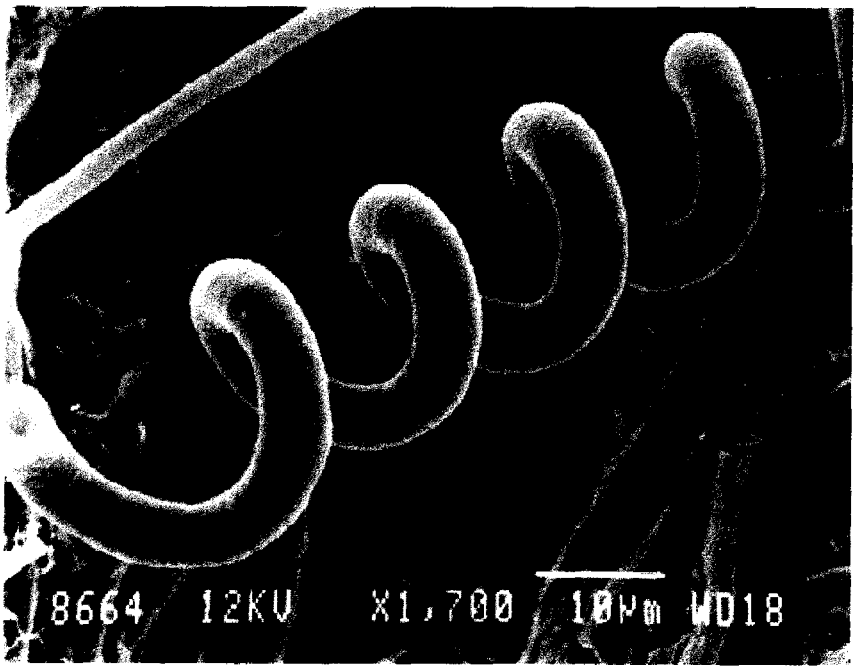

Figure 3.1: Scanning electron micrograph of healthy *Spirulina*

The cell wall of *Spirulina* is composed of four distinct layers. The outer layer consists of structural material analogous to the Gram negative bacterial cell wall. Below this is a layer of protein fibrils helically bound to the trichomes. The second layer is composed of peptidoglycan, which folds towards the inside of the filament. This second layer, together with the inner fibril

layer give rise to the septum, which separates the individual cells in the filament (Ciferri, 1983; Richmond, 1986).

3.2 Research aims

The primary aims of this section of the project were:

1) To evaluate *Spirulina* as a potential biosorbent for the heavy metals encountered in the mine effluent. To this end the adsorption capacity and kinetics of binding need to be determined.
2) To evaluate the efficiency of *Spirulina* as a treatment agent for the removal of heavy metals from an actual mine effluent.
3) To determine toxicity threshold levels for the various toxic heavy metals, above which the integrity of the treatment system would be compromised.

3.3 Materials and methods

3.3.1 Algal biomass

The *Spirulina* and *Oscillatoria* (expanded on in chapters 4 and 7) used in this study were cultivated under constant environment conditions (constant illumination at 27°C). The algal cultures were maintained in Zarrouk's chemically defined medium (Appendix B). Algae used in the experiments were harvested by filtering a portion of the stock culture through a nylon cloth (mesh size 0.2mm), washing twice with distilled water and resuspended in a 1g/l NaCl solution to form a concentrated slurry from which appropriate dilutions were made.

3.3.2 Determination of algal concentration

Both *Spirulina* and *Oscillatoria* are filamentous cyanobacteria, so cell counts could not be used to determine culture concentration. A chlorophyll extraction method and a photometric method were developed which could be accurately correlated to algal dry mass.

3.3.2.1 Dry mass determination

Porcelain crucibles were labelled, dried at 60°C for 3 hours and individually weighed. Volumes of 1, 2, 5, 7, 10 and 20ml were removed from the algal culture, spun down at 5000rpm for 5 minutes, and washed twice with distilled water. The washed cells were transferred to the crucibles and dried at 60°C for 12 hours, after which the dry mass was determined. Determinations were performed in triplicate and mean values used. A curve of dry mass against initial volume was plotted, with an r^2 value of 0.950 (Appendix C).

3.3.2.2 Photometric determination

Sample volumes of 1, 2, 5, 7, 10 and 20ml were removed from the stock culture and diluted to a final volume of 20ml with distilled water. The samples were thoroughly mixed to ensure even distribution and the optical density (OD) determined at 660nm. Determinations were made in triplicate and mean values were used to plot a curve of OD against initial volume, with an r^2 value of 0.998 (Appendix D).

3.3.2.3 Chlorophyll extractions

Similar volumes as previously used were filtered through a Whatman GF/C filter. The algal laden filters were transferred into foil covered bottles containing 10ml of acetone and crushed. The samples were stored at 4°C for 24 hours, after which they were filtered again and the absorbence determined at 661.6, 644.8 and 470nm. Chlorophyll concentrations were calculated from the equations given in Appendix E (Lichtenhaler, 1987). Extractions were performed in triplicate and mean values were used to plot a curve of chlorophyll *a* against initial volume, with an r^2 value of 0.995 (Appendix F).

The data from the OD_{660} measurements and chlorophyll extractions were plotted against the dry mass data and were found to be directly proportional (r^2 values of 0.972 and 0.965 respectively), indicating that algal mass could be accurately determined by either the photometric or chlorophyll extraction method.

3.3.3 Analytical techniques

All pH measurements were made using a Cyberscan 2500 pH meter. Metal analysis was performed using a GBC 909AA atomic absorption (AA) spectrophotometer, linked to a GBC integrator (Individual program parameters shown in Appendix G). Optical density measurements were made using a Shimadzu Mini 1240 UV-VIS spectrophotometer. All glassware was washed in 15% nitric acid followed by repeated rinses in distilled water.

3.3.3.1 Acid digests

Acid digests were performed to determine the amount of metal taken up by the algal cells. A 3ml sample was removed and filtered through a 0.45µm cellulose acetate filter. The filtrate was retained and used to determine the amount of metal remaining in solution. The filters containing the algae were placed in Pyrex boiling tubes to which 0.2ml 55% nitric acid was added. These were boiled for approximately 30 minutes (until all the nitrous oxide had dissipated). Once cooled 4ml of distilled water was added to each tube and the metal concentration was determined by AAS.

3.3.3.2 Carbohydrate determination

Carbohydrate determinations were performed to quantify extracellular polysaccharide. A sample was removed from the culture and filtered through a 0.45µm nylon membrane filter. 1ml of phenol reagent and 5ml 32% sulphuric acid were added to 1ml of the filtrate and mixed. The absorbance was read at 490nm and the results converted to glucose equivalents using a standard curve of glucose against absorbance (Appendix H).

3.3.3.3 Light microscopy

All light microscope preparations were made by mounting 25µl of sample on a glass slide. These were photographed at the Electron Microscopy Unit, Rhodes University, using an Olympus BX50 camera-microscope attached to an Olympus PM-30 exposure control unit.

3.3.3.4 Scanning electron microscopy (SEM)

Specimens were prepared either by filtering 5ml of sample through a Whatman GF/C filter or by evaporating a small volume onto a glass cover slip. The specimens were fixed in cold 2.5% gluteraldehyde in 0.1M phosphate buffer for 12 hours. After fixation the specimens were washed twice in phosphate buffer, followed by a 30% to 100% ethanol dehydration sequence, for 10min at each concentration. Specimens were then incubated in increasing concentrations of amyl acetate, prior to critical point drying. The dried specimens were mounted on copper stubs, coated in gold and observed using a JEOL JSM-80 SEM (Cross, 1987).

3.3.4 Adsorption isotherms

Adsorption isotherms were conducted, in triplicate, at 20°C for five hours. Viable *Spirulina*, equivalent to 100mg dry mass, was added to 100ml of the metal solutions (Cu^{2+}, Zn^{2+}, Fe^{2+}, Pb^{2+}) and shaken at 140rpm on a rotary shaker. Isotherm experiments were conducted at pH 6 and initial metal concentrations (C_0) varied from 20 to 1000μM. A pH of 6 was selected so that metal precipitation as hydroxides did not occur. After 5 hours a 5ml sample was removed, filtered through a 0.45μm nylon membrane filter and the metal remaining in solution was determined by AAS. The Langmuir sorption model was used to estimate the maximum metal uptake (X_m), where these could not be reached in the experiment (Holan *et al.*, 1993).

$$C_e/q_e = 1/(X_m b) + C_e/X_m$$

Where X_m represents the maximum adsorption capacity and b is the Langmuir constant, which is the ratio of sorption/desorption rates (Holan *et al.*, 1993). q_e is the metal uptake (mg metal/g of biomass) at equilibrium and C_e represents the equilibrium concentration of metal (mg/l). The Langmuir model makes four basic assumptions (Faust and Aly, 1987):

1) The molecules are adsorbed on definite sites on the surface of the adsorbent.
2) Each site can accommodate only one molecule.
3) The area of each site is a fixed quantity, determined solely by the geometry of the surface.
4) The adsorption energy is the same at all sites.

3.3.5 Adsorption kinetics

Viable *Spirulina* (300mg dry mass) was mixed with 300ml of metal solution at concentrations between 100 and 500μM. The solutions were shaken at 140rpm for 4 hours. Samples were taken at varying intervals and analysed as previously described.

3.3.6 Effluent treatment studies

Acid mine effluent was obtained from Black Mountain, a base metal mine in the Northern Cape Province, South Africa. The effluent was characterised by a low pH (1.99) and high concentrations of iron (1700μM), copper (17μM), lead (7μM) and zinc (33μM). A complete effluent profile is shown in appendix I.

Algal cultures were established in 400ml Zarrouk's medium, modified by omitting the iron and EDTA. The flasks were divided into five groups (three flasks per group), a control group and four experimental groups, to which increasing volumes of raw effluent were added. Chlorophyll extractions, heavy metal analysis (Cu, Fe, Zn and Pb) and pH measurements, as described previously, were performed on day 0. The flasks were incubated on a rotary shaker at 140rpm under constant environment conditions (constant illumination at 27°C).

On day 1 chlorophyll extractions were performed, after which the raw effluent was added to the flasks in the experimental groups (group 1 - 10ml, group 2 - 20ml, group 3 - 30ml and group 4 - 50ml). This was repeated on successive odd-numbered days. Prior to effluent addition the volume of the flasks was adjusted to 400ml, either by abstraction or addition of distilled water.

On day 2 and successive even-numbered days a 5ml sample was removed, filtered through a 0.45μm nylon membrane filter and the filtrate used to determine the concentration of heavy metals in solution.

The experiment was conducted over a 44 day period. The Zarrouk's media has a high pH and contains 16.8g/l of sodium bicarbonate which would lead to alkaline precipitation of the heavy

metals in the effluent. To determine the effect of the medium the experiments were repeated without the addition of algae to any of the flasks.

Data were analysed by determining the number of μmoles of each metal in the experimental flasks at day 0. This was determined each time heavy metal analysis was performed and allowed the metal removal to be evaluated for each two day period, as well as cumulatively over the duration of the experiment.

3.3.7 Toxicity studies

The loss of viability of the algal cultures during the effluent studies prompted the determination of the toxic effects of copper, lead and zinc on *Spirulina*. The following experiments were performed in triplicate.

Eighteen 500ml flasks were inoculated with 30ml of concentrated algal slurry and 270ml of Zarrouk's medium. A chlorophyll extraction, an acid digest and a pH reading were performed on each experimental flask. The cultures were allowed to stabilise for 24 hours under constant environment conditions.

On day 1 the appropriate volume of a 1M $CuSO_4$ was added to each flask to make the final concentrations up to 5, 10, 20, 30 and 50μM. Chlorophyll extractions, acid digests and pH readings were performed. This was repeated every second day thereafter. On day 4 additional copper was added to return the concentration in solution to the original levels. Carbohydrate determinations were performed every second day.

Light microscope and EM preparations of the algae were made at various stages.

The experiments were repeated using zinc (stock 1M $ZnSO_4$) and lead (stock 1M $PbCl_2$).

3.4 Results and discussion

3.4.1 Adsorption isotherms

The adsorption isotherm data for all three metals tested showed relatively good compliance to the Langmuir equation (Table 3.1). The correlation coefficients, r^2, for all the metals except iron were greater than 0.92, indicating a good relationship between the equilibrium metal concentration (C_e) and the metal uptake (q_e). The model assumes that no movement of adsorbed molecules occurs across the surface (Faust and Aly, 1978). As viable biomass was used in this study it is likely that there was some internalisation of adsorbed metal. This is evident from the kinetic data which indicate that there was a small increase in bound metal after equilibrium appeared to have been reached. The correlation coefficients would probably have been higher if the experiments had been performed over a shorter time period. The kinetic data (Figure 3.2) indicated that by five hours some internalisation of metal, particularly copper and zinc, would have occurred. There appeared to be a slight increase in metal removal after two hours, by which time adsorption equilibrium seemed to have been reached. This internalisation of metal would free additional binding sites and result in the overall binding being higher than would be expected assuming monolayer binding.

Table 3.1: Langmuir constants of metal-*Spirulina* binding (mean values, n = 3)

Metal	Temperature (°C)	X_m (mg/g)	Correlation (r^2)
Copper (Cu^{2+})	20.0	9.91	0.93
Zinc (Zn^{2+})	20.0	8.76	0.94
Lead (Pb^{2+})	20.0	65.36	0.96
Iron (Fe^{2+})	20.0	1.68	0.86

The isotherm data were substituted into the Langmuir equation to calculate the maximum adsorption capacity of *Spirulina* in terms of the various metals. Of the metals tested the capacity was highest for lead, followed by copper and zinc, with iron adsorbing poorly to the biomass. While the adsorption capacity of lead appeared to be almost 10 times higher than copper and zinc it must be remembered that the capacity is expressed in terms of mg/g and the atomic mass of lead

is considerably higher than copper or zinc. In terms of molar concentrations, the capacity for lead is just over double that of copper and zinc. This sequence is similar to that obtained by Pascucci (1993) using *Chlorella vulgaris*, Roy *et al.* (1993) using *Chlorella minutissima* and Hammaini *et al.* (1999) using activated sludge. Comparing the data from this study with published results for both algal and other biosorbents (Table 3.2) it is clear that *Spirulina* is not the most effective adsorbent. This is partly due to the filamentous nature of *Spirulina*, which leads to a smaller surface area to volume ratio than that of unicellular algae or yeast.

Table 3.2: Metal uptake capacity of various adsorbents

Metal	Adsorbent	X_m (mg/g)	Source
Copper	*Spirulina* sp.	9.91	This study
	Activated sludge	18.8	Hammaini *et al.* (1999)
	Sargassum fluitants	61.5	Kratochvil *et al.* (1995)
	AMT-BIOCLAIM™	152.0	Brierely *et al.* (1985)
Zinc	*Spirulina* sp.	8.76	This study
	Activated sludge	15.4	Hammaini *et al.* (1999)
	AMT-BIOCLAIM™	137.0	Brierely *et al.* (1985)
Lead	*Spirulina* sp.	68.36	This study
	Azolla filiculoides	100.0	Sanyahumbi (1998)
	Penicillium chrysogenum	116.0	Niu *et al.* (1993)
	Activated sludge	142.9	Hammaini *et al.* (1999)
	Sargassum fluitants	219.6	Fourest and Volesky (1996)
	AMT-BIOCLAIM™	601.0	Brierely *et al.* (1985)

3.4.2 Adsorption kinetics

The kinetic data indicate that in all cases initial binding of the metal to algae was rapid, with over 80% of the total accumulation occurring within the first 30 minutes. Figure 3.2 combines the data for all four metals at an initial concentration of 200μM. At lower concentrations the percentage removal was higher for all groups and the trends could not be seen as clearly. The kinetics of lead binding was the most rapid with over 95% of the total removal occurring within the first 60 seconds. This is consistent with the results of Sanyahumbi (1998). The kinetics of copper and zinc adsorption were slightly slower than that of lead. These are consistent with the results of Wilhelmi (1997), obtained using *Saccharomyces cerevisiae*. There appears to be a slight bi-phasic shape to the copper and zinc curves, suggesting some metal accumulation into the cells.

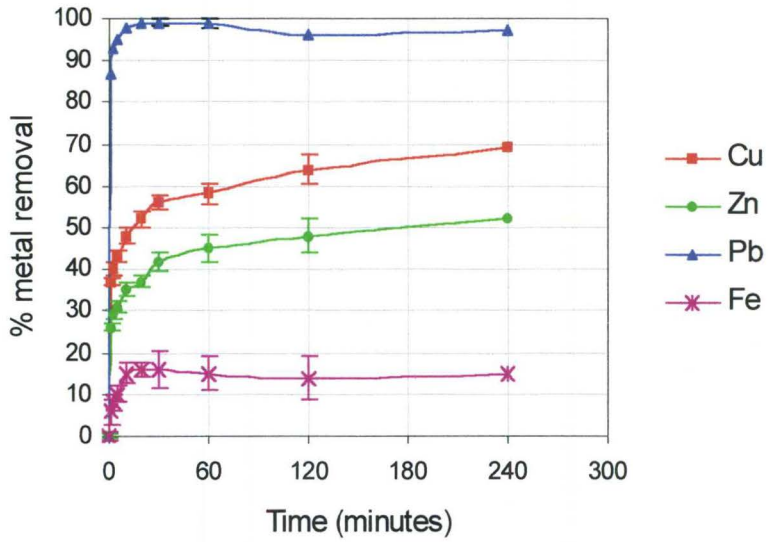

Figure 3.2: Percentage metal accumulation in batch flasks by *Spirulina* as a function of time (n=3 ± SD). Initial metal concentration 200μM. Data for individual metals obtained from separate experiments and are plotted on a single set of axes for comparative purposes

3.4.3 Effluent treatment studies

The treatment of raw AMD by direct contact with the algal culture was effective, although the algal cultures only remained viable for a short period of time. Figure (3.3) shows that the algal cultures in all groups remained healthy for the first seven days after which they began to decline rapidly. The decline in algal viability was most noticeable in the groups receiving the higher doses of AMD. Group one declined at a slower rate, while the control flasks essentially followed a standard growth curve pattern. The chlorophyll extractions were stopped after day 25 as most of the cultures in the experimental groups had died.

The pH data (Figure 3.4) mirrored the algal viability, with the pH in all flasks increasing by a similar degree over the first nine days. However, once the algal cultures began to deteriorate the pH no longer increased and subsequent addition of effluent resulted in a proportional decrease in pH. The pH of the flasks in the control group continued to increase until the cultures began to decline, due to nutrient depletion.

The legend for figures 3.3 to 3.7 is explained in table 3.3 below.

Table 3.3: Key to legends for figures 3.3 to 3.7

Group	Description of dosing on day 1 and subsequent odd-numbered days
Control	10ml Zarrouk's medium
Group 1	10ml raw mine effluent
Group 2	20ml raw mine effluent
Group 3	30ml raw mine effluent
Group 4	50ml raw mine effluent

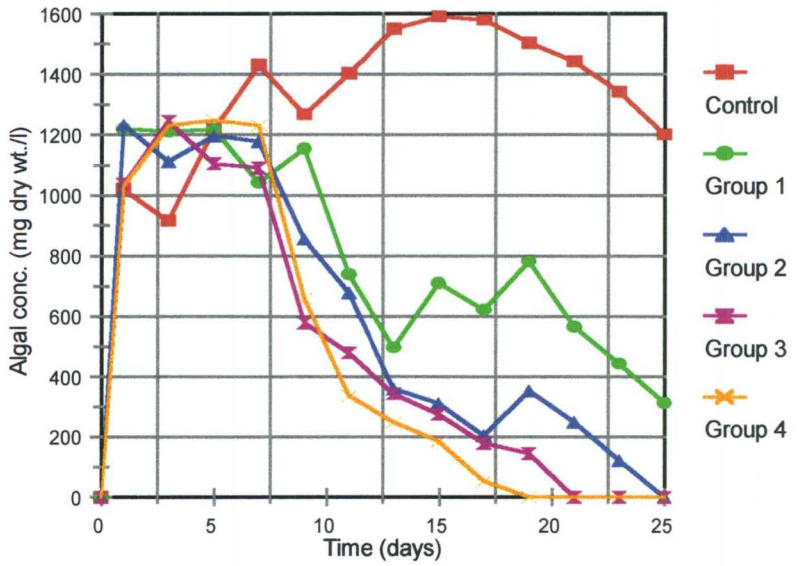

Figure 3.3: Graph showing mean (n = 3) algal concentration vs time for effluent treatment studies. Viable algal mass was determined using the linear relationship between Chlorophyll *a* and dry mass. Chlorophyll determinations terminated after day 25 due to death of most cultures

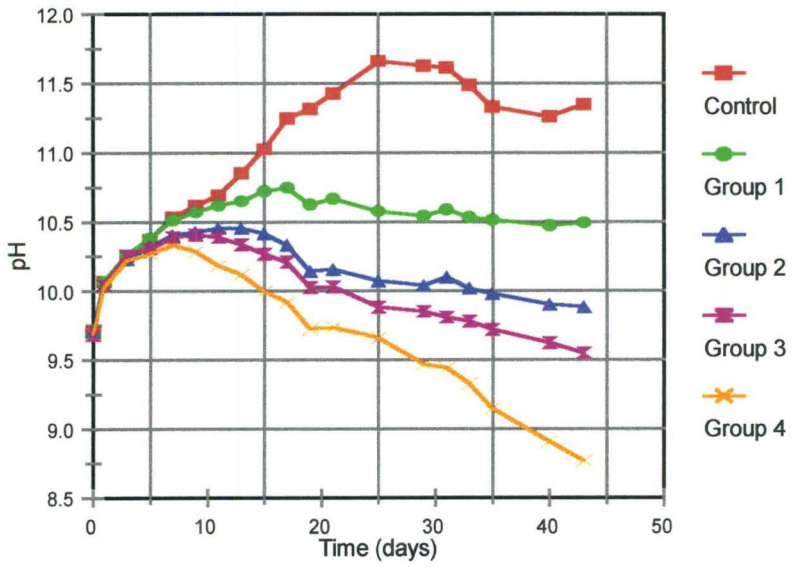

Figure 3.4: Graph of pH vs time for effluent treatment studies (mean values, n = 3)

Metal removal essentially appeared to be determined by pH. Due to the high pH and bicarbonate content of the algal growth medium the pH in all the groups did not fall significantly below 9.5 at any stage and only group four dropped below pH 9. As a result the metal removal percentages were high for all metals, especially the iron where over 99% was removed in all the groups. Copper showed an unusual trend (Figure 3.5), with a high percentage removal for the first eight days, most likely as a result of both precipitation and adsorption. However, there was a significant drop in efficiency after day eight, which coincided with the deterioration of the algal cultures (Figure 3.3). After day 14 the percentage removal began to increase again, particularly in groups 2-4, which coincided with the complete deterioration of the relevant algal cultures. The algal cultures in the group one flasks, although declining, had not died completely and the copper removal remained lowest in this group.

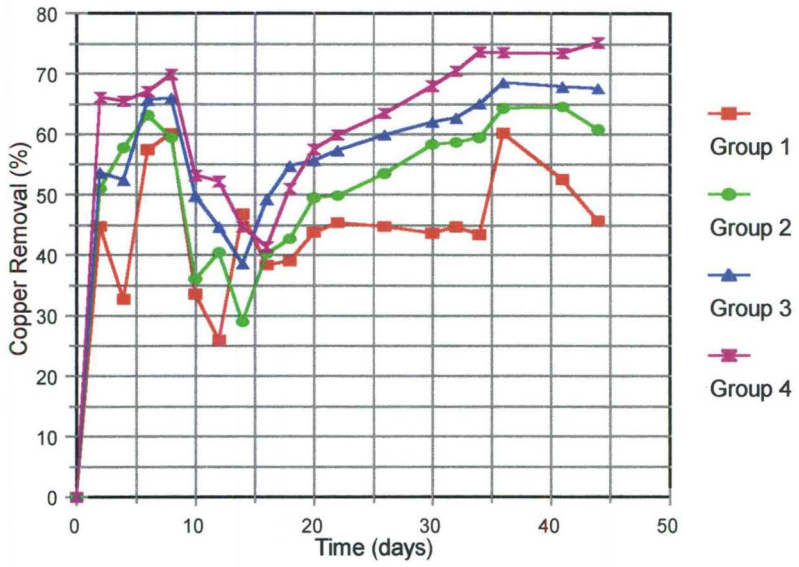

Figure 3.5: Graph of cumulative copper removal vs time for the effluent treatment studies (mean values, n = 3)

The trend observed for the copper suggests the release of exopolysaccharides and thiols by the metal stressed algae. These substances have been shown to chelate metals in solution, rendering them unavailable for accumulation (Kaplan *et al.*, 1987). Singh *et al.* (1999) found that the exposure of the cyanobacterium *Nostoc spongiaeforme* to elevated concentrations of copper, nickel and mercury significantly increased the production of both thiols and exopolysaccharide.

Exposure to 5μM copper resulted in a 50% increase in thiol production relative to the controls. A more significant increase in exopolysaccharide production was found. Kidambi *et al.*, (1995) showed that the gene responsible for alginate production in *Pseudomonas syringae* was transcriptionally activated by the presence of copper. A similar process may occur in cyanobacteria.

Once the affected cultures died the production of the metal complexing agents would cease and the copper added to the system during subsequent effluent additions would be free to precipitate. This would explain the increase in cumulative removal observed after the cultures had died. Group one showed the lowest copper removal, which can be attributed to the fact that the culture did not die completely.

The removal of zinc and lead showed very similar patterns. Zinc removal is shown in figure 3.6.

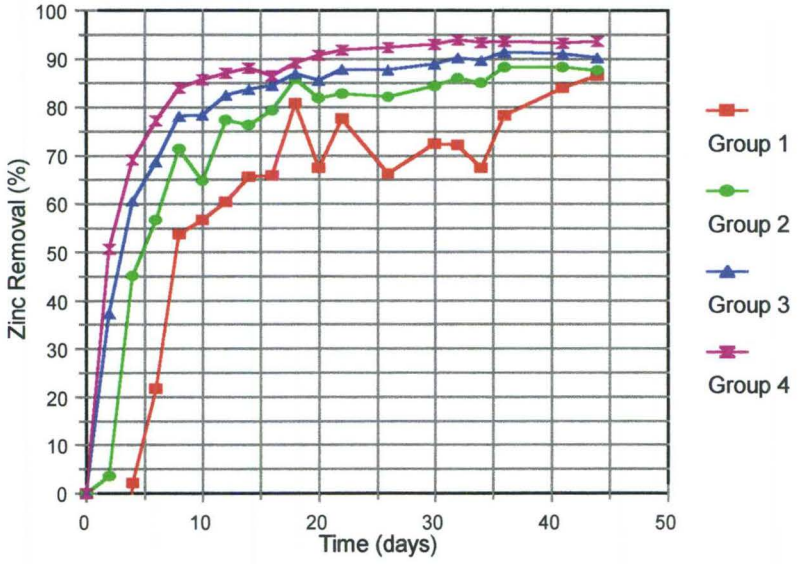

Figure 3.6: Graph of cumulative zinc removal vs time for effluent treatment studies (mean values, n = 3)

Metal removal can be attributed primarily to pH dependent alkaline precipitation as a result of the high bicarbonate content of the growth medium. The extracellular elements have been shown to have the highest affinity for copper, which would explain why the removal of the other metals was not affected. In all groups the amount of zinc and lead remaining in solution was similar, but as each group received an increasing dosage of effluent the percentage removal appears lower for group 1. The results suggest that precipitation is effective to a lower threshold level.

The results for the algal free control show a similar degree of metal removal as obtained in the experimental flasks. The copper flasks did not show the reduced metal removal between days 8-16, which further supports the assumption that thiols and polysaccharides were responsible for copper chelation in the experimental flasks. The rate of pH change between the experimental and control flasks was however, significantly different (Figure 3.7).

(a) (b)

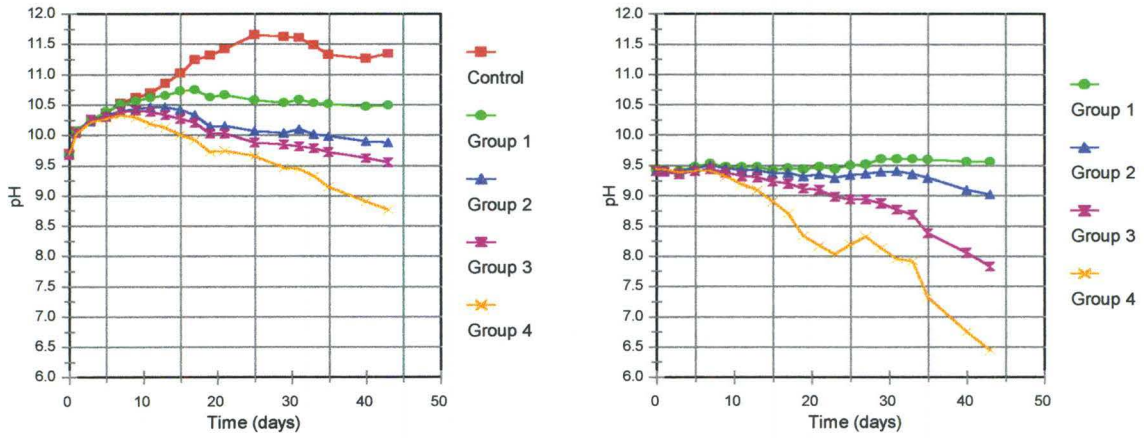

Figure 3.7: Comparison of pH change vs time for experimental (a) and algal free control (b) flasks (mean values, n = 3)

From the results it is clear that the presence of the algae has a significant effect on both maximum pH achieved and the rate of pH decrease. In both cases the volume of media added initially was the same, so the total amount of bicarbonate alkalinity (16.8g/l) present at the start was the same. The algae are able to modify the aqueous chemistry of their surrounding medium by utilising bicarbonate ions as a source of carbon dioxide for photosynthesis (Shiraiwa *et al.*, 1993). The remaining hydroxide ion is released back into the medium and results in the pH increase observed

in the control and group one in figure 3.7(a). The process does not increase the alkalinity, but rather reduces the acidity of the system. This phenomenon, and its potential application to AMD treatment will be discussed in chapter four.

As the pH in the group four flasks dropped below pH 7.5 the efficiency of the zinc removal decreased dramatically and a further drop in the pH to below 6.8 resulted in zinc that had been previously precipitated being remobilised.

3.4.4 Toxicity studies

3.4.4.1 Copper

The results for the algal concentration and pH are shown in figures 3.8 and 3.9. From the results it is clear that for the first three days all six groups exhibited essentially similar behaviour. Both the algal concentration and the pH increased steadily. Between days three and five the effects of acute copper toxicity become clearly evident, with the 20, 30 and 50µM copper groups showing a significant decline in both algal concentration and pH. By day 11 all the cultures exposed to 20-50µM Cu had no filaments and few cells still intact. By contrast, the control and 5µM cultures

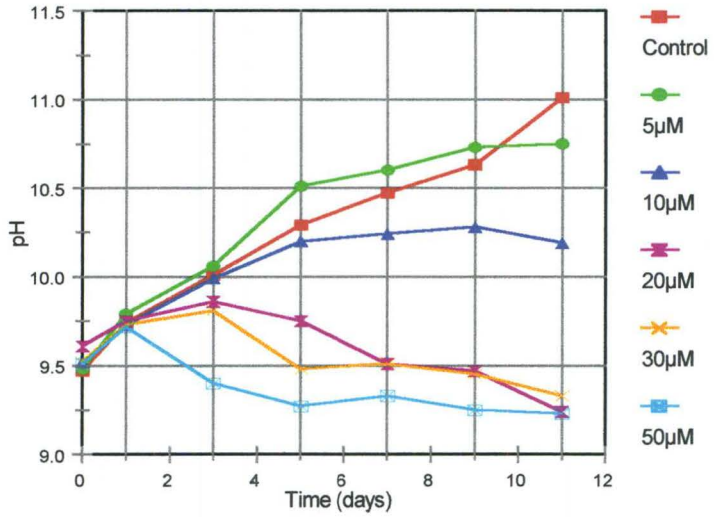

Figure 3.8: Mean pH vs time for copper toxicity study (n = 3)

appeared unaffected, while the 10μM cultures had begun to deteriorate.

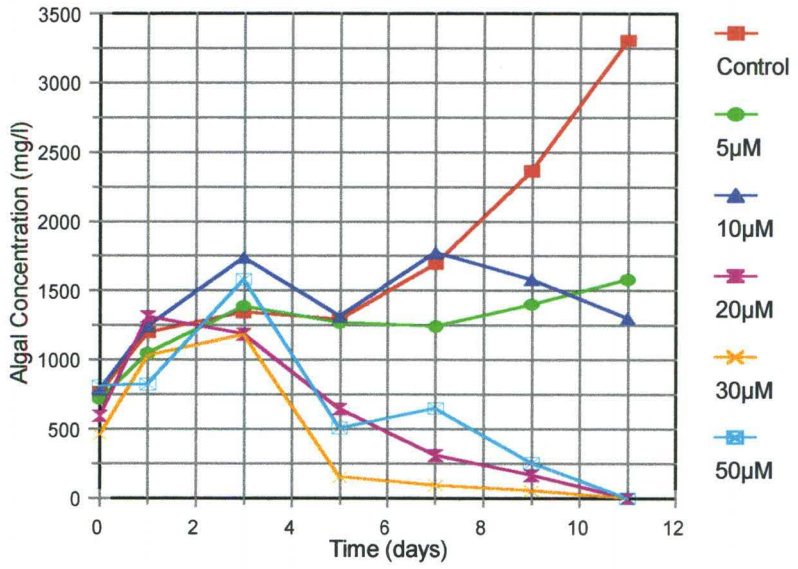

Figure 3.9: Mean algal concentration vs time for copper toxicity study (n = 3). Algal concentration determined from chlorophyll extractions

The effect of the copper on the cell morphology is shown in figures 3.10 to 3.13. A sequential degradation process can be observed, beginning with the unravelling of the coiled filaments (Figure 3.10) and progressing to complete disintegration of the filaments. After two days of exposure to copper at a concentration of 50μM the filaments had begun to uncoil and several had started to break up. After four days the disintegration process had progressed appreciably and large amounts of cell debris were visible (Figure 3.12). This appeared to be accompanied by the loss of a proportion of the cell contents, which resulted in some distortion of the individual cells (Figure 3.13), possibly as a result of reduced turgor pressure. Brady *et al.* (1994) found similar changes in the morphology of the yeast *Saccharomyces cerevisiae* following exposure to elevated concentrations of copper, with the cell surface becoming convoluted and the overall cell size decreasing slightly.

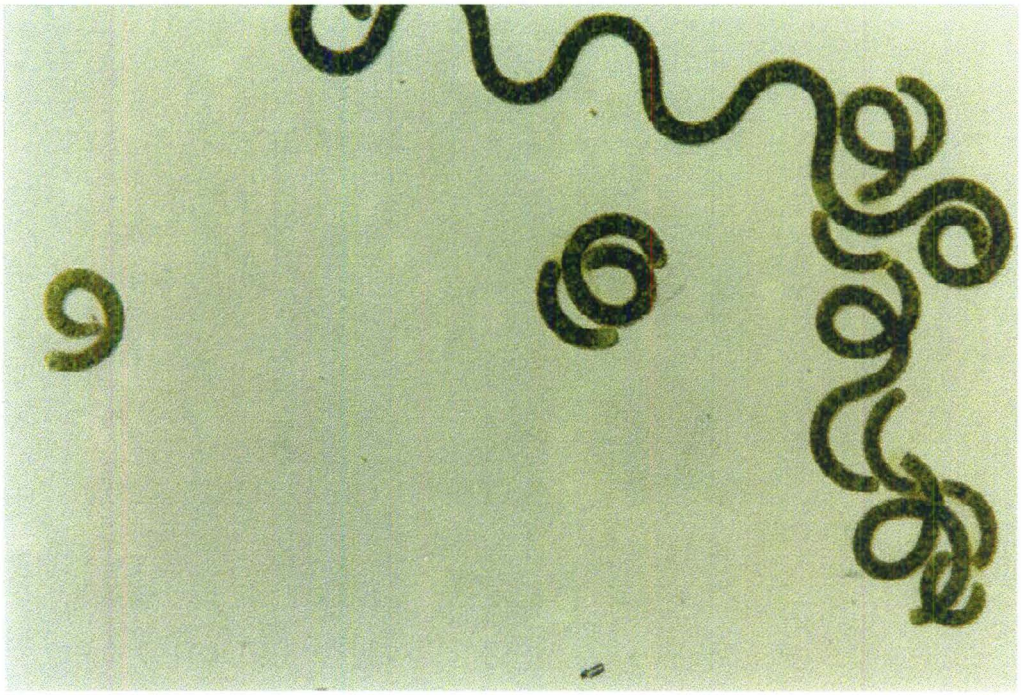

Figure 3.10: Light microscope preparation of *Spirulina* after two days exposure to 50μM Cu^{2+} showing uncoiling of the helical trichome

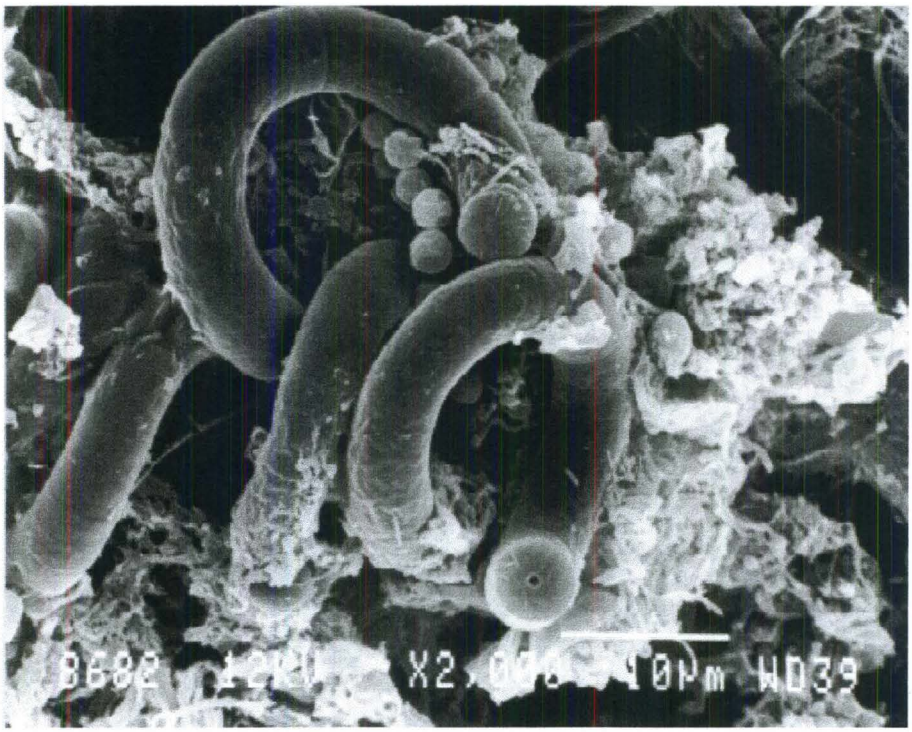

Figure 3.11: SEM preparation of *Spirulina* after two days exposure to 50μM Cu^{2+}

Figure 3.12: Light microscope preparation of *Spirulina* after four days exposure to 50μM Cu^{2+} showing yellowing and disintegration of filaments

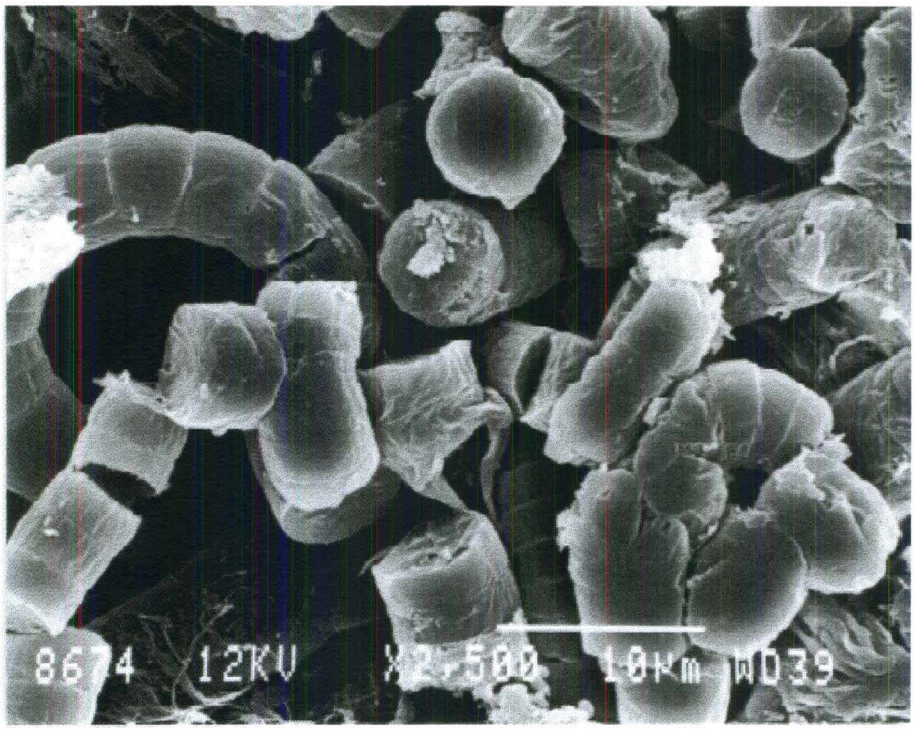

Figure 3.13: SEM preparation of *Spirulina* after four days exposure to 50μM Cu^{2+} showing extensive disruption of the filaments and distortion of the individual cells

The results from the acid digests, showing the amount of copper associated with the cell and remaining in solution are shown in figures 3.14 and 3.15. Figure 3.14 shows that there was a rapid increase in the copper accumulation after day three in the 20-50μM groups, but if one compares figure 3.14 to the graph of algal concentration (Figure 3.9) it can be seen that day three is when the cultures began to deteriorate. The data in figure 3.14 are expressed as μmoles of copper per gram of dry mass, which is determined from the chlorophyll *a* values. As the cells begin to die the chlorophyll concentration decreased, so while the actual mass was not affected the estimate of dry mass, based on the chlorophyll data, was reduced. Therefore, the graph only gives an accurate representation of the copper accumulation in the 20, 30 and 50μM groups up to day three. The data suggest that the threshold level for copper accumulation is approximately 7μmoles/g, because as soon as the amount of copper accumulated exceeded this value the cells began to die. The copper concentration in the cells in the control, 5 and 10μM groups never exceeded this value and the cultures remained viable after 11 days.

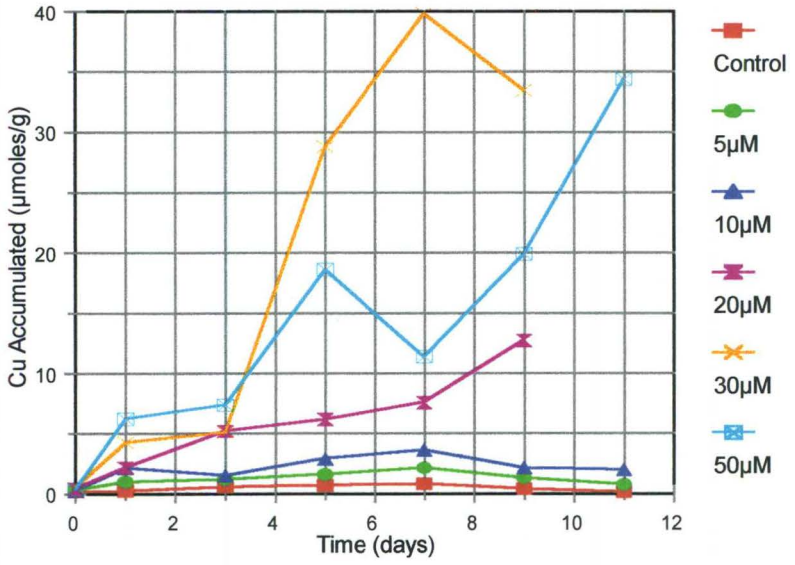

Figure 3.14: Copper accumulation by *Spirulina* over an 11 day period (mean values, n = 3)

Figure 3.15, showing copper concentration in solution, gives a clearer indication of what occurred. The peaks seen on day one were as a result of the initial spiking of the cultures. There was a steady decrease in the copper in solution in all groups as a result of accumulation by the cells. On day four, additional copper was added to restore the concentration of metal in solution to the initial levels. Following second dosing there was no significant decrease in the copper concentration. This is most likely due to the binding of copper to extracellular polysaccharides released by the algae. The bound copper stayed in solution, but couldn't be bound by the algae.

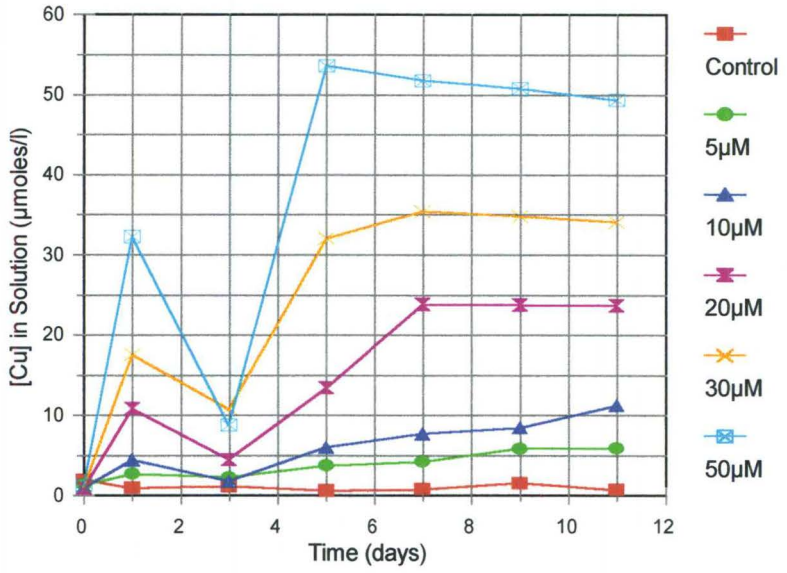

Figure 3.15: Concentration of copper remaining in solution over 11 day period. Initial dosing occurred on day 0 and subsequent dosing on day 4 (mean values, n = 3)

Figure 3.16 clearly shows a significant increase in extracellular carbohydrate following the addition of copper to the medium. The increase is proportional to the dosage with copper. The concentration of extracellular carbohydrate observed in the copper stressed cultures are in the same order of magnitude as observed by Singh *et al.* (1999) with *Nostoc spongiaeforme*. The increase in extracellular carbohydrate is less significant and slower in the control and 5µM cultures and is most likely due to nutrient stress. Brady *et al.* (1994) found that yeast cells which had been serially cultured in a medium containing copper showed reduced biosorptive capacity when exposed to high concentrations of copper.

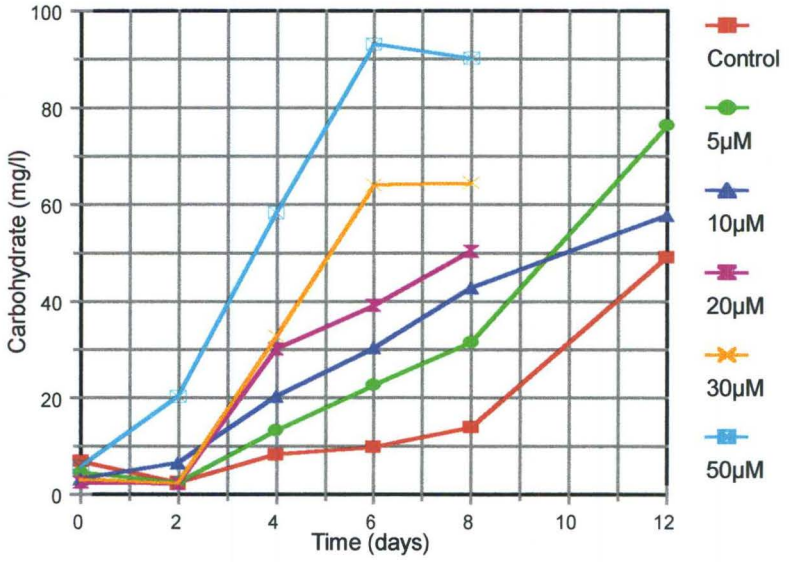

Figure 3.16: Concentration of extracellular carbohydrate vs time during copper toxicity studies. Carbohydrate concentration is expressed as mg/l glucose equivalents (mean values, n = 3)

3.4.4.2 Zinc

The results obtained for zinc showed the same basic trends as in the copper experiments. The onset of the toxic effects was rapid in the 20, 30 and 50µM groups (Figure 3.17) and although the affected groups took longer to die completely, this can be accounted for by the higher initial algal concentration. The studies on the different metals were performed consecutively and there was an initial acclimation period during which the algal growth rate in individual flasks may have differed. It was therefore not possible to ensure that the algal concentration at the time of metal dosing was the same in each flask. Figure 3.18 once again showed a strong positive correlation between algal culture strength and pH, indicating that pH is directly related to metabolic function.

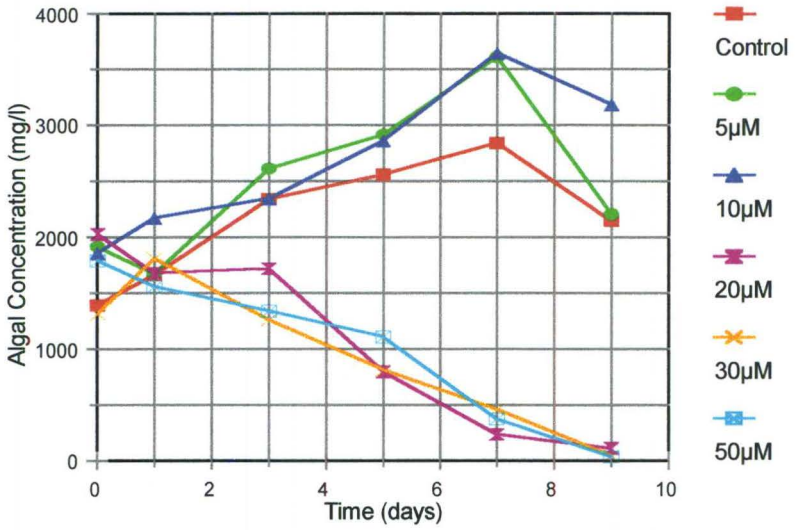

Figure 3.17: Mean algal concentration vs time for zinc toxicity study (n = 3). Algal concentration determined from chlorophyll extractions

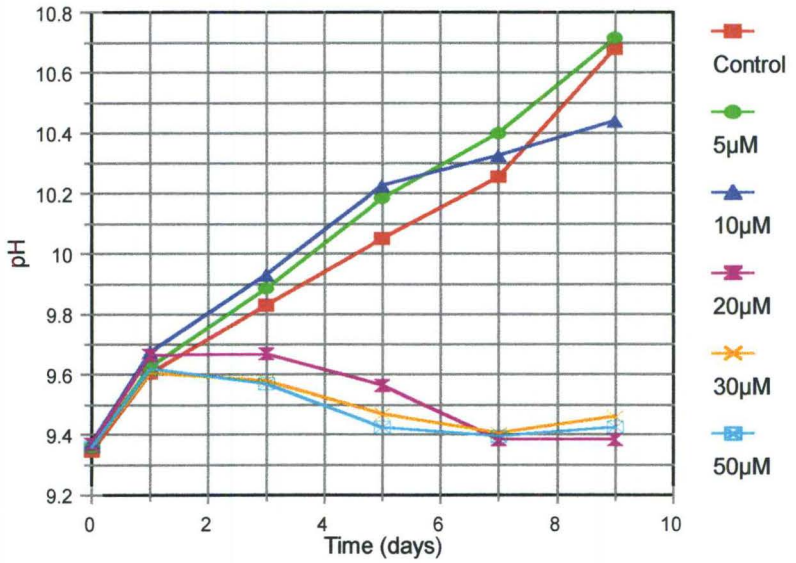

Figure 3.18: Graph of pH vs times for zinc toxicity study (mean values, n = 3)

Figure 3.19, showing zinc accumulation by the culture, suggests that the *Spirulina* is capable of tolerating approximately 5μmoles/g of zinc, as the cultures began to deteriorate once the concentration exceeded this. The reason for the dramatic increase in zinc accumulation seen in the 30 and 50μM groups after day five and seven respectively, is the same as for the similar trend observed during the copper study.

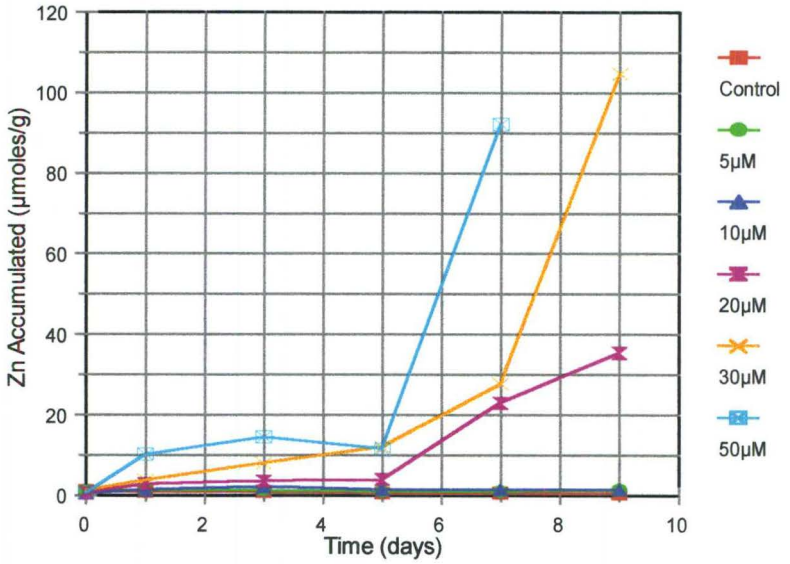

Figure 3.19: Zinc accumulated by *Spirulina* over 11 day period (mean values, n = 3)

The zinc in solution (results not shown) measured on day one was lower than the copper in the corresponding experiments and the reduction could not be attributed entirely to algal accumulation. This suggests that a portion of the zinc had either precipitated or been adsorbed to colloidal material, although the lack of significant amounts of extracellular carbohydrate (maximum concentration 30mg/l for 10μM culture) provides evidence for precipitation. There was a 5-10% increase in the zinc in solution between days three and five in the 20, 30 and 50μM groups, which was most likely as a result of metal being released as the cells began to disintegrate.

The deterioration of the cells can be seen in the photographs of the *Spirulina* grown in 50μM Zn^{2+} (Figures 3.20 and 3.21). The figures show the state of the cells after two days. At this point the cells looked healthier than at the corresponding time when challenged with copper. This could

be as a result of the higher initial algal concentration. After four days (Figures 3.22 and 3.23) the cells showed a greater degree of morphological damage, although they had not yellowed to the extent seen in the copper experiments. In addition the smooth appearance on the cell wall suggests that there has not been significant loss of cell contents.

Copper is known to affect photosynthetic electron transport, especially in photosystem II. In addition, copper has been shown to interfere with pigment and lipid biosynthesis and consequently chloroplast ultrastructure (Stauber and Florence, 1987; Guanzon *et al.*, 1994; Barón *et al.*, 1995). While zinc has also been shown to inhibit photosynthesis, it requires higher concentrations to have an equivalent effect on photosynthesis, as compared to copper (Davies, 1983). Therefore, the difference in colour between the cultures grown in zinc and copper could be due to the more acute affect of copper on the photosynthetic pigments.

Copper has also been shown to increase the permeability of algal cells, whereas zinc did not (Overnell, 1975). This would explain why the surface on the copper treated cells became distorted after a number of days, presumably as a result of the loss of turgor pressure.

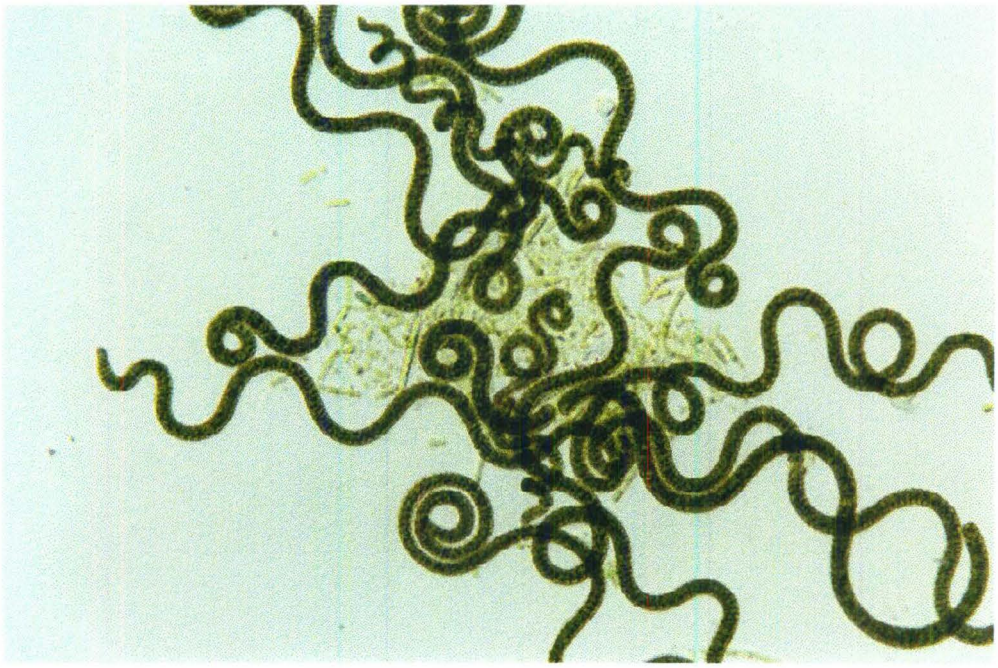

Figure 3.20: Light microscope preparation of *Spirulina* after exposure to 50μM Zn^{2+} for two days

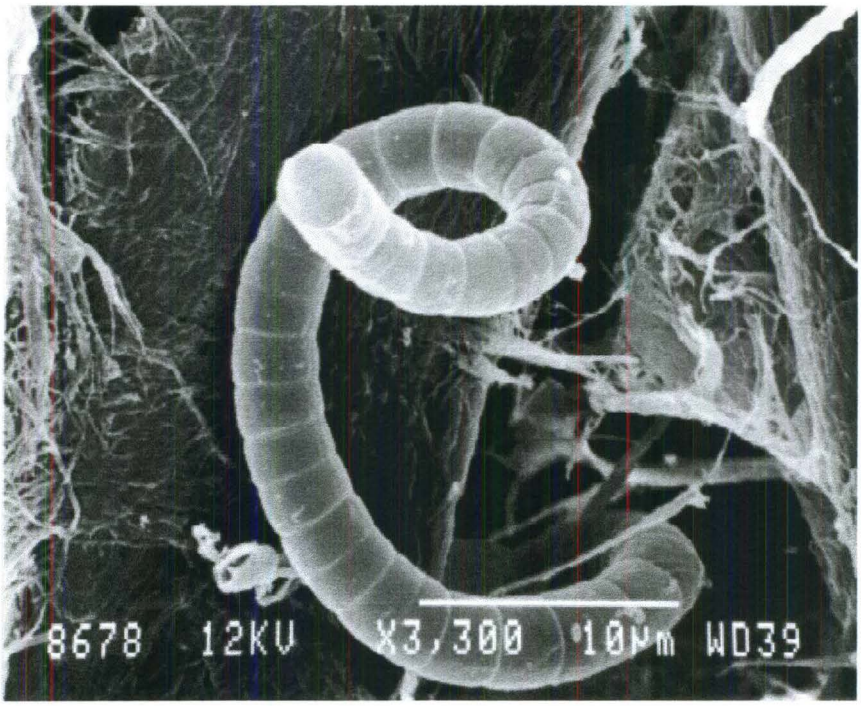

Figure 3.21: SEM preparation of *Spirulina* after exposure to 50μM Zn^{2+} for two days. Light specks on the cell surface represent electron dense regions possibly indicating metal accumulation

Figure 3.22: Light microscope preparation of *Spirulina* after exposure to 50μM Zn^{2+} for four days showing reduced degradation of photosynthetic pigments relative to copper treated cells

Figure 3.23: SEM preparation of *Spirulina* after exposure to 50μM Zn^{2+} for four days showing extensive filament degeneration without distortion of cell shape

3.4.4.3 Lead

The growth curve data (Figure 3.24) indicated that lead is not as toxic to *Spirulina* as copper or zinc. The first sign of any significant decline in algal concentration occurred on day 7, at which point all groups, including the control, began to decline. This suggests that nutrient depletion was a contributing factor. Lead clearly had an inhibitory effect at high concentrations, as the cultures subjected to 50μM Pb^{2+} showed a reduced increase in algal concentration (Figure 3.24) and a decrease in pH after day three (results not shown). This indicates that there was no active growth in that group after day three. All the other cultures appear to have been affected to a reduced degree until day seven when all began to decline. As a result a threshold level could not be determined for lead.

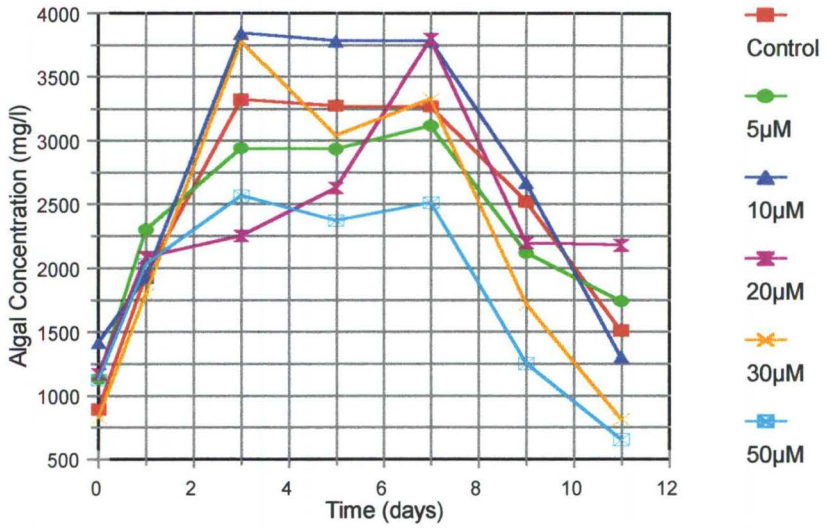

Figure 3.24: Mean algal concentration vs time for lead toxicity study (n = 3). Algal concentration determined from chlorophyll extractions

Lead has been shown to inhibit the electron transport chain (ETC) in *Spirulina platensis*, but had relatively little effect on the photsynthetic pathway compared to copper (Murthy and Mohanty, 1995). Results of work conducted by Murthy and Mohanty (1995) are summarised in table 3.4. The inhibition of the ETC would result in reduced energy being available for cellular metabolism, which would reduce cell growth and division. The results for the lead studies are consistent with this. The high level of inhibition of PSII by copper of similar concentrations to those used in this study provides further evidence to support the data presented in section 3.4.4.1.

Table 3.4: Effect of various concentrations of copper and lead on the electron transport chain (ETC) and photosystem II (PSII) activity in *Spirulina platensis* (Murthy and Mohanty, 1995).

Metal salt	Conc. (μM)	Inhibition of ETC (%)	Conc. (μM)	Inhibition of PSII (%)
Control	0	0	0	0
$CuCl_2$	6	5	6	7
	18	26	18	50
$Pb(NO_3)_2$	6	21	18	6
	18	35	36	16

While lead did not have the same level of acutely toxic effect on the algae it did induce gross changes in cell morphology (Figures 3.25 and 3.26). The filaments do not appear to break apart, but become shrivelled in appearance. As the experiment proceeded an increasing amount of cellular debris became apparent. As there was little evidence of gross cellular disintegration it appears the debris consisted of cellular contents that had leaked out of the cells. Due to the saline nature of the growth medium, water would not diffuse into the cells resulting in a loss of turgor pressure and the cells developing a shrivelled appearance.

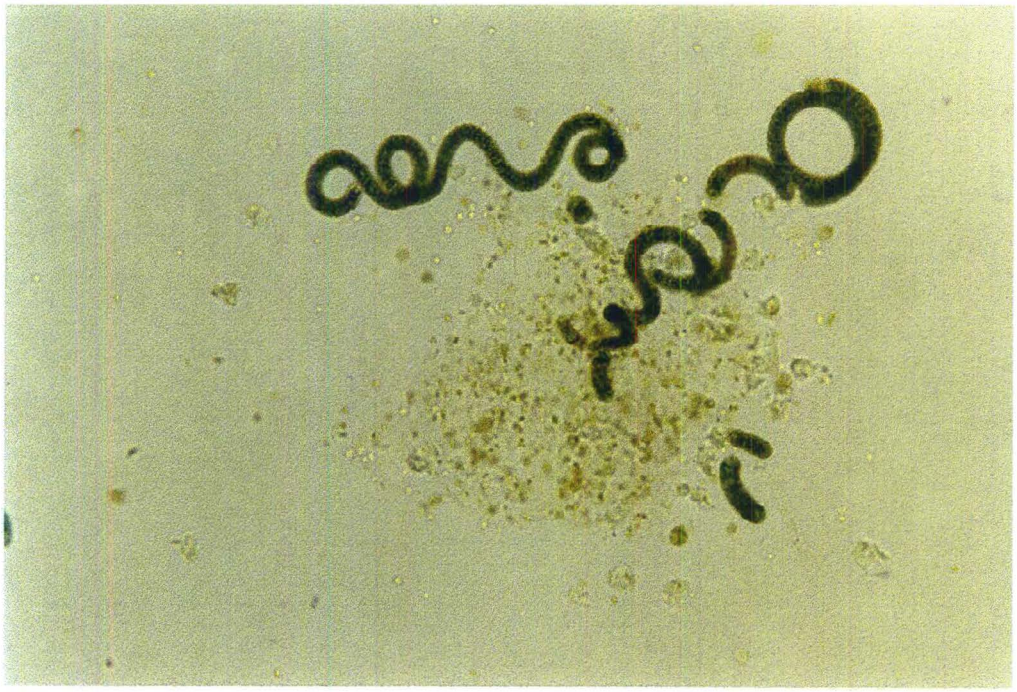

Figure 3.25: Light microscope preparation of *Spirulina* after exposure to 50μM Pb^{2+} for four days

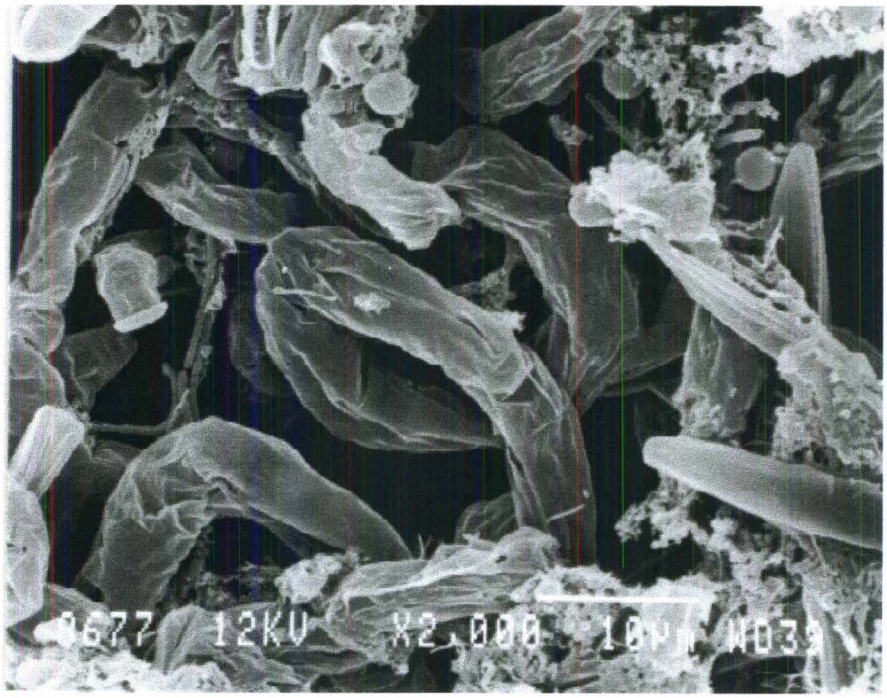

Figure 3.26: SEM preparation of *Spirulina* after exposure to 50μM Pb^{2+} for four days showing intact filaments, but grossly distorted cell surface

3.5 Conclusions

This study shows that using *Spirulina,* in a direct algal pond treatment system, for an effluent containing even moderate concentrations of toxic heavy metals, such as copper and zinc, is not a viable option.

The biosorption data indicate that the adsorption of heavy metals to the *Spirulina* biomass complies well ($r^2 > 0.92$) with the Langmuir monolayer model, until active transport across the cell wall begins to occur. The kinetics of metal adsorption follows a similar pattern to that reported for other biosorbents and the affinity series of Pb>Cu>Zn conforms to published results obtained using a variety of biomass types. The adsorption capacity of *Spirulina* is significantly lower than what has been reported for most other algal and fungal species. This was true for all the metals tested.

The treatment of an effluent from a base metal mine by direct contact with *Spirulina* cultures was effective for a period of time, although the majority of metal removal could be attributed to alkaline precipitation as a result of the high bicarbonate content of the growth medium.

The exposure of the algae to copper induced the excretion of copper complexing polysaccharides. The copper-polysaccharide complex remained in solution, but the copper in the complex did not appear available for algal binding or accumulation. In terms of effluent treatment the presence of high concentrations of polysaccharide is not desirable as it prevents effective copper removal from solution. Zinc and lead did not stimulate significant polysaccharide secretion.

The toxicity data show that copper and zinc are both acutely toxic to *Spirulina*, with threshold toxicity levels of below 10μmoles of metal per gram of biomass. The mechanism of toxicity appears different with the results suggesting copper affects the photosynthetic pigments and the integrity of the cell membrane, resulting in chlorophyll breakdown and the leakage of cell contents. Lead was less toxic, but did induce considerable changes in cell morphology with the cells becoming highly distorted. Lead has been reported to affect membrane stability and the

SEM images suggest that leakage of water and cellular components induced a loss of turgor pressure in the lead treated cells.

A significant finding was the ability of the algae to modify the aqueous chemistry of the surrounding medium through the utilisation of bicarbonate ions as a source of carbon dioxide for photosynthesis. The net result is an increase in pH and decrease in acidity of the system. This could be clearly seen by comparing the rate of pH change between the experimental and control groups in the effluent treatment study. The potential application of the phenomenon in wastewater treatment will be investigated in chapter four.

CHAPTER 4. ALGAL MODIFICATION OF THE AQUEOUS ENVIRONMENT - THE ROLE OF CARBONIC ANHYDRASE

4.1 Introduction

The data presented in the previous chapter showed that *Spirulina* was able to increase the pH of the surrounding medium and that, when dosed with an acidic effluent, the rate of pH decrease was significantly slower in flasks containing algae than the corresponding controls. This phenomenon, driven by the enzyme carbonic anhydrase, presents very real possibilities for the remediation of acidic effluents.

4.1.1 Carbonic anhydrase

Carbonic anhydrase (CA), also referred to as carbonate hydrolyase or carbonic dehydratase is a zinc containing metalloenzyme which catalyses the reversible interconversion of carbon dioxide (CO_2) and bicarbonate (HCO_3^-) with a maximum turnover number in excess of 10^6 s^{-1} (Braus-Stromeyer *et al.*, 1997; Eriksson *et al.*, 1996; Hiltonen *et al.*, 1998; So and Espie, 1998; Sültemeyer, 1998).

CA is a ubiquitous enzyme that has been isolated from a diverse range of organisms, including animals, plants, eubacteria, archaebacteria and viruses. To date no fungal CAs have been identified (Eriksson *et al.*, 1996; Hiltonen *et al.*, 1998; Sültemeyer, 1998). CA has been implicated in multiple and diverse physiological processes, including pH homeostasis, facilitated diffusion of CO_2, interconversion of CO_2 and HCO_3^-, ion transport, photosynthesis, efficient virus replication, calcification, bone resorption and the synthesis of urea, glucose and lipids (Braus-Stromeyer *et al.*, 1997; Eriksson *et al.*, 1996; Hiltonen *et al.*, 1998; So and Espie, 1998; Sültemeyer, 1998; Tashian, 1989).

The enzyme is classified into three independent CA gene families, namely α, ß and γ. There is little similarity in the DNA sequence between the three families, indicating that the genes have evolved independently at least three times. The α family is found primarily in animals, although

homologues have been found in the bacterium *Neisseria gonorrhoeae* and the periplasmic space of the green algae *Chlamydomonas reinhardtii*. This is the most extensively studied CA family and includes the mammalian CA isozymes. The ß family was originally isolated from the stroma of higher plants, but has subsequently been identified in various bacteria and algal species. The γ family has only recently been discovered with only one representative characterised to date (Eriksson *et al.*, 1996; Hiltonen *et al.*, 1998; Sültemeyer, 1998).

4.1.2 Structure of carbonic anhydrase

4.1.2.1 α-carbonic anhydrases

Mammalian CAs are divided into three groups, I, II and III, which share extensive homology in primary structure. All have a molecular mass of approximately 29kDa. In addition, crystal structures have shown that the secondary and tertiary structures are also similar (Tashian, 1989; Silverman, 1991).

Typically they are ellipsoidal molecules, approximately 5 x 4 x 4nm, which could be considered single-domain proteins were it not for the loosely connected amino terminal region of about 24 amino acids. A 10-stranded, twisted ß-sheet is the dominant tertiary structure (Figure 4.1), which divides the molecule into two halves. The upper half includes the N-terminal helical region and the active site, while the lower half contains a large hydrophobic core. The ß-sheets, with the exception of two pairs of parallel strands, are antiparallel and are connected by hairpin loops and some helices. A number of relatively short helices are present on the surface of the molecule (Freskgård *et al.*, 1991; Lindskog, 1997).

The active site is located in a large, cone shaped cavity that penetrates close to the centre of the molecule. The zinc ion occurs at the base of the cleft (Figure 4.1) and is tetrahedrally co-ordinated to the imidazole rings of three histidine residues. The fourth co-ordination position is occupied by a water molecule. The ionisation of the water molecule is critical to the catalytic pathway (Silverman, 1991). The water ligand is hydrogen bonded to the side chain of Thr_{199},

which in turn is hydrogen bonded to the side chain of Glu_{106}. These two amino acids are conserved in all α-CAs.

Figure 4.1: Tertiary structure of human carbonic anhydrase II. Cylinders represent α-helices and arrows the ß-sheets. Zinc ion shown in green

4.1.2.2 ß-carbonic anhydrases

While no crystal structures of ß-CAs have yet been determined, they differ considerably from α-CAs in several respects. Their primary structure is entirely different which has made it impossible to identify any active site residues from sequence alignments (Johansson and Forsman, 1993). The ß-CAs contain a greater number of cysteine residues, compared to the α-CAs. Furthermore the oligomeric structure is different, although there has been some debate as to whether the molecule is a hexamer (Silverman, 1991) or an octomer (Johansson and Forsman, 1993). The ß-CAs also appear to have a greater number of α-helices compared to the α-CAs, which are composed primarily of ß-sheets.

4.1.3 Catalytic mechanism

The catalytic mechanism has been extensively studied using human carbonic anhydrase II (HCA II) and can be divided into two parts. The first part involves the interconversion of CO_2 and HCO_3^- (Equation 1). This is controlled by the catalytically active zinc-bound water molecule, which can be hydrolysed to a hydroxide ion. The second part is the regeneration of the active form of the enzyme (E), which involves the transfer of a proton from the catalytic site to the surrounding medium (Equation 2). The zinc bound hydroxide ion attacks a carbon dioxide molecule to form a metal bound bicarbonate ion, which is then displaced by a water molecule (Equation 1). The zinc bound hydroxide is regenerated by a rate-limiting transfer of a zinc-bound water proton to the His-64 residue, which delivers the proton to a buffer base (Equation 2). The reactions are shown in greater detail in figure 4.2 (Lindskog, 1997).

$$EZnOH^- + CO_2 \leftrightarrows EZnH_2O + HCO_3^- \quad (1)$$

$$EZnH_2O + B \leftrightarrows EZnOH^- + BH^+ \quad (2)$$

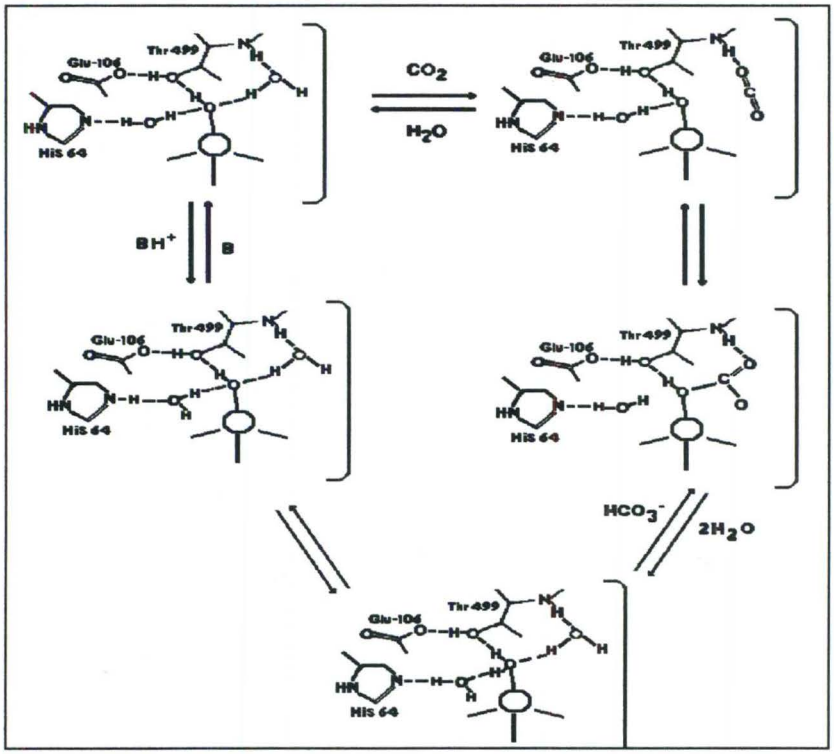

Figure 4.2: Schematic representation of the catalytic mechanism of HCA II (Lindskog, 1997)

4.1.3.1 ß-carbonic anhydrases

The catalytic capabilities of the ß-CAs are similar to those of the α-CAs, despite their different evolutionary origin. The kinetic parameters relating to the hydration of carbon dioxide by pea carbonic anhydrase indicated that the enzyme was as efficient as HCA II, although the observed kinetic patterns were more complex. The results were consistent with a zinc-hydroxide mechanism and the presence of a buffer-dependent proton-transfer step, although the proton transfer mechanism appeared different (Johansson and Forsman, 1993; Lindskog, 1997).

4.1.4 Inhibitors of carbonic anhydrase

The most extensively studied CA inhibitors are the sulfonamides. Aromatic and some heterocyclic sulfonamides, possessing the general formula $R\text{-}SO_2NH_2$ (or $R\text{-}SO_2NH(OH)$) are powerful and specific inhibitors of most CAs. They bind to the zinc ion as anions, via the nitrogen atom of the sulfonamide group (Lindskog, 1997; Moroney *et al.*, 1985). The NH group of the ionised sulfonamide replaces the zinc-bound water molecule and hydrogen bonds to the OH group of Thr_{199}.

Most monovalent anions are able to inhibit CA function, although the dissociation constants of the enzyme-anion complex vary considerably, from a few μM for CN^- to about 1M for F^-. The monovalent anions interfere with the hydrogen bonds formed between the zinc-bound water and the associated amino acid side chains (Lindskog, 1997).

4.1.5 Carbonic anhydrase in microalgae and cyanobacteria

The primary function of CA in algae, as in higher plants, is to increase the concentration of carbon dioxide around the photosynthetic enzyme ribulose biphosphate carboxylase (Rubisco). Both microalgae and cyanobacteria live in an aqueous medium where the concentration of carbon dioxide surrounding the cells is significantly less than that surrounding aerial plants. In order to maintain optimal photosynthetic rates these organisms have developed a carbon concentrating mechanism (CCM) that functions to raise the intracellular carbon dioxide concentration to a level

far in excess of that present in the surrounding environment. Carbon dioxide derived from this internal pool is used by Rubisco to initiate the first reaction in the Calvin cycle, the carboxylation of ribulose biphosphate. The inorganic carbon (C_i) transport system and CA are critical to the functioning of the CCM. The enzyme is induced by low levels of dissolved CO_2 and light (Badger and Price, 1992; Beardall *et al.*, 1998; Moroney and Chen, 1998; Sültemeyer, 1998).

4.1.5.1 Microalgae

The majority of the research into algal carbonic anhydrase has been conducted using *Chlamydomonas reinhardtii*, and the data accumulated have led to a broad understanding of the CCM in eukaryotic algae. A model of the CCM is shown in figure 4.3 (Sültemeyer, 1998). This shows that the inorganic carbon needs to cross the cell wall, the plasma membrane and the membranes of the chloroplast envelope before it reaches the pyrenoid containing the Rubisco (Badger and Price, 1992).

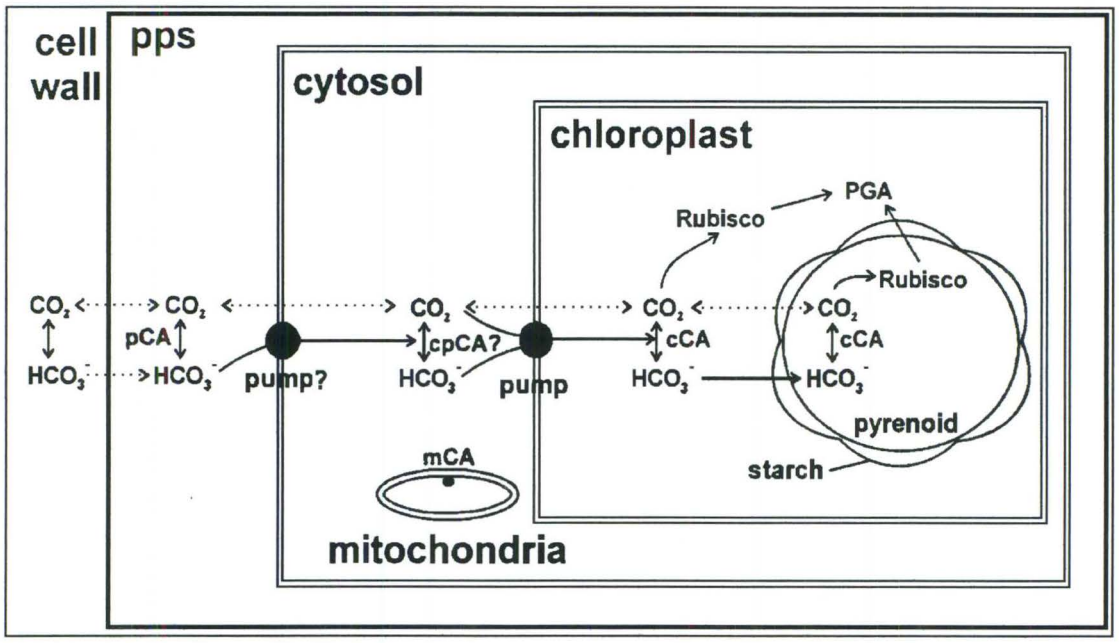

Figure 4.3: Proposed model for the carbon concentrating mechanism of *Chlamydomonas reinhardtii* as a model organism for microalgae (Sültemeyer, 1998)

There has been considerable debate as to which inorganic carbon species is actively transported across the membranes. Historically, it was assumed that bicarbonate was the species involved, but recent research has indicated that an active CO_2 uptake system exists in some organisms

(Sültemeyer *et al.*, 1989) and that plastids are able to actively transport both CO_2 and HCO_3^- (Amaroso *et al.*, 1996).

Both extracellular and intracellular forms of the enzyme have been isolated from a variety of algal species (Williams and Coleman, 1996; Flores-Moya and Fernández, 1998). It is believed that the extracellular form accelerates the extracellular equilibration of CO_2 and HCO_3^- to provide CO_2 at a sufficient rate to enter the cell and serve as a substrate for photosynthetic reduction. The periplasmic enzymes are particularly important for the acquisition of inorganic carbon under alkaline pH conditions, where HCO_3^- is the predominant species (Husic and Marcus, 1994).

4.1.5.2 Cyanobacteria

Cyanobacteria are structurally different from eukaryotic algae, lacking discrete chloroplasts. The photosynthetic pigments are concentrated in carboxysomes. CA activities have been found to be lower and more variable in cyanobacteria. The enzyme appears to be either granular or soluble in nature, depending on the species (Badger and Price, 1989).

The mechanisms by which C_i transport occurs in cyanobacteria is still not well understood. A number of methods have been used to try and discriminate between transport of CO_2 and HCO_3^- and a general picture has emerged which indicates that the C_i transport system can utilise both species as substrates. The transport of CO_2 is, however, considered constitutive while the ability to accumulate HCO_3^- appears to be induced as a response to low external CO_2 concentrations. Regardless of the species accumulated from the external medium, it is HCO_3^- that is delivered into the cytosol. This HCO_3^- penetrates the carboxysomes, which contain the vast majority of the cell's Rubisco. In the carboxysomes specifically located CAs generate CO_2 in the immediate vicinity of the Rubisco (Al-Moghrabi *et al.*, 1996; Badger and Price, 1992; Sültemeyer *et al.*, 1995).

4.1.6 Implications for aqueous species equilibrium

Carbonic anhydrase, which is a critical component of the CCM of algae and cyanobacteria, is able to increase the CO_2 concentration around the photosynthetic enzyme Rubisco. The enzyme catalyses the interconversion of CO_2, H_2CO_3 and HCO_3^- via enhanced rates of hydration/dehydration. The simplified reactions involved in this process are as follows:

$$CO_2 + H_2O \rightleftharpoons H_2CO_3 \quad (3)$$

$$H_2CO_3 \rightleftharpoons HCO_3^- + H^+ \quad (4)$$

$$HCO_3^- \rightarrow CO_2 \text{ (inside cell)} + OH^- \text{ (outside cell)} \quad (5)$$

In the presence of elevated concentrations of bicarbonate in the surrounding medium equations (3) and (4) become negligible and equation (5) dominates. This leads to an accumulation of hydroxide ions in the medium, resulting in an increase in pH (Shiraiwa *et al.*, 1993). The increased pH shifts the bicarbonate/carbonate aqueous equilibrium towards carbonate formation. This phenomenon has been termed "alkalisation" (Haglund *et al.*, 1992; Shiraiwa *et al.*, 1993), but a closer look at the chemistry reveals that the total alkalinity of the system does not change, rather the increase in pH represents a decrease in the acidity of the system. The net result of the accumulation of inorganic carbon, from bicarbonate, by algae and cyanobacteria is an increase in pH and the shift in carbonate species equilibrium from bicarbonate to the more reactive carbonate and hydroxide species.

This chapter will examine the efficiency of this mechanism and evaluate its potential application in the generation of reactive alkaline species for the remediation of metal contaminated acidic wastewaters.

4.2 Research aims

The primary aims of this section of the project were:

1) To extract carbonic anhydrase from *Spirulina* and determine enzyme activity.
2) To quantify the generation of reactive alkaline species from bicarbonate.
3) To evaluate the potential for remediation of heavy metal contaminated acidic wastewaters.

4.3 Materials and methods

4.3.1 Algal biomass

Algal biomass was obtained from stock cultures as described in chapter 3.

4.3.2 Carbonic anhydrase assay

4.3.2.1 Assay system

The assay system was based on that of Wilbur and Anderson (1948) and modified according to Hiltonen *et al.* (1995) and Yang *et al.* (1985). The enzyme activity was determined electrochemically by measuring the time required for the pH to decrease from 8.2 to 7.2 when 2ml of ice-cold CO_2 saturated deionised water was added to 4ml of Veronal buffer (20mM, pH 8.3, 4°C) containing the test material. One unit of activity (Wilbur Anderson Unit (WAU)) was defined as:

$$WAU = t_0/t - 1$$

where t_0 was the time taken in an enzyme-free buffer (control) and t was the time taken in the experimental samples. Commercially pure bovine carbonic anhydrase, with an activity of 8100 WAU, was obtained from Sigma Aldrich. Carbonic anhydrase standards (10-150 WAU/ml) were prepared by diluting the stock solution. 100µl aliquots of standard were used in each individual

assay. Carbon dioxide saturated water was prepared by bubbling CO_2 through 400ml of double distilled water (ddH_2O) at 4°C for one hour just prior to use.

4.2.3.2 Sample preparation and partial purification

Initial whole cell assays using *Spirulina* yielded negative values so after consultation with Professor David Husic (Lafayette College, Pennsylvania) it was decided to use a sample which had been boiled for five minutes as a control to remove any variable that may have resulted from the presence of algae in the assay system.

Algal samples were prepared by centrifuging 1ml of culture at 2000g for 10min in an Eppendorf 5403 centrifuge. Pellets were washed in an equivalent volume of 1g/l NaCl (to avoid osmotic shock) and centrifuged at 7000g for 20min. The pellets were then resuspended in an appropriate volume of 20mM Veronal buffer (pH 8.3). A 200µl aliquot was used for each individual determination.

Partial purification was achieved by subjecting the sample to two passes through a French pressure cell at 1500psi. The homogenate was centrifuged at 11 500g for 20min in an Eppendorf 5403 centrifuge. The resulting supernatant was ultracentrifuged at 100 000g for 60min in a Beckman L-70 ultracentrifuge. All fractions were assayed for CA activity.

4.3.3 Titration method for determining the effect of algae on the aqueous chemistry

4.3.3.1 Analytical technique

An indirect method for assaying carbonic anhydrase activity by analysing the effect of the algae on the aqueous chemistry of the medium was developed as a result of the inaccuracies of the Wilbur Anderson method. A titration based system was developed to compare the effect of inorganic carbon accumulation by algae to the addition of sodium hydroxide (NaOH). The experiments were performed using 50mM sodium bicarbonate ($NaHCO_3$) in 1g/l NaCl. The number of moles of hydroxide ions required to increase the pH of 50ml of bicarbonate solution

from 7.0 to11.5 was determined. Titrations were repeated five times and the mean data used to generate formulae for the relevant conditions. The results showed that there were two phases over which the relationship between OH^- added and pH change were essentially linear. Regression analysis allowed the generation of the following formulae:

pH 7-9: $\mu moles\ OH^- = (\Delta pH \times 2.804) \times 100$ $(r^2 = 0.97)$

pH 9-11.5: $\mu moles\ OH^- = (\Delta pH \times 10.819) \times 100$ $(r^2 = 0.99)$

4.3.3.2 Batch experiments

For the batch experiments 50ml of 50mM $NaHCO_3$ in 1g/l NaCl, adjusted to pH 7, was inoculated with viable algae (20-500mg dry mass equivalent) that had been washed twice with 1g/l NaCl to remove any traces of alkalinity. The culture was agitated at 120rpm, using a magnetic stirrer and flea. The experiments were initiated by switching on a bank of six cold, white fluorescent lights. pH measurements were taken each minute for the first 30 minutes and at five minute intervals thereafter. The temperature was maintained between 25 and 27°C. Control experiments were conducted without addition of algae and in the absence of light. All experiments were repeated five times and mean values reported. The experiments were repeated using 50mg of algae, but after 60 minutes the pH was reduced to 8.3 by the addition of 0.02N sulphuric acid (H_2SO_4). Following the pH adjustment the reaction was again initiated by illumination and the pH change recorded.

4.3.3.3 Effect of substrate concentration

Flasks were set up as for section 4.3.3.2 (five replicates), but at bicarbonate concentrations of 5, 10, 25 and 50mM. The pH was adjusted to 8.3 to ensure maximum alkalinity as bicarbonate. The experiment was conducted for 30 hours, with pH measurements recorded hourly for the first 5 hours and at five hour intervals thereafter.

4.3.3.4 Inhibitor studies

Flasks were set up as in section 4.3.3.2 (five replicates) and the initial pH adjusted to 8.3. The effect of the CA inhibitor acetazolamide (AZ) was determined by dosing the cultures with the appropriate volume of 10mM AZ stock to achieve inhibitor concentrations of 25, 50, 75 and 100μM. The experiment was initiated as before and the pH recorded at five minute intervals for 60 minutes.

4.3.4 Alkalinity assay

A second indirect method was used to determine the change in the aqueous alkaline species. A suitable volume of sample was filtered through a 0.45μm GF/C filter to remove algal biomass. The pH was recorded after which 0.02N sulphuric acid (H_2SO_4) was added using a burette. The pH was monitored continuously and the volume of acid added was recorded at pH 8.3 and 4.5. The total alkalinity was calculated using the equation below:

Total alkalinity as mg/l $CaCO_3$ equivalents = ml acid added x (1000/sample vol)

The alkaline species could theoretically be determined by using the volume of acid required to reduce the pH to 8.3 and comparing it to the amount needed to reach pH 4.5, but the results for the OH^- component proved inaccurate. A more accurate picture was obtained by using the aqueous species modelling software, MinteqA2, to predict the species present at a specific pH and total alkalinity.

4.3.5 Analysis and modelling of long term changes in aqueous chemistry

Spirulina cultures were set up in two litre culture flasks of Zarrouk's medium with an initial bicarbonate concentration of 16.8g/l. The cultures were maintained at 25°C with a light/dark cycle of 12 hours. Each day the pH of the cultures were recorded and a 10ml sample was removed, filtered through a 0.45μm GF/C filter and the alkalinity of the filtrate determined. The

pH and alkalinity data were entered into Minteq to generate a comprehensive model of aqueous species present in the solution.

4.4 Results and discussion

4.4.1 Carbonic anhydrase assay

The Wilbur Anderson assay method did not prove accurate, even when used to test the commercially pure enzyme. In all cases the calculated enzyme activity was significantly higher than what was predicted from the dilutions (Table 4.1), with the degree of error generally increasing with increased enzyme concentration, with the exception of the highest concentration.

Table 4.1: Comparison between expected and observed carbonic anhydrase activity units from commercially pure bovine carbonic anhydrase (n=5)

Expected activity WAUs	Observed activity WAUs	Standard deviation	Difference
1.000	1.296	0.351	0.296
2.000	4.107	0.496	2.107
3.000	7.791	0.256	4.791
4.000	10.114	0.560	6.114
5.000	12.579	0.570	7.579
15.000	21.179	0.748	6.579

The results of the carbonic anhydrase assays performed on the various fractions obtained from the partial purification are shown in figure 4.4. The results clearly show that the Wilbur Anderson assay method is not reliable. The standard deviations are unacceptably high, in most cases exceeding the mean value. The highest enzyme activity was found in pellets resulting from the ultracentrifugation step (P2). This would suggest that the enzyme is membrane bound, but if this was the case the supernatant from the first centrifugation step (S1) should have had the highest activity as P2 is derived from S1. A number of authors have noted that the Wilbur Anderson method can be fairly rough and insensitive, with very little or no activity being detected in

situations where substantial activity has been detected using alternative methods such as mass spectroscopy (Badger and Price, 1989; Haglund *et al.*, 1992; Raven, 1995). The methods however, require a pure enzyme preparation.

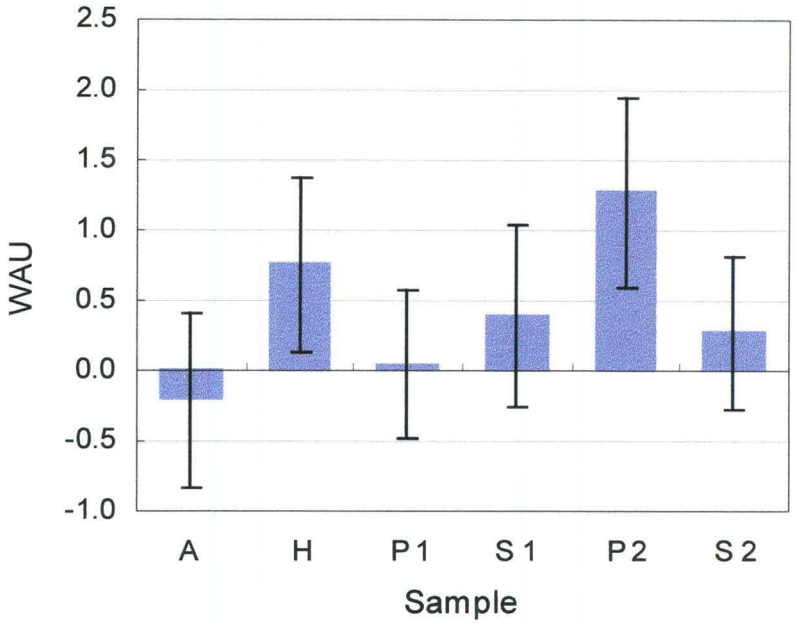

Figure 4.4: Carbonic anhydrase activity of partially purified fractions determined by Wilbur Anderson method. A = harvested algae, H = algal homogenate, P1 = pellet from 1st centrifugation, S1 = supernatant from 1st centrifugation, P2 = pellet from ultracentrifugation and S2 = supernatant from ultracentrifugation (n=5 ± SD)

4.4.2 Batch experiments

For the batch experiments 100mg of algae provided optimal results. The combined data from the batch experiment replicates are shown in figure 4.5. The net pH change over the 60 minute period was 1.31 units. By substituting the pH change into the equation derived from the standard curve this represents the equivalent of adding 367µmoles of OH^- ions. Therefore, it can be estimated that 1g of *Spirulina* (dry mass) is capable of generating the equivalent of 3670µmoles of OH^- ions per hour under the experimental conditions.

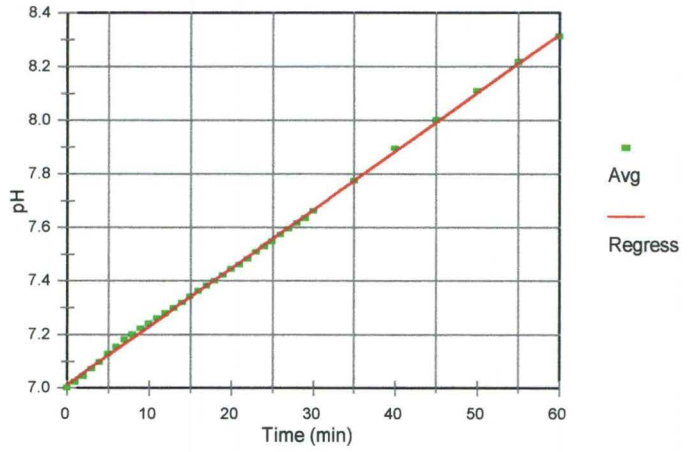

Figure 4.5: Mean data for pH increase vs time for batch experiments (n=5, SD<0.1 for all points, $R^2 = 0.999$)

No increase in pH occurred in the absence of algae or in the dark (results not shown). Figure 4.6 confirms the reduction of acidity during the accumulation of inorganic carbon. After the first 60 minutes the pH was adjusted back to 8.3 by the addition of 1.6ml of 0.02N H_2SO_4.

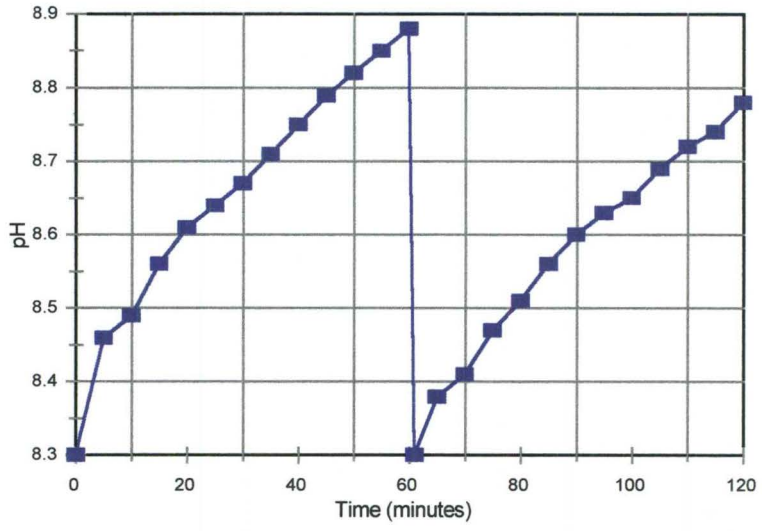

Figure 4.6: Change in pH vs time as a result of inorganic carbon accumulation. pH adjusted to 8.3 after 60 minutes by adding H_2SO_4 (mean values, n = 5)

The phenomenon can be explained in terms of acid and alkaline potential of the various species. The effect on alkalinity and acidity of the addition of various chemicals to water is summarised in table 4.2.

Table 4.2: Effect on alkalinity and acidity of the addition of various chemicals to water

X ppm of chemical added (expressed as $CaCO_3$)	Alkalinity change (as ppm $CaCO_3$)	Acidity change (as ppm $CaCO_3$)
NaOH	+ X	- X
$NaHCO_3$	+ X	+ X
CO_2	0	+ X

In the case of the carbonic anhydrase catalysed utilisation of bicarbonate by algae, the substrate (HCO_3^-) has an acid and an alkaline potential. The bicarbonate is split into CO_2 and OH^-, with the CO_2 being utilised for photosynthesis. This removes the acid potential from the right hand side of the equation. The hydroxide ion is released into the medium so the net change in the acid/alkaline potential of the medium from +1 acid and +1 alkaline to +1 alkaline and -1 acid. Therefore, the term "alkalisation" is not strictly correct as the alkaline potential has not changed, rather the acidity of the system has been reduced and hence the pH has increased.

The OH^- ions that are released into the medium affect the equilibrium between HCO_3^- and CO_3^{2-}, shown below.

$$HCO_3^- \rightleftharpoons CO_3^{2-} + H^+$$

The acid ionisation constant (K_a) for HCO_3^- (4.8×10^{-11}) suggests that at pH values below 8.3 all the carbonate alkalinity will be in the bicarbonate form. In the presence of a strong base, such as OH^- ($K_b = 1$), the reaction is driven to the right. The released protons equilibrate with the OH^- ions.

The validity of the reaction series proposed above can be tested by using Minteq to model the predicted pH at the end of the experiment. The proposed mechanism suggests that for each mole

of carbon dioxide that is derived from bicarbonate, a further mole of bicarbonate is converted to carbonate as a result of the release of hydroxide ions into solution. Using the data shown in figure 4.5 (first 60 minutes) it can be calculated that the pH change was equivalent to adding 160μmoles of OH^- ions. The proposed changes in alkaline species are shown in table 4.3.

Table 4.3: Proposed changes in alkaline species induced by algal uptake of inorganic carbon

Component	Time = 0	Time = 60min	Change
pH	8.30	8.89	+0.69
Na^+ (μM)	3 355	3 355	0
Cl^- (μM)	855	855	0
HCO_3^- (μM)	2500	2180	-320
CO_3^{2-} (μM)	0	160	+160

The pH is determined by the ions in solution. Therefore, if the proposed system is correct, the equilibrium pH predicted by Minteq using the ion concentrations from table 4.3 should be the same as the measured pH. Minteq predicted an equilibrium pH of 9.06 which is not significantly different ($P = 0.065$, $n=5$) from the experimental mean. The slightly lower pH measured in the experimental flasks is most likely as a result of the system being open, which would allow some carbon dioxide to diffuse into the medium and reduce the pH.

4.4.2.1 Effect of substrate concentration

The effect of initial substrate concentration on the rate of pH change induced by algal accumulation of inorganic carbon is shown in figure 4.7, which shows that the initial rate of pH increase is rapid. The pH change during the first hour is highest where the bicarbonate concentration is lowest. This is expected because the higher concentrations have a higher capacity to buffer change in pH. The effect of substrate limitation is clearly visible in the 0.5 and 1mM cultures. It has previously (section 4.4.2) been calculated that, under similar reaction conditions, *Spirulina* is capable of utilising up to 367μmoles of HCO_3^- per hour. It has also been demonstrated that a maximum of 50% of the bicarbonate is available for accumulation as the other 50% is converted to carbonate as a result of the release of hydroxide ions. The 5 and 10mM

$NaHCO_3$ cultures initially contained only 250 and 500µmoles of HCO_3^- ions respectively, so it is clear that this would rapidly become limiting and the pH would cease to increase. The decrease in pH observed in the 5mM cultures most likely occurred due to the release of carbon dioxide as a result of cellular respiration.

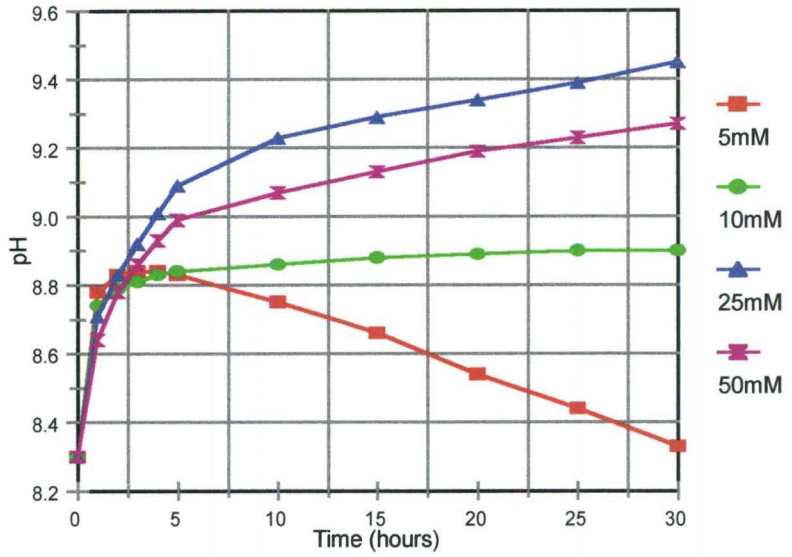

Figure 4.7: The effect of bicarbonate concentration on the rate of pH change induced by the utilisation of inorganic carbon by 100mg *Spirulina* (mean values, n = 5)

4.4.2.2 Inhibitor studies

The effect of the addition of a carbonic anhydrase inhibitor to the cultures is shown in figure 4.8. Acetazolamide (AZ) is a specific inhibitor of external CA. The molecule cannot enter the cell, so only affects enzyme that is associated with the cell wall and membrane. The results indicate that AZ has a significant effect on carbonic anhydrase at a concentration of 50µM and above, although the effect did not appear proportional to the concentration of inhibitor. The fact that there is still an increase in pH in the cultures grown at AZ concentrations of over 50µM suggests that both an internal and external CA enzyme are present in *Spirulina*. Sültemeyer *et al.*, (1998) has demonstrated that direct HCO_3^- transport can still occur in cells with an external CA. The HCO_3^- ions that are transported across the membrane can be utilised by internal CA in the region of the

carboxysomes. The OH^- ions generated inside the cell will still be released to the external environment, resulting in an increase in pH.

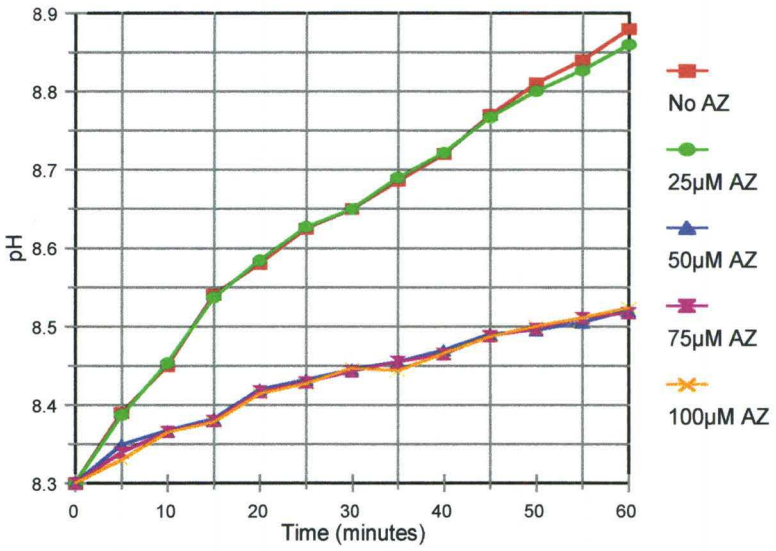

Figure 4.8: The effect of acetazolamide on carbonic anhydrase activity in *Spirulina* (mean values, n = 5)

4.4.3 Assessment of bioremediation potential

The effect of the change in carbonate species, induced by the algal accumulation of inorganic carbon, on the metal precipitation potential was assessed by direct measurement and predictive modelling. The two litre *Spirulina* cultures were maintained for a period of 13 days, at which point the cultures began to show signs of nutrient depletion. Over this period the pH increased from 8.6 to 9.8. Figure 4.9, which shows the change in alkaline species in solution over the experimental period, indicates a reduction of over 70% in the bicarbonate concentration by the end of the experimental period. There was a corresponding increase in the carbonate concentration. The molar relationship of carbonate generated relative to bicarbonate reduced is slightly below 50%. This is consistent with the proposed mechanism, as half the carbon is incorporated into the cells during photosynthesis. The increase in pH represents an increase in the concentration of OH^- ions relative to H^+ ions, but this could not be determined by the

alkalinity assay. To accurately determine the hydroxide concentration the data from figure 4.9 was entered into Minteq and the pH regulated speciation determined. The results are summarised in figure 4.10.

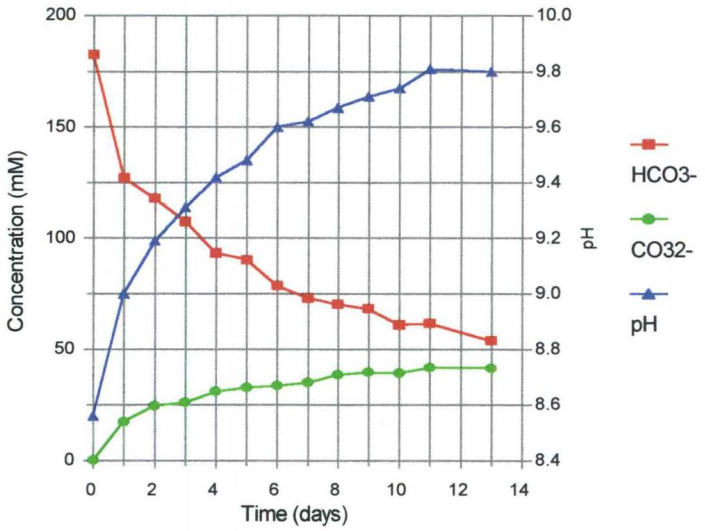

Figure 4.9: Changes in pH and alkaline species induced by cultivation of *Spirulina* in 2l Zarrouk's medium (16.8g/l $NaHCO_3$). Alkaline species determined by titration

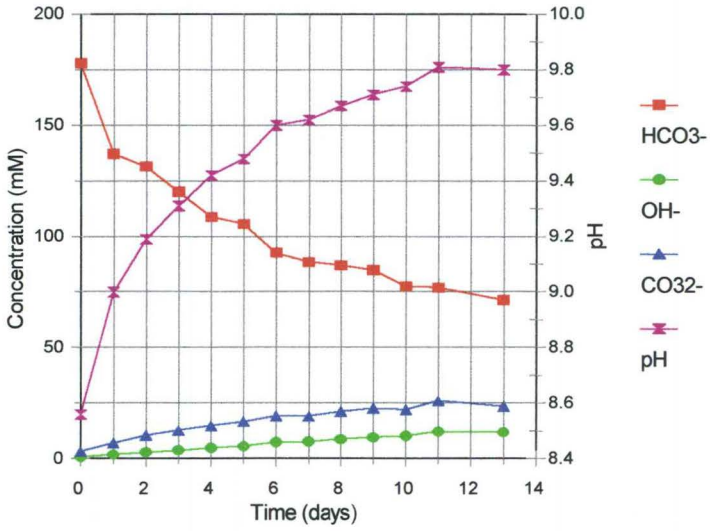

Figure 4.10: Changes in pH and alkaline species induced by cultivation of *Spirulina* in 2l Zarrouk's medium (16.8g/l $NaHCO_3$). Alkaline species determined by MinteqA2

Comparisons of figure 4.8 and figure 4.9 show that predicted species at the specific pH values determined by the modelling software differ somewhat from those determined by the alkalinity titration method. The increase in hydroxide ions is expected due to the increase in pH and as the titration method cannot account for the hydroxide ions, the concentration of carbonate is overestimated.

Further modelling was conducted, using the Minteq programme, to determine the predicted effect of the change in alkaline species and pH on the precipitation of a range of metals commonly found in mining and industrial effluents. It was calculated that 333µl of filtered medium from day 0 would provide sufficient HCO_3^- to react with 60ml of 500µM metal solution, with a base to metal ratio of 2:1. From day 0-13 the precipitation was modelled by calculating the concentration of the various species that would result from adding 333µl of algal filtrate from the specific day to 60ml of metal solution. The change in predicted precipitation from day 0 to day 13 is shown in table 4.4.

Table 4.4: Percentage precipitation, predicted by Minteq, of various metals by the addition of 333µl of algal filtrate to 60ml of 500µM metal solution. Initial bicarbonate to metal ratio of 2:1

Metal salt	% precipitation (d0)	% precipitation (d13)	Precipitated species
$CaCl_2$	0.0	39.7	$CaCO_3$
$CuSO_4$[1]	82.8	68.4	$Cu_3(OH)_2CO_3$
	(47.5)	(47.6)	$Cu(OH)_2$
$FeSO_4$	46.7	47.7	$FeCO_3$
$MgCl_2$	0.0	25.6	$MgCO_3$
$MnCl_2$	41.4	51.8	$MnCO_3$
$NiCl_2$[2]	0.0	0.0	-
$PbCl_2$	49.8	61.4	$PbCO_3$
$ZnSO_4$	31.5	46.2	$ZnCO_3.H_2O$

[1] The predicted precipitating species, malachite, while thermodynamically the most stable is kinetically unlikely to form in a short time. The results in parentheses are for $Cu(OH)_2$ which should be favoured kinetically. This will be further investigated in chapter 6.

[2] At the 2:1 ratio of base to metal, nickel is not predicted to precipitate, although 53.8% of the nickel in solution is in the form $NiCO_{3(aq)}$ which increased to 51.7% by day 13. Doubling the bicarbonate concentration resulted in a predicted precipitation of 12.2% as $Ni(OH)_2$

The predicted results show that for copper and nickel, which precipitate as hydroxides, the generation of reactive alkaline species will not increase the efficiency of precipitation. Iron, manganese, lead and zinc are predicted to precipitate as carbonates. These metals are acidic, which means that they are able to drive the dissociation of bicarbonate to carbonate and a proton. This explains the predicted precipitation on day 0, prior to the formation of significant amounts of carbonate. The biologically mediated generation of carbonate and hydroxide ions is likely to increase the efficiency of precipitation by 15-20%. Calcium and magnesium are also predicted to precipitate as carbonates, but they are not acidic and are only predicted to precipitate once the action of the algae has resulted in the formation of free carbonate ions (Greenwood and Earnshaw, 1984). The modelled data confirm the potential of the algal mediated modification of alkaline species to enhance metal precipitation and acid neutralisation.

4.5 Conclusions

The results presented in this chapter clearly show that the Wilbur Anderson method of assaying carbonic anhydrase activity is not consistently accurate, particularly when applied to raw and partially purified material. The activity of the enzyme could be indirectly assessed by measuring the rate of pH increase of a solution containing a predetermined concentration of bicarbonate. This could be compared to results from standard titrations using sodium hydroxide which allowed the expression of the enzyme activity in terms of a hydroxide equivalent.

The experiments indicated that a *Spirulina* concentration of 2000mg dry mass/l (100mg in 50ml) was optimal and resulted in acidity reduction equivalent to the addition of 3670μmoles OH^- g^{-1} $hour^{-1}$. This efficiency will most likely be somewhat reduced under environmental conditions. Ideally the results should be expressed in terms of OH^- equivalents per mg enzyme, but attempts in this laboratory to isolate and purify carbonic anhydrase from *Spirulina* have proved unsuccessful (Payne, 2000).

There is strong evidence to suggest that the proposed mechanism for the accumulation of inorganic carbon and the subsequent modification of alkaline species in solution is correct. The aqueous species modelling software MinteqA2 was used to predict the pH after various time

intervals based on the expected change in alkaline species. The results were not significantly different to those recorded experimentally.

Inhibitor studies performed using various concentrations of acetazolamide clearly indicated significant inhibition of carbonic anhydrase at inhibitor concentrations of 50μM and above. Acetazolamide cannot enter the cell, so the fact that there was a significant, although reduced, increase in pH in the cultures subjected to high doses of inhibitor suggests that *Spirulina* has both an internal and external carbonic anhydrase. Furthermore, the data suggest that *Spirulina* has some capacity to directly transport bicarbonate ions into the cell.

Experiments conducted with larger volumes and for up to 13 days indicated that *Spirulina* was able to increase the pH to almost 10. Alkalinity measurements confirmed that despite the increase in pH there was no increase in alkalinity. The algae were able to reduce the initial bicarbonate concentration by up to 70% through carbon dioxide accumulation and by conversion to carbonate and hydroxide. Predictive modelling was conducted assuming the addition of 333μl of filtered medium to 50ml of 500μM metal solution, an alkalinity to metal ratio of 2:1. The results indicated that over the 13 day period the potential of the medium to precipitate iron, manganese, lead and zinc increased by 15-20%, while the potential to precipitate the hardness causing metals, calcium and magnesium, increased from zero to up to 40%. There was no effect on the precipitation of copper and nickel which are thought to precipitate as hydroxides. Further modelling and experimental data to determine the optimal mixing regime for the effective remediation of a complex effluent will be discussed in chapter 7.

From the data it can be concluded that the biological modification of alkaline species can significantly enhance the ability of alkaline streams to reduce acidity and precipitate metals. The requirements for such a system are a source of bicarbonate alkalinity and conditions conducive to the culture of algae. On an industrial scale the provision of bicarbonate as a chemical salt would not be a sustainable or cost effective option. A system for the biological generation of bicarbonate alkalinity is described in chapter 5.

CHAPTER 5. BIOLOGICAL GENERATION OF BICARBONATE AND SULPHIDE IONS

5.1 Introduction

Sulphur is a vital component of the amino acids cysteine and methionine and as such is required by all plants, animals and bacteria for the synthesis of protein. The biological cycling of sulphur in the natural environment comprises both aerobic and anaerobic processes (Postgate, 1984). In its highest oxidation state, sulphur exists as the sulphate ion (SO_4^{2-}) which is reduced to sulphide (S^{2-}) by most bacteria, fungi and plants before incorporation into amino acids. This process is known as assimilatory sulphate reduction and is purely a biosynthetic process (Gibson, 1990).

However, any sulphur compound with an oxidation state above that of sulphide (-2) can potentially function as an electron acceptor for the biological oxidation of carbon substrates by biological processes. This process is termed dissimilatory sulphate reduction and is carried out by a specialised group of anaerobic bacteria, the sulphate reducing bacteria (SRB).

5.1.1 Sulphate reducing bacteria

Sulphate reducing bacteria are a large, physiologically diverse group of anaerobic bacteria which are defined by their ability to utilise inorganic sulphate in an ATP-requiring reaction as one of their terminal electron acceptors (Peck and Lissolo, 1988). The generalised reaction is shown below.

$$2CH_2O + SO_4^{2-} \rightarrow 2HCO_3^- + H_2S$$

The speciation of the carbonate and sulphide will depend on the pH of the surrounding media, but generally they will take the form of HCO_3^- and HS^-.

The physiology and growth requirements of these bacteria have been extensively studied (Holland *et al.*, 1987; Hansen, 1988; Gibson, 1990; Elliot *et al.*, 1998; Heider *et al.*, 1998; Phelps *et al.*,

1998). The initial research concentrated on two groups of SRB, the genus *Desulfotomaculum*, which comprises straight or curved rods which are spore forming, and *Desulfovibrio*, which are non-spore forming vibrios. The two groups differed in terms of the enzymes involved in the removal of the pyrophosphate formed during the activation of the sulphate by ATP sulphurylase (Liu and Peck, 1981). Early research showed that field data tended to contradict results obtained in laboratory studies which suggested the presence of previously unclassified strains. Further research led to the discovery and classification of numerous additional genera including, *Desulfobacter, Desulfonema, Desulfomicrobium, Desulfococcus, Desulfobulbus, Desulfomonas, Desulfosarcina, Thermodesulfobacterium* and *Archaeoglobus* (Gibson, 1990).

The ecology, physiology and bioenergetics of this group have been reviewed by a number of authors (Widdel, 1988; Gibson, 1990). Sulphate reducing bacteria have been isolated from a wide range of anaerobic environments, including estuarine sediments (Sahm *et al.*, 1999), acid mine water (Herlihy *et al.*, 1987), saline water (Banat *et al.*, 1981), freshwater and most soils (Watanabe and Furusaka, 1980). SRB strains have been isolated that are able to tolerate a wide range of temperatures, with thermophilic SRBs having been isolated from deep aquifers where temperatures exceed 60°C (Olson *et al.*, 1981).

While it was originally thought that SRB were obligate anaerobes, new evidence from community structures in floating cyanobacterial mats has established that some SRB strains are able to tolerate oxygen, while others are even capable of limited aerobic respiration (Stal, 2001).

5.1.2 Dissimilatory sulphate reduction

The initial step of biological sulphate reduction involves the transport of exogenous sulphate across the bacterial membrane into the cell. Once inside the cell sulphate dissimilation proceeds via the action of ATP sulphurylase. Sulphate combines with ATP to produce the highly activated molecule adenosine phosphosulphate (APS) and pyrophosphate (PPi), which may subsequently be cleaved to yield inorganic phosphate. APS is rapidly converted to sulphite (SO_3^-) by the cytoplasmic enzyme APS reductase. Sulphite may be reduced by a number of intermediates to form the sulphide ion (Gibson, 1990). The pathway is shown in figure 5.1.

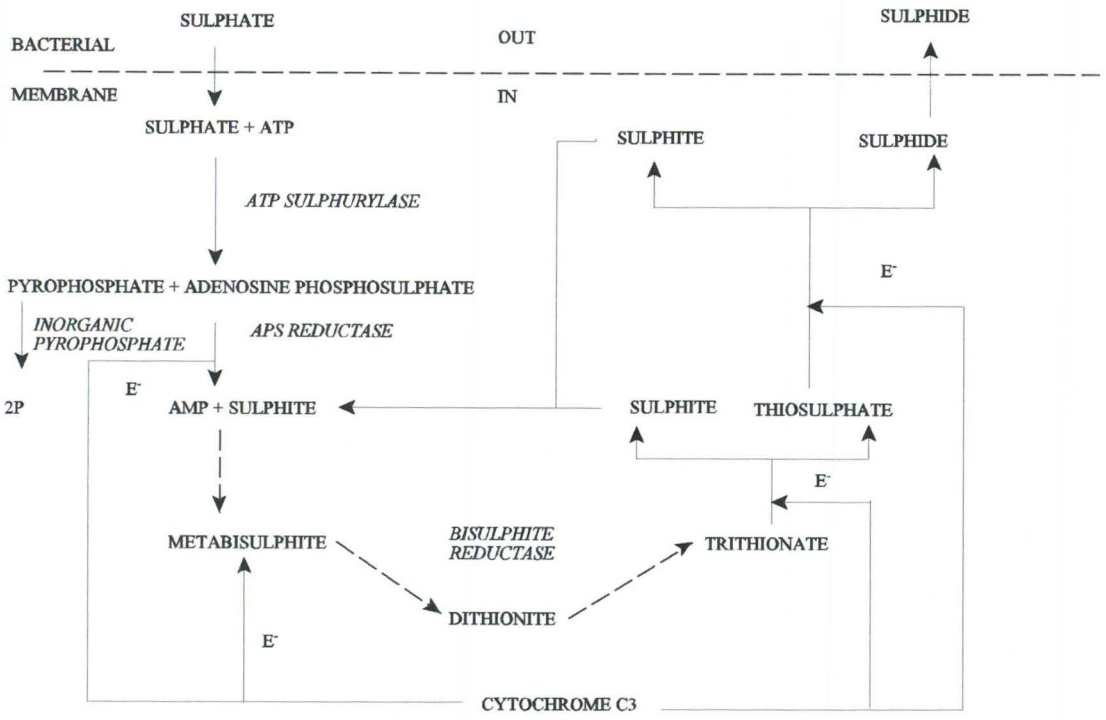

Figure 5.1: Schematic representation of the dissimilatory sulphate reduction pathway (E = electron), modified from Gibson (1990)

Essentially, sulphate is reduced to sulphide using electron donors such as lactate, malate, pyruvate, acetate, formate, hydrogen and ethanol. ATP is produced by electron transport level phosphorylation (ETLP) with various electron and hydrogen carriers involved between the donor and acceptor molecules (Odom and Peck, 1984). The arrangement of these components, in *Desulfovibrio*, and the enzymes involved are shown in figure 5.2. The bacteria contain two C_3 cytochromes, a low (13 000) and a high (26 000) molecular weight protein. Although the high molecular weight protein is twice the size of the smaller one it does not represent a dimer. The C_3 13 000 protein is periplasmic and acts as an electron carrier for the hydrogenase found on the periplasmic side of the cytoplasmic membrane. It is thought to have replaced the function of ferrodoxin, found in other bacteria. The larger protein acts as an electron carrier for the cytoplasmic hydrogenase (Holland *et al.*, 1987).

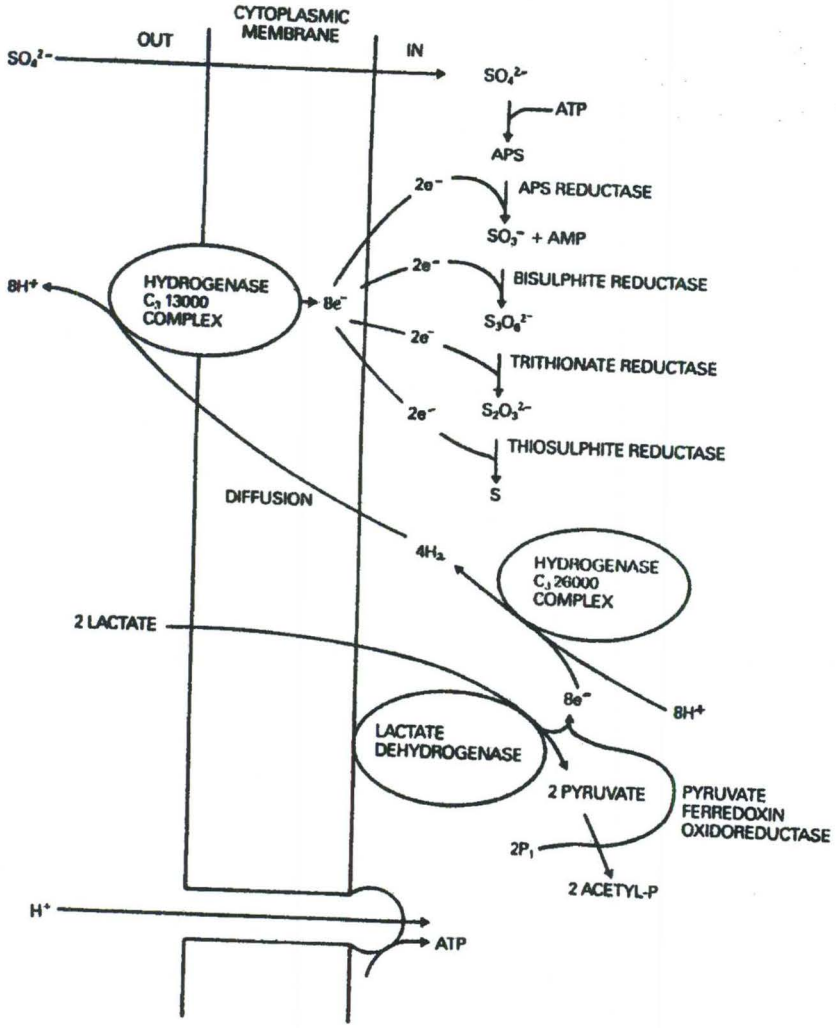

Figure 5.2: Schematic representation of energy production in sulphidogenic bacteria (Holland *et al.*, 1987)

The bacteria are able to obtain energy by ETLP or substrate level phosphorylation (SLP), depending on the availability of an organic electron donor and sulphate. When sulphate is not limiting ETLP dominates and sulphate entering the cell is activated to adenosine phosphosulphate (APS), giving a redox potential (-60mV) high enough to be an electron acceptor. The APS is reduced by the enzyme APS reductase and the sulphite (SO_3^-) sequentially, by three reductase enzymes, to sulphide. Eight electrons are required for the reduction of sulphate to sulphide and this is associated with the expulsion of eight protons from the cytoplasm. The protons are transduced into ATP on their return, via the ATPase. The formation of APS requires 19.6kJ

mole^{-1} of energy. A possible 171kJ mole^{-1} of energy is released during the reduction of APS to sulphide, a net gain of 151.4kJ mole^{-1} (Holland *et al.*, 1987).

In the presence of low environmental sulphate concentrations the bacteria are unable to utilise an electron transport chain between the periplasmic hydrogenase and the sulphate reduction system. As a result the four protons leaving the cell per two molecules of lactate oxidised (Figure 5.2) will be available for other bacteria. The net gain of ATP is possible from the hydrolysis of acetyl phosphate. The excess reducing power ($8e^-$) is expelled from the cell as hydrogen, which can be used by other bacteria in the environment. If the sulphate concentration is low and the expelled hydrogen is not utilised by other bacteria the partial pressure of hydrogen in the surrounding environment increases, inhibiting the further oxidation of lactate (Holland *et al.*, 1987; Widdel, 1988).

5.1.3 Growth requirements for sulphate reducing bacteria

Sulphate reducing bacteria have fairly simple nutritional requirements. An inorganic electron acceptor is required by most strains and this is generally provided by the sulphate ion, although some species are able to utilise other oxidised sulphur compounds, such as thiosulphate, tetrathionate and sulphite (Cypionka, 1987). In the absence of an inorganic electron acceptor some strains are able to ferment substrates such as malate, lactate, fumarate and pyruvate. The ability of some species of *Desulfovibrio* and *Desulfobulbus* to reduce nitrate and nitrite has also been demonstrated (Seitz and Cypionka, 1986).

The sulphate reducing bacteria have been shown to utilise a wide variety of carbon sources, with the specific electron donor depending on the genus in question (Gibson, 1990). The range of carbon sources which can be utilised is shown in table 5.1.

Table 5.1: Compounds that can be used as energy substrates by sulphate reducing bacteria (Boshoff, 1999)

Group	Specific compounds
Inorganic	hydrogen, carbon monoxide
Monocarboxylic acids	formate, acetate, propionate, butyrate, isobutyrate, 2- and 3-methylbutyrate, higher fatty acids up to C_{18}, pyruvate and lactate
Dicarboxylic acids	succinate, fumarate, malate, oxalate, maleinate, glutarate, pimelate
Alcohols	methanol, ethanol, propanol, butanol, ethylene, glycols, 1,2- and 1,3-propanediol and glycerol
Amino acids	glycine, serine, cysteine, threonine, valine, leucine, isoleucine, aspartate, glutamate and phenylalanine
Miscellaneous	choline, oxamate, fructose, benzoate, nicotinic acid, indole, phenol, anthraline, p-cresol, catechol, hydroquinone and aminobenzoate

The ability of SRBs to utilise complex organic carbon sources has not been demonstrated, although SRB activity has been achieved where a microbial consortium has been cultivated on a range of complex carbon sources, such as tannery effluent, primary sewage sludge, wood chips, sawdust and a variety of cellulose containing feedstocks. The action of other fermentative bacteria is responsible for the partial degradation of the complex carbon, releasing substrates that are available to the SRBs (Béchard *et al.*, 1994; Boshoff, 1999; Whittington-Jones, 2000).

The nitrogen source of choice for most SRBs is ammonia, although the dissimilatory reduction of nitrate and nitrite has been shown to provide nitrogen in some cases. In general, however, SRBs are inhibited by high nitrate concentrations, which increase the redox potential of the medium (Jenneman *et al.*, 1986). Furthermore, some sulphate reducers are able to fix nitrogen or utilise amino acids as their nitrogen source (Gibson, 1990). Iron and phosphorus have also been shown to be important nutrients (Postgate, 1994).

The growth of SRB cultures is stimulated by a low E_H medium. This effect may be achieved by the addition of E_H poising agents such as sodium sulphide, sodium dithionite, sodium ascorbate or sodium thioglycollate, which was used in this study (Postgate, 1994).

5.2 Research aims

The primary aims of this section of the project were:

1) To quantify bicarbonate and sulphide generation by SRB cultured in a variety of chemically defined media.
2) To investigate the effect of upscale to a simplified reactor design.
3) To investigate the efficiency of sparging with nitrogen and air to reduce the sulphide concentration in anaerobic digester overflow (ADO) prior to its use as an algal feed.
4) To assess the suitability of enriched, partially treated acid mine drainage as a growth medium for SRB.

5.3 Materials and methods

5.3.1 Bacterial biomass

Sulphate reducing bacteria and fermentative bacteria cultures were isolated from the algal integrated ponding system (AIPS) at the Grahamstown sewage treatment works and enriched in modified Postgate medium (Appendix J). All subsequent cultures were initiated using a 10% inoculum of the stock cultures.

5.3.2 Determination of bacterial concentration

A variety of methods have been attempted to determine the concentration of bacterial cultures, including cell counts, optical density readings (600nm), dry mass and fluorescence assays. However, none of the methods proved accurate, primarily as a result of interference from the extracellular polymeric substances associated with the cells and the reaction of iron in the media with sulphide.

5.3.3 Analytical techniques

All experiments were conducted using acid-washed glassware, as before. Measurements of alkalinity and pH were performed as previously described. The presence of sulphide contributed to the total alkalinity. In instances where bicarbonate concentrations were determined from the alkalinity data the contribution of the sulphide have been accounted for. Assays for phosphate, nitrate and ammonia were performed using Merck Spectroquant® reagent kits and analysed using a Merck Spectroquant® NOVA 60 photometer.

Gram staining (Appendix K) was performed on samples extracted from the lactate fed reactors. Light microscope and scanning electron microscope images were produced as described in chapter 3.

5.3.3.1 Sulphide assay

Total free sulphide (H_2S, HS^- and S^{2-}) in solution was determined using a colorimetric method based on the reaction of sulphide with p-phenylene diamine. The assay system is only precise to concentrations of 1mg/l so appropriate dilutions were necessary. A suitable volume of sample was transferred to a test tube, to which 200µl of 15% zinc acetate was added. The volume was made up to 5ml by the addition of oxygen-free, triple distilled water ($dddH_2O$). A volume of 500µl of N,N-dimethyl-p-phenylene diamine hydrochloride solution, followed by 500µl of ferric chloride solution were added to the sample, which was mixed thoroughly and allowed to react for 60 minutes. The absorbance was read at 665nm and concentration determined off the standard curve. Standard curve and recipes are shown in appendix L.

5.3.3.2 Sulphate assay

Sulphate ions in solution were generally determined using the Merck Spectroquant® reagent kit. However, in some cases the addition of the final reagent (tannin) in the kit resulted in the formation of a complex which resulted in a turbid sample. In these cases the sulphate was

determined using a high performance liquid chromatography (HPLC) method. In both cases the accuracy of the method was confirmed by testing a standard copper sulphate solution.

Samples for the HPLC method were prepared by filtering 5ml of sample through a 0.45µm nylon membrane filter after which 2ml of the filtrate was treated with 1ml of 0.1M zinc acetate and centrifuged at 12 000rpm for 30 seconds. The supernatant was filtered through a 0.22µm nylon membrane filter and 2ml of the filtrate was passed through an Isolute C18 (EC) column to exclude any organic material.

The samples (20µl) were run through a Hamilton PRP-X100 HPLC column (10µ, 150 x 4.1mm) at a flow rate of 2ml/min, under pressure generated by a Waters model 510 pump. A Waters 430 Conductivity Detector was coupled to the column and the data was integrated using the BORWIN 1.5x software package. The sulphate peak exhibited a retention time of approximately 10 minutes. A sulphate standard curve was prepared using sodium sulphate (0.3g Na_2SO_4 in 200ml dddH_2O for a 100mg/l standard). The mobile phase is described in appendix M.

5.3.3.3 Sulphur assay

A 500µl sample was placed in an eppendorf tube and centrifuged at 13 000rpm in a Heraeus microfuge for 10 minutes. The supernatant was discarded and the pellet resuspended in 1ml of HPLC grade acetone. After 60 minutes the sample was filtered through a 0.45µm nylon membrane filter. The samples were run through a Phenomenex LUNA C18 (5µm, 150 x 4.6mm) column at a flow rate of 2ml/min, under pressure from a Waters model 510 pump. A Waters 484 Tunable Absorbance Detector was coupled to the column and the data was integrated using the BORWIN 1.5x software package. The mobile phase is described in appendix M.

5.3.4 The effect of different electron donors

Four 1.8l reactors were inoculated (20% V/V) with a bacterial consortium isolated from a lactate-fed anaerobic digester. Three of the reactors were operated as sulphate reducing systems, fed lactate, phenol and glucose respectively, and the fourth as a fermentative system, fed lactate.

Experiments were performed in duplicate. The proposed metabolic reactions involving the sulphate reducing bacteria are summarised in table 5.2.

Table 5.2: Metabolic reactions involving sulphate reducing bacteria (Gibson, 1990)

Oxidative reactions
$2C_3H_6O_3 + SO_4^{2-} + H^+ \rightarrow 2C_2H_4O_2 + 2HCO_3^- + H^+ + HS^-$
$C_2H_4O_2 + SO_4^{2-} \rightarrow HS^- + 2HCO_3^-$
$C_6H_{12}O_6 + SO_4^{2-} + H^+ \rightarrow 2C_2H_4O_2 + 2CO_2 + HS^- + 4H_2O$
$2\ Phenol + 7SO_4^{2-} + 6H_2O \rightarrow 12HCO_3^- + 5H^+ + 7HS^-$
Fermentative reaction
$3C_3H_6O_3 \rightarrow C_2H_4O_2 + 2C_3H_6O_2 + HCO_3^- + H^+$

In all cases the organic carbon concentration corresponded to a COD of 2000mg/l and where sulphate was added the sulphate concentration was 2000mg/l, giving a COD:SO_4 ratio of 1:1. The pH of the media was adjusted to 7.0 prior to autoclaving and all reactors were fed at a constant rate of 37.5ml/hour, giving a hydraulic retention time of 48 hours. Reactors were shaken at 120rpm on an orbital shaker and the temperature was maintained at 25°C. The composition of the media is detailed in table 5.3 below.

Table 5.3: Composition of nutrient media for bicarbonate generating bacterial reactors

Compound	Lactate - fermentative	Lactate - SO_4 reducing	Glucose - SO_4 reducing	Phenol - SO_4 reducing
Na-lactate 60%	4.2ml	4.2ml	-	-
Glucose	-	-	1.88g	-
Phenol	-	-	-	0.89g
K_2SO_4	3.63g	3.63g	3.63g	3.63g
NH_4Cl	0.1g	0.1g	0.1g	0.1g
K_2HPO_4	0.1g	0.1g	0.1g	0.1g
ddH_2O	995.8ml	995.8ml	1000ml	1000ml

Sulphate, sulphide, pH, COD and total alkalinity measurements were taken daily. The COD measurements were highly variable and did not show a clear reduction over time. While COD has been used to measure carbon utilisation in large scale reactors it can be concluded that for small reactors, COD measurement is not a viable method for determining alkalinity production as a function of organic carbon utilisation.

5.3.5 Scale-up of lactate fed reactor

The lactate fed sulphidogenic reactor was scaled-up to a volume of 28l using a 10% inoculum from the previous experiments. The reactor was not fed for the first seven days, while the culture became established, after which modified Postgate B medium (Appendix J) was pumped into the bottom of the reactor at a flow rate of 2ml/min, giving a hydraulic retention time of approximately 10 days. The reactor was not stirred or agitated in any way and an overflow port, connected to an anti-siphon loop, was positioned 5cm from the top of the reactor. The pH, sulphate, sulphide and alkalinity were measured on a daily basis until a steady state was established and at various intervals thereafter, while phosphate, nitrate and ammonia levels were measured at various intervals.

5.3.6 The effect of sparging on sulphide levels in anaerobic digester overflow (ADO)

Sulphide in solution has been shown to be toxic to algae so for the ADO to be used as a bicarbonate source for the cultivation of algae, the concentration of sulphide in solution would need to be reduced. Sparging with air and nitrogen was used to strip sulphide from H_2S from the solution. A volume of ADO was transferred to a stoppered Schott bottle. Air or nitrogen was pumped in at a rate of 38.6ml/s and dispersed through an air stone. The sulphide laden carrier gas was passed through two sulphide traps, consisting of 400ml of 0.125M NaOH. The gas stream was again dispersed using air stones. The initial experiments were conducted for 60 minutes, with subsequent experiments extending for up to eight hours. The pH, sulphide, sulphate, sulphur concentrations in the ADO, as well as the sulphide trapped by NaOH, were measured at various intervals.

5.4 Results and discussion

5.4.1 Investigation of the bacterial consortium

There appear to be at least three distinctive bacterial species making up the consortium isolated from the AIPS, based on the gram stain results and the gross morphology of the cells depicted in the light microscope and SEM preparations. Figure 5.3 shows a light microscope preparation of a gram stained sample from the 28l, lactate fed reactor. Figure 5.4 shows an SEM preparation of the same sample. The majority of the cells appear gram negative, consisting of short and longer rods, characteristic of the genus *Desulfovibrio*. There are also a number of cells which appear gram positive, which is indicative of the genus *Desulfotomaculum*. Bowker and Chauke (unpublished results) extracted DNA from the initial inoculum and classified over 20 strains on the basis of 16S RNA sequences. Representatives of both genera mentioned above were isolated from the inoculum and characterised.

Both *Desulfovibrio* and *Desulfotomaculum* have similar preferred carbon sources, which include the organic acids, lactate, pyruvate and malate, and alcohols such as ethanol, propanol and butanol. For the majority of the species making up the two genera, the oxidation of the preferred substrates is incomplete with acetate being formed as an end product (Gibson, 1990).

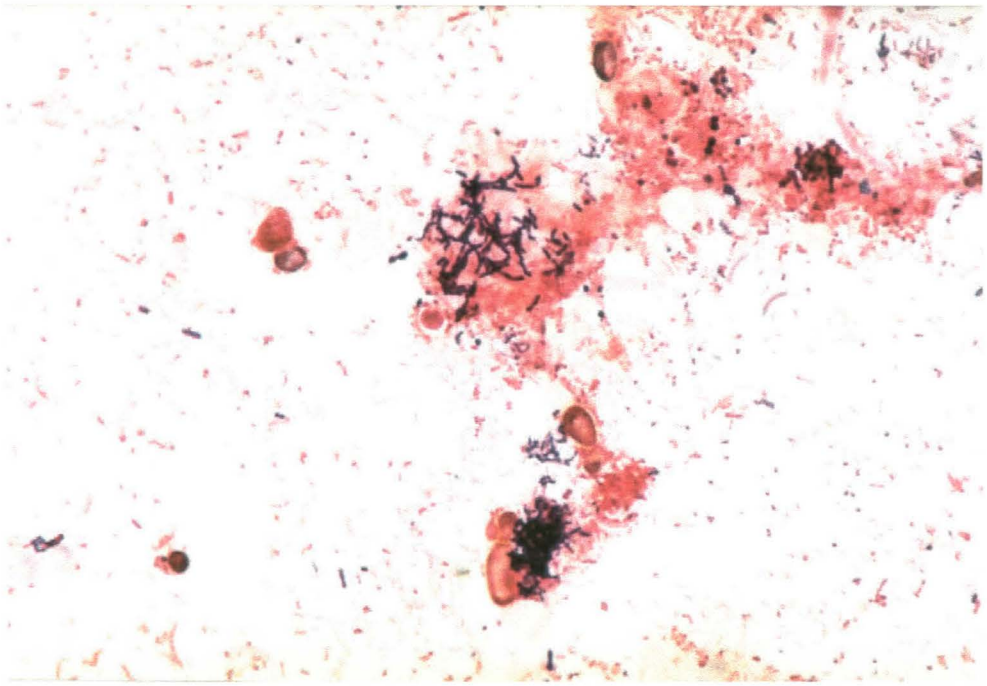

Figure 5.3: Light microscope preparation of gram stained sample from the 28l, lactate fed, anaerobic digester, showing the presence of both gram positive and gram negative cells.

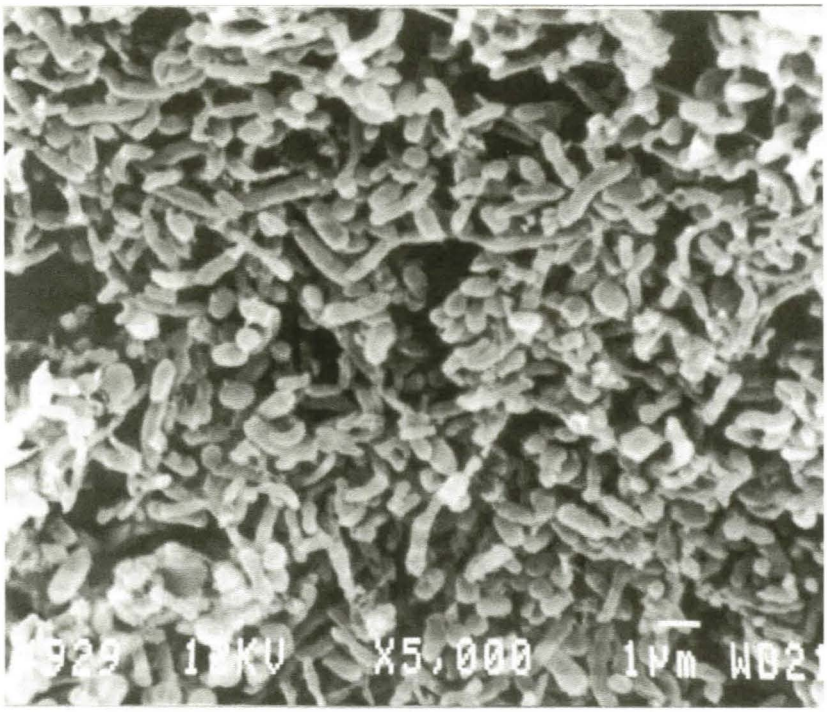

Figure 5.4: SEM preparation of bacterial consortium extracted from the 28l, lactate fed, anaerobic digester

5.4.2 The effect of different electron donors

The results from the studies on the various electron donors clearly indicate that the sulphate reducing bacteria in the original isolate favour lactate as the preferential carbon source. This is consistent with the crude identification, based on morphology, of the presence of species from the genera *Desulfovibrio* and *Desulfotomaculum*. The pH data (Figure 5.5) show that the pH in the lactate fed reactors stabilised at approximately 6.2 in the fermentative reactors and just above 7 in the sulphidogenic reactors. The pH in the reactors fed on phenol remained relatively constant, while the glucose fed reactor demonstrated a steady decline in pH, stabilising between 3.4 and 3.5.

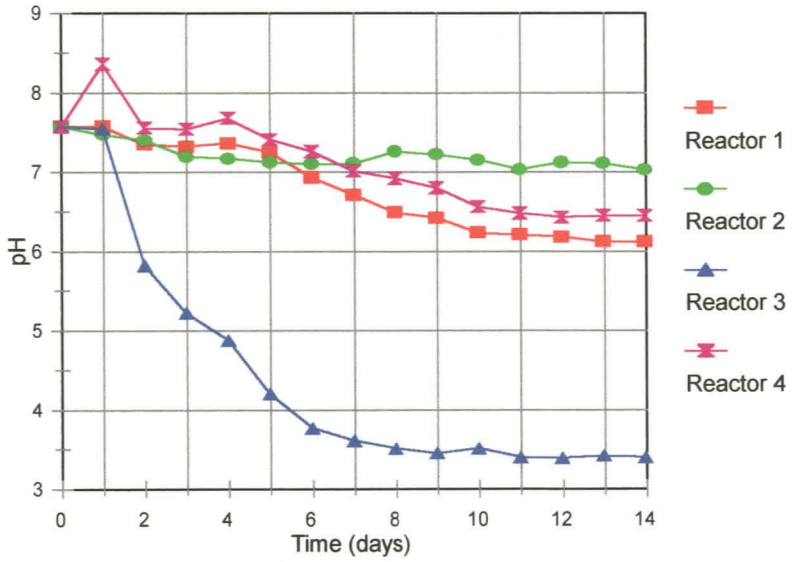

Figure 5.5: Graph of pH vs time for anaerobic reactors fed different carbon sources. Reactor 1 = lactate, no sulphate, Reactor 2 = lactate + sulphate, Reactor 3 = glucose + sulphate and Reactor 4 = phenol + sulphate. Carbon source concentration equivalent to COD of 2000mg/l and sulphate concentration 2000mg/l (mean values, n=2)

The pH values in the lactate fed reactors are consistent with expectations, based on the proposed reaction pathways (Table 5.2). The higher pH value in the sulphidogenic reactor is due to the generation of sulphide by sulphate reduction (Figure 5.6) and a greater amount of alkalinity (Figure 5.7). The dramatic decrease in the pH of the glucose fed reactors suggests the presence

of acetogenic bacteria in the original inoculum. Acetogenic bacteria, such as *Acetobacterium woodi*, have a greater affinity for glucose than most SRB. They ferment glucose to acetate according to the following equation:

$$C_6H_{12}O_6 \rightarrow 3CH_3COO^- + 3H^+$$

This generation of hydrogen ions results in the decrease in pH. While acetate can be used as a carbon source for some sulphate reducing bacteria, particularly of the genus *Desulfobacter*, it is not a preferred carbon source for most *Desulfovibrio* and *Desulfotomaculum* species (Widdel, 1988; Gibson, 1990). The absence of any sulphate reduction in the glucose fed reactors (Figure 5.6) confirms the absence of *Desulfobacter* species in the inoculum.

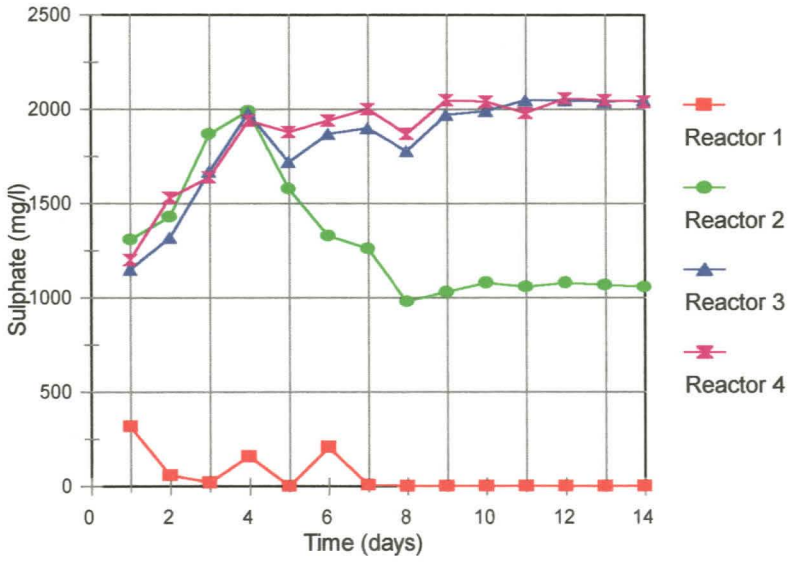

Figure 5.6: Graph of sulphate concentration in solution vs time for anaerobic reactors fed different carbon sources. Legend description as for figure 5.5

Figure 5.6 shows that active sulphate reduction only took place in the reactors receiving both lactate and sulphate in the feed. The cultures required a four day period to acclimatise before a significant decrease in sulphate was detected. By day eight the reactor conditions had stabilised

with a sulphate reduction efficiency of 50%. This represents a sulphate conversion rate of 500mg SO_4 l^{-1} day^{-1}. The data for sulphide generation followed an identical pattern, with appreciable sulphide concentrations only being detected in the reactors fed both lactate and sulphate. Sulphide levels increased after day four and stabilised after day eight at between 145 and 155mg/l. In terms of sulphur mass balance this represents 46% of the sulphate reduced. The sulphide in solution exists in a state of dynamic equilibrium between $H_2S_{(aq)}$, HS^- and S^{2-}, with the relative percentages dependent on the pH (Stumm and Morgan, 1996). Modelling with MinteqA2 indicated that at pH 7, 56.8% of the sulphide would exist as HS^- and 43.2% as H_2S. It is, therefore, reasonable to assume that part of the unaccounted for sulphide had been lost to the head-space as hydrogen sulphide gas. A certain percentage of the reduced sulphate would also have been assimilated into the cell (Widdel, 1988).

The alkalinity generated by the various reactors is shown in figure 5.7.

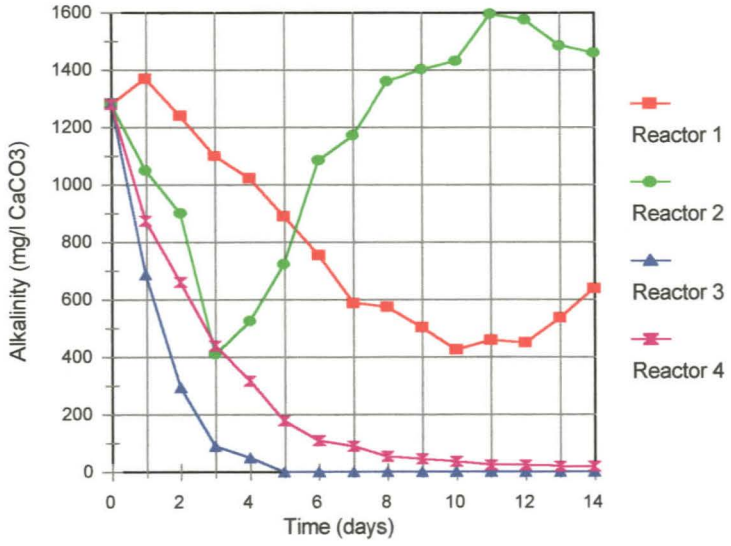

Figure 5.7: Graph of alkalinity generation vs time for anaerobic reactors fed different carbon sources. Legend description as for figure 5.5

The results clearly show the relationship between sulphate reduction and alkalinity generation, with the alkalinity profile for reactor two, mirroring that for the sulphide generation (Figure 5.6).

The low pH of the glucose fed reactors means that any carbonate present will be in the form of carbonic acid (H_2CO_3) and will not contribute towards alkalinity (Stumm and Morgan, 1996). The bacteria were unable to utilise phenol as a carbon source, so no alkalinity was generated in those reactors. The results for reactor one indicate that substrate level phosphorylation of the lactate occurred from the onset of the experiment and that alkalinity production stabilised at approximately 500mg/l as $CaCO_3$. The predicted reactions for the utilisation of lactate in a sulphidogenic and fermentative system (Table 5.2) suggest that the sulphidogenic system should produce three times as much bicarbonate as the fermentative system for an equivalent amount of lactate utilised, which is demonstrated by the experimental data (Gibson, 1990).

5.4.3 Scale-up of the lactate fed, sulphidogenic reactor

The lactate-fed sulphidogenic reactor was successfully scaled up to a volume of 28l. The relationship between pH, sulphate and sulphide is shown in figure 5.8. The use of an inoculum from a reactor with a similar nutrient regime reduced the lag period which was observed in the initial experiments (Section 5.4.2). The reactor was run as a batch system for the first seven days, after which media was continuously pumped through. The reactor has been operated on a continuous basis for over three months. During the initial phase the sulphate concentration decreased steadily to approximately 200mg/l. After switching to a continuous operation mode, where the feedstock had a sulphate concentration of approximately 1900mg/l, the sulphate concentration increased, stabilising at between 550 and 600mg/l, which represented a mean sulphate conversion rate of 135.20 ± 6.78mg l^{-1} day^{-1} (1406.25 ± 70.63µmoles l^{-1} day^{-1}). This was lower than the stirred reactors, due to the lack of agitation which resulted in the majority of the bacteria being concentrated near the bottom of the reactor, creating a vertical stratification in terms of efficiency.

The pH increased rapidly during the batch reactor phase, increasing from 6.5 to 7.05, as a result of the generation of sulphide and bicarbonate. After the switch to a continuous system the pH increase slowed, stabilising at between 7.2 and 7.4, which represents the pH optimum of most SRB species (Widdel and Pfennig, 1984; Gibson, 1990). The concentration of dissolved sulphide

remained stable at between 200 and 250mg/l from day six onward and was not affected by the change in reactor configuration.

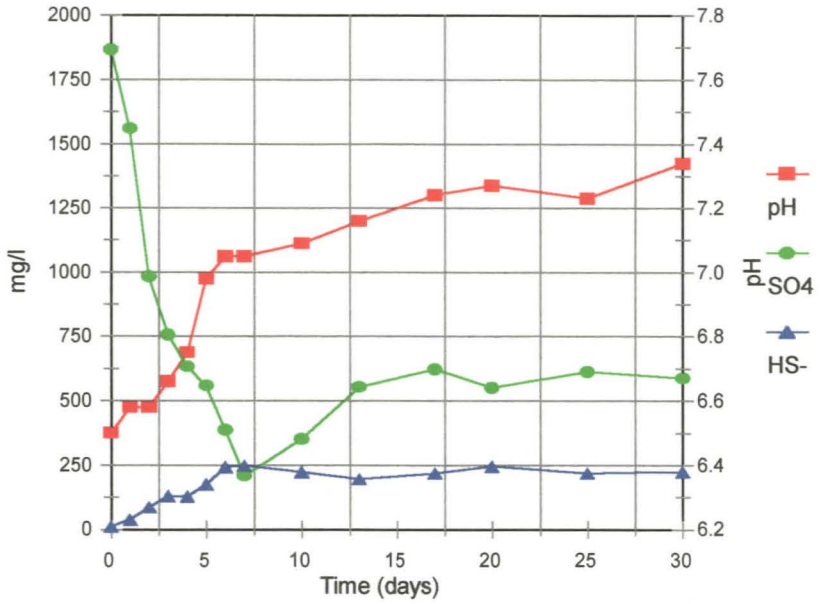

Figure 5.8: Relationship between pH, SO_4^{2-} and HS^- during scale-up of the lactate fed sulphidogenic reactor. Reactor operated as a batch system for seven days, after which modified Postgate B medium was pumped in continuously at a rate of 2ml/min

The bicarbonate generation in the reactor was determined using the alkalinity titration method and adjusting the value to take into account the contribution of the sulphide. The results for the bicarbonate generation (Figure 5.9) confirm the relationship between bicarbonate production and sulphate reduction. The bicarbonate concentration in the reactor increased rapidly during the batch phase of operation from 19mM to approximately 40mM. Once the reactor was switched to a continuous mode of operation the bicarbonate concentration stabilised between 40 and 44mM, with a mean value of 42.20 ± 1.51mM. The feedstock had a pH of 5.20 and an alkalinity of 2.99mM. The productivity of the reactor, in terms of bicarbonate generation, was calculated as 4033 ± 83μmoles l^{-1} day^{-1}.

The molar ratio of bicarbonate to sulphide in the reactor was initially high, during the lag phase of growth. This decreased during the batch operation and stabilised once the reactor was fed continuously. The mean bicarbonate to sulphide ratio during the continuous phase was calculated

as 6.15 ± 0.44. This is three times higher than the predicted value, based on the published reactions for lactate utilisation by SRB (Widdel, 1988), assuming conservation of the species involved.

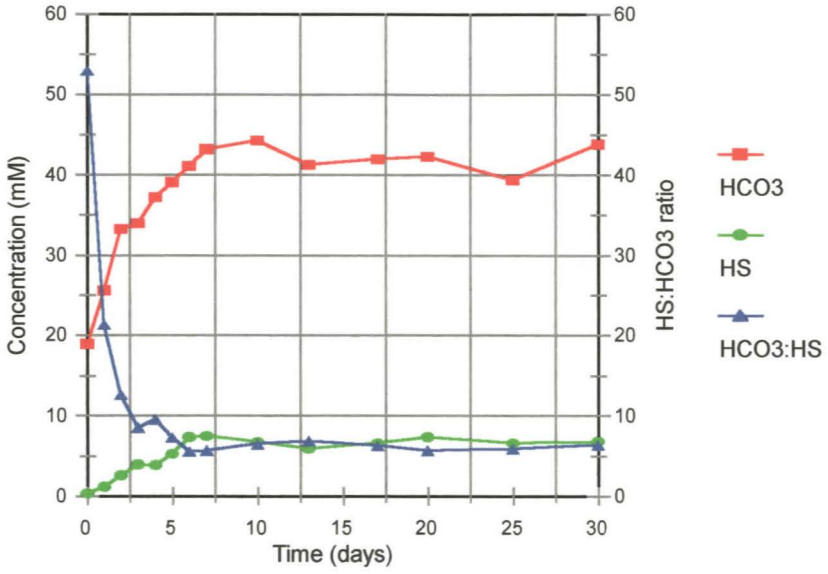

Figure 5.9: Relationship between biologically generated bicarbonate and sulphide in the 28l, lactate fed, anaerobic digester

The unexpectedly high bicarbonate to sulphide ratio can be partially accounted for by the loss of sulphide as H_2S gas. Furthermore, the overflow from the reactor contained cream/white particulate matter, which proved to be elemental sulphur. Opening the reactor showed that a floating crust of sulphur had formed at the liquid-air interface. The oxidation of sulphide to sulphur can occur chemically or biologically, as a result of sulphur oxidising bacteria (Zopfi *et al.*, 2001). As a result of the small head-space and hence, limited oxygen availability, in the reactor the ratio of sulphide to oxygen is high and sulphide oxidation does not proceed fully to sulphate, thiosulphate or sulphite, but instead results in the formation of polysulphide (S_n^{2-}) and elemental sulphur (S^0) (Chen and Morris, 1972). The formation of these products would reduce the amount of sulphide in solution.

An analysis of bicarbonate generation relative to sulphate reduction in the reactor allowed the determination of the ratio of bicarbonate generated per sulphate reduced. The published reactions

would yield a molar ratio of 2:1 for lactate as the sole carbon source. The experimental data yielded a molar ratio of 2.86:1, which indicates that additional alkalinity was produced, most likely by the fermentative degradation of lactate. The lack of mixing in the reactor could lead to the formation of transient microenvironments that are low in sulphate, which would promote the fermentative pathway.

A general decrease in the COD of the effluent relative to the feed-stock was noted, however, the high degree of variability, both on a daily basis and between replicates, precluded the generation of a statistically significant relationship between COD reduction and sulphide or bicarbonate generation. The direct measurement of lactate and acetate would be needed.

The modified Postgate B medium contains high concentrations of phosphate (350mg/l) and ammonia (336mg/l). As a result these nutrients never became limiting. During the continuous phase of operation only 9.89 ± 0.31% of the ammonia and 37.7 ± 0.86% of the phosphate was being utilised.

5.4.4 The effect of sparging on aqueous sulphide concentration

Elevated levels of aqueous sulphide are toxic to both bacteria and algae. Boshoff *et al.* (1998) demonstrated that sulphide concentrations in excess of 200mg/l led to the rapid deterioration in viability of both *Spirulina* sp. and *Dunaliella salina*. For the ADO to be used as an algal feed the sulphide concentration needed to be decreased. Biogenic hydrogen sulphide has also been shown to have the ability to selectively precipitate metals from solution (Hammack *et al.*, 1994).

Sparging the overflow from the 28l reactor with nitrogen and air significantly reduced the concentration of aqueous sulphide. This coincided with an increase in pH (Figure 5.10). The sulphide in solution exists in a dynamic equilibrium, and at the pH values of the ADO, the predominant species were H_2S and HS^-. Similarly the H_2S is in a state of two-phase equilibrium, between the liquid fraction and the head-space (Stumm and Morgan, 1996). Sparging flushes the head-space which results in a lower P_{H_2S} and drives the equilibrium towards the gaseous phase.

This, in turn drives the equilibrium between HS^- and H_2S towards the formation of H_2S, which requires a hydrogen ion and therefore results in an increase in pH.

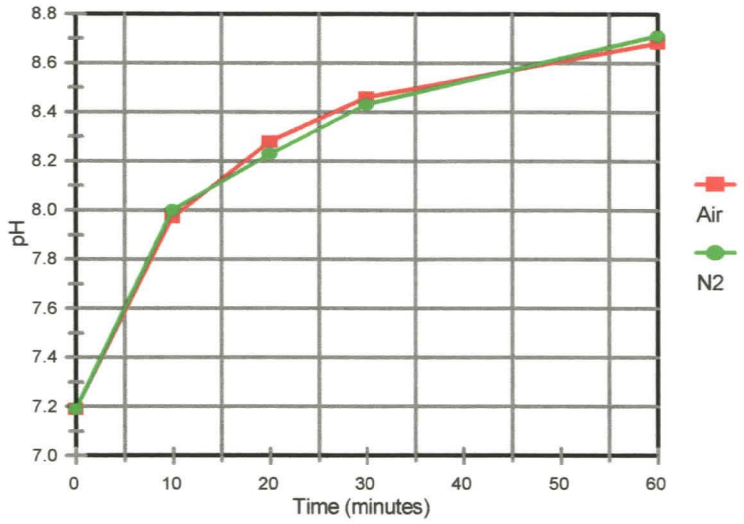

Figure 5.10: The effect on pH of sparging anaerobic digester overflow with nitrogen and air at a flow rate of 38.6ml/s (mean values, n=3)

The effect on the speciation of the sulphur was markedly different, depending on whether air (Figure 5.11) or nitrogen (Figure 5.12) was used. The situation was similar in both cases for the first 20 minutes, with no significant difference ($P = 0.056$) in the amount of sulphide scrubbed by the first sodium hydroxide trap (Figure 5.13). After 20 minutes, however, no further sulphide was stripped from the ADO in the air sparged samples. The introduction of oxygen into the system resulted in the oxidation of the remaining aqueous sulphide. This was complete after 30 minutes. The presence of elemental sulphur was detected after 10 minutes and its concentration continued to increase until all the sulphide was oxidised. The total sulphide species data indicate that not all the sulphur can be accounted for. The chemical oxidation of sulphide passes through a number of intermediates, notably polysulphide, which cannot be adequately quantified (Steudel, 1996; Schippers and Sand, 1999). It is most likely that these intermediates account for the rest of the sulphur. The absence of significant amounts of sulphate is due to the duration of the experiment, which did not allow the complete oxidation of sulphide to sulphate. This was confirmed by

extending the duration of the experiment to eight hours, during which an increase in the sulphate concentration was noted (results not shown).

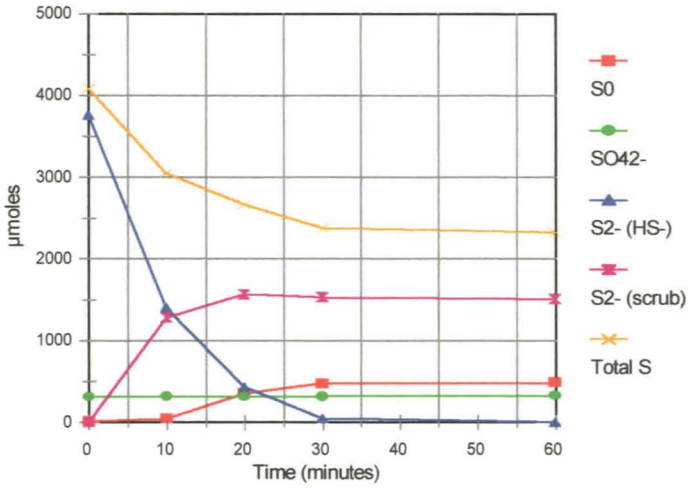

Figure 5.11: Changes in sulphur species in solution as a result of sparging with air (mean values, n=3)

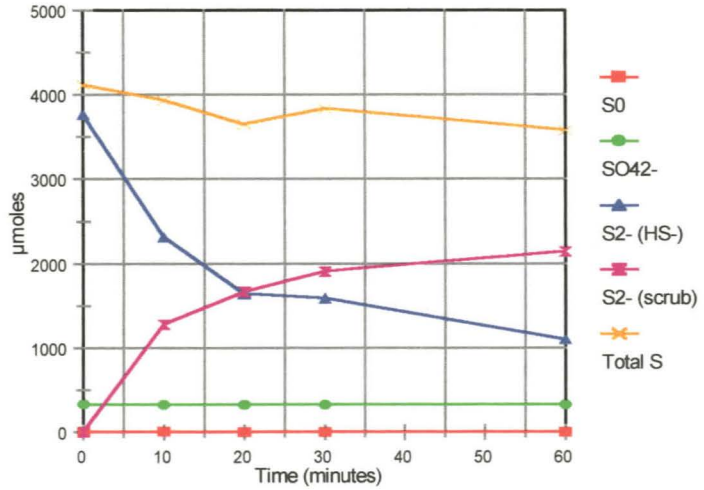

Figure 5.12: Changes in sulphur species in solution as a result of sparging with nitrogen (mean values, n=3)

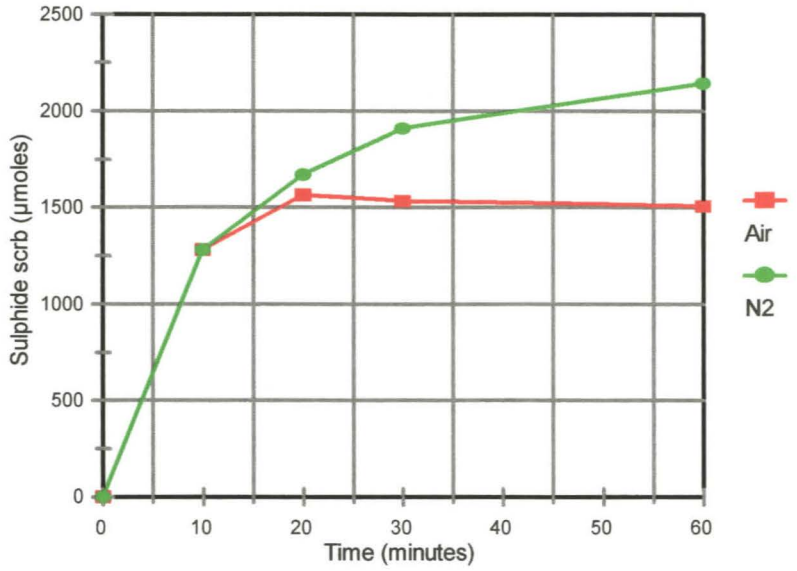

Figure 5.13: Sulphide scrubbed by the first NaOH trap. No sulphide was detected in the second trap at any stage (mean values, n=3)

Figure 5.13, shows the amount of sulphide trapped in the first of the two serially connected, sodium hydroxide traps. The absence of any sulphide in the second trap confirms that 100% of the H_2S stripped from the digester overflow has been trapped. The rate of H_2S stripping was unaffected by the gas type for the first 20 minutes, suggesting that it is governed by physical principles. The oxidation of aqueous sulphide in the air sparged samples resulted in no further sulphide stripping occurring after 20 minutes. Continued sulphide stripping was observed in the nitrogen sparged system, although the rate decreased as the pH increased. As the pH increased the aqueous sulphide equilibrium shifted more towards HS^-, thereby decreasing the amount of H_2S in solution (Stumm and Morgan, 1996). Sparging with nitrogen for eight hours did not result in a greatly improved yield, with only 7.52% more sulphide being recovered.

Sparging with both air and nitrogen resulted in a substantial decrease in the phosphate concentration. There was no significant difference ($P = 0.07$, $n = 3$) in the percentage phosphate reduction between the air sparged ($90.34 \pm 2.66\%$) and the nitrogen sparged ($89.67 \pm 3.01\%$) system. The most likely reason for the reduction in phosphate is a pH dependent precipitation reaction. Sparging with nitrogen had little effect on the concentration of ammonia in solution,

while a 15% reduction in ammonia was observed in the air sparged system, most likely as a result of chemical oxidation to nitrate.

5.5 Conclusions

Morphological and physiological data suggest that the bacterial consortium, isolated from the AIPS, contains at least two species of the genus *Desulfovibrio* as well as a species of gram positive SRB of the genus *Desulfotomaculum*. Lactate is the preferred carbon source for both genera. The bacterial consortium was able to utilise lactate as the sole electron donor under both sulphate reducing and fermentative conditions. The results from the glucose fed reactors confirm the presence of acetogenic bacteria in the consortium and the inability of the sulphate reducers to utilise the acetate produced suggests that the consortium does not contain *Desulfobacter* species.

The agitated, lactate fed reactor was able to reduce sulphate at a rate of 500mg SO_4 l^{-1} day^{-1}, although only 50% of the reduced sulphate was detectable as aqueous sulphide. Modelling of the sulphide speciation at the relevant pH indicated that 43% of the sulphide would exist as H_2S, which could be lost to the air. The lactate fed reactor was successfully scaled up to a volume of 28l. The lack of agitation in the 28l reactor led to stratification of the bacteria and reduced mass transfer rates. As a result the efficiency of sulphate reduction decreased to 135mg l^{-1} day^{-1} (1406μmoles l^{-1} day^{-1}). The bicarbonate generation rate was calculated as 4033μmoles l^{-1} day^{-1}, which yielded a molar ratio of bicarbonate to sulphate three times higher than expected, primarily as a result of the loss of hydrogen sulphide gas and the oxidation of sulphide to elemental sulphur near the air-water interface. The molar ratio of bicarbonate generated to sulphate reduced was 2.86:1. A ratio of 2:1 would be expected in an ideal situation and the discrepancy can be attributed to lactate fermentation, most likely in sulphate depleted microenvironments.

Sparging the anaerobic digester overflow with air and nitrogen appreciably reduced the concentration of aqueous sulphide. Sparging with air reduced the aqueous sulphide concentration to zero within 60 minutes, although only 41% was recovered as hydrogen sulphide with the remainder converted to a variety of oxidation products. Sparging with nitrogen did not induce

any oxidation and after 60 minutes 70% of the sulphide had been stripped from solution. Further sparging for an additional seven hours only resulted in the stripping of a further 7%.

The sulphate reducing bacteria system was able to generate a considerable amount of bicarbonate alkalinity and sparging with air or nitrogen reduced the aqueous sulphide concentration to levels which would not be toxic to algae. This system therefore, represents an ideal and sustainable source of bicarbonate to drive the algal catalysed reactions described in chapter 4.

Should such a system be implemented on an industrial scale it would be impractical and expensive to use a chemically defined medium. Professor Peter Rose's research group at Rhodes University, and other researchers, have conducted extensive research into the utilisation of complex organic carbon sources, such as tannery effluent (Boshoff, 1999), sewage sludge (Pletschke *et al.*, 2001; Whiteley *et al.*, in preparation), wood chips (Chang *et al.*, 2000), sawdust (Wakao *et al.*, 1979), whey (Christensen *et al.*, 1996) and other cellulose based products (Chang *et al.*, 2000), to drive sulphate reducing systems and the design of reactors to optimise their performance. The data indicate that rates of sulphate reduction and bicarbonate production similar to those presented here can be achieved using an inexpensive complex carbon source and a suitably adapted bacterial consortium.

The efficiency and characteristics of metal precipitation, from both single metal solutions and artificial acid mine drainage, induced by the addition of the biologically generated alkaline species was investigated, and will be discussed in chapter six.

CHAPTER 6. METAL PRECIPITATION: REACTION DYNAMICS AND THE IMPLICATIONS FOR PROCESS DESIGN

6.1 Introduction

The chemical precipitation of heavy metals, primarily by lime addition, has historically been the preferred method for the treatment of acid mine drainage (Dean *et al.*, 1972). This process is efficient for the removal of most metals and is relatively cost effective, when compared to more complex physico-chemical strategies.

Lime treatment requires a relatively short reaction time, due to the high solubility of lime (0.15%). This advantage is offset by the fact that the minimum solubilities for the different metals typically found in AMD occur at different pH values. The metal hydroxides are amphoteric in nature and as such, maximum metal removal cannot be achieved at a single precipitation pH level (Feng *et al.*, 2000). This has necessitated the introduction of multi-stage systems.

The removal of heavy metals from wastewater by sulphide precipitation, with Na_2S, NaHS or CaS, has become an increasingly popular option (Bhattacharyya *et al.*, 1981; Feng *et al.*, 2000). Sulphide precipitation is an attractive option as precipitation occurs effectively over a broad pH range and precipitation of certain metals can be achieved at very low pH values. Sulphide dosing, however, needs to be carefully controlled, particularly in the treatment of acidic effluents, due to the liberation of toxic H_2S gas at low pH. A number of authors (Hammack *et al.*, 1993; Hammack *et al.*, 1994; Foucher *et al.*, 2001) have reported on the use of biologically generated hydrogen sulphide gas to selectively precipitate heavy metals from mixed effluents. These systems are advantageous as the metal sulphides can be generated at low pHs.

More recently, the focus of attention has shifted towards active and passive biological treatment systems as they offer a more cost effective and potentially sustainable option. Many of these systems, such as artificial wetlands and sulphate reducing bacteria based systems, still rely heavily on precipitation as the primary mechanism for removing metals from solution. While the reactive

alkaline species may be of biological origin, the precipitation process is essentially the same as that which occurs in chemical based systems.

6.1.1 Alkaline species in biological systems

The biological systems described in chapters three to five contain three weak acid-base systems, which are responsible for determining the pH. They are the carbonate system (H_2CO_3, HCO_3^- and CO_3^{2-} species), the sulphide system (H_2S, HS^- and S^{2-} species) and the water dissociation system (H^+ and OH^- species). The equilibrium reactions and pK values are shown in table 6.1.

Table 6.1: Equilibrium reactions and pK values for the biologically influenced acid-base systems (Stumm and Morgan, 1996)

$H_2S \rightleftharpoons H^+ + HS^-$	$pK_1 = 7.06$ at 20°C
$HS^- \rightleftharpoons H^+ + S^{2-}$	$pK_2 = 13.89$ at 20°C
$H_2CO_3 \rightleftharpoons H^+ + HCO_3^-$	$pK_1 = 6.38$ at 20°C
$HCO_3^- \rightleftharpoons H^+ + CO_3^{2-}$	$pK_2 = 10.32$ at 20°C
$H_2O \rightleftharpoons H^+ + OH^-$	$pK_w = 7.00$ at 20°C

From table 6.1 it can be seen that the pK value for the equilibrium between HS^- and S^{2-} suggests that S^{2-} will not be present in a significant quantity in any biological reactors. Similarly, the value for the equilibrium between HCO_3^- and CO_3^{2-} suggests that CO_3^{2-} is unlikely to be present in the sulphate reducing components of biological systems, where the pH rarely exceeds 8 (Gibson, 1990).

6.1.2 Limitations to understanding biologically mediated precipitation

Numerous authors (Rose *et al.*, 1998; Chang *et al.*, 2000; Corbett, 2001; Foucher *et al.*, 2001; Glombitza, 2001; Shutes, 2001) have reported on the remediation of acid mine drainage using systems dependent on biologically generated sulphide and alkalinity. In these cases metal precipitation is typically expressed in terms of percentage removal or reduction in aqueous concentration, while neutralisation is regarded in terms of pH only. There appears to be little

information available on aspects such as the acidity of the effluents, mixing regimes based on molar or acidity/alkalinity ratios and analysis of the eventual precipitate. The result is that fairly broad assumptions are made as to the nature of the precipitate formed.

Chemical species modelling is a popular technique which can be used to predict the equilibrium condition existing in treated acid mine waters. As the models are based on thermodynamic rather than kinetic data, some of the species predicted to occur at equilibrium may not have been formed during the timescale of the experiment, which can reduce the validity of the model.

The results presented in this chapter aim to provide more focused information regarding metal precipitation by hydroxide, sulphide and carbonate species as well as assessing the validity of using the chemical speciation software MinteqA2 to model simple and more complex situations.

6.2 Research aims

The primary aims of this section of the project were:

1) To investigate the precipitation of individual metal species and a simulated acid mine drainage by individual anion species, anaerobic digester overflow and algal overflow.
2) To assess the accuracy of equilibrium species predictions generated by MinteqA2 compared to the experimental data.
3) To assess the potential for selective metal precipitation by biologically generated hydrogen sulphide.
4) To compare the settling properties of sludges generated by conventional hydroxide and sulphide treatments to those generated using biological sulphide and alkalinity.
5) To investigate the composition of the precipitates using wavelength dispersive X-ray spectrometry.

6.3 Materials and methods

6.3.1 Analytical techniques

All pH measurements were made using a Cyberscan 2500 pH meter. Alkalinity was measured using the method described in section 4.3.4. Acidity was determined according to Standard Methods (APHA, 1998), with the samples pretreated with 30% hydrogen peroxide, to oxidise all reduced iron and manganese, prior to titration. Metal analysis was performed using a GBC 909AA atomic absorption (AA) spectrophotometer, linked to a GBC integrator (Individual program parameters shown in Appendix G). Redox measurements were made using a redox probe integrated to purpose developed computer software, designed and constructed by Professor Justin Jonas and Anthony Sullivan of the Physics Department at Rhodes University.

6.3.1.1 Wavelength dispersive X-ray spectrometry (WDS)

Precipitate samples were finely ground using a mortar and pestle, loaded into a brass cylinder (8mm high with an internal diameter of 3mm). The samples were set in a boric acid case by applying seven tons of force for two minutes, using a hydraulic press. The samples were carbon coated and analysed using a JEOL superprobe 733, linked to a computer running the Probe for Windows software package. An accelerating voltage of 20kV and a beam current of 200nA were employed. An 80μm defocused beam was used to prevent degradation of the samples and compensate for any lack of uniformity in the sample surface. ZAF corrections were applied throughout. The detection limits, read times and peak analysed for each element are shown in appendix N.

6.3.2 Artificial acid mine drainage

A chemically defined artificial acid mine drainage (artAMD) was made up to closely resemble the profile of the water pumped from the East Rand Basin at Grootvlei. The concentration of the base metals, copper, lead, zinc, nickel and manganese were elevated above those found in the

Grootvlei water, so that the results could be considered applicable to both a typical gold and base metal type acid mine drainage. The composition of the artAMD is shown in table 6.2.

Table 6.2: Composition of the artificial acid mine drainage

Component	Reagent added	Mass (g) for 1l	Conc. (mg/l)	Conc. (μM)
Ca^{2+}	$CaCl_2.2H_2O$	0.850	231.65	5780
Cu^{2+}	$CuSO_4.5H_2O$	0.079	20.02	315
Fe^{2+}	$FeSO_4.7H_2O$	1.045	209.98	3760
H^+	H_2SO_4	2ml (1N)	2.00	2000
K^+	KCl	0.037	26.00	665
	KNO_3	0.017		
Mg^{2+}	$MgSO_4.7H_2O$	1.752	172.78	7109
Mn^{2+}	$MnCl_2.4H_2O$	0.144	39.99	728
Na^+	Na_2SO_4	0.803	278.41	12110
NH_4^+	NH_4Cl	0.021	6.57	386
Ni^{2+}	$NiCl_2.6H_2O$	0.081	20.01	341
Pb^{2+}	$PbCl_2$	0.027	20.10	97
Zn^{2+}	$ZnSO_4.7H_2O$	0.088	20.01	306
Cl^-	-	-	499.49	14090
NO_3^-	-	-	10.60	171
SO_4^{2-}	-	-	1741.92	18145

The pH of the artAMD varied between 2.96 and 3.04, with a mean acidity of 756 ± 4mg/l $CaCO_3$ equivalents. The aqueous species were modelled using the Minteq software (Appendix O). The model predicted the precipitation of $PbSO_4$. The aqueous species concentration of the individual components was confirmed by AAS for the cations and Spectroquant tests for the anions and NH_4. The detected lead concentration was 19.31μM, confirming the Minteq prediction.

6.3.3 Batch flask experiments

Batch flask experiments were conducted using 60ml of a 500µM metal solution. This corresponded to 30µmoles of metal. A suitable volume of 1M base stock solution (NaOH, $NaHCO_3$, Na_2CO_3 and Na_2S) was added to give the desired metal to base molar ratio. The flasks were agitated at 120rpm on an orbital shaker for 60 seconds and then allowed to stand for 30 minutes. A 5ml sample was removed and filtered through a 0.45µm nylon membrane filter. A second 5ml sample was centrifuged at 5000rpm for 5 minutes. The metal remaining in solution was determined using AAS. The pH was recorded at the beginning and end of the experiment. Minteq was used to model the equilibrium situation, predicting supersaturated species, the most likely precipitate, the percentage precipitation and equilibrium pH. Experiments were conducted in triplicate.

6.3.4 Settling cone experiments

The settling rates of the various precipitates were recorded by conducting the experiments in 1l Imhoff cones. Individual metal solutions (1mM) and artAMD were reacted with a suitable volume of stock solution or overflow from the 28l anaerobic digester or the algal gutters (described in chapter seven) at specific molar ratios or acidity/alkalinity ratios. The pH, aqueous metal concentration, volume of settled precipitate and, where appropriate, redox potential were measured at various intervals. The settled precipitate was collected, dried at 30°C and used for SEM and wavelength dispersive spectroscopy. Minteq was used to model the equilibrium situation as previously described. Experiments were conducted in triplicate.

The effect of hydrogen sulphide gas addition was determined by sparging a suitable volume of anaerobic digester overflow as described in the previous chapter. The stripped H_2S was bubbled through the metal solution using an air-stone at the bottom of the cone.

For the artAMD studies, settling efficiency was calculated in terms of moles of metal precipitated per volume of precipitate after six hours.

6.3.5. Statistical analysis

Unless otherwise stated, the results reported represent the mean of triplicate samples. The error bars are not shown in the figures to avoid over-complication. The P values were obtained using T-tests and were generated using Statistica, a statistical analysis package.

6.4 Results and discussion

While copper, lead, zinc and iron were studied, the preliminary data suggested that copper, lead and zinc reacted in a similar manner. Therefore, copper and iron were more extensively studies and those results are presented in this chapter, along with the artificial acid mine drainage data.

6.4.1 Copper

The results for the batch flask experiments using $CuSO_4$ as the metal salt are shown in figures 6.1 and 6.2.

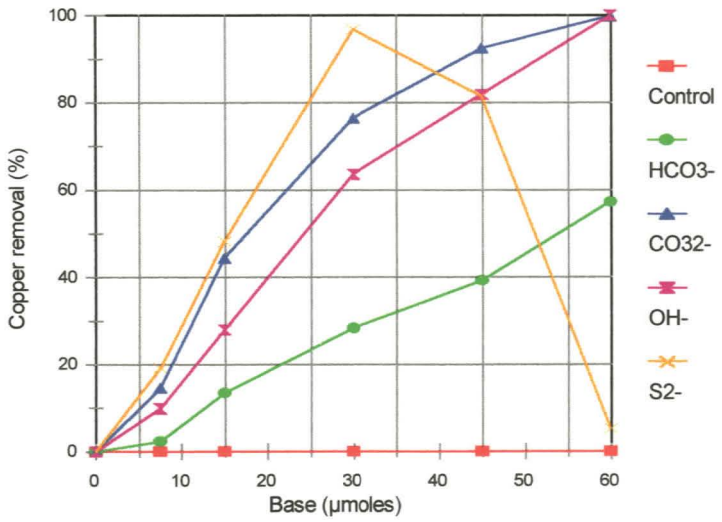

Figure 6.1: Precipitation of copper (30µmoles) by various bases at increasing molar ratios (mean values, n = 3). Samples filtered through 0.45µm nylon membrane filter

The results show an essentially linear relationship between the amount of base added and the amount of copper precipitated in all cases except sulphide. In all cases the addition of sulphide resulted in an instant reaction, with the appearance of the copper solution changing from clear to brown (Figure 6.3). Figure 6.1 shows that, at copper to sulphide ratios of 1:1 and above, the copper sulphide complex was effectively filtered out and that sulphide was the most effective base. However, at copper to sulphide ratios below one, an increasing percentage of the complex passes through the filter, with the percentage removal dropping to 5% at a ratio of 1:2.

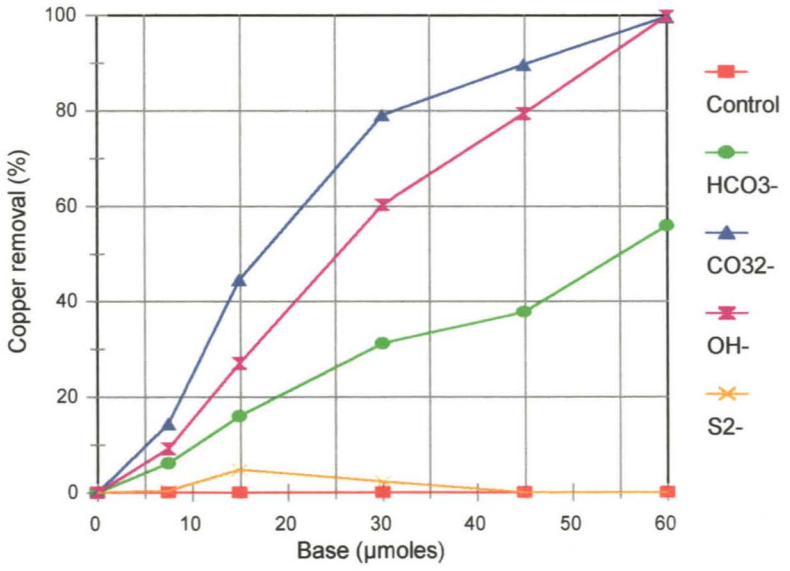

Figure 6.2: Precipitation of copper (30µmoles) by various bases at increasing molar ratios (mean values, n = 3). Samples centrifuged at 5000rpm for 5min

An evaluation of the data in figures 6.1 and 6.2 showed that there was no significant difference ($P > 0.05$, $n = 3$) in the percentage removal achieved by filtration and centrifugation for the addition of OH^-, HCO_3^- and CO_3^{2-}. There was, however, a clearly significant difference in the case of sulphide, with only negligible settling of the copper sulphide complex being achieved by centrifugation.

In addition, the results clearly show that despite a similar molar ratio in all cases there is significant difference ($P < 0.001$ in all cases) in the copper removal achieved by the different bases. Despite the OH^- and HCO_3^- having the same charge, the hydroxide precipitated almost two and a half times the amount of copper. The OH^- results are interesting as the precipitation

achieved is over 50% which would be the theoretical maximum, assuming precipitation as $Cu(OH)_2$. The CO_3^{2-} and S^{2-} achieved a greater degree of precipitation, as would be expected as they carry a greater negative charge. The removal achieved by carbonate addition was, however, significantly below the theoretical maximum if $CuCO_3$ is assumed to precipitate. The results of the equilibrium modelling are presented in table 6.3 and help to explain the observed results.

Table 6.3: Comparison of the experimental results obtained by precipitating $CuSO_4$ with a variety of bases, at a copper to base ratio of 1:1, to those predicted using MinteqA2

	Experimental		Predicted		
Base	pH	% prec.	pH	% prec.	Precipitating species
OH^-	6.13	63.6	5.72	66.6	Bronchantite - $Cu_4(OH)_6SO_4$
HCO_3^-	6.27	28.3	5.58	46.0	Malachite - $Cu(OH)_2CO_3$ and Bronchantite - $Cu_4(OH)_6SO_4$
CO_3^{2-}	6.63	76.4	6.04	90.3	Malachite - $Cu(OH)_2CO_3$
S^{2-}	6.61	96.88	7.00	100.0	Covellite - CuS

The data presented in table 6.3 show that the predicted situation in the case of OH^- and S^{2-} addition is relatively accurate in terms of the percentage removal, despite the equilibrium pH differing quite considerably. The formation of bronchantite following the addition of hydroxide would explain why the observed precipitation was over 50% at the 1:1 ratio. The increased precipitation was a result of the incorporation of a sulphate molecule which means that only 1.5 OH^- ions are required per Cu^{2+} ion, rather than two. The WDS analysis of the precipitate revealed a copper content of 54% and a sulphur content of 8%. Pure bronchantite would have a copper content of 56% and a sulphur content of 7%. Therefore, there is sufficient evidence to confirm the prediction of bronchantite. In the case of the precipitation with sulphide, the WDS data shows a copper to sulphide mass percentage ratio of 1.95, which is acceptably close to the ratio of 1.98 for pure covellite to confirm the prediction.

The predicted situation for the addition of bicarbonate and carbonate differ markedly from the experimental results. While malachite may be the most thermodynamically stable form, it requires a considerable period of time to form (Cairncross and Dixon, 1999) and can therefore be excluded

as a potential component of the precipitate. The addition of both bicarbonate and carbonate yields a mixture that is supersaturated with respect to a number of species. These are: $Cu(OH)_2$, bronchantite, antlerite ($Cu_3(OH)_4SO_4$), langite ($Cu_4(OH)_6SO_4.H_2O$), malachite and azurite ($Cu_3(OH)_2(CO_3)_2$). If the precipitation species is set as $Cu(OH)_2$ then the predicted precipitation is 24.1% for bicarbonate addition and 69.9% for carbonate, which while lower than the measured removal is considerably closer. The presence of sulphur, at between 4-6% (wt %), in both precipitates suggests the presence of some bronchantite, which would result in a slightly higher percentage removal than $Cu(OH)_2$ alone.

6.4.1.1 The copper-sulphide system

The copper-sulphide system was investigate further by repeating the experiments, but extending the reaction time to seven days. The copper sulphide complex underwent a distinctive change after approximately three and a half days, with a progressive colour change from brown to a dark green/black, followed by eventual settling of the precipitate after six days. This transition is shown in figure 6.3.

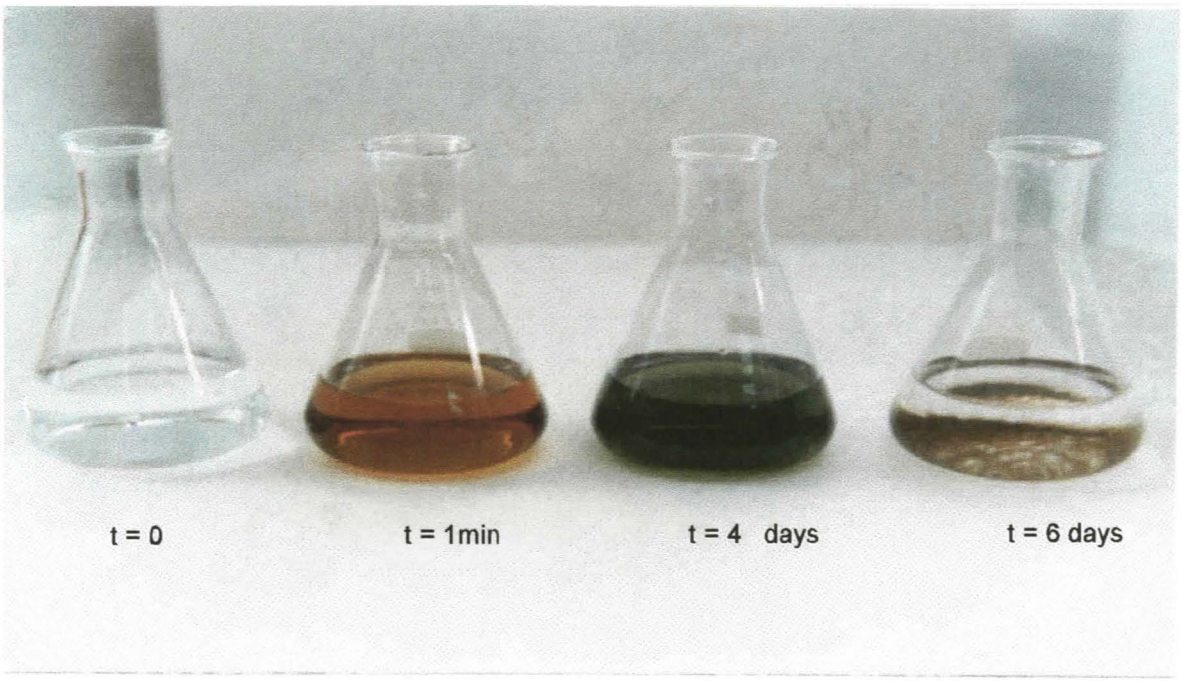

Figure 6.3: Evolution of a readily settling precipitate following the addition of aqueous sulphide to copper sulphate at a molar ratio of 1:1

These results are consistent with those obtained by Silvester *et al.* (1991) and Pattrick *et al.* (1997), who showed changes in copper sulphide precipitates in response to ageing and heating. The colour changes were initially attributed to a change in the formal oxidation state (Silvester *et al.*, 1991), but this was discounted by Pattrick *et al.* (1997), who showed that in all cases the precipitates contained only Cu(I).

Pattrick *et al.* (1997) concluded that the addition of sulphide led to the formation of a very fine grained, metastable precipitate. The fine grain size resulted in the precipitate effectively forming a dilute suspension (Figure 6.3), which could not be removed by centrifugation. Ageing resulted in the formation of large fused aggregates of grains, which readily settled. Particle size has been shown to be an important control of the apparent colour of very fine grained precipitates (Chow and Zukoski, 1994). The small size of the brown precipitate means that the colour observed will be the result of both light scattering and electronic transitions. Pattrick *et al.* (1997) used X-ray absorption near edge structure analysis of the brown precipitate to show that the electronic structure was poorly developed and, therefore, the ordered electronic transitions that lead to the blue/green colour may not have been possible.

The phenomenon of the formation of a primitive CuS precipitate was only observed where aqueous sulphide was added. When gaseous hydrogen sulphide was used, a more coarse, dark green/black, precipitate formed almost immediately. This was accompanied by a decrease in pH, as shown in table 6.4.

Table 6.4: Copper precipitation by gaseous hydrogen sulphide. A 1mM $CuSO_4$ solution (1l) was sparged with biogenic H_2S for two minute periods, followed by a ten minute settling period (mean values, n = 3)

Time (min)	pH	Settled volume (ml)	Copper in solution (μM)
0	5.47	0.0	1000.00
12	3.47	0.2	842.34
24	3.07	2.5	444.39
36	2.88	1.6	207.716
48	2.69	1.5	9.38
60	2.67	1.5	0.24

Table 6.4 shows that 10 minutes of sparging is a sufficient time to introduce enough hydrogen sulphide to effect the precipitation of all the copper in solution. The sulphide stripping experiments described in the previous chapter showed that 10 minutes of sparging with either nitrogen (Figure 5.12) or air (Figure 5.11) resulted in the stripping off of almost 1400μmoles of H_2S, which would be sufficient to precipitate all the copper. The associated decrease in pH is as a result of the liberation of hydrogen ions by the reaction shown below.

$$H_2S_{(gas)} + Cu^{2+}_{(aq)} \rightarrow CuS_{(s)} + 2H^{+}_{(aq)}$$

The introduction of additional hydrogen sulphide gas did not affect the precipitation process or significantly ($P > 0.095$) change the pH and redox potential. This is in contrast to the situation with aqueous sulphide, where the addition of excess sulphide resulted in a substantial increase in pH, decrease in the redox potential, and retarded the formation of a precipitate which settled out of suspension. This suggests that pH and redox may play a significant role in the aggregation of the fine grained precipitate.

6.4.1.2 Settling cone experiments

The settling cone experiments confirmed the results obtained in the batch experiments with similar copper removal percentages being recorded for the various bases. In addition, the settling cone experiments highlighted the effect the non-alkaline anion species present in the solution can have on the efficiency of precipitation. Figures 6.4 and 6.5 show the results obtained by the addition of hydroxide (Cu to OH^- ratio of 1:1) to solutions of copper sulphate and copper chloride respectively. From the batch experiments it was confirmed that bronchantite was the precipitating species in the copper sulphate system. Modelling of the copper chloride system predicted tenorite, a form of $Cu(OH)_2$, to be the precipitating species. The maximum theoretical percentage precipitation for tenorite at a Cu to OH^- ratio of 1:1 is 49.9%, compared to the 66.6% for bronchantite. While figure 6.5 shows a percentage copper precipitation in the $CuCl_2$ system of slightly over 50%, it is still considerably lower than that achieved in the $CuSO_4$ system. In both cases the precipitate formed was fine grained and blue in colour, although the bronchantite was lighter in colour. The bronchantite clearly had superior settling characteristics, demonstrated by the fact that it had begun to settle to the bottom of the cone, while the tenorite remained in suspension. Addition of sodium sulphate to the $CuCl_2$ system resulted in bronchantite precipitation.

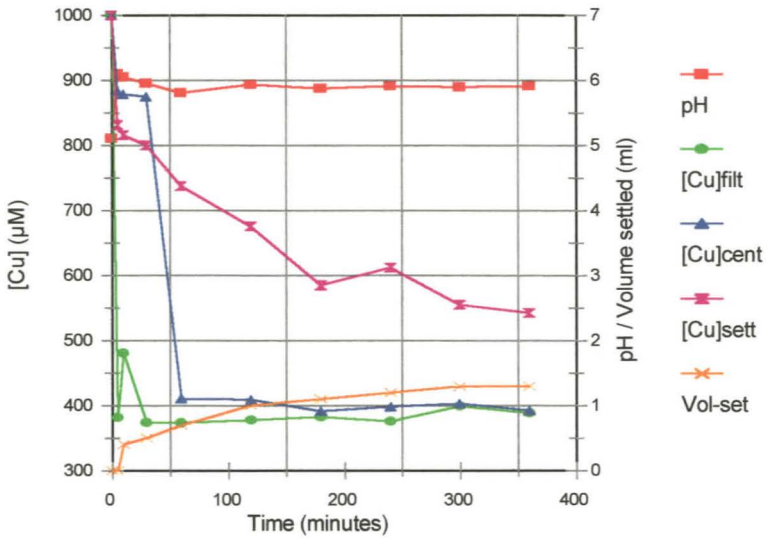

Figure 6.4: Copper precipitation and settling achieved by the addition of NaOH to 1mM $CuSO_4$ at a molar ratio of 1:1 (mean values, n = 3). Experiments conducted in a 1l Imhoff cone. Samples were filtered through a 0.45µm nylon membrane filter (filt), centrifuged at 5000rpm for 5min (cent) and untreated (sett). Vol-set = volume of settled precipitate

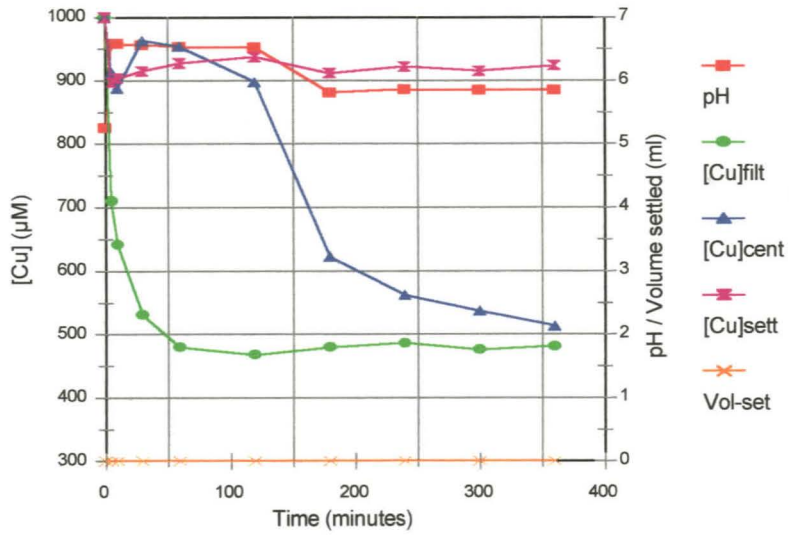

Figure 6.5: Copper precipitation and settling achieved by the addition of NaOH to 1mM $CuCl_2$ at a molar ratio of 1:1 (mean values, n = 3). Legend explanation as for figure 6.4

Changing the copper to hydroxide ratio to 1:2 resulted in over 99% copper precipitation in both the $CuSO_4$ and $CuCl_2$ system. There was, however, a significant difference ($P < 0.001$) in the settling rate and settling volume of the precipitates as can be seen in figure 6.6.

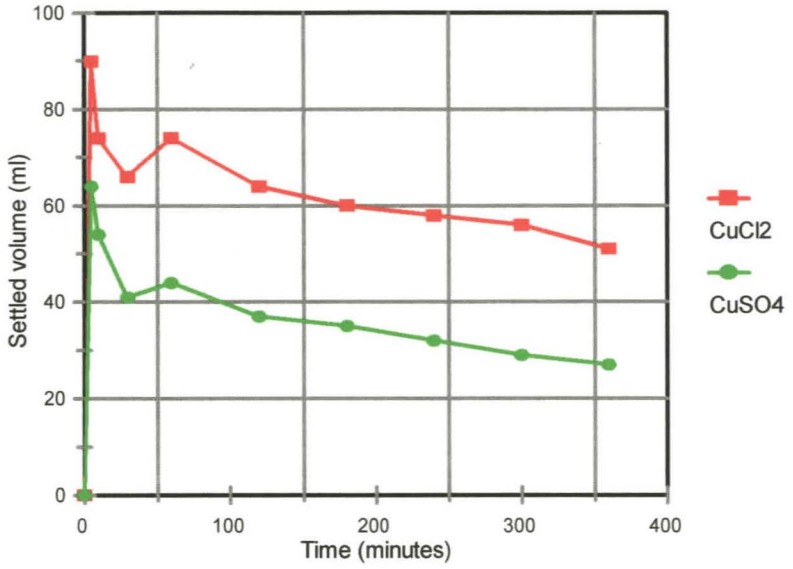

Figure 6.6: Settling rate and volume for precipitates generated by the addition of NaOH to 1mM $CuCl_2$ and $CuSO_4$ in a 1l Imhoff cone (mean values, n = 3). Cu to OH^- ratio 1:2

The initial reaction, upon the addition of the hydroxide, resulted in similar looking precipitates to those formed at the 1:1 ratio. However, after 30 minutes the colour in the $CuCl_2$ cones began changing from blue to green, which became progressively dark blue/black after 120 minutes. A similar trend was observed in the $CuSO_4$ cones, but the change only began after 90 minutes. Minteq predicted tenorite precipitation in both cases. Tenorite should have a Cu weight percentage of 65.16%, but the WDS data indicated a Cu wt% of 71.4% for the chloride system and 66.83% in the sulphate system. In addition, sulphur was detected at a wt% of 3.7% in the precipitate from the $CuSO_4$, which suggests the presence of some bronchantite. The change of the precipitate from blue to black suggests the maturation of $Cu(OH)_2$ to CuO, which would have a Cu wt% of 79.8%. Therefore, the data suggest that in the chloride system the tenorite is in the process of maturing to CuO, while the sulphate system appears to contain a mixture of

bronchantite and CuO. A mixture of 52% bronchantite and 48% CuO would result in the correct sulphur content and a copper content of 67.4%, which is close to the measured percentage of 66.83%. The presence of bronchantite would result in the more compact precipitate which was observed (Figure 6.6).

The addition of sulphide achieved 100% copper removal, although this required 88 hours at a copper to sulphide ratio of 1:1 and 116 hours at a ratio of 1:2. At the 1:2 ratio, free sulphide at a concentration of 28.95mg/l, was detected in solution after five minutes. This concentration gradually decreased over time until it had all been oxidised, after 104 hours. This was accompanied by a decrease in pH from 11.02 to 5.56. The colour change from brown to green only began after all the free sulphide had been oxidised, which reinforces the suggestion that the maturation of amorphous CuS to stable covellite is pH and redox dependent. The WDS analysis of the precipitate formed at both copper to sulphide ratios indicated a stoichiometric relationship between copper and sulphide of one to one, which is consistent with covellite.

Overflow from the 28l anaerobic digester (ADO) was used to precipitate $CuSO_4$ at metal to alkaline species ratios of 1:1 and 1:2. The alkaline species in the ADO were calculated at concentrations of 38.84mM for HCO_3^- and 7.95mM for HS^-. These values were used to determine the volume of ADO to add for the specific ratios. The results from the settling cones are shown in figures 6.7 and 6.8 and indicate copper removal of 44% and 68% respectively after 10 hours. The modelled equilibrium situation generated by Minteq predicts a copper removal percentage of 51.9% at the 1:1 ratio and 87.1% at the 1:2 ratio. In both cases covellite and malachite are predicted to precipitate, with bronchantite also predicted to exist at the 1:1 ratio. From the results generated using individual basic species, it can be assumed that the covellite and bronchantite are accurate predictions. Similarly, malachite is unlikely to exist after only 10 hours. The other precipitating species is most likely to be $Cu(OH)_2$ rather than malachite and this would explain why the observed percentage removals were lower than the predicted. In addition, this would result in the equilibrium pH being higher than those predicted (5.41 and 5.66), which was indeed observed.

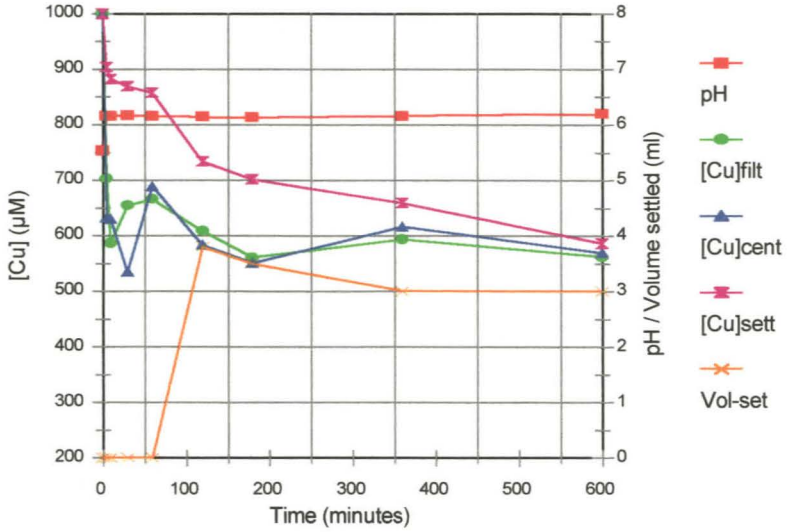

Figure 6.7: Copper precipitation and settling achieved by the addition of anaerobic digester overflow to 1mM $CuSO_4$ at a molar ratio of 1:1 (mean values, n = 3). Experiments conducted in a 1l Imhoff cone. Samples were filtered through a 0.45µm nylon membrane filter (filt), centrifuged at 5000rpm for 5min (cent) and untreated (sett). Vol-set = volume of settled precipitate

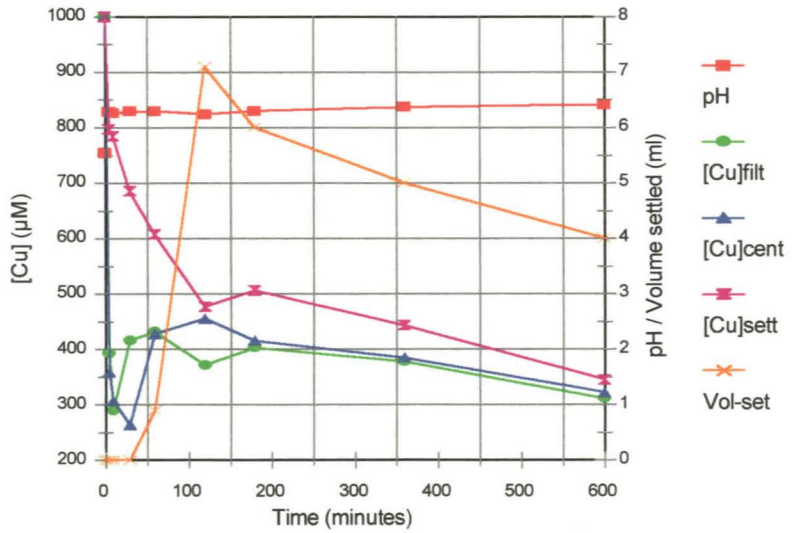

Figure 6.8: Copper precipitation and settling achieved by the addition of anaerobic digester overflow to 1mM $CuSO_4$ at a metal to base ratio of 1:2 (mean values, n = 3). Explanation of legend as for figure 6.7

Anaerobic digester overflow that had been sparged with air as described in chapter five was also tested. The metal precipitation percentage was similar to that achieved using the unaerated ADO, but the characteristics of the precipitate differed markedly in colour and settling characteristics. The precipitate generated by the aerated ADO was blue, rather than dark brown, and settled faster than the precipitate from the unaerated ADO. This advantage was, however, offset by the bulky nature of the precipitate, which had a volume over four times as large. The difference in the precipitate properties is due to the absence of sulphide from the aerated ADO, which would result in a blue coloured, more bulky hydroxide-based precipitate.

6.4.2 Iron

Iron forms the major heavy metal component of most acid mine drainage discharges and as such, an understanding of its precipitation is of critical importance in developing precipitation based systems for treating acid mine drainage. At the point of discharge to the surface from the previously anoxic environment, the majority of the iron will be in the ferrous form so this was the form used in most of the experiments.

The batch experiments showed a similar trend for iron as with copper, with the hydroxide, bicarbonate and carbonate exhibiting a proportional relationship between the amount of base added and the amount of iron precipitated. The addition of sulphide, however, once again led to the formation of an amorphous complex which passed through the 0.45μm filter when the sulphide to iron ratio was greater than 1:1.

As with the copper, if the duration of the experiment was extended, the suspension underwent a change in appearance and a precipitate that readily settled evolved. The change in appearance occurred more rapidly than with copper, with colour changing from black to yellow within 60 minutes and settling occurring within 240 minutes in the 60ml batch flasks (Figure 6.9). The observed change was intimately linked to the presence of oxygen. The changes in pH and free sulphide present in solution, following the addition of Na_2S to a solution of $FeSO_4$ at a sulphide to iron ratio of 2:1, under aerobic and anaerobic conditions are shown in figure 6.10.

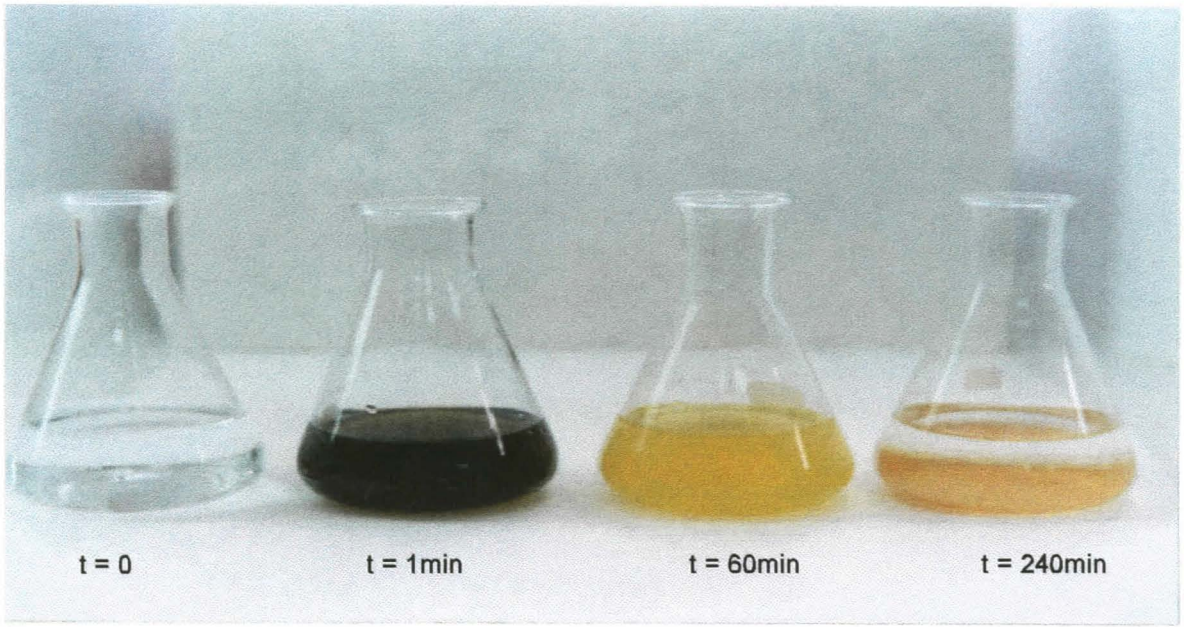

Figure 6.9: Evolution of a readily settling precipitate following the addition of aqueous sulphide to 500μM ferrous sulphate at a molar ratio of 1:1

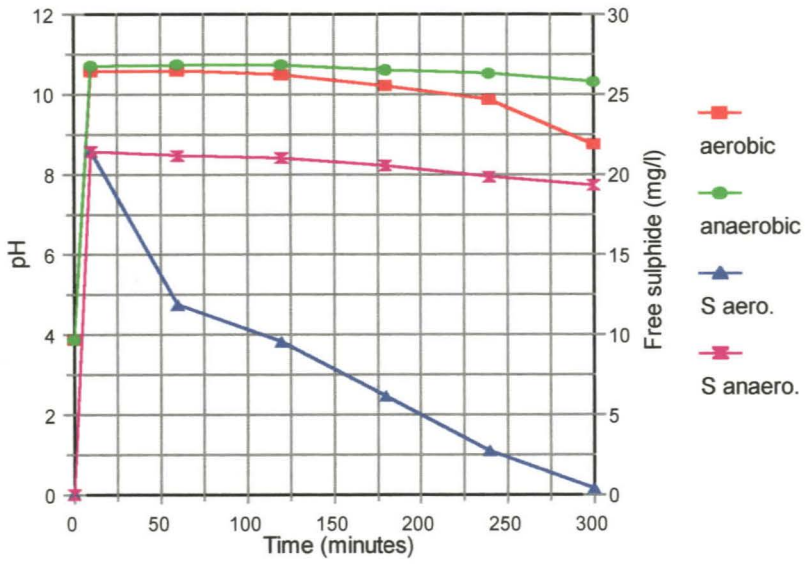

Figure 6.10: Changes in pH and free sulphide in solution, following the addition of Na_2S to $FeSO_4$ at a molar ratio of 2:1, under aerobic and anaerobic conditions (mean values, n = 3)

Figure 6.10 shows that complete oxidation of the free sulphide occurs within five hours. Associated with the oxidation of the sulphide is a reduction in pH. The sulphide oxidation and reduction in pH are negligible in the flasks maintained under anaerobic conditions. The effect of this on the concentration of iron in solution is shown in figure 6.11.

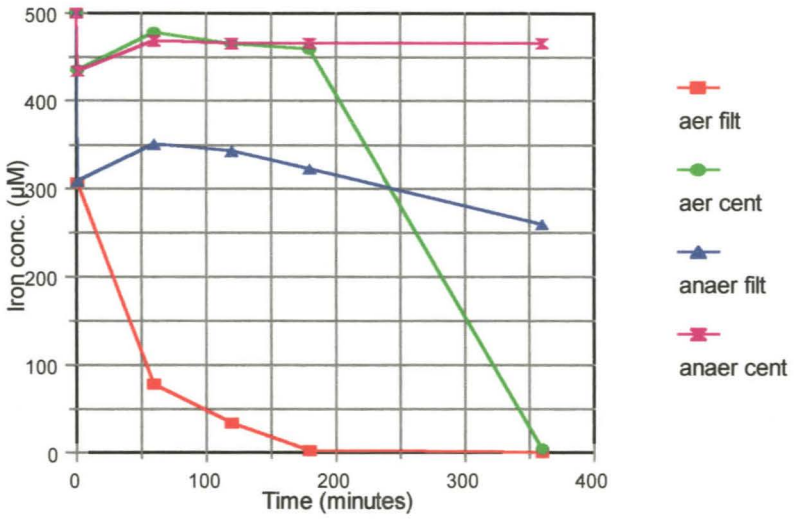

Figure 6.11: Concentration of iron remaining in solution, following the addition of Na_2S to a solution of $FeSO_4$ at a molar ratio of 2:1, under aerobic and anaerobic conditions (mean values, n = 3). Samples were filtered through a 0.45µm nylon membrane filter (filt) or centrifuged at 5000rpm for 5min (cent)

The effect of the exclusion of oxygen on the rate and efficiency of iron precipitation is clearly shown in figure 6.11. In the flasks exposed to the air the free sulphide concentration after 180 minutes had been reduced to 6mg/l and the precipitate had begun to change colour and aggregate. By 360 minutes complete removal was achieved by centrifugation, while in the flasks kept anaerobic, no maturation of the precipitate had occurred and iron removal by centrifugation remained negligible.

The precipitation of FeS, under anaerobic conditions, and the subsequent formation of pyrite has been fairly extensively researched (Rickard, 1995; Wilkin and Barnes, 1996; Rickard 1997a and 1997b). Rickard (1995) proposed two competing mechanisms for the formation of FeS. These are shown below:

$$Fe^{2+} + H_2S \rightarrow FeS_{(s)} + 2H^+ \text{ and}$$
$$Fe^{2+} + 2HS^- \rightarrow Fe(HS)_{2\,(s)}$$

The bisulphide ($Fe(HS)_2$) pathway requires a second stage, which involves the condensation of $Fe(HS)_2$ to FeS and H_2S.

A combination of experimental and theoretical data allowed Rickard (1995) to conclude that the dominant reaction was determined by pH and sulphide concentration. In general, environments with high dissolved sulphide concentrations ($\geq 10^{-3}$M) have pHs greater than seven. In these systems the bisulphide pathway dominated, while at lower sulphide concentrations the pH was typically below seven and the H_2S pathway dominated.

The initial precipitate formed by the addition of sulphide to aqueous iron is amorphous and was found to contain an excess of sulphide in the formula, which could not be explained by simple nonstoichiometry (Sweeny and Kaplan, 1973). The amorphous precipitate developed long-range structural ordering after two days, developing X-ray peaks equivalent to mackinawite. The formation of well crystalline mackinawite in aqueous solutions at 25°C was, however, found to take up to two years (Sweeny and Kaplan, 1973). Voltammetric studies of the aqueous iron(II) sulphide system led to the proposed existence of a number of iron sulphide complexes including $Fe(SH)^+$, Fe_2SH^{3+} (Luther and Ferdelman, 1993) and $Fe(SH)S_x^-$ (Luther, 1991). The formation of a negatively charged iron polysulphide complex would explain the results shown in figures 6.10 and 6.11, where free sulphide species were detected by the sulphide assay. However, sparging of the solution with nitrogen did not reduce the concentration of detectable sulphide. The polysulphide complex contains a terminal, charged sulphide which would be detected by the assay, but would not have been stripped off by sparging, while aqueous H_2S would.

The data on FeS precipitation and pyrite formation were experimentally obtained in systems devoid of oxygen and would be applicable to anaerobic sediments and SRB reactors. However, in a practical AMD treatment operation it would be impossible to exclude oxygen from the precipitators and clarifiers. Therefore, while the mechanisms described above may play a minor role in these systems the effect of oxygen cannot be ignored.

The mechanism of air oxidation of pyrrhotite (Fe_7S_8) was determined by Pratt *et al.* (1994). Native pyrrhotite typically contains 68% Fe(II) and 32% Fe(III). They used mineral fragments 2 x 2 x 5mm in size and investigated the effect of exposure to oxygen for various time periods. The proposed mechanism involved the bonding of molecular oxygen to the pyrrhotite surface, followed by its reduction, through a number of intermediates, to O^{2-}. They showed that Fe(III) bonded to sulphur was the most reactive pyrrhotite component to oxygen and that there were lattice vacancies associated with Fe(III)-S bonding. Molecular oxygen adsorbed at the surface-exposed lattice vacancies may be rapidly reduced through the transfer of electrons from the interior. The electrons were derived from either Fe(II) or S^{2-}, resulting in an increase in the Fe(III) percentage. The presence of Fe(III) adjacent to the vacancy promoted electron transfer, as the transfer of electrons between Fe(II) and Fe(III) is exceptionally fast. By this mechanism, virtually all the Fe(III)-S bonds were converted to Fe(III)-O bonds and Fe(III)-oxyhydroxide was formed. The research indicated that the rate of growth of the oxyhydroxide layer decreased with time (4Å after 6.5h, 8Å after 50h), due to diffusion considerations (Pratt *et al.*, 1994).

The results from this study suggest a similar mechanism is at work with the oxidation of the Fe(II) in the amorphous FeS to Fe(III) followed by the replacement of the bonded sulphur by oxygen and the eventual maturation of the precipitate from FeOOH to Fe_2O_3. The small grain size of the amorphous FeS would negate the diffusion problems encountered in the pyrrhotite experiments.

6.4.2.1 Settling cone experiments

The settling cone experiments concentrated on the effect of oxygen on the settling rates and final volume of the precipitate generated by the addition of sulphide to iron. The role played by pH and redox potential were also assessed.

The relationship between redox potential and settling of the precipitate is shown in figure 6.12.

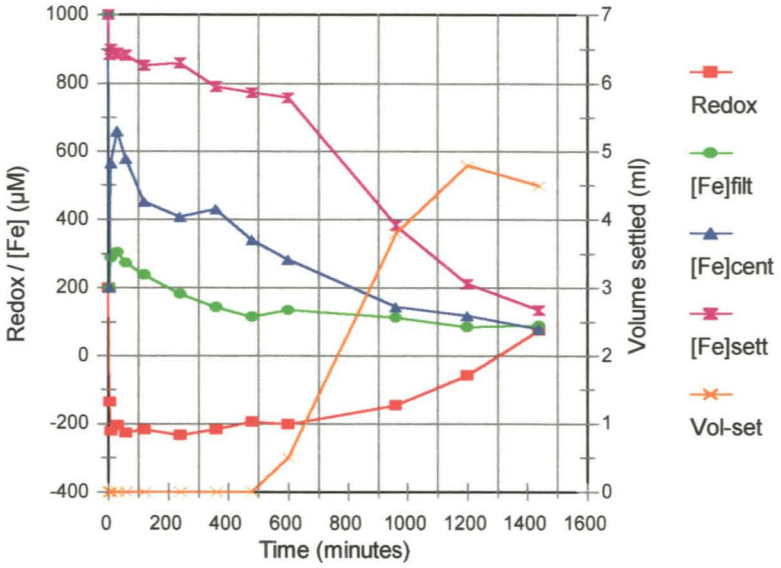

Figure 6.12: The relationship between redox potential and the settling rate and volume of the precipitate generated by the addition of aqueous sulphide to a 1mM $FeSO_4$ solution at a molar ratio of 1:1 (mean values, n = 3). Explanation of legend as for figure 6.7

Figure 6.12 shows that the addition of sulphide to the $FeSO_4$ produced a dramatic change in redox from 199 to below -200mV. This was associated with an increase in pH from 4.7 to 7.3 (data not shown in figure 6.12) and the formation of an inky black amorphous precipitate. The amorphous Fe-S complex remained in suspension for over 10 hours before a precipitate began to settle. This was accompanied by an increase in the redox potential and a decrease in pH. The data from the batch experiments suggest that this is a result of the oxidation of free sulphide groups. The appearance of the liquid in the cone also began to change from inky black to a dark brown/orange colour, which became more prevalent as the redox approached a positive value. The WDS analysis of the precipitate collected after 24 hours indicated an iron percentage of 68% and a sulphur content of 4%. Pure FeS would have a sulphur content of 36.8%, clearly indicating that the initial Fe-S complex has been oxidised. The weight percentage of iron in the precipitate was slightly lower than that of Fe_2O_3 (69.6%) and higher than that for FeOOH (62.5%). This suggests that the precipitate was predominantly Fe_2O_3 with lower percentages of FeOOH and unoxidised

FeS. Such a situation would be consistent with the mechanism proposed by Pratt *et al.* (1994) with the final maturation of FeOOH to the more stable Fe_2O_3.

The active sparging of the system with air at a rate of 40ml/s greatly increased the oxidation rate and resulted in complete settling of the precipitate in three hours after the pump had been switched off (Figure 6.13).

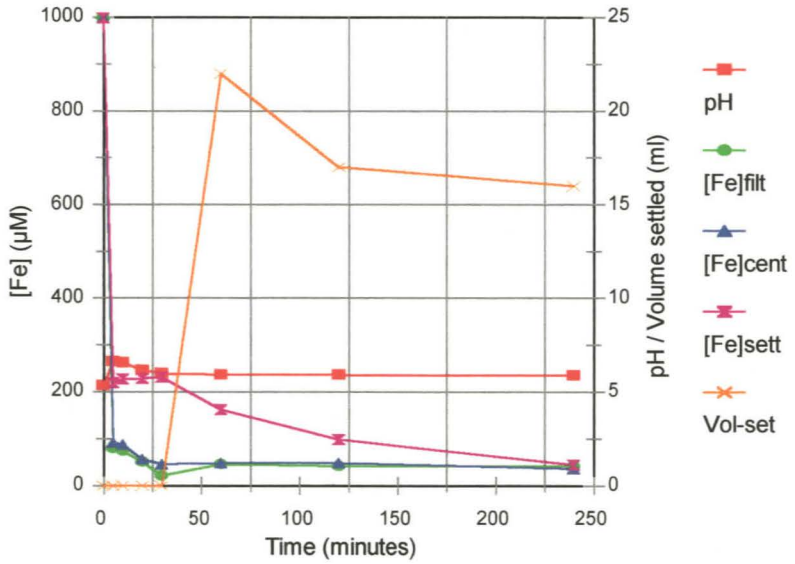

Figure 6.13: The effect of air sparging for 30 minutes on the settling rate and volume of precipitate generated by the addition of aqueous sulphide to a 1mM $FeSO_4$ solution at a molar ratio of 1:1 (mean values, n = 3). Legend description as for figure 6.7

While the total iron removal was only slightly higher than in the unaerated system, the volume of the precipitate was over three times greater. The most likely explanation for this is that the precipitate was predominantly FeOOH, which forms a less dense precipitate than Fe_2O_3. The shorter duration of the experiment, four hours as opposed to 24 hours, would have resulted in a lower proportion of the precipitate maturing to Fe_2O_3. Further evidence for this was the characteristic bright orange colour and the lower weight percentage (65.6%) of iron in the precipitate.

6.4.3 Artificial acid mine drainage

Settling cone experiments were conducted using artAMD treated with NaOH (OH^-), Na_2S (S^{2-}), nitrogen sparged (N_2spADO) and unsparged anaerobic digester overflow (ADO) and overflow from the algal reactors (Alg OF). The hydroxide and sulphide experiments were conducted to evaluate conventional chemical treatments, while the various digester overflows and algal overflow were used to evaluate the individual components of the integrated system. Acidity to alkalinity ratios of 1:1 and 1:2 were used. In all cases 628ml of the artAMD was used, to which the specific volume of basic solution was added. The volume was made up to 1l using ddH_2O. The metals remaining in solution were measured after three hours, sufficient time to allow precipitate settling without the oxidation and subsequent precipitation of ferrous iron and reduced manganese to occur. The settled volume was measured at various intervals for six hours and the combined results are shown in figure 6.14.

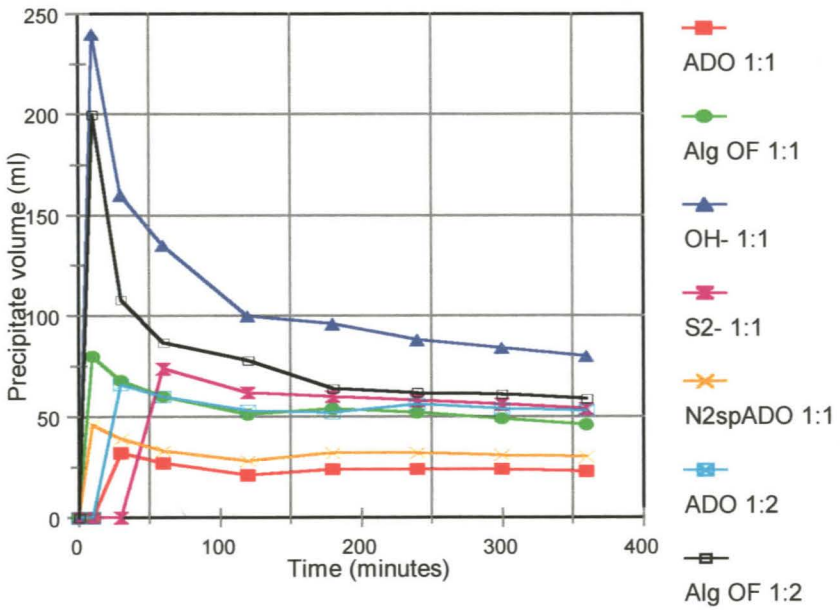

Figure 6.14: Settling rates and volumes of precipitates generated by the addition of various basic solutions to artificial acid mine drainage in 1l Imhoff cones (mean values, n = 3). Acidity to alkalinity ratios of 1:1 and 1:2 were used.

Figure 6.14 shows that the precipitate formed by the addition of hydroxide was the most voluminous, followed by those formed by the addition of overflow from the algal reactors. The

precipitates formed by the addition anaerobic digester overflow appeared considerably less bulky than those where algal overflow was added, suggesting that the presence of sulphide results in less bulky precipitates. The precipitates formed by the addition of ADO and S^{2-} took longer to begin settling due to the initial formation of amorphous metal sulphides. This is shown in figure 6.15. Figure 6.14 is slightly deceiving as it does not take into account the amount of metal precipitated. A clearer picture is evident from table 6.5, which shows the percentage metal removal in each case and expresses the precipitate data in terms of μmoles of metal per ml of precipitate.

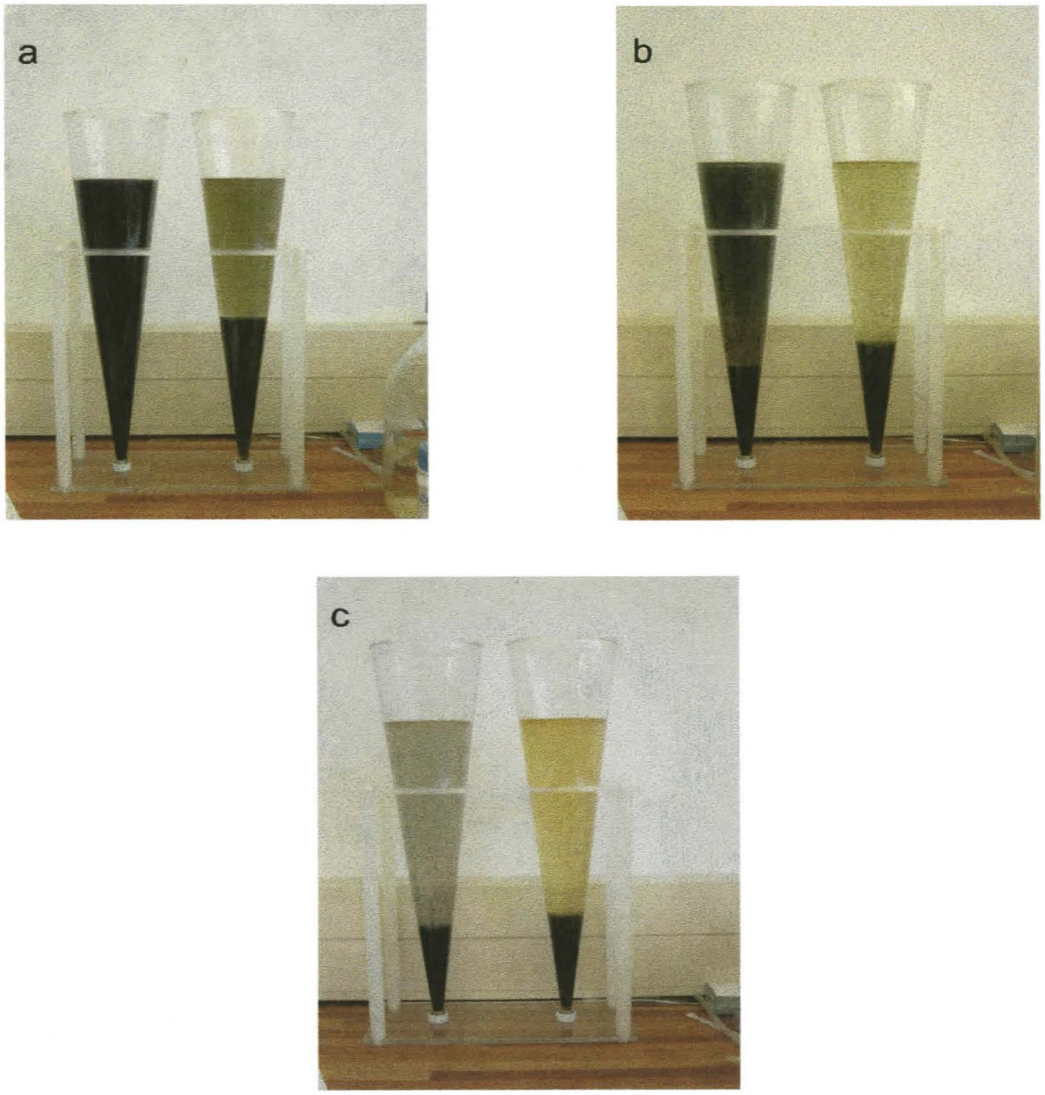

Figure 6.15: The appearance and rate of precipitate formation following the addition of anaerobic digester overflow (left cone) and algal vessel overflow (right cone) to artificial acid mine drainage. Time after mixing is (a) 10 minutes, (b) 60 minutes and (c) 180 minutes

Table 6.5: Metal removal after 180 minutes in settling cone experiments using artificial acid mine drainage and a range of basic solutions (mean values, n = 3). For metal removal, settled data was used

	Percentage metal removal								Precipitate	
Base	Ca	Cu	Fe	Mg	Mn	Ni	Pb	Zn	Total µmoles	µmoles per ml
Initial (µM)	3630	198	2361	4465	457	214	61	192	11578	-
OH^- 1:1	27.1	99.2	99.8	21.2	64.0	89.6	100.0	94.3	5096	63.7
S^{2-} 1:1	24.5	99.3	97.4	17.4	47.0	98.3	100.0	98.1	4748	87.9
ADO 1:1	30.4	99.7	41.3	25.2	15.9	19.0	100.0	98.3	3222	140.1
N_2spADO 1:1	46.4	99.2	61.8	6.6	18.4	13.3	100.0	65.3	3137	104.6
Alg OF 1:1	48.9	98.2	83.4	1.9	24.0	27.3	100.0	53.5	4215	91.6
ADO 1:2	28.1	99.1	80.1	1.4	29.2	92.4	100.0	99.6	3833	67.3
Alg OF 1:2	25.8	98.6	99.7	9.6	54.9	93.6	100.0	99.0	4625	72.3

The data from table 6.5 highlight a number of important facts. The total metal removed by the hydroxide and sulphide is similar, but considerably higher than those for the biologically generated bases at the acidity to alkalinity ratio of 1:1. This can be explained by the presence of a high concentration of bicarbonate, which as previously shown, has an acid and a basic potential in the biogenic streams. The sulphide and hydroxide solutions have no acid potential. The algal overflow sample performed appreciably better than the anaerobic digester overflow, which can be accounted for by the conversion of bicarbonate to carbonate ions.

A consistently high percentage of copper and lead removal was achieved. Zinc removal was consistently higher in the samples containing aqueous sulphide, suggesting precipitation as a sulphide, but was also effective in the presence of higher concentrations of hydroxide (OH^- and Alg OF 1:2). In contrast, nickel did not appear to precipitate as a sulphide and as was only effectively removed in the presence of excess alkalinity, suggesting precipitation as a hydroxide. A similar trend was observed for manganese, although manganese removal was generally ineffective. The hardness metals, calcium and magnesium, were also not effectively removed. This problem was exacerbated by the presence of a high concentration of magnesium in the anaerobic digester overflow, due to the use of magnesium sulphate in the Postgate medium.

In terms of the metal precipitated per ml of precipitate the biogenic samples at the 1:1 ratio performed best, although the inefficient removal of particularly iron means that this ratio could not be applied in a treatment system. Comparing the biogenic streams at the 1:2 ratio with the sulphide and hydroxide it is clear that the hydroxide produces the most voluminous precipitate and sulphide the least, which has been reported in the literature (Boshoff, 1999). As far as the biogenic samples were concerned, the algal overflow precipitated more metal per volume of precipitate than the anaerobic digester overflow.

Attempts to model the complex artAMD cone experiments did not yield accurate results. For example, the modelled predictions for the addition of algal overflow at an acidity to alkalinity ratio of 1:2 were, 81% iron removal (as siderite - $FeCO_3$), 95% lead removal (as cerrusite - $PbCO_3$) and 96% copper removal (as malachite - $Cu_2(OH)_2CO_3$). While the predicted equilibrium pH (6.50) was similar to the observed results the model underestimated the efficiency of the system. Similarly, while the WDS data showed weight percentages for the individual metals that were consistent with the amounts that had been removed from solution, little information on the precipitated species could be gathered.

6.4.4 Selective metal precipitation with H_2S gas

The results for the selective precipitation of metals from the artificial acid mine drainage are shown in figures 6.16 and 6.17. Figure 6.16 shows the effect of sparging with nitrogen on the pH and aqueous sulphide concentrations of the anaerobic digester overflow and the AMD solution. As previously noted, the stripping of H_2S from the ADO results in an increase in pH as a result of the loss of hydrogen ions as the sulphide equilibrium is driven from HS^- to H_2S formation. Similarly, the pH of the AMD solution decreases as the two hydrogen ions from the H_2S gas are released as the sulphide binds to the metals.

Figure 6.17, showing the concentration of metals remaining in solution in the AMD, clearly indicates that copper and lead react rapidly with the H_2S to form insoluble sulphide precipitates, while no reaction occurs with zinc and nickel. The appearance of sulphide in the post-reaction NaOH trap after 10 minutes indicates that the lack of reaction by zinc and nickel was not due to insufficient H_2S. Similarly, no reduction in the concentration of dissolved manganese, iron,

calcium or magnesium was noted. The lack of reactivity of zinc, at pHs up to six, is contrary to the results of Hammack *et al.* (1993) who reported good zinc removal at pHs between two and four. Experiments conducted with pure zinc sulphate and zinc chloride solutions (results not shown) confirmed the results achieved with the AMD, with only a small reduction (4-7%) in the zinc concentration at pH 4 and 5, with no precipitation above pH 5.

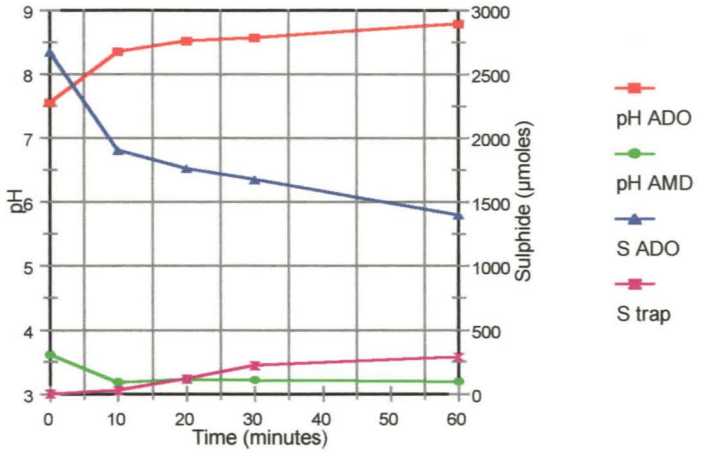

Figure 6.16: The effect on pH and aqueous sulphide of sparging artificial acid mine drainage with biogenic H_2S (mean values, n = 5). S trap = post sparging NaOH trap

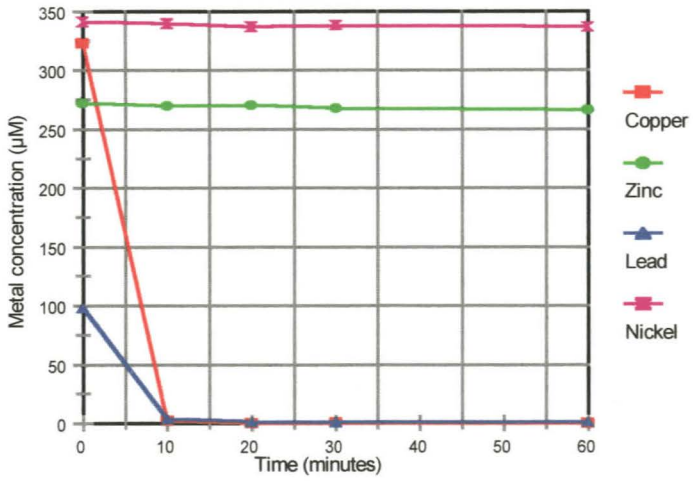

Figure 6.17: Metal removal from artificial acid mine drainage by biogenic H_2S (mean values, n = 5)

6.5 Conclusions

The results from this chapter show that the precipitation of copper and ferrous iron by the addition of hydroxide, bicarbonate and carbonate ions resulted in the rapid formation of a precipitate that settled readily. The amount of metal removed was proportional to the amount of base added up to the point of maximum removal. The addition of base in excess of that required for complete removal led to a decrease in efficiency, due to the formation of soluble, anionic hydroxide complexes (eg $Me(OH)_3^-$). In the case of copper, the presence of sulphate in solution led to the precipitation of bronchantite ($Cu_4(OH)_6SO_4$), which had preferential settling properties to $Cu(OH)_2$. In addition, the incorporation of a sulphate ion into the precipitate resulted in an increase in the efficiency of copper removal per base ion added.

The addition of aqueous sulphide resulted in the formation of amorphous precipitates for both copper and iron. At sulphide to metal ratios of up to 1:1 this precipitate could be readily removed by filtration through a 0.45μm filter, but centrifugation at 5000rpm proved ineffective. At increased sulphide concentrations the precipitate could no longer be filtered.

Ageing of the amorphous metal sulphide precipitates resulted in the evolution of a more stable crystalline structure, which promoted aggregation and settling. This took several days in the case of copper and resulted in the precipitation of covellite. In the case of iron, the exposure of the amorphous precipitate to oxygen led to the oxidation of the FeS to FeOOH, which evolved to the more stable Fe_2CO_3. This process occurred over a period of hours and was accelerated by the active aeration of the suspension. Under anaerobic conditions the amorphous FeS remained in suspension, with published data indicating that fully crystalline mackinawite (FeS) may take up to two years to form.

The settling cone experiments utilising the artificial acid mine drainage at prescribed acidity to alkalinity ratios showed that the presence of bicarbonate, which has an acid and a basic potential, resulted in reduced metal precipitation when compared to hydroxide, sulphide and carbonate, which have no acid potential. The ability of the algae to extract carbon dioxide from bicarbonate and thus reduce the acidity of the system, led to the algal overflow outperforming the anaerobic digester overflow in terms of metal precipitation efficiency. In addition, the precipitate generated

by the addition of algal overflow was second only to the sulphide in terms of metal removed per volume of precipitate. This confirms the importance of the algal component to the integrated treatment system. The presence of aqueous sulphide appeared to enhance the precipitation of copper and zinc.

Bubbling biogenic hydrogen sulphide gas through the artificial acid mine drainage resulted in the rapid and complete precipitation of copper and lead from solution, even at pHs below three. In addition, the precipitate which formed, aggregated and settled rapidly, without requiring the ageing period observed when aqueous sulphide was added. The continued addition of excess gaseous sulphide did not affect the precipitation process in any way. The gaseous sulphide did not react with any of the other metals. This could form an important pretreatment step in the integrated system, allowing the efficient recovery of valuable metals from effluents dominated by iron, manganese and hardness metals.

Attempts to model the formation of the precipitates using MinteqA2 were relatively successful for the simple systems, although the prediction of thermodynamically stable but kinetically unlikely species was a problem. This could be overcome by the exclusion of certain species which were considered kinetically unsuitable. The attempts to model the more complex, artificial acid mine drainage system was not successful, despite knowing the precise composition of both the streams to be blended. It is possible that the presence of dissolved organic components from the anaerobic digester and algal reactors affected the metal removal, resulting in a system that could not be considered purely inorganic.

The wavelength dispersive X-ray spectroscopy (WDS) analysis of the precipitates provided valuable information on their composition. This information could be used to accurately determine the precipitating species in the simple systems. However, the number of metals precipitated in the acid mine drainage situation made it impossible to assign individual anionic components. To be able to achieve this each individual metal would have needed to be extensively studied, not only copper and iron.

The work presented in this chapter has a number of important implications for the design of the integrated system. Hydrogen sulphide gas can be used in a pretreatment step for the complete

removal of copper and iron. The presence of aqueous sulphide is undesirable, due to the formation of amorphous precipitates, especially of iron. In a scaled-up treatment system the treated volume would be too large to allow efficient oxidation of the FeS without an active aeration step, which has cost implications. The use of the algal overflow to facilitate the bulk of the precipitation would be advantageous due to the high percentage of carbonate, which unlike bicarbonate has no acid potential. As a result a smaller volume would be needed to neutralise the acidity of the effluent. This presence of carbonate would result in the rapid precipitation of ferrous iron as siderite ($FeCO_3$) and would also enhance manganese removal.

The major problems to be overcome are the precipitation of manganese, which was not effectively removed by any of the bases, and the reduction of the hardness of the water.

The data presented in chapters three to six were used to develop two integrated biological systems. A description of these systems and the results of their operation in a laboratory-scale pilot study are presented in chapter seven.

CHAPTER 7. PILOT PLANT STUDIES

7.1 Introduction

The previous chapters have indicated that an extensive body of literature exists relating to the biology, ecology and physiology of a wide range of organisms, which have been evaluated in terms of their ability to reduce aqueous metal and sulphate concentrations. Similarly, a number of reactor configurations and electron donors have been investigated for the cultivation of sulphate reducing bacteria (Maree *et al.*, 1987; Maree and Hill, 1989; Barnes *et al.*, 1991; Hammack and Edenborn, 1992; van Houten *et al.*, 1994) and the ability of large scale algal ponds to treat a number of domestic and industrial effluents has also been demonstrated (Oswald, 1990; Mara *et al.*, 1996; Rose *et al.*, 1996).

Notwithstanding this, there has been very little work published on the integration of algal and bacterial processes for the treatment of industrial effluents. The major contribution in this field has come from Professor Peter Rose and his research group at Rhodes University. The pioneering work was undertaken by Boshoff *et al.* (1996) and Dunn (1998) and concentrated on the co-disposal of sewage sludge and saline wastewaters, derived from the tanning process. The results showed that sewage sludge and tannery effluent could be used effectively as electron donors and carbon sources, particularly for sulphate-salinity reduction applications. The work progressed further and resulted in the conceptual development of the 'Algal Sulphate Reducing Process for Acid and Metal Wastewater Treatment' - the ASPAM Process (Rose *et al.*, 1998).

Initial plans to scale up the ASPAM process using tannery effluent as the electron donor were put on hold as a result of the Grootvlei mine incident, described in chapter two. The initial results obtained by Boshoff *et al.* (1996), Dunn (1998) and Whittington-Jones (2000), on the accelerated hydrolysis of primary sewage sludge indicated the potential to use an integrated system, utilising sewage sludge as the carbon source, to treat the water being pumped from Grootvlei. This led to the conceptualisation of the patented Rhodes BioSURE Process, which was later piloted on site (Rose and Hart, 1998). The pilot plant was able to treat approximately 140 000l of mine water per day, with a sulphate removal efficiency of between 14.8% and 55.3% during the

initialisation phase, stabilising between 65-70% once the system had been optimised (Corbett, 2001).

While the ASPAM and BioSURE Processes both contain SRB and algal components, in both cases the role of the algae is primarily as a polishing step, to remove trace amounts of metal, oxidise any remaining sulphide and reduce nutrients. The metal precipitation in these processes is achieved by blending the recycled, sulphide-rich, treated water with the AMD. Metal precipitation is presumed to occur as sulphides and possibly carbonates (Corbett, 2001).

The results described in chapter 6, comparing the metal precipitation achieved using sulphide-rich anaerobic digester overflow to carbonate-rich algal overflow, clearly indicate the benefit of utilising the sulphide-free system, particularly to achieve iron removal. The two integrated systems described in this chapter, while essentially containing the same components as the ASPAM and BioSURE Processes, differ in that the role of the algae is far more integral and the metals are not precipitated as sulphides. The exception to this is where gaseous hydrogen sulphide is used to achieve selective precipitation of some metals, prior to the blending with the algal overflow.

7.2 Research aims

The primary aims of this section of the project were:

1) To evaluate a number of reactor configurations for the continuous treatment of acidic, metal-laden effluents at a laboratory pilot scale.
2) To assess the suitability of enriched, partially treated effluent as a feed for the sulphate reducing bacteria.
3) To assess the accuracy of using MinteqA2 to model the metal precipitation occurring in reaction vessel during the continuous operation phase.

7.3 Treatment of a base metal effluent by a *Spirulina* based system

The results shown in chapter three demonstrated the potential of a *Spirulina* based system for the treatment of AMD, although a direct contact system did not prove sustainable due to the acute toxic effects of copper and zinc. The ability of algae to generate reactive alkaline species through the accumulation of inorganic carbon was demonstrated in chapter four. This led to the development of a non-contact system for the continuous treatment of AMD, described below.

7.3.1 Process description

A schematic representation of the non-contact system is shown in figure 7.1.

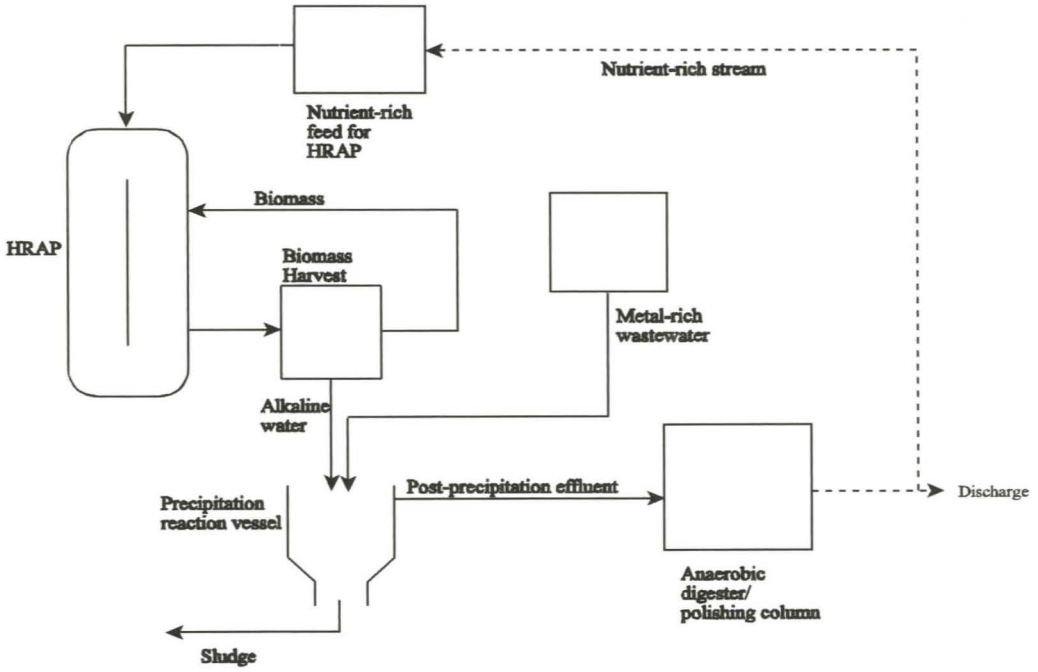

Figure 7.1: A generalised description of a process for the treatment of acidic, metal-laden effluents (van Hille *et al.*, 1999)

The nutrient and bicarbonate-rich algal feed is pumped into the high rate algal pond (HRAP), where the bicarbonate is utilised by the algae to obtain carbon for photosynthesis. The reactions involved result in an increase in pH and a shift in carbonate species equilibrium towards carbonate and hydroxide. The overflow from the HRAP passes through a biomass harvest and recycle step

and the aqueous alkaline component passes into the precipitation reaction vessel, where it is blended with raw effluent. The rate of effluent addition is determined by calculating the optimum mixing ratio, based on the alkalinity of the HRAP overflow and the acidity of the effluent. The resulting metal sludge settles at the bottom of the cone shaped reaction vessel, from where it can be drained off. The clarified liquid can either be discharged or if necessary passed through a polishing step to remove trace amounts of metals. If the initial effluent is high in sulphate it will be necessary to pass the post precipitation effluent through a sulphate reduction step as no sulphate is removed during the alkaline precipitation step.

7.3.2 Materials and methods

7.3.2.1 Analytical techniques

The determination of pH, acidity, alkalinity, chlorophyll content, sulphate, sulphide, phosphate, ammonia and metal concentrations were conducted as described in previous chapters. In all cases samples from the individual reactors were performed in triplicate and mean values are presented.

7.3.2.2 Effluent pH profile

A pH profile was performed on the base metal effluent (appendix I) to determine the pH dependency of the metal precipitation. Twelve 100ml samples of the effluent were removed and the pH of the samples were increased by the addition of 1M NaOH. A pH range of 2-13 was used. All samples were allowed to react for 60 minutes after which a sample was removed and filtered through a 0.45µm nylon membrane filter. The concentration of metal in the filtrate was determined by AA spectroscopy and the percentage metal removal was determined. The pH profile was performed in triplicate.

7.3.2.3 Control reactors

Prior to the continuous operation phase, a number of control reactors were set up, similar to those described in section 3.3.6. The initial algal culture was established in Zarrouk's medium which

has a high alkalinity due to the sodium bicarbonate. To determine the metal precipitation potential of this in the continuous system, two five litre reactors were set up. The first contained a culture of *Spirulina* in Zarrouk's medium and the second, only media. In both cases tap water was pumped into the reactors at a rate of 1ml/min. The overflow from the reactors passed into the reaction vessel, into which the effluent was pumped at a rate of 1ml/min. The pH and algal concentration in the 5l growth vessel were measured daily. The pH and metal concentrations in the reaction vessel were also measured on a daily basis.

7.3.2.4 Continuous operation

For the continuous operation of the system, the *Spirulina* was maintained in a 30l, oval, raceway pond. The algae were maintained in suspension through the action of a paddle wheel. The algal culture was fed at a rate of 1.4ml/min on the liquid overflow of an anaerobic digester treating primary sewage sludge, obtained from the Grahamstown municipal sewage treatment works. Overflow from the algal growth vessel was passed through a filtration step (nylon mesh, 0.2mm mesh size). The filtrate passed into the reaction vessel and the algal biomass was returned to the growth vessel. Effluent was pumped into the reaction vessel, at a rate of 1.4ml/min, where metal precipitation occurred. The overflow from the reaction vessel was collected and supplemented with yeast extract (1g/l), 60% sodium lactate (6ml/l), ammonium chloride (1g/l) and potassium dihydrogen orthophosphate (0.5g/l). The mixture was pumped into a 20l anaerobic digester, seeded with an SRB consortium, at a rate of 2.8ml/min. The overflow from the reactor was sampled daily to determine pH, sulphate, sulphide and metal concentrations.

7.3.3 Results and discussion

7.3.3.1 Effluent pH profile

The results of the pH profile are shown in figure 7.2 and indicate that for effective precipitation of all four metals to be achieved, the pH in the reaction vessel would need to be maintained above pH 8. The pH profile suggests that should the pH decrease below 8 the efficiency of zinc removal would be affected first, followed by copper, lead and eventually iron. This sequence is consistent

with theoretical values (Greenwood and Earnshaw, 1984) and modelled predictions generated by MinteqA2.

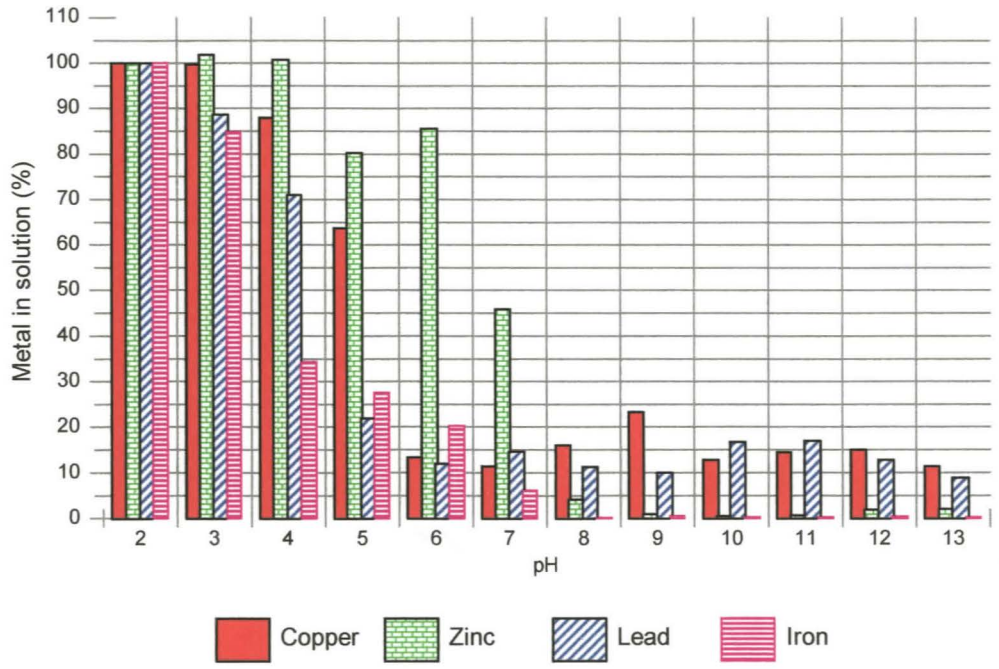

Figure 7.2: pH profile of effluent from the Black Mountain base metal mine illustrating the percentage of each metal remaining in solution following the increase of the pH from 1.99 by the addition of NaOH. (mean values, n = 3)

7.3.3.2 Control reactors

The algal concentration in the 5l growth vessel remained relatively constant during the first five days, during which time the pH increased from 9.00 to 9.85, due to the accumulation of inorganic carbon. After day five, the algal concentration began to decrease, primarily as a result of nutrient stress, but also as a result of biomass washout due to the nylon mesh not being a totally effective filter. The pH decreased steadily over the same period, to pH 9.03 on day 14, due to replacement of alkaline Zarrouk's medium with tap water. The pH change in the algal free control was more dramatic, with the pH decreasing from 9.00 to 7.67 over the corresponding period.

Figures 7.3 and 7.4, showing the changes in pH and metal removal observed in the reaction vessel, clearly demonstrate the contribution of the algae to the efficiency of the process.

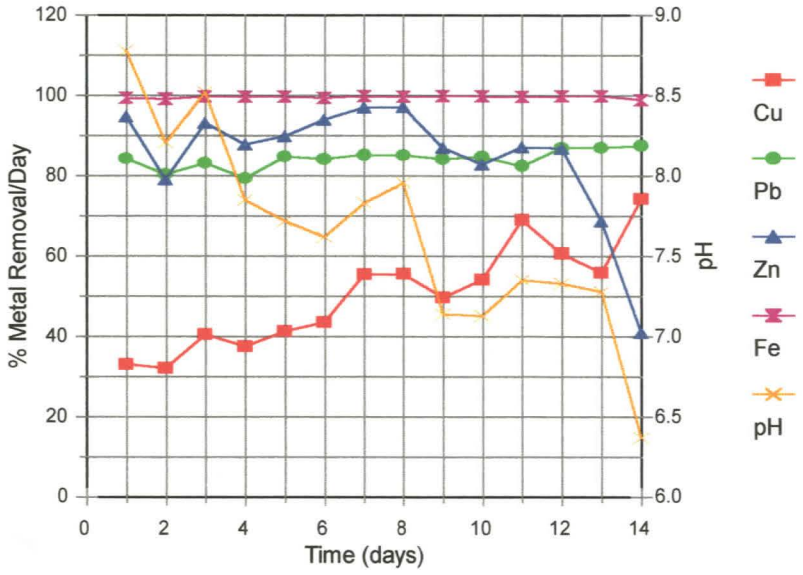

Figure 7.3: Relationship between metal removal for each 24 hour period and pH in the reaction vessel for the control system containing algae. Metal removal calculated by analysing the reaction vessel overflow

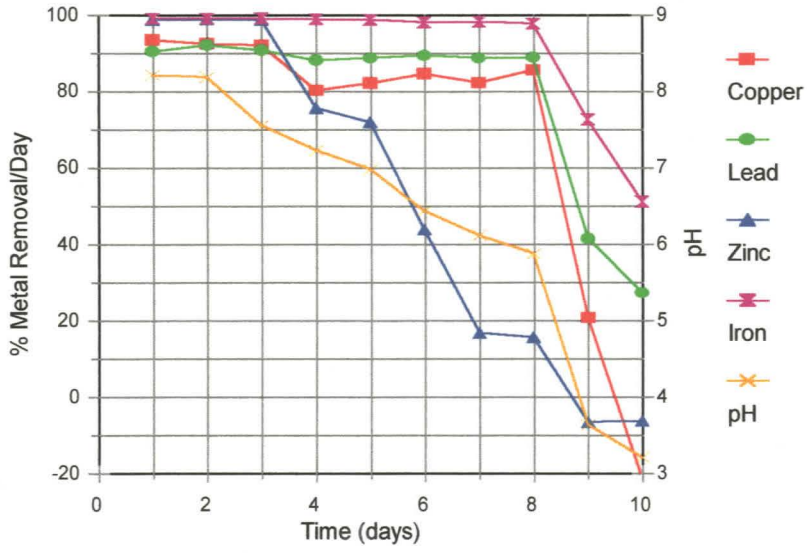

Figure 7.4: Relationship between metal removal for each 24 hour period and pH in the reaction vessel for the algal free control system. Metal removal calculated by analysing reaction vessel overflow

In both cases the pH in the reactor vessel decreases, although the decrease in the algal free control system is far more rapid and significant. In both cases, the initial concentration of alkalinity was the same. The results presented in chapter four show that accumulation of inorganic carbon, from bicarbonate, by the algae does not lead to an increase in total alkalinity but rather reduces the acidity of the system. The rate of effluent addition and hence acidity addition was the same in both systems. Therefore, the overflow entering the reaction vessel had the same alkalinity in both cases, but the overflow from the system containing the algae had a greatly reduced acidity, allowing it to buffer the acidity of the effluent more effectively and for a longer period of time.

The metal removal is essentially pH dependent and follows the trend observed in the pH profile (Figure 7.2). In both systems there was a proportional decrease in zinc removal after the pH fell below 7.5. The zinc removal in the algal free system was negative on days 9 and 10 and the copper removal on day 10, after the pH had dropped to 4, as a result of some precipitated metal redissolving. The removal of lead and iron remained constant in the system containing algae for all 14 days, but began to decrease after day eight in the algal free system, as the pH fell below 6.

The copper removal in the system containing algae showed an opposite trend, with a low initial percentage removal, which increased as the experiment progressed. This can be attributed to the presence of copper complexing extracellular polymeric substances (EPS), as described in chapter three. They have been shown to be released as a result of nutrient stress, which would be induced as the tap water diluted the growth medium (Singh *et al.*, 1999). At low concentrations of EPS the complex remains soluble, but as the concentration increases it forms insoluble aggregates (Boshoff, unpublished results). As the experiment progressed the nutrient stress became more acute and hence the EPS production increased, accounting for the increase in percentage copper removal.

7.3.3.3 Continuous operation

The results of the continuous operation of the system are summarised in table 7.1 and indicate that the system was able to run effectively for a 30 day period, reducing the concentration of all four heavy metals to below the acceptable risk criteria determined by the Department of Water Affairs and Forestry (1998).

Table 7.1: Summary of the performance of the *Spirulina* based integrated process for the treatment of a base metal effluent. The results (mean ± SD) represent a combination of the daily measurements over a 30 day period. RV = reaction vessel, AD = anaerobic digester, AR = acceptable risk level

Component	Units	Effluent	After RV	After AD	% reduction	AR
pH	-	1.99	8.26 ± 0.37	8.12 ± 0.16	-	-
Sulphate	mg/l	4415	2236 ± 63	295 ± 27	89.1	-
Copper	µM	54.90	1.52 ± 0.11	1.42 ± 0.09	94.3	1.6
Iron	µM	1771.8	8.3 ± 4.1	4.7 ± 2.5	99.5	161.2
Lead	µM	11.30	0.27 ± 0.08	0.27 ± 0.06	95.1	0.5
Zinc	µM	109.50	2.98 ± 0.68	3.37 ± 0.46	93.8	10.7

It is clear from table 7.1 that the majority of the metal removal occurs as precipitation in the reaction vessel as a result of mixing the effluent with the alkaline overflow from the algal growth vessel. During the continuous operation phase the algae were fed on overflow from an anaerobic digester treating sewage sludge. This feed had a bicarbonate alkalinity of between 1100 and 1300mg/l $CaCO_3$ equivalents and also contained sufficient nitrogen and phosphorous to prevent the algae from suffering nutrient stress. As a result, the overflow from the algal growth vessel contained EPS concentrations low enough (18 ± 13mg/l) not to affect copper precipitation.

It is also clear that the alkaline precipitation step did not reduce sulphate concentration, other than by dilution, resulting from the mixing of the two streams. This necessitated an additional anaerobic digestion step. The combination of the dilution and anaerobic digestion steps resulted in an 89% reduction in the sulphate concentration.

The advantage of the system described above, stems from the fact that neither the algal or bacterial components come into direct contact with the effluent. This allows both components to operate under optimal conditions, without any stress related to toxic heavy metals or acidic pH values. The system did, however, have a number of shortcomings. The most significant were the problems related to using an algal species which was suspended in the liquid medium. This necessitated constant agitation, which would increase the operational cost, as well as a solid-liquid separation stage, to avoid biomass loss. The nylon-mesh filter was not entirely effective and by day 30 the biomass concentration in the algal growth vessel was 32% lower than at the start, which led to a reduction in efficiency. In addition, if the system where to be scaled up the nylon-mesh filter would not be appropriate. A second shortcoming lay in the fact that the system had no potential to facilitate the selective recovery of potentially valuable metals.

A second system was developed, that depended on the same basic principles, but overcame the problems described above. The *Spirulina* was replaced by *Oscillatoria* sp., another filamentous cyanobacteria, which has a similar CA enzyme system and adheres firmly to solid surfaces. A selective precipitation, utilising gaseous hydrogen sulphide, was incorporated for the recovery of copper and lead. The modified system is described below.

7.4 Treatment of a synthetic acid mine drainage by an *Oscillatoria* sp. based system

7.4.1 Process description

The design of the continuous system, utilising *Oscillatoria* (Figures 7.5 and 7.6) rather than *Spirulina* to generate carbonate and hydroxide alkalinity, is illustrated in figure 7.7 . The system essentially contains the same components as those described in section 7.3, but utilises biogenic hydrogen sulphide to selectively precipitate copper and lead, as metal sulphides, prior to the precipitation of the bulk of the metals in the reaction vessel.

The high rate algal pond has been replaced by a simulated stream reactor, in which the algae are attached to stones lining the surface of the reactor. The bicarbonate rich overflow from the anaerobic digester flows over the algae by means of gravity.

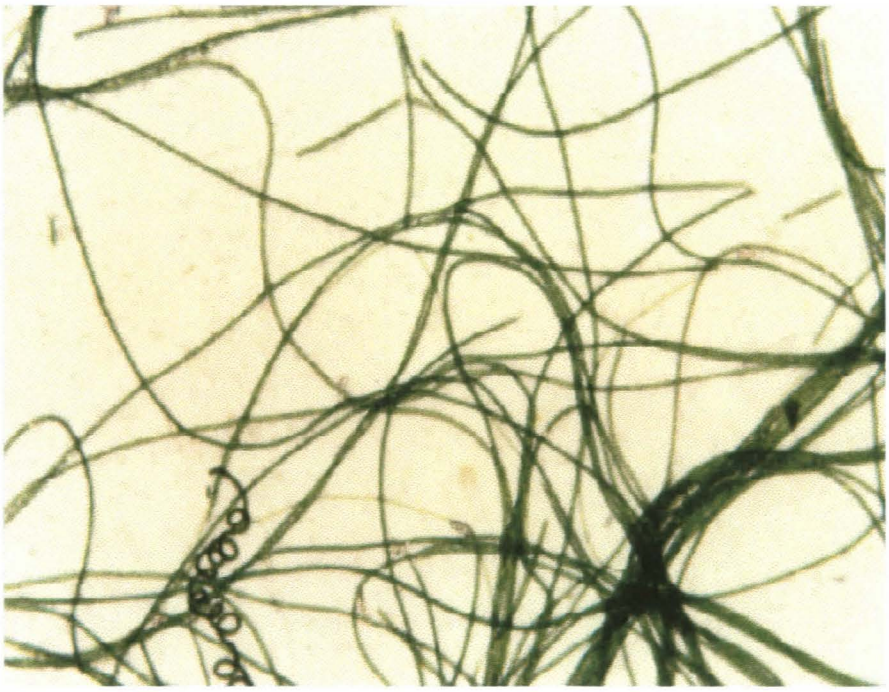

Figure 7.5: Light microscope preparation of *Oscillatoria* sp.

Figure 7.6: Seeding of the *Oscillatoria* culture in the simulated stream (gutter) reactors showing the adhesion of the algae to the solid supports and the subsequent extension of the filaments

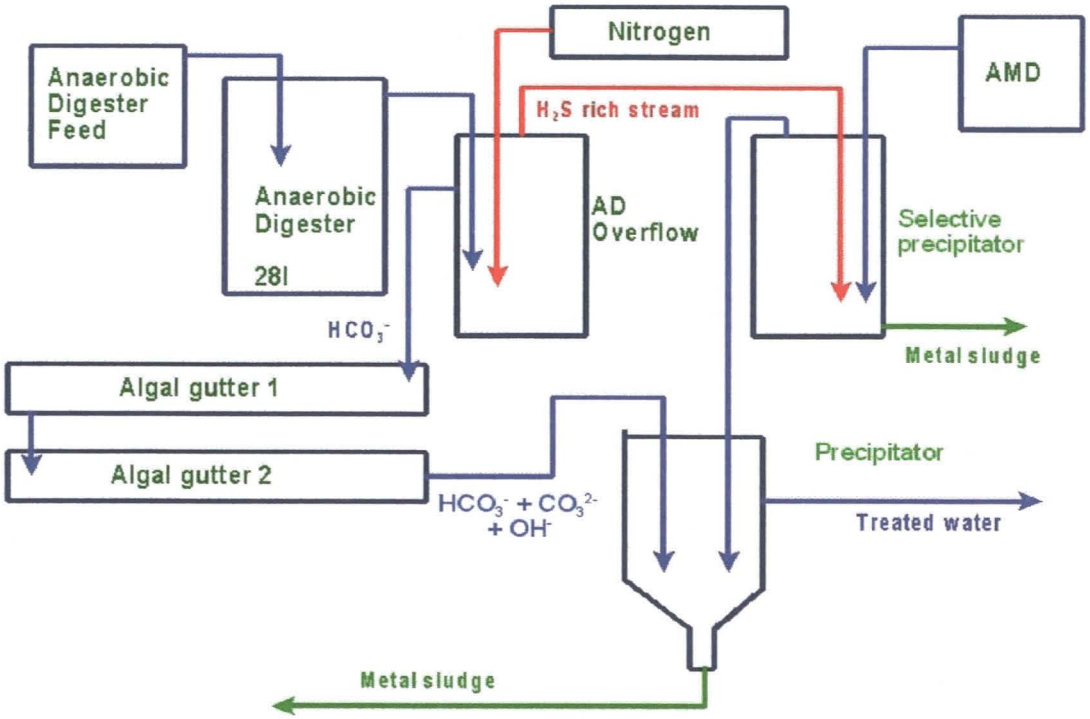

Figure 7.7: Schematic diagram illustrating the integrated biological system for the treatment of acidic, metal-laden wastewaters. Blue lines represent liquid streams and red lines gaseous streams

7.4.2 Materials and methods

7.4.2.1 Analytical techniques

The determination of pH, acidity, alkalinity, sulphate, sulphide and metal concentrations were conducted as described in previous chapters. In all cases samples from the individual reactors were performed in triplicate and mean values are presented.

7.4.2.2. Operational parameters

The pilot plant was operated for a period of 100 days, the first 10 of which were used to optimise the various parameters. The full bench-scale pilot system is shown in figure 7.8. Modified Postgate B medium was fed into the 28l anaerobic digester at a rate of 2ml/min. The overflow from the anaerobic digester was collected in a stoppered, 2l Schott bottle which was periodically

Figure 7.8: Bench scale integrated biological system showing the various components, a = anaerobic digester feed, b = 28l anaerobic digester, c = algal gutters, d = selective precipitation vessel, e = acid mine drainage, f = nitrogen source and g = precipitation vessel

sparged with nitrogen at a rate of 40ml/s for 60 minutes. The hydrogen sulphide rich gas stream was passed into an airtight, 10l selective precipitation vessel, where copper and lead were removed (Figure 7.9). The nitrogen sparged ADO was fed into the first algal gutter at a rate of 2ml/min. The combined volume of the algal gutters was 7l, giving a retention time of 2.4 days. The overflow from the algal gutters was blended with the acid mine drainage, exiting the selective precipitation vessel, into the precipitation vessel. The rate of blending was controlled to ensure an acidity to alkalinity ratio in the precipitation vessel of 1:2. The metal precipitate formed in the precipitation vessel settled in the cone at the base of the reactor, from where it could be removed, and the clarified liquid was drawn off through a port situated 10cm below the top of the reactor. The clarified liquid could be subjected to a final polishing step, prior to discharge.

The following measurements were taken on a regular basis: anaerobic digester - pH, sulphate, sulphide and alkalinity; algal gutters - pH and alkalinity; selective precipitation vessel - pH and dissolved metal concentration; overflow from precipitation vessel - pH, alkalinity, sulphate and dissolved metal concentration.

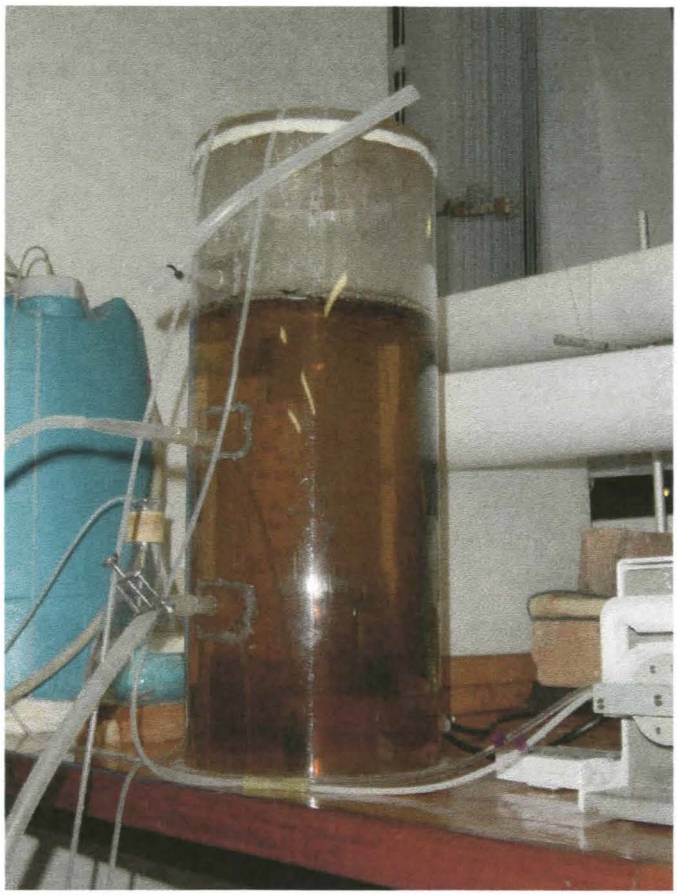

Figure 7.9: The selective precipitation vessel showing the formation of the brown copper and lead sulphide precipitate

7.4.3 Results and discussion

The results from the analyses performed on the overflow from the 28l anaerobic digester over the 100 day operation period are shown in figure 7.10. The initial optimisation period, day 0 to 10, was split into two phases. For the first seven days the reactor was operated as a batch system. This phase was characterised by a rapid drop in the sulphate concentration and a corresponding increase in the pH and aqueous sulphide concentration. Figure 7.11 shows that, over the same period, there was a rise in the bicarbonate alkalinity in the reactor. The ratio of alkalinity to sulphide was initially very high (53:1), but dropped rapidly as the sulphate reducing bacteria became established. From day seven onward the medium was pumped into the reactor at a constant rate of 2ml/min. This resulted in an initial increase in the sulphate concentration, until a steady state was reached by day 10.

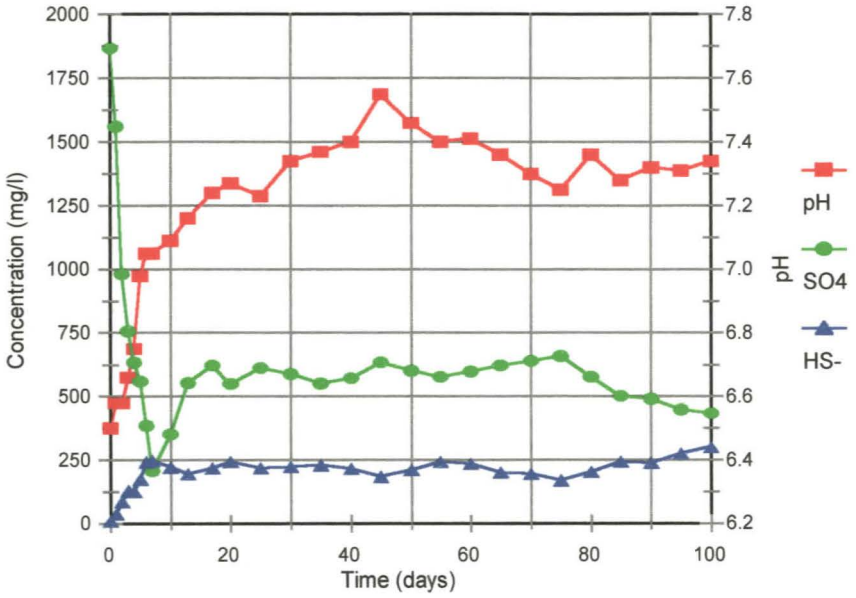

Figure 7.10: pH, sulphate and sulphide concentrations recorded in the overflow from the 28l anaerobic digester over the 100 day pilot study period. The reactor was operated as a batch system for 7 days after which medium was pumped in at a constant rate of 2ml/min

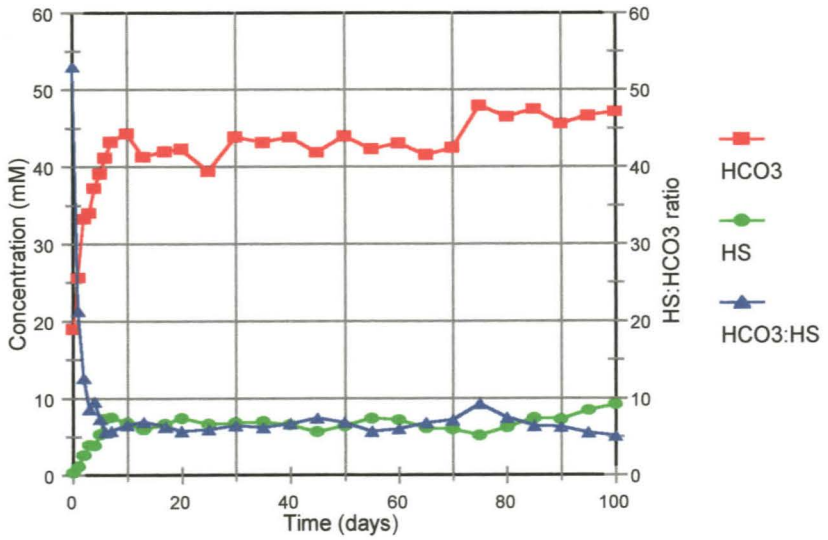

Figure 7.11: Bicarbonate, sulphide and bicarbonate to sulphide ratio recorded in the overflow from the 28l anaerobic digester over the 100 day pilot study period

During the 90 day period when the reactor was essentially in a steady state, the concentration of sulphate and sulphide, as well as the pH and alkalinity, fluctuated within a narrow range. The mean values for the parameters measured, between day 10 and day 100, are shown in table 7.2.

Table 7.2: Mean (± SD) values for pH, sulphate, sulphide, bicarbonate and the ratio of bicarbonate to sulphide recorded for the anaerobic digester overflow, for the period between day 10 and day 100

Component	mg/l	mM
pH	7.32 ± 0.10	-
Sulphate	559.62 ± 74.66	5.80 ± 0.80
Sulphide	224.46 ± 29.04	6.80 ± 0.88
Bicarbonate	2192.54 ± 95.45	43.85 ± 2.24
HCO_3^- to HS^- ratio	6.55 ± 0.88	

This represented a mean sulphate conversion rate of 141.96 ± 15.61mg l^{-1} day^{-1} (1478.75 ± 162.58μmoles l^{-1} day^{-1}) for the steady state period. This value is lower than that reported by Boshoff (1999) for a stirred tank reactor, fed tannery effluent. The sulphate conversion rate could be significantly increased by introducing some form of agitation to enhance the mass transfer within the reactor (as shown in section 5.4.2), but this would have significant cost implications on a larger scale. The mean bicarbonate generation was calculated as 252.60 ± 10.61mg l^{-1} day^{-1} (4200.50 ± 176.40μmoles l^{-1} day^{-1}), which proved sufficient to maintain optimum performance of the algal system.

The sparging of the anaerobic digester overflow with nitrogen resulted in a reduction in aqueous sulphide of between 62 and 68% and an associated increase in pH from approximately 7.3 to between 8.44 and 8.71. This increase in pH initiated the shift in carbonate species equilibrium from bicarbonate to carbonate and effectively provided a "head start" for the algal system. The combined performance of the two gutter reactors, as measured from the overflow of the second gutter, over the 100 day trial period is summarised in figure 7.12.

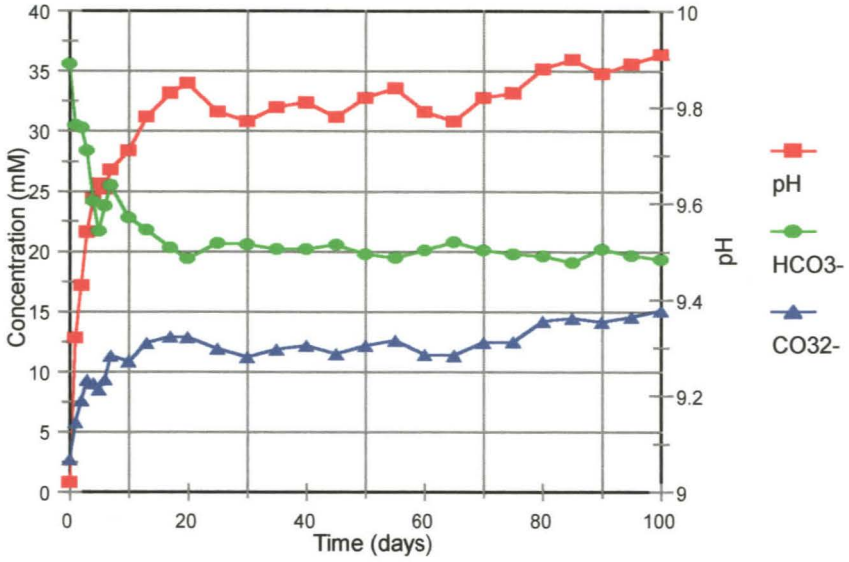

Figure 7.12: pH, bicarbonate and carbonate concentrations recorded in the overflow from the second algal gutter reactor over the 100 day pilot study period

The algal culture was initially established in Zarrouk's defined medium, which accounts for the high initial bicarbonate concentration. During the first seven days, while the anaerobic digester was in the batch phase, the liquid in the gutters was re-circulated. Tap water was added to the system to overcome the effect of evaporation and as such there was little change in the total alkalinity of the system. Figure 7.12, however, shows that carbonate species equilibrium changed dramatically during this period, as a result of the algal accumulation of inorganic carbon. The ratio of bicarbonate to carbonate decreased from 13.04 to 2.54. The change from batch to continuous operation of the anaerobic digester resulted in the continuous feed to the algal reactors and the re-circulation was terminated. A small increase in the bicarbonate concentration, resulting from the influx of anaerobic digester overflow, can be seen between days 7 and 9, after which a steady state is established. The total alkalinity in the gutter reactors was consistently higher than that of the anaerobic digester overflow, which can be accounted for by the evaporation of a certain fraction of the liquid. During the 90 day steady state phase, the gutter reactors showed a reduction in the bicarbonate concentration of over 50%, relative to the anaerobic digester overflow. The combined effect of the sparging of the digester overflow and the action of the

algae resulted in a mean increase in carbonate concentration from 0.07 ± 0.01mM (ADO) to 12.65 ± 1.20mM, or 5070 ± 410μmoles l^{-1} day^{-1}.

The selective precipitation stage consistently removed over 99% of the copper and lead from solution, as metal sulphides. The effect on the aqueous concentration of the other metals was negligible. The precipitation of copper and lead was accompanied by a reduction in the mean pH, over the trial period, from 3.12 ± 11.64 to 2.96 ± 5.38.

The mean overflow rate from the second algal gutter was 1.76 ± 0.15ml/min, with the fluctuation resulting from differing evaporation rates. This resulted in a mean overflow volume of 2.53l/day, which at a mean alkalinity concentration of 4017mg/l $CaCO_3$ equivalents, constituted the addition of 10179mg of alkalinity to the precipitation vessel. As the mean acidity of the artificial acid mine drainage was 760mg/l $CaCO_3$ equivalents, this facilitated the treatment of 6.7l/day of acid mine drainage at an acidity to alkalinity ratio of 1:2.

The results of the metal removal in the selective precipitator and the precipitation vessel, from day 10 to day 100, are summarised in table 7.3.

Table 7.3: Mean (± SD) results for the heavy metal precipitation, from the artificial acid mine drainage, achieved from day 10 to day 100. artAMD = artificial acid mine drainage, Sel. prep. = selective precipitator, AER = acceptable environmental risk

Metal	artAMD conc. (μM)	Sel. prep. conc. (μM)	% removal	Precipitator conc (μM)	Combined % removal[1]	AER conc.
Cu	315 ± 6	1.3 ± 0.6	99.6	0.7 ± 0.8	99.8	1.6
Fe	3760 ± 32	3748 ±36	0.3	8.7 ± 4.6	99.8	161.2
Mn	728 ± 17	730 ± 11	< 0.1	234 ± 21	67.9	5.5
Ni	341 ± 9	336 ± 12	1.5	15.2 ± 5.7	95.5	19.4
Pb	97 ± 2	0.1 ± 0.2	99.9	0.1 ± 0.3	99.9	0.5
Zn	306 ± 22	298 ± 13	2.6	3.1 ± 2.2	99.0	10.7

[1]The combined percentage removal includes precipitation in both the selective precipitator and the bulk precipitation reactor, as well as a dilution factor associated with blending the streams together

The data from table 7.3 clearly show that for all the heavy metals, with the exception of manganese, the concentration in the precipitation vessel overflow stream is below the acceptable environmental risk criteria laid down by the Department of Water Affairs and Forestry (1998).

The concentrations of calcium (2720 ± 62μM), magnesium (4867 ± 131μM) and sulphate (1860 ± 24mg/l) in the precipitation vessel overflow stream were still appreciable, although the pH of 7.86 ± 0.09 was within prescribed limits. Much of the magnesium and sulphate was derived from the initial anaerobic digester feed. If the anaerobic digester could be run on enriched, partially treated acid mine drainage, these concentrations could be significantly reduced.

7.5 Cultivation of SRB on enriched, partially treated artAMD

7.5.1 Materials and methods

Three 2l anaerobic digesters were set up on partially treated artificial acid mine drainage that had been enriched with KH_2PO_4 (0.5g/l), NH_4Cl (1.0g/l), yeast extract (1.0g/l) and sodium lactate (6ml of a 60% solution). The reactors were inoculated with a 10% (v/v) inoculum from the 28l anaerobic digester and shaken at 120rpm on an orbital shaker. The reactors were operated as batch systems for 13 days, and pH, sulphate, sulphide and alkalinity were measured daily. The concentration of metals remaining in solution was determined after seven days.

7.5.2 Results and discussion

The performance of the reactors is summarised in figure 7.13, which shows that the SRB were able to successfully grow on the enriched AMD, despite the high manganese concentration. The reactors had essentially achieved maximum (95.8%) sulphate reduction by day 10. During this period, the pH had increased from 7.20 to 7.40 and the sulphide and alkalinity levels had stabilised at approximately 250mg/l and 3300mg/l $CaCO_3$ equivalents respectively. These values are consistent with the levels observed during the steady state operation of the 28l reactor and suggest that the addition of nutrients to the partially treated acid mine drainage could generate a feed suitable to run the entire system.

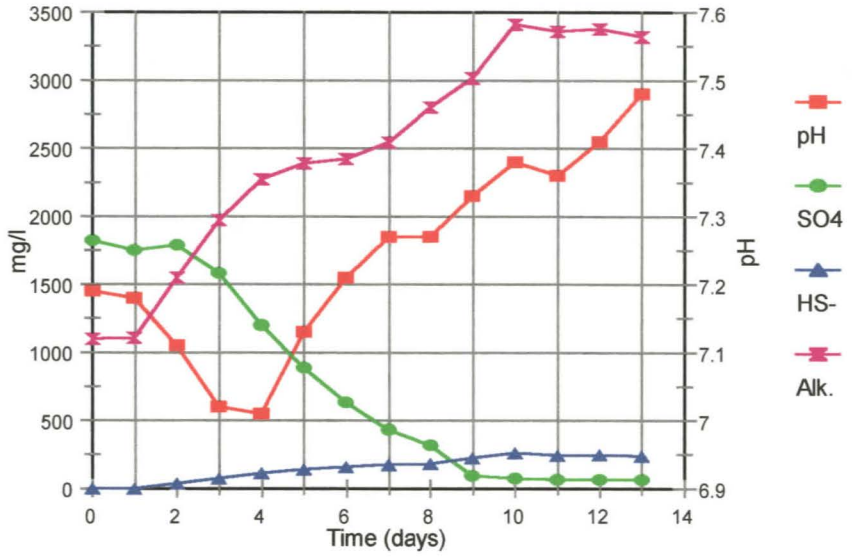

Figure 7.13: Performance of a sulphate reducing system with lactate enriched, partially treated acid mine drainage as the electron donor and carbon source (mean values, n = 3)

The analysis of the metal content on day seven showed a dramatic decrease in the manganese content, from a mean value of 226μM to 4.5μM, which is below the acceptable environmental risk level. Similarly, the mean concentration of calcium and magnesium in the three reactors had fallen to 1078μM (43.2mg/l) and 3402μM (82.7mg/l) respectively.

The blending of 6.7l of acid mine drainage with 2.5l of algal overflow would theoretically generate 9.2l of partially treated acid mine drainage each day. Diverting 30% of this stream and enriching it with nutrients could create an effective feed for the large anaerobic digester. The remaining 70% of the stream could be polished to final discharge quality, perhaps utilising a small anaerobic wetland.

The attempts to model the precipitation reactions occurring due to the blending of the acid mine drainage with the algal overflow did not prove successful. The results showed the same inaccuracies as explained in chapter six.

7.6 Scale-up considerations

Treating a volume of acid mine drainage similar to the predicted discharge volume from the East Rand Basin, would require the scaling-up of all parameters of the system proposed above, by a factor of approximately five million. Assuming no significant loss in the efficiency of the system, this would require an anaerobic digester with a volume of 140m^3, being fed at a rate of 60kl/h. Some form of active mixing would be required to achieve efficient mass transfer in a reactor of such size. It would be possible to use the gas stream exiting the selective precipitator to facilitate this in an airlift system, as the gas would be oxygen-free. The simulated stream (algal reactor) would require a volume of 35Ml. The stream would need to be relatively shallow, with an approximate depth of 50cm. This would require a land area of 70m^2. If a portion of the partially treated minewater was supplemented with a carbon source and used as the feed for the main anaerobic digester, this would result in the discharge of 32.2Ml/day of treated water, with an elevated manganese and sulphate content. Due to the absence of high concentrations of iron and acidity (pH ± 7.8), this stream could be effectively treated to strict discharge criteria in an anaerobic wetland of approximately 200 000m^2.

The formulation of a cost estimate for such a system fell beyond the scope of this project. However, the individual components of such a system are significantly more "low-tech" than the systems covered in chapter 2. In addition, the potential to use a waste carbon source to provide the nutrients for the anaerobic digestion would have a significant cost benefit. The system is also able to recover all the copper and lead from the minewater, which would result in the generation of revenue from their sale. The fact that the system is entirely dependent on biologically mediated processes to generate the reactive anionic species means that, once operational, the system could become essentially self-sustaining.

7.7 Conclusions

The results from the two pilot plant studies illustrated the potential of an integrated biological system for the treatment of acid mine drainage. While the *Spirulina* based system was effective in the treatment of the base metal effluent, the problems associated with maintaining the culture

in suspension and preventing the loss of excessive biomass, introduced practical problems. These problems would be exaggerated should the system have been scaled up.

The modification of the algal vessel design to accommodate *Oscillatoria*, which adhered firmly to the solid supports, removed the problem of solid-liquid separation. The addition of a selective precipitation step allowed the recovery of all the copper and lead from the artificial acid mine drainage, while reducing the sulphide concentration of the anaerobic digester overflow to a level which was not toxic to the algae.

After a 10 day optimisation period the integrated system was operated for 90 days, without any loss of efficiency. The anaerobic digester operated at a mean sulphate conversion rate of 1479μmoles l^{-1} day^{-1}, while generating bicarbonate at a rate of 4200μmoles l^{-1} day^{-1}. The bicarbonate to sulphide ratio remained consistent at approximately 6:1.

The combination of the nitrogen sparging and the action of the algae raised the pH of the anaerobic digester overflow from 7.3 to 9.7. The concentration of bicarbonate in the algal overflow was over 50% less than the anaerobic digester overflow and the concentration of carbonate had increased from 0.07mM to 12.65mM. This represented a significant reduction in acidity.

The selective precipitation of copper and lead by gaseous hydrogen sulphide resulted in the removal of over 99% of each metal from solution. The gaseous sulphide has little effect on the other metals. The blending of the post H_2S-treated acid mine drainage with the algal overflow, at an acidity to alkalinity ratio of 1:2, resulted in the precipitation of iron, nickel and zinc to concentrations below the acceptable environmental risk levels. Only manganese was not efficiently removed. The mean pH of the overflow from the precipitator was 7.86, which was within acceptable limits.

The precipitator overflow did still contain appreciable amounts of calcium, magnesium and sulphate. The enrichment of this stream with ammonia, phosphate and lactate resulted in an effective feed for the sulphate reducing bacteria. The treatment of the enriched stream in a second

anaerobic digester resulted in the almost complete removal of the manganese and sulphate, and a reduction in the calcium and magnesium concentrations. The enrichment of 30% of the precipitator overflow could provide the feed for the large anaerobic digester. Due to low acidity and iron content of the precipitator overflow, the remaining 70% could easily be polished by an anaerobic wetland.

As shown in the previous chapter, the ability of MinteqA2 to generate an accurate model of such a complex precipitation system was limited.

There are no major obstacles to the scaling up of an integrated biological system such as the one proposed here. The individual reactor components are relatively "low-tech" as are the required control mechanisms. The system has the additional advantage that once the biological components are established, the system is essentially self-sustaining, provided a suitable carbon source is provided. It has been previously noted that considerable research is being conducted into the utilisation of low cost and waste carbon sources as feeds for sulphate reducing systems. The results presented in this chapter clearly indicate that this type of system could be a viable treatment option for the uncontrolled, long-term discharge of acid mine drainage from abandoned mines.

CHAPTER 8. GENERAL DISCUSSION

Increasing urbanisation, industrialisation and the provision of water to a large sector of the population who were previously deprived are placing an ever increasing burden on South Africa's limited water reserves. The Government has recently introduced pro-active legislation, aimed at ensuring the management and conservation of these water resources for future generations.

The contamination of surface and groundwater reserves by heavy metals is a major concern. Historically these metals have originated from active mining operations, manufacturing and urban run-off. While leaching mine dumps and abandoned coal mines are a factor, the volume of these discharges are limited. However, economic pressure on the gold mining industry has resulted in the decommissioning of an increasing number of mines, particularly on the East Rand. In the near future all gold mining on the East Rand and eventually throughout the Witwatersrand will cease. As a consequence, the dewatering of the vast underground basins, which have resulted from mining operations, will stop and the groundwater will rebound. The rising groundwater will dissolve acid generating salts, which formed from the oxidation of sulphide minerals (mainly pyrite) under non-saturated conditions. This will most likely result in the dramatic deterioration of the groundwater quality, and where the groundwater discharges to the surface, a serious and long term environmental problem.

The conventional methods for treating acid mine drainage have focused on chemical precipitation, typically by lime addition, in a high density sludge process. While such systems are effective, they are expensive and are not a feasible long term option. There has been an increasing amount of interest shown in biological systems, ranging from active, sulphate reducing bacteria systems, to passive, artificial wetlands for acid mine drainage remediation. This project focused on the development of an integrated biological system, driven by the biological generation of reactive alkaline species, for the long term, sustainable treatment of acid mine drainage.

The initial work concentrated on the binding and accumulation of heavy metals by the blue-green alga, *Spirulina* sp. Metal binding was rapid and the binding affinity series of Pb > Cu > Zn >> Fe was consistent with published data for other algal species. The binding capacity was, however, lower than that determined for most other microbial biomasses. Furthermore, the acute toxicity of copper and zinc resulted in the rapid deterioration of the algal culture. This precluded the algae from being used in a treatment system where they came into direct contact with toxic metals. The algae were able to increase the pH of the surrounding medium when external bicarbonate concentrations were high.

The ability of the algae to modify the aqueous environment was studied in greater detail. The phenomenon is controlled by the enzyme carbonic anhydrase, which plays an integral part in the carbon concentrating mechanism of the algae. In the presence of light and reduced concentrations of external carbon dioxide, the algae are able to utilise bicarbonate as a source of carbon dioxide for photosynthesis. This results in the release of a hydroxide ion to the external medium and an increase in pH. The process does not increase the alkalinity of the medium, but rather reduces the acidity by driving the equilibrium between bicarbonate and carbonate towards carbonate formation. Bicarbonate is able to act as both an acid and a base, and is considered to have one acid and one basic potential. Carbonate has only one basic potential. Experimental evidence showed that *Spirulina* was able to reduce the acidity of the medium by an amount equivalent to the addition of 3670μmoles of hydroxide per gram of biomass per hour, at an optimal biomass concentration of 2000mg dry mass/1.

Attempts to quantify the enzyme activity directly were unsuccessful, due to the inaccuracies of the Wilbur-Anderson method. An indirect method was developed which analysed the change in carbonate species equilibrium. The carbonic anhydrase inhibitor, acetazolamide, significantly reduced, but did not completely inhibit the enzyme activity at external concentrations of 50μM and above. The inhibitor cannot enter the cell so the fact that there was an incomplete inhibition of enzyme activity, even at inhibitor concentrations in excess of 100μM, suggests the presence of both an internal and external carbonic anhydrase enzyme. Experiments conducted with increased volumes (2l) of algal culture, showed a pH increase from 8.3 to almost 10 and a 70% reduction in the bicarbonate concentration over a 13 day period.

Predictive modelling, using MinteqA2, on the potential of the algal treated, liquid medium to precipitate a variety of metals showed that over the 13 day period of the experiment, the potential of the medium to precipitate iron, manganese, lead and zinc increased by 15-20%. Over the same period, the potential to precipitate calcium and magnesium increased from 0 up to 40%. This highlighted the potential of using the algal mechanism in a remediation context.

In order for such a system to be sustainable, a readily available source of bicarbonate is needed. Clearly the continuous addition of bicarbonate salts would not be a cost effective solution. The biological generation of bicarbonate by sulphate reducing bacteria was investigated. While sulphate reducing bacteria have been the focus of a considerable amount of research, the majority of this has focused on desalination and the production of sulphide for metal precipitation. For most carbon sources, the amount of bicarbonate generated per sulphate reduced is significantly greater than the sulphide produced.

A bacterial consortium was isolated from an anaerobic pond at the Grahamstown sewage treatment works and maintained in a lactate based medium. Morphological and physiological data suggested the presence of at least two species of *Desulfovibrio* and one of *Desulfotomaculum*. Results obtained from experiments utilising glucose as a carbon source suggested the presence of acetogenic bacteria in the consortium, as well as the absence of acetate utilising SRB, such as *Desulfobacter* species. The consortium was able to reduce sulphate at a rate of up to 500mg l^{-1} day^{-1} in an agitated, 2l reactor. The sulphate reduction rate dropped to 135mg l^{-1} day^{-1} in a 28l, non-agitated reactor. This was most likely due to reduced mass transfer. The ratio of bicarbonate to sulphide generated in the reactor was 6:1, which was three times higher than expected. This could be attributed to the loss of sulphide, as hydrogen sulphide gas, to the headspace as well as the oxidation of sulphide to elemental sulphur. Additional bicarbonate could also have been produced in sulphate poor microenvironments within the non-agitated reactor. In these environments, substrate level phosphorylation would dominate.

The sulphide concentration in the overflow from the anaerobic digester was high enough (> 200mg/l) to be toxic to the algae. This was reduced by sparging the overflow with air or nitrogen. Sparging with air at 40ml/s reduced the aqueous sulphide concentration to zero within

60 minutes, although only 41% of the sulphide was recovered as H_2S, with the remainder converted to a variety of oxidation products. Sparging with nitrogen did not induce oxidation and allowed the recovery of 70% of the sulphide as H_2S after 60 minutes of sparging. The remainder of the sulphide remained in solution. The stripping off of H_2S resulted in an increase in the pH of the anaerobic digester overflow. The sparging resulted in the loss of all H_2S in the headspace, which resulted in the equilibrium between $H_2S_{(aq)}$ and $H_2S_{(g)}$ at the air-liquid interface needing to be re-established. This led to a shift in the equilibrium between $HS^-_{(aq)}$ and $H_2S_{(aq)}$, which removed a hydrogen ion from solution.

The mechanisms involved in the precipitation of individual metal species and a complex acid mine drainage, by reactive alkaline species were investigated. The accuracy of using chemical speciation software to model simple and complex precipitation systems was also evaluated. In addition, the precipitates were analysed using wavelength dispersive X-ray spectroscopy to try and determine their composition.

The precipitation of individual metal species by the addition of hydroxide, bicarbonate and carbonate was relatively straightforward and a combination of precipitate analysis and information from the modelling allowed the determination of the precipitated species. The addition of sulphide resulted in a more complex situation, with the initial formation of metastable, amorphous precipitates for both copper and iron. These precipitates required an extended period of time to evolve into a stable crystalline form, which settled out of suspension. The addition of an excess of sulphide resulted in a retardation of the evolution process, suggesting the formation of more complex associations, such as charged polysulphide complexes. In the case of copper, the stable precipitate was determined to be covellite (CuS). In the case of iron, the oxidation of the amorphous FeS to FeOOH and eventually Fe_2O_3 occurred before the evolution to a stable mackinawite (FeS) could occur. The active aeration of the amorphous FeS increased the oxidation and settling rate.

The precipitation of the artificial acid mine drainage by hydroxide, sulphide and the biologically generated anaerobic digester overflow and algal overflow, at various acidity to alkalinity ratios, clearly showed how the acid potential of bicarbonate reduced the precipitation efficiency. The

sulphide and hydroxide resulted in the greatest amount of precipitation, followed by algal overflow and the anaerobic digester overflow. The precipitation with sulphide produced the most compact sludge, followed by the algal overflow, the anaerobic digester overflow and hydroxide. In terms of the behaviour of the individual metals in the mixed solution, zinc and copper appeared to precipitate more effectively in systems where aqueous sulphide was present. In contrast, nickel precipitation appeared to be primarily pH dependent, while iron and manganese were preferentially precipitated in the presence of carbonate. From these data, it could be concluded that the algal overflow led to more efficient metal precipitation than the anaerobic digester overflow.

The use of Minteq to predict the amount of metal precipitated and the species involved did not generate accurate results, due to the complexity of the system. Similarly, the precipitate analysis, using wavelength dispersive X-ray spectroscopy, could only confirm the composition of the precipitate in terms of weight percentages for the individual metals, but could not provide information on the precipitating species.

Biologically generated hydrogen sulphide gas was shown to effect the rapid and complete removal of the copper and lead from the acid mine drainage, without reacting with any of the other metals present.

The bench scale pilot operation of the integrated biological systems highlighted their potential for the remediation of acid mine drainage effluents. The *Spirulina* based system was effective, but suffered from problems associated with maintaining the algae in suspension and preventing biomass loss. These problems were overcome by using *Oscillatoria* in the simulated stream reactors and the system was operated without a loss of efficiency for 90 days. The anaerobic digester component of the integrated system was able to consistently generate bicarbonate at a rate of 4200μmoles l^{-1} day^{-1}. The combination of the nitrogen sparging step and the action of the algae was able to reduce the bicarbonate concentration by over 50% and increase the carbonate concentration from 0.07mM to 12.65mM. In terms of metal removal, the selective precipitation of over 99% of copper and lead, using hydrogen sulphide gas, was consistently achieved. The blending of the hydrogen sulphide treated acid mine drainage and the algal overflow at an acidity

to alkalinity ratio of 1:2 resulted in the precipitation of all the heavy metal, except manganese, to concentrations below the acceptable environmental risk level. It was shown that a portion of the overflow stream from the precipitator could be enriched with a carbon source, ammonia and phosphate, and used as a feed for the large anaerobic digester. The remainder of the stream could be discharged to a final polishing step, possibly an anaerobic wetland.

There are no obvious obstacles preventing the scale-up of the integrated biological system presented here. As such, the use of biologically generated reactive alkaline species has been shown to provide a possible treatment option for the long term, sustainable remediation of future, high volume, acid mine drainage discharges.

APPENDICES

Appendix A

Acceptable risk levels and hazard ratings of the metals encountered in this study. Guidelines determined by the Department of Water Affairs and Forestry (1998)

Acceptable environmental risk			
Metal	ppm	µM	Hazard rating
Copper	0.1	1.6	2
Iron	9.0	161.2	3
Lead	0.1	0.5	2
Manganese	0.3	5.5	2
Nickel	1.14	19.4	2
Zinc	0.7	10.7	2

Explanation of hazard rating

Hazard rating	Oral toxicity - LD_{50} (mg/kg)	Dermal toxicity - LD_{50} (mg/kg)
1	Up to 5	Up to 40
2	5-50	40-200
3	50-200	200-1000
4	>200	>1000

Appendix B

Zarrouk's medium for the cultivation of *Spirulina* sp.

Component	Mass/volume
NaCl	1g/l
K_2SO_4	1g/l
KNO_3	3g/l
H_3PO_4	0.25ml/l
$NaHCO_3$	16.8g/l
EDTA	0.08g/l
$FeSO_4.7H_2O$	0.01g/l

The H_3PO_4 was added after the salts had been dissolved

In experiments where metal precipitation was measured the EDTA was omitted from the media as it acts as a metal complexing agent

Appendix C

Standard curve of dry mass of *Spirulina* against volume of algal culture dried ($n = 5$, $r^2 = 0.950$)

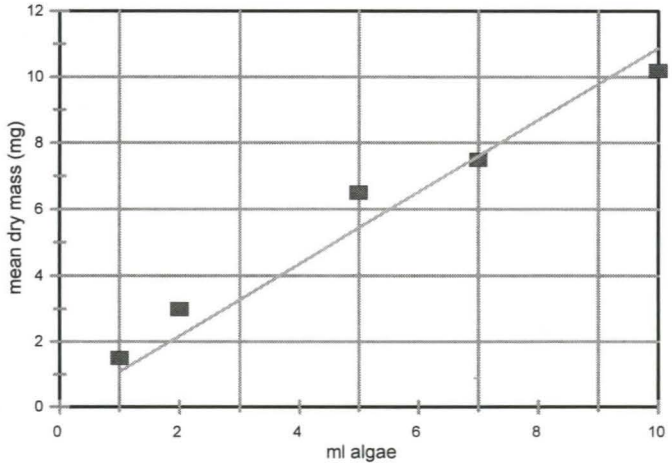

Appendix D

Standard curve of optical density (660nm) against volume of algae (n = 5, $r^2 = 0.998$)

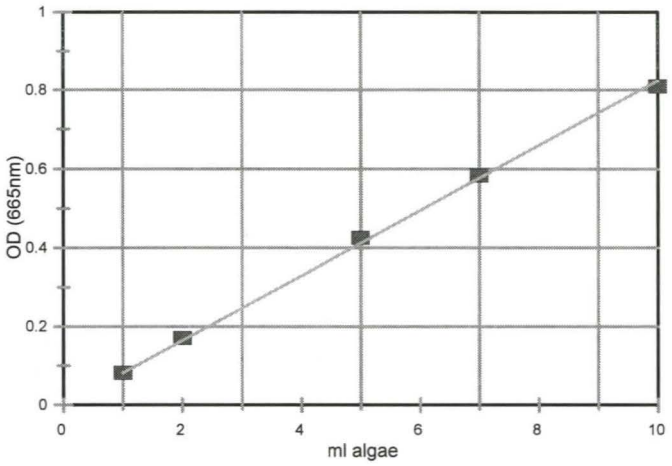

Appendix E

Equations for calculating chlorophyll concentrations (mg/l) from acetone extraction data

Chlorophyll *a* : $C_a = 11.24A_{661.6} - 2.04A_{644.8}$

Chlorophyll *b* : $C_b = 20.13A_{644.8} - 4.19A_{661.6}$

Xanthophylls and Carotenoids : $C_{x+c} = (1000A_{470} - 190C_a - 63.4C_b)/214$

Appendix F

Standard curve of chlorophyll *a* against volume of algae used for extraction (n = 5, $r^2 = 0.995$)

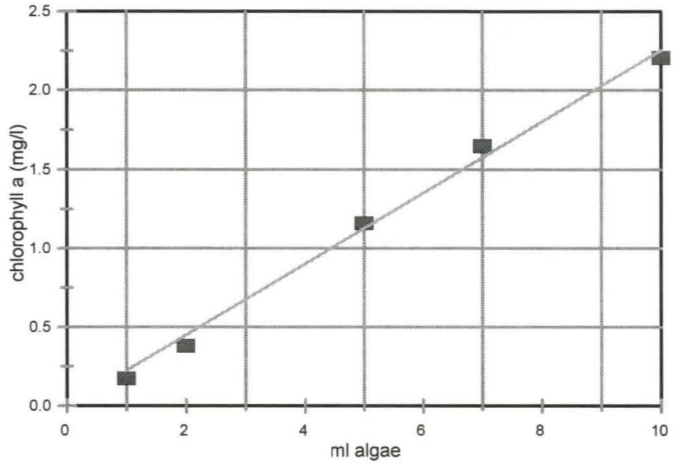

Appendix G

Atomic absorption spectrophotometer program parameters for individual metal windows

Range	Wavelength	Slit width
Calcium: Nitrous oxide-acetylene, lamp current 10.0mA		
10-100µM	422.7nm	0.5nm
Copper: Air-acetylene flame, lamp current 3.0mA		
2-50µM	324.7nm	0.5nm
100-500µM	217.9nm	0.2nm
500-2500µM	222.6nm	1.0nm
Iron: Air acetylene flame, lamp current 7.0mA		
10-150µM	248.3nm	0.2nm
50-1000µM	372.0nm	0.2nm
500-2500µM	386.9nm	0.2nm
Potassium: Air-acetylene flame, lamp current 6.0mA		
25-125µM	769.9nm	0.5nm
Magnesium: Air-acetylene flame, lamp current 3.0mA		
20-500µM	202.6nm	1.0nm
Manganese: Air-acetylene flame, lamp current 5.0mA		
25-100µM	280.1nm	0.2nm
100-500µM	403.1nm	0.2nm
Sodium: Air-acetylene flame, lamp current 5.0mA		
4000-15000µM	330.2nm	0.5nm
Nickel: Air-acetylene flame, lamp current 4.0mA		
25-125µM	232.0nm	0.2nm
Lead: Air-acetylene flame, lamp current 5.0mA		
10-100µM	217.0nm	1.0nm
50-250µM	283.3nm	0.5nm
250-2000µM	261.4nm	0.5nm
Zinc: Air-acetylene flame, lamp current 5.0mA		
2-50µM	213.9nm	0.5nm

Appendix H

Standard curve for carbohydrate determinations (n = 5, $r^2 = 0.984$)

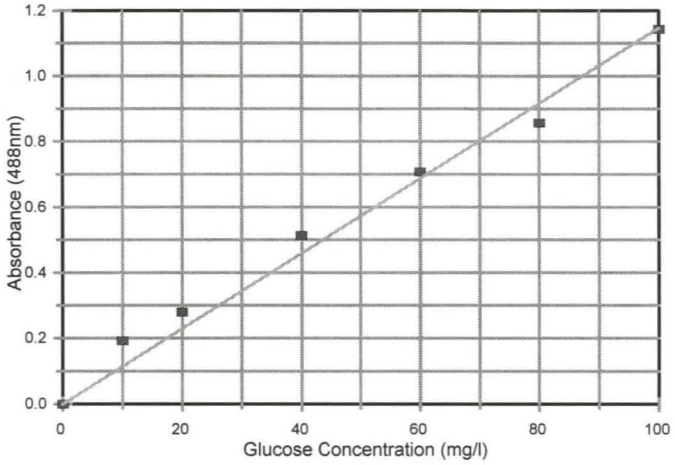

Appendix I

Analysis of effluent from the Black Mountain base metal mine. pH = 1.99

Component	Concentration (mg/l)	Concentration (μM)
Chemical Oxygen Demand (COD)	148	-
Calcium as Ca	890	22 206
Magnesium as Mg	121	4 978
Copper as Cu	1.08	17.00
Lead as Pb	1.52	7.34
Zinc as Zn	2.20	33.64
Iron as Fe	95	1 701
Chloride as Cl	621	17 516
Sulphate as SO_4	3620	37 708
Nitrate as N	1.4	100
Total hardness as $CaCO_3$	2718	-
Calcium hardness as $CaCO_3$	2220	-
Magnesium hardness as $CaCO_3$	498	-
Bicarbonate as $CaCO_3$	0	-

Appendix J

Recipe for modified Postgate B medium for cultivation of SRB

Component	Mass/volume
KH_2PO_4	0.5g
NH_4Cl	1.0g
$MgSO_4.7H_2O$	2.0g
Yeast extract	1.0g
Na_2SO_4	1.0g
60% Na lactate	6ml

Ascorbic acid (0.001g/l) and sodium thioglycollate (0.001g/l) were added to the medium only for the initial establishment of the SRB culture in the 28l anaerobic digester.

Appendix K

Method for gram staining bacterial samples

1) Heat fix bacteria on a microscope slide and stain with crystal violet - 60s
2) Wash smear with water - 2s
3) Flood smear with iodine - 60s
4) Wash with water - 2s
5) Flood smear with 95% ethanol - 30s
6) Counterstain with safranin - 10s
7) Wash with water

Appendix L

Reagents for sulphide analysis

Zinc acetate

10.55g $(CH_3COO)_2Zn.2H_2O$

Make up to 1l with $dddH_2O$

Ferric chloride

8g $FeCl_3$

500ml 6M HCl

Store in a dark bottle at room temperature

Amide-sulphuric acid stock solution

2g N-N dimethyl-p-phenylene diamine dihydrochloride

500ml 6M HCl

Store in a dark bottle at room temperature

Standard curve

Mean values (n = 5), $R^2 = 0.999$

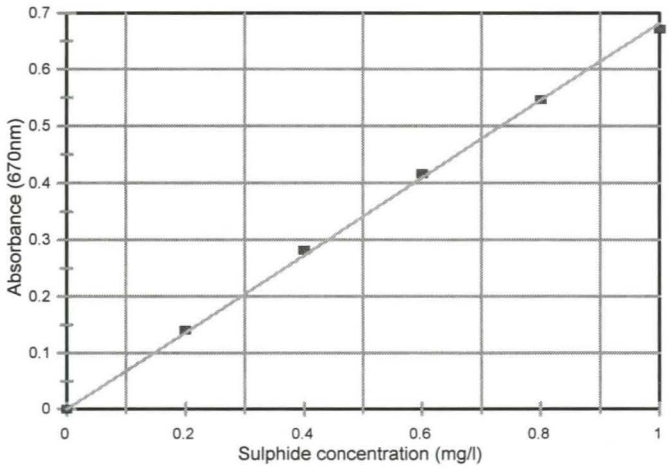

Appendix M

Mobile phases for detection of sulphate and sulphur by HPLC

Anion (sulphate) HPLC mobile phase

5.52g para-hydroxybenzoic acid

250ml methanol

Make up to 2l with $dddH_2O$

For running buffer, use 300ml of the above concentrate and make up to 1l with $dddH_2O$. Filter through a 0.45µm nylon membrane filter and de-gas

Sulphur HPLC mobile phase

950ml methanol

50ml $dddH_2O$

Filter through a 0.45µm nylon membrane filter and de-gas

Appendix N

Detection limits, read times and peak analysed for the individual elements used in the wavelength dispersive x-ray spectrocopy

Element	Det. Limit (ppm)	Read time (low)	Read time (peak)	Read time (high)	Peak
Cu	0.071	5s	10s	5s	kα
Fe	0.044	5s	10s	5s	kα
Mg	0.260	5s	10s	5s	kα
Mn	0.036	5s	10s	5s	kα
Ni	0.077	5s	10s	5s	kα
Pb[1]	0.201	15s	30s	15s	mα
S	0.073	5s	10s	5s	kα
Zn	0.087	5s	10s	5s	kα

[1] The m orbital is more difficult to excite, resulting in lower counts. Therefore, the read time for lead was set at three times longer than the elements in which the kα peak was read.

Appendix O

Major metal species present in the artificial acid mine drainage, as predicted by MinteqA2

Metal species	Concentration (μM)
Ca^{2+}	4093
$CaSO_{4\,(aq)}$	1687
Cu^{2+}	221
$CuSO_{4\,(aq)}$	91
Fe^{2+}	2765
$FeSO_{4\,(aq)}$	995
Mg^{2+}	5228
$MgSO_{4\,(aq)}$	1881
Mn^{2+}	523
$MnSO_{4\,(aq)}$	192
Ni^{2+}	242
$NiSO_{4\,(aq)}$	95
$NiCl^{+}$	4
Pb^{2+}	39
$PbSO_{4\,(aq)}$	45
$PbCl^{+}$	9
Zn^{2+}	199
$ZnSO_{4\,(aq)}$	94
$Zn(SO_4)_2^{2-}$	9

REFERENCES

Abalde, J., Cid, A., Reiriz, S., Torres, E. and Herrero, C. 1995. Response of the marine microalga *Dunaliella tetiolecta* (Chlorophyceae) to copper toxicity in short time experiments, *Bulletin of Environmental Contamination and Toxicity,* **54:** 317-324

Adams, B., Gale, I., Younger, P.L., Lerner, D. and Chilton, J. 2000. Groundwater. In: Acreman, M. (ed.) *The Hydrology of the UK. A study of change*, Routledge, London, pp 150-179

Ahmed, S., Chughtai, S. and Keane, M.A. 1998. The removal of cadmium and lead from aqueous solution by ion exchange with Na-Y zeolite, *Separation and Purification Technology,* **13:** 57-64

Al-Moghrabi, S., Goiran, C., Allemand, D., Speziale, N. and Jaubert, J. 1996. Inorganic carbon uptake for photosynthesis by the symbiotic coral-dinoflagellate association II. Mechanisms for bicarbonate uptake, *Journal of Experimental Marine Biology and Ecology*, **199:** 227-248

Amaroso, G., Weber, C., Sültemeyer, D. and Fock, H. 1996. Intracellular carbonic anhydrase activities in *Dunaliella tetiolecta* (Butcher) and *Chlamydomonas reinhardtii* (Dangeard) in relation to inorganic carbon concentration during growth: further evidence for the existence of two distinct carbonic anhydrases associated with the chloroplasts, *Planta*, **199:** 177-184

APHA. 1998. *Standard Methods for the Examination of Water and Wastewater*, 20th Edition, American Public Health Association, Washington, USA

Appelo, C.A.J. and Postma, D. 1993. *Geochemistry, Groundwater and Pollution,* Balkema, Rotterdam, 536pp

Ashkenazy, R., Gottlieb, L. and Yannai, S. 1997. Characterization of acetone-washed yeast biomass functional groups involved in lead biosorption, *Biotechnology and Bioengineering*, **55:** 1-10

Asthana, R.K., Singh, S.P. and Singh, R.K. 1992. Nickel effects on phosphate uptake, alkaline phosphotase, and ATPase of a cyanobacterium, *Bulletin of Environmental Contamination and Toxicity,* **48:** 45-54

Backeberg, G.R., Bembridge, T.J., Bennie, A.T.P., Groenewald, J.A., Hammes, P.S., Pullen, R.A. and Thompson, H. 1996. Policy proposal for irrigated agriculture in South Africa, WRC Report No. KV96/96, Water Research Commission, Pretoria, South Africa

Badger, M.B. and Price, G.D. 1989. Carbonic anhydrase associated with the cyanobacterium *Synechococcus* PCC7942, *Plant Physiology*, **89:** 51-60

Badger, M.B. and Price, G.D. 1992. The CO_2 concentrating mechanism in cyanobacteria and microalgae, *Physiologia Plantarum*, **84:** 606-615

Banat, I.M., Lindstrom, E., Nedwell, D.B. and Balba, M.T. 1981. Evidence for co-existence of two distinct functional groups of sulphate-reducing bacteria in salt marsh sediment, *Applied and Environmental Microbiology*, **42:** 985-992

Barnes, L.J., Janssen, F.J., Scheeren, P.J.H., Versteegh, J.H. and Koch, R.O. 1991. Simultaneous microbial removal of sulphate and heavy metals from waste water, *Proceedings of EMC91: Non-ferrous metallurgy - present and future*, Elsevier, pp 391-401

Barón, M., Arellano, J.B. and López Georgé, J. 1995. Copper and photosystem II: A controversial relationship, *Physiologia Plantarum*, **94:** 174-180

Barrado, E., Prieto, F., Vega, M. and Fernandez-Polanco, F. 1998. Optimization of the operational variables of a medium-scale reactor for metal-containing wastewater purification by ferrite process, *Water Research*, **32:** 3055-3061

Bayless, E.R. and Olyphant, G.A. 1993. Acid-generating salts and their relationship to the chemistry of groundwater and storm runoff at an abandoned mine site in southwestern Indiana,

USA, *Journal of Contaminant Hydrology,* **12:** 313-328

Beardall, J., Johnston, A. and Raven, J. 1998. Environmental regulation of CO_2-concentrating mechanisms in microalgae, *Canadian Journal of Botany*, **76:** 1010-1017

Béchard, G., Yamazaki, H., Gould, D. and Bédard, P. 1994. Use of cellulosic substances for the microbial treatment of acid mine drainage, *Journal of Environmental Quality,* **23:** 111-116

Bhattacharyya, D., Sun, G., Sund-Hagelberg, C. and Schwitzgebel, K. 1981. Precipitation of heavy metals with sodium sulphide: bench-scale and full-scale experimental results, *AIChE Symposium Series*, **77(209):** 31-38

Boshoff, G.A. 1999. Development of integrated biological processing for the biodesalination of sulphate- and metal-rich wastewaters, PhD Thesis, Rhodes University, Grahamstown, South Africa

Boshoff, G.A., Duncan, J.R. and Rose, P.D. 1996. An algal-bacterial integrated ponding system for the treatment of mine drainage waters, *Journal of Applied Phycology*, **8:** 442

Boshoff, G.A., Duncan, J.R. and Rose, P.D. 1998. Sulphide toxicity to algae, *Proceedings of the Biennial Conference of the Water Institute of South Africa (WISA 98)*, WISA, Cape Town

Brady, D. and Duncan, J.R. 1994. Binding of heavy metals by the cell walls of *Saccharomyces cerevisiae, Enzyme and Microbial Technology,* **16:** 633-636

Brady, D., Glaum, D. and Duncan, J.R. 1994. Copper tolerance in *Saccharomyces cerevisiae*, *Letters in Applied Microbiology*, **18:** 245-250

Braus-Stromeyer, S.A., Schnappauf, G., Braus, G.H., Göbner, A.S. and Drake, H.L. 1997. Carbonic anhydrase in *Acetobacterium woodii* and other acetogenic bacteria, *Journal of Bacteriology*, **179:** 7179-7200

Brierley, J.A., Brierley, C.L. and Goyak, G.M. 1985. AMT-BIOCLAIM™: A new wastewater treatment and metal recovery technology. In: *Fundamental and Applied Biohydrometallurgy*, Elsevier, Amsterdam, pp 291-304

Cairncross, B. and Dixon, R. 1999. *Minerals of South Africa*, The Geological Society of South Africa, South Africa, 290 pp

Casey, N.H., Meyer, J.A., Coetzee, C. and van Niekerk, W.A. 1996. An investigation into the quality of water for animal production, WRC Report No. 301/1/96, Water Research Commission, Pretoria, South Africa

Chang, I.S., Shin, P.K. and Kim, B.H. 2000. Biological treatment of acid mine drainage under sulphate-reducing conditions with solid waste materials as substrate, *Water Research*, **34:** 1269-1277

Chiarle, S., Ratto, M. and Rovatti, M. 2000. Mercury removal from water by ion exchange resins adsorption, *Water Research*, **34:** 2971-2978

Chian, E.S.K. and De Walle, F.B. 1983. Removal of heavy metals from a fatty acid wastewater with a complex mixed anaerobic filter, *Proceedings of the 38th Industrial Waste Conference*, Purdue University, West Lafayette, IN, pp 920-927

Chen, K.Y. and Morris, J.C. 1972. Kinetics of oxidation of aqueous sulfide by O_2, *Environmental Science and Technology*, **6:** 529-537

Chow, M.K. and Zukoski, C.F. 1994. Gold sol formation mechanisms - role of colloidal stability, *Journal of Colloid and Interface Science*, **165:** 97-109

Christensen, B., Laake, M. and Lien, T. 1996. Treatment of acid mine water by sulphate-reducing bacteria: results from bench scale experiment, *Water Research*, **30:** 1617-1624

Chutter, F.M. 1998. *Research on the Rapid Biological Assessment of Water Quality Impacts in Streams and Rivers*, Water Research Commission Report No. 422/1/98, Pretoria, South Africa

Ciferri, O. 1983. *Spirulina*, the edible microorganism, *Microbiology Reviews*, **47:** 551-578

Corbett, C.J. 2001. The Rhodes BioSURE Process in the treatment of acid mine drainage wastewaters, MSc Thesis, Rhodes University, Grahamstown, South Africa

Crist, D.R., Crist, R.H., Martin, J.R. and Watson, J.R. 1994a. Ion exchange systems in proton-metal reactions with algal cell walls, *FEMS Microbiology Reviews*, **14:** 309-313

Crist, R.H., Martin, J.R., Carr, D., Watson, J.R., Clarke, H.J. and Crist, D.R. 1994b. Interactions of metals and protons with algae. 4. Ion exchange vs adsorption models and a reassessment of Scatchard plots, ion-exchange rates and equilibria compared with calcium alginate, *Environmental Science and Technology*, **28:** 1859-1866

Cross, R.H.M. 1987. *A handbook on the preparation of biological material for electron microscopy*, Rhodes University, Grahamstown, pp 5-12, 34-37

Cypionka, H. 1987. Uptake of sulfate, sulfite and thiosulfate by proton-ion symport in *Desulfovibrio desulfuricans*, *Archives of Microbiology*, **148:** 144-149

Davies, A.D. 1983. In: Rourd, F.E. and Chapman, D.J. (eds), *Progress in phycological research*, Elsevier Science Publishers, Netherlands, pp 113-145

Dean, J.G., Bosqui, F.L. and Lanouette, K.H. 1972. Removing heavy metals from waste water, *Environmental Science and Technology*, **6:** 518-522

De Jager, F.S.J. 1986. The East Rand Gold Field and the South Rand Gold Field. In: Antrobus, E.S.A. (ed.) *Witwatersrand Gold - 100 Years*, Geological Society of South Africa, Johannesburg

Department of Water Affairs and Forestry (DWAF). 1998. Waste Management Series: Minimum requirements for the handling, classification and disposal of hazardous waste. Second edition, CTP Book Printers, Cape Town, 171 pp

Department of Water Affairs and Forestry (DWAF). 1999. Draft Water Conservation and Demand Management National Strategy Framework, Department of Water Affairs and Forestry, pp 7-28

Dunn, K.M. 1998. The biotechnology of high rate algal ponding systems in the treatment of saline tannery wastewaters, PhD Thesis, Rhodes University, Grahamstown, South Africa

Elliot, P., Ragusa, S. and Catcheside, D. 1998. Growth of sulphate-reducing bacteria under acidic conditions in an upflow anaerobic bioreactor as a treatment system for acid mine drainage, *Water Research*, **32:** 3724-3730

Eriksson, M., Karlsson, J., Ramazanov, Z., Gardeström, P. and Samuelsson, G. 1996. Discovery of an algal mitochondrial carbonic anhydrase and characterisation of a low-CO_2-induced polypeptide in *Chlamydomonas reinhardtii*, *Proceedings of the National Academy of Sciences USA*, **91:** 12031-12034

Faust, S.D. and Aly, O.M. 1987. *Adsorption Processes for Water Treatment*, Butterworth Publishers, Stoneham, MA, USA

Feng, D., Aldrich, C. and Tan, H. 2000. Treatment of acid mine water by use of heavy metal precipitation and ion exchange, *Minerals Engineering*, **13:** 623-642

Flores-Moya, A. and Fernández, J.A. 1998. The role of external carbonic anhydrase in the photosynthetic use of inorganic carbon in the deep-water alga *Phyllariopsis purpurascens* (Laminariales, Phaeophyta), *Planta*, **207:** 115-119

Foucher, S., Battaglia-Brunet, F., Ignatiadis, I. and Morin, D. 2001. Treatment by sulfate-

reducing bacteria of Chessy acid-mine drainage and metals recovery, *Chemical Engineering Science*, **56:** 1639-1645

Fourest, E. and Volesky, B. 1996. Contribution of sulfonate groups and alginate to heavy metal biosorption by the dry biomass of *Sargassum fluitans*, *Environmental Science and Technology*, **30:** 277-282

Franklin, N.M., Stauber, J.L., Markich, S.J. and Lim, R.P. 2000. pH-dependent toxicity of copper and uranium to a tropical freshwater alga (*Chlorella* sp.), *Aquatic Toxicology*, **48:** 275-289

Freskgård, P.O., Carlsson, U., Mårtensson, L.G. and Jonsson, B.H. 1991. Folding around the C-terminus of carbonic anhydrase II, *FEBS Letters*, **289:** 117-122

Frost, R.C. 1979. Evaluation of the rate of decrease in the iron content of water pumped from a flooded shaft mine in County Durham, England, *Journal of Hydrology,* **40:** 101-111

Gadd, G.M. and White, C. 1993. Microbial treatment of metal pollution - a working biotechnology? *Trends in Biotechnology*, **11:** 353-359

Gardea-Torresdey, J.L., Becker-Hapak, M.K., Hosea, J.M. and Darnell, D.W. 1990. Effect of chemical modification of algal carboxyl groups on metal ion binding, *Environmental Science and Technology*, **24:** 1372-1378

Garnham, G.W., Codd, G.A. and Gadd, G.M. 1993. Uptake of cobalt and cesium by microalgal- and cyanobacterial-clay mixtures, *Microbial Ecology*, **25:** 71-82

Gazea, B., Adam, K. and Kontopoulos, A. 1996. A review of passive systems for the treatment of acid mine drainage, *Minerals Engineering*, **9:** 23-42

Gibson, G.R. 1990. Physiology and ecology of the sulphate-reducing bacteria, *Journal of*

Applied Bacteriology, **69:** 769-797

Glombitza, F. 2001. Treatment of acid lignite mine flooding water by means of microbial sulfate reduction, *Waste Management*, **21:** 197-203

Glover, H.G. 1975. Acidic and ferruginous mine drainages. In: Chadwick, M.J. and Goodman, G.T. (eds) *The Ecology of Resource Degradation and Renewal,* Proceedings of the 15th Symposium of the British Ecological Society, 10-12 July 1973, Blackwell, Oxford, pp 173-195

Glover, H.G. 1983. Mine water pollution - an overview of problems and control strategies in the United Kingdom, *Water Science and Technology,* **15:** 59-70

Greene, B., McPherson, R. and Darnell, D.W. 1987. In: Patterson, J. and Pasino, R. (eds), *Metals, Speciation, Separation and Recovery*, Lewis Publishers, Inc., Chelsea, MI, pp 53-70

Greenwood, N.N. and Earnshaw, A. 1984. *Chemistry of the Elements*, Pergamon Press, Oxford, England, 1542pp

Guanzon, N.G. Jr., Nakahara, H. and Yoshida, Y. 1994. Inhibitory effects of heavy metals on growth and photosynthesis of three freshwater microalgae, *Fisheries Science*, **60:** 379-384

Haglund, K., Ramazanov, Z., Mtolera, M. and Pedersen, M. 1992. Role of external carbonic anhydrase in light-dependent alkalization by *Fucus serratus* L. and *Laminaria saccharina* (L.) Lamour. (Phaeophyta), *Planta*, **188:** 1-6

Hammack, R.W., Dvorak, D.H. and Edenborn, H.M. 1993. The use of biogenic hydrogen sulfide to selectively recover copper and zinc from severely contaminated mine drainage. In: Torma, A.E., Wey, J.E. and Lakshmanan, V.L. (eds) *Biohydrometallurgical Technologies,* The Minerals, Metals & Materials Society, pp 631-639

Hammack, R.W. and Edenborn, H.M. 1992. The removal of nickel from minewater using

bacterial sulfate reduction, *Applied Microbiology and Biotechnology*, **37:** 674-678

Hammack, R.W., Edenborn, H.M. and Dvorak, D.H. 1994. Treatment of water from an open-pit copper mine using biogenic sulfide and limestone: A feasibility study, *Water Research*, **28:** 2321-2329

Hammaini, A., Ballester, A., González, F., Blázquez, M.L. and Muñoz, J.A. 1999. Activated sludge as a biosorbent of heavy metals. In: Amils, R. and Ballester, A. (eds), Proceedings of the International Biohydrometallurgy Symposium (IBS '99), Part B, Elsevier, Amsterdam, pp 185-192

Hansen, T.A. 1988. Physiology of sulphate reducing bacteria, *Microbiological Sciences*, **5:** 81-84

Harris, J., van Vliet, H.R. and MacKay, H.M. 1999. Water resource quality policy: The approach adopted by the Department of Water Affairs and Forestry under the water law principles, *Water Science and Technology,* **39:** 31-37

Hedin, R.S. 1997. Passive mine water treatment in the eastern United States. In: Younger, P.L. (ed.) *Minewater Treatment Using Wetlands,* Chartered Institution of Water and Environment Management, London, pp 1-15

Hedin, R.S., Nairn, R.W. and Kleinmann, P.L.P. 1994. *Passive Treatment of Coal Mine Drainage*, US Bureau of Mines Information Circular 9389, US Department of the Interior, Bureau of Mines, Pittsburgh, PA., pp 1-35

Heider, J., Spormann, A.M., Beller, H.R. and Widdel, F. 1998. Anaerobic bacterial metabolism of hydrocarbons, *FEMS Microbiology Reviews*, **22:** 459-473

Herlihy, A.T., Mills, A.L., Hornberger, G.M. and Bruckner, A.E. 1987. The importance of sediment sulphate reduction to the sulphate budget of an impoundment receiving acid mine

drainage, *Water Resources Research*, **23:** 287-292

Herrera, L.J., Hernàndez, P., Ruíz, R. and Gantenbein, S. 1991. *Desulfovibrio desulfuricans* growth kinetics, *Environmental Toxicology and Water Quality*, **6:** 225-238

Hiltonen T., Björkbacka, H., Forsman, C., Clarke, A.K. and Samuelsson, G. 1998. Intracellular ß-carbonic anhydrase of the unicellular green alga *Coccomyxa*, *Plant Physiology*, **117:** 1341-1349

Hiltonen, T., Karlsson, J., Palmqvist, K., Clarke, A.K. and Samuelsson, G. 1995. Purification and characterisation of an intracellular carbonic anhydrase from the unicellular green alga *Coccomyxa*, *Planta*, **195:** 345-351

Holan, Z.R., Volesky, B. and Prasetyo, I. 1993. Biosorption of cadmium by biomass of marine algae, *Biotechnology and Bioengineering,* **41:** 819-825

Holland, K.T., Knapp, J.S. and Shoesmith, J.G. 1987. *Anaerobic Bacteria*, Blackie & Son Ltd., Glasgow, pp 137-197

Husic, H.D. and Marcus, C.A. 1994. Identification of intracellular carbonic anhydrase in *Chlamydomonas reinhardtii* with a carbonic anhydrase-directed photoaffinity label, *Plant Physiology*, **105:** 133-139

Jarvis, A.P. and Younger, P.L. 2000. Broadening the scope of mine water environmental impact assessment: a UK perspective, *Environmental Impact Assessment Review,* **20:** 85-96

Jenneman, G.E., McInerney, M.J. and Knapp, R.M. 1986. Effect of nitrate on biogenic sulphide production, *Applied and Environmental Microbiology*, **51:** 1205-1211

Jin, X., Nalewajko, C. and Kushner, D.J. 1996. Comparative study of nickel toxicity to growth and photosynthesis in nickel-resistant and -sensitive strains of *Scenedesmus acutus* f. *alternans*

(Chlorophyceae), *Microbial Ecology*, **31:** 103-114

Johansson, I.J. and Forsman, C. 1993. Kinetic studies of pea carbonic anhydrase, *European Journal of Biochemistry*, **218:** 439-446

Johnson, D.B. 1995. Acidophilic microbial communities: Candidates for bioremediation of acidic mine effluents, *International Biodeterioration and Biodegradation,* Elsevier Science, 41-58

Jooste, S. and Thirion, C. 1999. An ecological risk assessment for a South African acid mine drainage, *Water Science and Technology*, **39:** 297-303

Juby, G.J.G., Schutte, C.F. and van Leeuwen, J. 1996. Desalination of calcium sulphate scaling mine water: Design and operation of the SPARRO process, *Water SA,* **22:** 161-172

Kalin, M., Cairns, J. and McCready, R. 1991. Ecological engineering methods for acid mine drainage treatment of coal wastes, *Resources, Conservation and Recycling*, **5:** 265-275

Kaplan, D., Christiaen, D. and Arad, S.M. 1987. Chelating properties of extracellular polysaccharides from *Chlorella* spp., *Applied and Environmental Microbiology*, **53:** 2953-2956

Karamushka, V.I., Gruzina, T.G. and Ul'berg, Z.R. 1995. Accumulation of gold(III) by the cells of cyanobacterium *Spirulina platensis*, *Microbiology*, **64:** 157-160

Kidambi, S.P., Sundin, G.W., Palmer, D.A., Chakrabarty, A.M. and Bender, C.L. 1995. Copper as a signal for alginate synthesis in *Pseudomonas syringae*, *Applied and Environmental Microbiology*, **61:** 2172-2179

Kratochvil, D., Fourest, E. and Volesky, B. 1995. Biosorption of copper by *Sargassum fluitans* biomass in a fixed bed column, *Biotechnology Letters*, **17:** 777-782

Kratochvil, D. and Volesky, B. 1998. Biosorption of Cu from ferruginous wastewater by algal biomass, *Water Research*, **32:** 2760-2768

Lam, P.K.S., Wut, P.F., Chan, A.C.W. and Wu, R.S.S. 1999. Individual and combined effects of cadmium and copper on the growth response of *Chlorella vulgaris*, *Environmental Toxicology*, **14:** 347-353

Larson, H.P., Shou, J.K.P. and Ross, L.W. 1973. Chemical treatment of metal-bearing mine drainage, *Journal of the Water Pollution Control Federation,* **45:** 1682-1695

Lawrence, J.R., Swerhone, G.D.W. and Kwong, Y.T.J. 1998. Natural attenuation of aqueous metal contamination by an algal mat, *Canadian Journal of Microbiology*, **44:** 825-832

Leusch, A. and Volesky, B. 1995. The influence of film diffusion on cadmium biosorption by marine biomass, *Journal of Biotechnology*, **43:** 1-10

Lichtenhaler, H.K. 1987. Chlorophylls and carotenoids: pigments of the photosynthetic biomembranes, *Methods in Enzymology*, **148:** 350-371

Lindskog, S. 1997. Structure and mechanism of carbonic anhydrase, *Pharmacology and Therapeutics,* **74:** 1-20

Liu, C.L. and Peck, H.D. 1981. Comparative bioenergetics of sulfate reduction in *Desulfovibrio* and *Desulfotomaculum* spp., *Journal of Bacteriology*, **145:** 966-973

Loewenthal, R.E., Morgan, B.E. and Lahav, O. 2001. Iron and heavy metals in acid mine drainage waters - equilibrium and treatment considerations, *Water Sewage & Effluent,* **21:** 15-23

Luther III, G.W. 1991. Pyrite synthesis via polysulfide compounds, *Geochimica et Cosmochimica Acta*, **55:** 2829-2849

Luther III, G.W. and Ferdelman, T.G. 1993. Voltammetric characterization of iron(II) sulfide complexes in laboratory solutions and in marine waters and porewaters, *Environmental Science and Technology*, **27:** 1154-1163

Mara, D.D., Pearson, H.W. and Silva, S.A. 1996. Waste stabilisation ponds: technology and applications, *Water Science and Technology*, **33:** 1-262

Maree, J.P., Du Plessis, P. and Van der Walt, C.J. 1992. Treatment of acidic effluents with limestone instead of lime, *Water Science and Technology,* **26:** 345-355

Maree, J.P., Gerber, A. and Hill, E. 1987. An integrated process for biological treatment of sulphate containing industrial effluents, *Journal of the Water Pollution Control Federation,* **59:** 1069-1074

Maree, J.P. and Hill, E. 1989. Biological removal of sulphate from industrial effluents and concomitant production of sulphur, *Water Science and Technology*, **21:** 265-276

Martel, A., Yu, S., Garcia-Reina, G., Lindblad, P. and Pederson, M. 1992. Osmotic adjustment in the cyanobacterium *Spirulina platensis*: Presence of an α-glucosidase, *Plant Physiology and Biochemistry*, **30:** 573-578

Meador, J.P., Sibley, T.H., Swartzman, G.L. and Taub, F.B. 1998. Copper tolerance by the freshwater algal species *Oocystis pusilla*, *Aquatic Toxicology*, **44:** 69-82

Moroney, J.V. and Chen, Z.Y. 1998. The role of the chloroplast in inorganic carbon acquisition by eukaryotic algae, *Canadian Journal of Botany*, **76:** 1025-1035

Moroney, J.V., Husic, H.D. and Tolbert, N.E. 1985. Effect of carbonic anhydrase inhibitors on inorganic accumulation by *Chlamydomonas reinhardtii*, *Plant Physiology*, **79:** 177-183

Murthy, S.D.S. and Mohanty, P. 1995. Action of selected heavy metal ions on the photosystem

2 activity of the cyanobacterium *Spirulina platensis*, *Biologia Plantarum*, **37:** 79-84

Neytzell-De Wilde, F.G. 1992. Reassessment of the strategy with respect to industrial effluent discharge with special reference to advanced technology treatment methods. Phase 1: Industrial effluent discharge problem areas, WRC Report No. 407/1/92, Water Research Commission, Pretoria, South Africa

Niu, H., Xu, X.S. and Wang, J.H. 1993. Removal of lead ions from aqueous solutions by *Penicillium* biomass, *Biotechnology and Bioengineering*, **42:** 785-787

Nordstrom, D.K., Jenne, F.A. and Ball, J.W. 1979. Redox equilibria of iron in acid mine waters, *American Chemical Society, Symposium Series*, **93:** 51-79

Odendaal, P. 1997. The future role and functions of the Water Research Commission, *Proceedings of the Water Institute of Southern Africa Biennial Conference and Exhibition*, Cape Town, 4-7 May

Odom, J.M. and Peck, H.D. 1984. Hydrogenase, electron-transfer proteins, and energy coupling in the sulphate-reducing bacteria *Desulphovibrio*, *Annual Review of Microbiology*, **38:** 551-592

Olson, G.J., Dockins, W.S. McFeters, G.A. and Inverson, W.P. 1981. Sulphate-reducing and methanogenic bacteria from deep aquifers in Montana, *Geomicrobiology Journal,* **2:** 327-340

Oswald, W.J. 1990. Advanced integrated wastewater pond systems, *Proceedings of the 1990 ASCE Convention EE Div/ASCE*, San Francisco, California

Oswald, W.J. 1991. Waste treatment by pond systems. Engineering aspects, *Proceedings of the IAWPRC conference on appropriate waste management technologies,* Perth, Australia

Overnell, J. 1975. The effect of heavy metals on photosynthesis and loss of potassium in two species of marine algae, *Dunaliella tertiolecta* and *Phaedoctylum tricornutum*, *Marine Biology*,

29: 99-103

Payne, R.A. 2000. *Spirulina* as a bioremediation agent: Interaction with metals and involvement of carbonic anhydrase, MSc Thesis, Rhodes University, Grahamstown, South Africa

Pascucci, P.R. 1993. Simultaneous multi-element study of the binding of metals in solution by an algal biomass, *Chlorella vulgaris*, *Analytical Letters*, **26:** 445-455

Pattrick, R.A.D., Mosselmans, J.F.W., Charnock, J.M., England, K.E.R., Helz, G.R., Garner, C.D. and Vaughan, D.J. 1997. The structure of amorphous copper sulphide precipitates: An X-ray absorption study, *Geochimica et Cosmochimica Acta*, **61:** 2023-2036

Peck, H.D. and Lissolo, T. 1988. Assimilatory and dissimilatory sulphate reduction: Enzymology and bioenergetics, *Society of General Microbiology Symposium*, **42:** 99-132

Perez, O.P., Umetsu, Y. and Sasaki, H. 1998. Precipitation and densification of magnetic iron compounds from aqueous solutions at room temperature, *Hydrometallurgy,* **50:** 223-242

Phelps, C.D., Kerkhof, L.J. and Young, L.Y. 1998. Molecular characterization of a sulphate-reducing consortium which mineralizes benzene, *FEMS Microbiology Ecology*, **27:** 269-279

Pletschke, B.I., Rose, P.D. and Whiteley, C.G. 2001. The enzymology of accelerated primary sludge solubilisation utilising sulphate reducing systems. The role of ATP-Sulphurylase. In: van Velsen, A.F.M. and Verstraete, W.H. (eds), *Proceedings of the 9th World Congress on Anaerobic Digestion*, Antwerpen, Belgium

Postgate, J.R. 1984. *The Sulphate-Reducing Bacteria* 2nd Edn. Cambridge University Press

Pratt, A.R., Muir, I.J. and Nesbitt, H.W. 1994. X-ray photoelectron and Auger electron spectroscopic studies of pyrrhotite and mechanism of air oxidation, *Geochimica et Cosmochimica Acta*, **58:** 827-841

Raven, J.A. 1995. Photosynthetic and non-photosynthetic roles of carbonic anhydrase in algae and cyanobacteria, *Phycologia*, **34:** 93-101

Richmond, A. 1986. In: *Handbook of microalgal mass culture*, CRC Press Inc., USA, pp 117-145, 212-230

Rickard, D. 1995. Kinetics of FeS precipitation: Part 1. Competing reaction mechanisms, *Geochimica et Cosmochimica Acta,* **59:** 4367-4379

Rickard, D. 1997a. Kinetics of pyrite formation by the H_2S oxidation of iron (II) monosulphide in aqueous solutions between 25 and 125°C: The rate equation, *Geochimica et Cosmochimica Acta*, **61:** 115-134

Rickard, D. 1997b. Kinetics of pyrite formation by the H_2S oxidation of iron (II) monosulphide in aqueous solutions between 25 and 125°C: The mechanism, *Geochimica et Cosmochimica Acta*, **61:** 135-147

Rose, P.D., Boshoff, G.A., van Hille, R.P., Wallace, L.C.M., Dunn, K.M. and Duncan, J.R. 1998. An integrated algal sulphate reducing high rate ponding process for the treatment of acid mine drainage wastewaters, *Biodegradation*, **9:** 247-257

Rose, P.D. and Hart, O.O. 1998. Retreatment of water, SA Patent 99/6546, ARIPO/99/01683, Australia 54004/99, USA 09/418.326, Namibia 99/0057

Rose, P.D., Maart, B.A., Dunn, K.M., Rowswell, R.A. and Britz, P. 1996. High rate algal oxidation ponding for the treatment of tannery effluents, *Water Science and Technology*, **33:** 219-227

Roy, D., Greenlaw, P.N. and Shane, B.S. 1993. Adsorption of heavy metals by green algae and ground rice hulls, *Journal of Environmental Science and Health*, **A28:** 37-50

Sahm, K., MacGregor, B.J., Jørgensen, B.B. and Stahl, D.A. 1999. Sulphate reduction and vertical distribution of sulphate-reducing bacteria quantified by rRNA slot-blot hybridization in a coastal marine sediment, *Environmental Microbiology*, **1:** 65-74

Sanyahumbi, D. 1998. Removal of lead from solution by the non-viable biomass of the water fern *Azolla filiculoides*, MSc thesis, Rhodes University, South Africa

Sanyahumbi, D., Duncan, J.R., Zhao, M. and van Hille, R.P. 1998. Removal of lead from solution by the non-viable biomass of the aquatic fern *Azolla filiculoides*, *Biotechnology Letters*, **20:** 173-183

Sauty, J-P. 1980. An analysis of hydrodispersive transfer in aquifers, *Water Resources Research*, **16:** 145-158

Schippers, A. and Sand, W. 1999. Bacterial leaching of metal sulfides proceeds by two indirect mechanisms via thiosulfate or via polysulfides and sulfur, *Applied and Environmental Microbiology*, **65:** 319-321

Schoeman, J.J. and Steyn, A. 2001. Investigation into alternative water treatment technologies for the treatment of underground mine water discharged by Grootvlei Propriety Mines Ltd into the Blesbokspruit in South Africa, *Desalination* **133:** 13-30

Scott, R. 1995. *Flooding of Central and East Rand gold mines: An investigation into controls over the inflow rate, water quality and the predicted impacts of flooded mines*, Water Research Commission Report No. 486/1/95, 238pp

Seitz, H.J. and Cypionka, H. 1986. Chemolithotrophic growth of *Desulfovibrio desulfuricans* with hydrogen coupled to ammonification of nitrate or nitrite, *Archives of Microbiology*, **146:** 63-67

Sherwood, J.M. and Younger, P.L. 1994. Modelling groundwater rebound after coalfield closure: An example from County Durham, UK. In: Reddish, D.J. (ed.) *Proceedings of the 5th International Mine Water Congress, Volume 2,* 769-777

Sherwood, J.M. and Younger, P.L. 1997. Modelling groundwater rebound after coalfield closure. In: Chilton, P.J. (ed.) *Proceedings of the XXVII Congress of the International Association of Hydrogeologists*, **1:** 165-170

Shiraiwa, Y., Goyal, A. and Tolbert, N.E. 1993. Alkalization of the medium by unicellular green algae during the uptake of dissolved inorganic carbon, *Plant Cell Physiology*, **34:** 649-657

Shutes, R.B.E. 2001. Artificial wetlands and water quality improvement, *Environment International*, **26:** 441-447

Silverman, D.N. 1991. The catalytic mechanism of carbonic anhydrase, *Canadian Journal of Botany*, **69:** 1070-1078

Silvester, E.J., Grieser, F., Sexton, B.A. and Healy, T.W. 1991. Spectroscopic studies of copper sulfide sols, *Langmuir*, **7:** 2917-2922

Singh, M. and Constantinides, G. 2000. The National Water Conservation and Demand Management Strategy: A local authorities' perspective, *Proceeding of the Biennial Conference of the Water Institute of Southern Africa (WISA 2000)*, 17-21

Singh, N., Asthana, R.K., Kayastha, A.M., Pandey, S., Chaudhary, A.K. and Singh, S.P. 1999. Thiol and exopolysaccharide production in a cyanobacterium under heavy metal stress, *Process Biochemistry*, **35:** 63-68

So, A.K.C. and Espie, G.S. 1998. Cloning, characterisation and expression of carbonic anhydrase from the cyanobacterium *Synechocystis* PCC6803, *Plant Molecular Biology*, **37:** 205-215

Spratt, A.K. and Wieder, R.K. 1988. Growth responses and iron uptake in *Sphagnum* plants and their relations to acid mine drainage (AMD) treatment, *Mine Drainage and Surface Mine Reclamation,* **1:** 279-286

Stal, L.J. 2001. Coastal microbial mats: the physiology of a small-scale ecosystem, *South African Journal of Botany*, **67:** 399-410

Stauber, J.L. and Florence, T.M. 1987. Mechanism of toxicity of ionic copper and copper complexes to algae, *Marine Biology*, **94:** 511-519

Steudel, R. 1996. Mechanism for the formation of elemental sulfur from aqueous sulfide in chemical and microbiological desulfurization processes, *Industrial and Engineering Chemistry Research*, **35:** 1417-1423

Stumm, W. and Morgan, J.J. 1996. *Aquatic Chemistry*, Third edition, John Wiley and Sons, New York

Sültemeyer, D., Price, G.D., Yu, J.W. and Badger, M.B. 1995. Characterisation of carbon dioxide and bicarbonate transport during steady-state photosynthesis in the marine cyanobacterium *Synechococcus* strain PCC7002, *Planta*, **197:** 597-607

Sültemeyer, D., Miller, A.G., Espie, G.S., Fock, H.P. and Canvin, D.T. 1989. Active CO_2 transport by the green alga *Chlamydomonas reinhardtii*, *Plant Physiology*, **89:** 1213-1219

Sültemeyer, D. 1998. Carbonic anhydrase in eukaryotic algae: characterization, regulation and possible function during photosynthesis, *Canadian Journal of Botany*, **76:** 962-972

Sweeny, R.E. and Kaplan, I.R. 1973. Pyrite framboid formation: laboratory synthesis and marine sediments, *Economic Geology*, **68:** 618-634

Tashian, R.E. 1989. The carbonic anhydrases: Widening perspectives on their evolution,

expression and function, *Bioessays*, **10:** 186-192

Teisseire, H. and Vernet, G. 2000. Copper-induced changes in antioxidant enzymes activities in fronds of duckweed (*Lemna minor*), *Plant Science*, **153:** 65-72

Ting, Y.P., Lawson, F. and Prince, I.G. 1989. Uptake of cadmium and zinc by the alga *Chlorella vulgaris*: Part 1. Individual ion species, *Biotechnology and Bioengineering*, **34:** 990-999

Tobin, J.M., Cooper, D.G. and Neufeld, R.J. 1990. Investigation of the mechanism of metal uptake by denatured *Rhizopus arrhizus*, *Enzyme and Microbial Technology*, **12:** 591-595

Tobin, J.M., L'homme, B. and Roux, J.C. 1993. Immobilisation protocols and effects of cadmium uptake by *Rhizopus arrhizus* biosorbents, *Biotechnology Techniques*, **7:** 739-744

van Hille, R.P., Boshoff, G.A., Rose, P.D. and Duncan, J.R. 1999. A continuous process for the biological treatment of heavy metal contaminated acid mine water, *Resources, Conservation and Recycling*, **27:** 157-167

van Houten, R.T., Hulshoff Pol, L.W. and Lettinga, G. 1994. Biological sulphate reduction using gas-lift reactors fed with hydrogen and carbon dioxide as energy and carbon source, *Biotechnology and Bioengineering*, **44:** 586-594

van Tonder, G.J. and Kirchner, J. 1990. Estimation of natural groundwater recharge into Karoo aquifers in South Africa, *Journal of Hydrology*, **121:** 395-419

van Wyk, J.J. and Munnik, R. 1998. Dewatering of the Far East Rand mining basin: A critical evaluation of Government's approach towards solving the associated environmental problems, *Proceedings of Biennial Conference and Exhibition of the Water Institute of South Africa,* **3C:** 1-9

Vile, M.A. and Wieder, R.K. 1993. Alkalinity generation by Fe(III) reduction vs sulphate reduction in wetlands constructed for acid mine drainage treatment, *Water, Air and Soil Pollution,* **69:** 425-441

Volesky, B. 1987. Biosorbents for metal recovery, *TIBTECH*, **5:** 96-101

Vonshak, A., Kancharaska, N., Bunnag, B. and Tanticharoen, M. 1996. Role of light and photosynthesis on the acclimation process of the cyanobacterium *Spirulina platensis* to salinity stress, *Journal of Applied Phycology*, **8:** 119-124

Wagener, G.F. 1972. *Sedimentary tectonics of the East Rand Basin, with special reference to the Brakpan formation*, MSc thesis, University of Stellenbosch

Wakao, N., Takahashi, T., Sakurai, Y. and Shiota, H. 1979. A treatment of acid mine water using sulphate-reducing bacteria, *Journal of Fermentation Technology*, **57:** 445-452

Wang, W., Zhenghe, X.U. and Finch, J. 1996. Fundamental study of an ambient temperature ferrite process in the treatment of acid mine drainage, *Environmental Science and Technology,* **30:** 2604-2608

Warwick, D.W., Brackley, I.J.A. and Connelly, R.J. 1987. The dewatering of dolomite by deep mining in the West Rand, South Africa, *Proceedings of the 2nd Multidisciplinary Conference on Sinkholes and the Environmental Impacts of Karst*, 349-358

Watanabe, I. and Furusaka, C. 1980. Microbial ecology of flooded rice fields, *Advances in Microbial Ecology*, **4:** 125-168

Whittington-Jones, K. 2000. Sulphide-enhanced hydrolysis of primary sewage sludge: Implications for the bioremediation of sulphate-enriched wastewaters, PhD thesis, Rhodes University, Grahamstown, South Africa

Widdel, F. 1988. Microbiology and ecology of sulphate and sulphur reducing bacteria, In: Zehnder, A. (ed.), *Biology of anaerobic microorganisms.* Wiley Interscience, pp 469-485

Widdel, F. and Pfennig, N. 1984. Dissimilatory sulphate- or sulphur-reducing bacteria, In: Krieg, N.R. and Holt, J.G. (eds), *Bergey's Manual of Systematic Bacteriology, Volume 1*, Williams & Wilkins, London, pp 663-679

Wieder, R.K. 1989. A survey of constructed wetlands for acid coal mine drainage in the eastern United States, *Wetlands,* **9:** 299-315

Wieder, R.K. and Lang, G.E. 1992. Modification of acid mine drainage in a freshwater wetland. In: McDonald, B.R. (ed.) *Proceedings of the Symposium on Wetlands of the Unglaciated Appalachian Region,* 43-53

Wilbur, K.M. and Anderson, N.G. 1948. Electromeric and colorimetric determination of carbonic anhydrase, *Journal of Biological Chemistry*, **176:** 147-154

Wilde, E and Benemann, J.R. 1993. Bioremoval of heavy metals by the use of microalgae, *Biotechnology Advances,* **11:** 781-812

Wilhelmi, B.S. 1997. The removal and recovery of toxic and valuable metals from aqueous solution by the yeast *Saccharomyces cerevisiae*, PhD thesis, Rhodes University, South Africa

Wilkin, R.T. and Barnes, H.L. 1996. Pyrite formation by reactions of iron monosulfides with dissolved inorganic and organic sulfur species, *Geochimica et Cosmochimica Acta,* **60:** 4167-4179

Williams, T.G. and Coleman, B. 1996. The effects of pH and dissolved inorganic carbon on external carbonic anhydrase activity in *Chlorella saccharophila*, *Plant Cell and Environment*, **19:** 485-489

Wood, S.C., Younger, P.L. and Robins, N.S. 1999. Long-term changes in the quality of polluted water discharges from abandoned underground coal workings in Scotland, *Quarterly Journal of Engineering Geology,* **32:** 69-79

Yang, S., Tsuzuki, M. and Miyachi, S. 1985. Carbonic anhydrase of *Chlamydomonas*: Purification and studies on its induction using antiserum against *Chlamydomonas* carbonic anhydrase, *Plant and Cell Physiology*, **25:** 25-34

Younger, P.L. 1995. Hydrogeochemistry of minewaters flowing from abandoned coal workings in County Durham, *Quarterly Journal of Engineering Geology,* **28:** S101-S113

Younger, P.L. 1997. The longevity of minewater pollution: a basis for decision making, *The Science of the Total Environment,* **194/195:** 457-466

Younger, P.L. 1998. Coalfield abandonment: geochemical processes and hydrochemical products. In: Nicholson, K. (ed.) *Energy and the Environment: Geochemistry of fossil, nuclear and renewable resources*, MacGregor Science, pp 1-29

Younger, P.L. 2000. Predicting temporal changes in total iron concentrations in groundwaters flowing from abandoned deep mines: a first approximation, *Journal of Contaminant Hydrology,* **44:** 47-69

Younger, P.L. 2001. Mine water pollution in Scotland: nature, extent and preventative strategies, *The Science of the Total Environment,* **265:** 309-326

Younger, P.L. and LaPierre, A.B. 2000. '*Uisge Mèinne*': mine water hydrogeology in the Celtic lands, from *Kernow* (Cornwall, UK) to *Ceap Breattain* (Cape Brenton, Canada). In: Robins, S. and Misstear, B.D.R. (eds) *Groundwater in the Celtic Regions: Studies in Hard Rock and Quaternary Hydrogeology,* Geological Society, London, Special Publications, **182:** 35-52

Zhao, M. and Duncan, J.R. 1998. Removal and recovery of nickel from aqueous solution and

electroplating rinse effluent using *Azolla filiculoides*, *Process Biochemistry*, **33:** 249-255

Zopfi, J., Ferdelman, T.G., Jørgensen, B.B., Teske, A. and Thamdrup, B. 2001. Influence of water column dynamics on sulfide oxidation and other major biogeochemical processes in the chemocline of Mariager Fjord (Denmark), *Marine Chemistry*, **74:** 29-51